On deterministic and statistical consistency for nonlinear inverse problems

Rasmussen, Aksel Kaastrup

Publication date:
2023

Document Version
Publisher's PDF, also known as Version of record

On deterministic and statistical consistency for nonlinear inverse problems

Aksel Kaastrup Rasmussen

Kongens Lyngby 2023

Technical University of Denmark
Department of Applied Mathematics and Computer Science
Richard Petersens Plads, building 324,
2800 Kongens Lyngby, Denmark
Phone +45 4525 3031
compute@compute.dtu.dk
www.compute.dtu.dk

Summary

This thesis studies consistent reconstruction for nonlinear inverse problems from the perspective of regularization theory and the Bayesian approach.

It focuses on three nonlinear inverse problems: the Calderón problem, an inverse problem in photoacoustic tomography, and an inverse Robin problem. These problems have applications across the fields of medical imaging, industrial testing, and, in the case of the latter, even in large-scale ice sheet modeling for sea level predictions.

The regularization perspective considers consistency as a property attributed to methods whose reconstructions improve toward the ground truth as the deterministic noise decreases. For a large class of penalized least-squares methods, consistency is guaranteed, while computability is harder to guarantee. In contrast, we offer, in this thesis, a direct, consistent, and computable regularization strategy for the three-dimensional Calderón problem. It is based on truncated frequency information under a prior assumption of a smooth ground truth. Further, we demonstrate the convergence property numerically on synthetic data.

The Bayesian perspective has become the preferred perspective when it comes to handling random noise, incorporating prior knowledge, and quantifying uncertainty. Here, consistency enters as a property of a posterior distribution that increasingly concentrates around the ground truth as the random data improves. Guaranteeing consistency is often a first step in reliable estimation and uncertainty quantification for high-dimensional nonlinear inverse problems. We will review the Bayesian perspective, recent consistency results, and offer parallels to the perspective of regularization theory.

Among new contributions, we address consistent Bayesian reconstruction of piecewise constant parameters: We provide consistent methods for inclusion detection and apply them to a problem in the photoacoustic tomography setting, demonstrating the consistency in a numerical example. Furthermore, we address how to consistently and efficiently reconstruct real analytic parameters with the use of a strong smoothness prior in a Bayesian approach. Here, the inverse Robin problem serves as motivation and a theoretical case study.

Resumé (summary in Danish)

Denne afhandling undersøger konsistent rekonstruktion for ikkelineære inverse problemer fra perspektivet af regulariseringssteori og Bayesiansk inferens.

Den fokuserer på tre ikkelineære inverse problemer: Calderón problemet, et inverst problem inden for fotoakustisk tomografi, og et såkaldt inverst Robin problem. Disse problemer har anvendelser inden for medicinsk billeddannelse, industrielle tests og i tilfældet af det sidstnævnte endda i storskala ismodellering til nytte i langsigtede fremskrivninger af det globale havniveau.

Fra perspektivet af regulariseringsteori er konsistens en egenskab tillagt metoder, hvis rekonstruktioner forbedres mod den sande parameter, når den deterministiske støj aftager. For en stor klasse af metoder baseret på mindste kvadraters metode er konsistens garanteret, mens beregnelighed er sværere at garantere. I modsætning hertil præsenterer vi i denne afhandling en direkte, konsistent og beregnelig regulariseringsstrategi for Calderón problemet i tre dimensioner. Den er baseret på trunkeret frekvensinformation under en *a priori* antagelse om en vis glathed af den sande parameter. Endvidere demonstrerer vi konsistensegenskaben af metoden i numeriske eksempler.

Det Bayesianske perspektiv er blevet det foretrukne perspektiv, når det kommer til håndtering af stokastisk støj, indkorporering af *a priori* antagelser og kvantificering af usikkerhed. Her optræder konsistens som en egenskab tillagt en såkaldt *a posteriori*-sandsynlighedsfordeling, hvis den i stigende grad koncentrerer sig omkring den sande parameter, når kvaliteten af den stokastiske data forbedres. At garantere konsistens er ofte et første skridt i pålidelig estimering og kvantificering af usikkerhed i højdimensionale ikkelineære inverse problemer.

Vi vil gennemgå relevante dele af det Bayesianske perspektiv, diskutere nylige konsistensresultater og fremføre paralleller til regulariseringsteoriens perspektiv.

Blandt nye bidrag adresserer vi konsistent Bayesiansk rekonstruktion af stykvis konstante parametre: Vi betragter konsistente metoder til inklusionsdetektion og anvender dem på et inverst problem i fotoakustisk tomografi, hvor vi demonstrerer konsistensegenskaben i et numerisk eksempel. Ydermere beskæftiger vi os med, hvordan man konsistent og effektivt rekonstruerer en klasse af analytiske parametre ved brug af en *a priori*-sandsynlighedsfordeling, der modellerer stærk glathed. Her fungerer det inverse Robin problem som den konkrete motivation og teoretiske ramme.

Preface

This thesis presents the results of my work as a PhD student at the Department of Applied Mathematics and Computer Science, Technical University of Denmark (DTU), in the period September 1 2020 - August 31 2023. The work was carried out under the supervision of Professor Kim Knudsen, DTU, and Professor Tanja Tarvainen, University of Eastern Finland.

The obtained results concern reconstruction and consistency for some nonlinear inverse problems and are detailed in the papers:

PAPER A Kim Knudsen and Aksel Kaastrup Rasmussen. Direct regularized reconstruction for the three-dimensional Calderón problem. Inverse Probl. Imaging, 16(4):871–894, 2022. See [KR22b].

PAPER B Babak Maboudi Afkham, Kim Knudsen, Aksel Kaastrup Rasmussen, and Tanja Tarvainen. A Bayesian approach for consistent reconstruction of inclusions. arXiv preprint, arXiv:2308.13673, 2023. In submission. See [AKRT23].

PAPER C Ieva Kazlauskaite, Aksel Kaastrup Rasmussen, and Fanny Seizilles. The Bayesian approach to inverse Robin problems. In preparation, 2023. See [KRS23].

The papers are summarized in Chapter 2 and 4 in a proper given context, where in the first summary, I include results from the unpublished technical report [KR22a]. I remark that PAPER C is subject to an ongoing numerical study and is therefore still in preparation. Some preliminary numerical results

figure in its summary in Section 4.3. The papers and the report can be found in Appendix A-D. In Appendix E, a summary of the notation is given. Note there are discrepancies in notation between the summaries and the corresponding papers, since the thesis attempts to unify the notation.

I am grateful to my main supervisor Professor Kim Knudsen for his advice, encouragement and curiosity, and to my co-supervisor Professor Tanja Tarvainen for her everlasting support. I had the pleasure of visiting Tanja and the University of Eastern Finland in the Fall of 2021 and extend sincere thanks to everybody at the Department of Technical Physics who made it a special and memorable experience.

I would like to give my best thanks to Professor Per Christian Hansen and the CUQI group for a stimulating and cooperative research environment. I would also like to thank Babak Maboudi Afkham and Amal Alghamdi, postdoctoral researchers in the CUQI project, whom I had the pleasure of collaborating with. I am grateful to the Villum Foundation (grant no. 25893) for funding the CUQI project and my PhD.

Special thanks to the thesis assessment committee consisting of Professor Josselin Garnier, Assistant Professor Hanne Kekkonen and Associate Professor Mirza Karamehmedovic for the evaluation of the thesis.

Part of the work was undertaken at an external stay at Cambridge University in the winter of 2022-2023 under the supervision of Professor Richard Nickl. I would like to give my sincere thanks to Richard for making this wonderful experience possible. I am grateful for his expertise, guidance and engaging discussions. I would like to thank Kweku Abraham for a good office climate, great mathematics discussions and a memorable introduction to lacrosse. I also thank Ieva Kazlauskaite and Fanny Seizilles for great collaboration.

The Scientific Computing Section at DTU has provided great work relationships. In particular, I would like to thank Frederik for his friendship and courage in trying to learn golf and Silja for being a great office mate.

Finally, I would like to thank Astrid for always being there for me and providing distractions when I needed them the most.

Kgs. Lyngby, Denmark, August 2023

Aksel Kaastrup Rasmussen

Contents

Chapter 1

Introduction

Nonlinear inverse problems play a crucial role across many scientific fields. In the field of medical imaging, for example, we find novel technologies that allow doctors to look inside the human body - technologies that are based on mathematical methods for solving nonlinear inverse problems. At a much larger scale, some of the same underlying mathematical methods may be used to learn the structure of massive glaciers.

In this thesis, we look at nonlinear inverse problems that share the goal of recovering a parameter γ (a cause) indirectly through an observation (the effect) that depends on the parameter in a nonlinear way. Such problems arise for example in inverse problems in which the link between cause and effect is modelled by a partial differential equation (PDE). In many such cases, one seeks to recover a spatially variant coefficient γ in a PDE from observations of its solution on the whole or parts of the domain in question. This is the setting of many nonlinear imaging technologies and, for example, inverse problems in ice sheet modelling for glaciers.

To formalize this link, we denote by $\mathcal{G}$ the forward map that takes γ to the observation $\mathcal{G}(\gamma)$. For now we define this map on a subset Γ of the normed space $\mathcal{X}$ (parameter space) and consider the normed space $\mathcal{Y}$ (observation space) as the codomain:

$$\mathcal{G} : \Gamma \to \mathcal{Y}.$$

One can for example think of $\mathcal{X}$ as the space of all bounded functions on some domain, and Γ as the subset of positive such functions.

The nonlinearity of $\mathcal{G}$ often adds to the difficulty of inverting it, since the analysis has to be tailored to the problem at hand. Indeed, most interesting inverse problems are already difficult to solve; they are ill-posed in the sense of Hadamard [Had53]. That is, mathematically speaking, given a set of admissible observations $\mathcal{Z} \subset \mathcal{Y}$ one of the following properties does not hold:

1. Existence: for all $y \in \mathcal{Z}$, there exists $\gamma \in \Gamma$ such that $y = \mathcal{G}(\gamma)$
2. Uniqueness: $\mathcal{G}(\gamma_1) = \mathcal{G}(\gamma_2)$ implies $\gamma_1 = \gamma_2$, when $\mathcal{G}(\gamma_1), \mathcal{G}(\gamma_2) \in \mathcal{Z}$.
3. Stability: $\mathcal{G}^{-1}$ is continuous on $\mathcal{Z}$.

To make the list concrete, we have to specify $\mathcal{Z}$ and in which sense we mean continuous. The list inspires the following antithesis of questions one usually poses to an inverse problem when studying it:

1'. Can we characterize the range of $\mathcal{G}$?

2'. For which sets $\mathcal{A} \subset \Gamma$ is $\mathcal{G}|_{\mathcal{A}}$ injective?

3'. For which sets $\mathcal{Z} \subset \mathcal{G}(\mathcal{A})$ is $\mathcal{G}^{-1}|_{\mathcal{Z}}$ continuous?

Occasionally in this thesis, we will redefine $\mathcal{G}$ to its restriction to a set $\mathcal{A} \subset \Gamma$ such that $\mathcal{G}$ is both injective and continuous. If such sets exists we call the corresponding inverse problem conditionally well-posed. Not the least since Calderón's emphasis on reconstructing γ from observations in his influential paper [Cal80], it has been common to add a fourth question:

4'. How do we compute γ from the observations in a stable way?

Here the word 'stable' is a call-back to Hadamard's third property of well-posedness. Indeed, a violation of this often leaves approximations of $\mathcal{G}^{-1}$ numerically unstable. To make matters worse, measurements are always contaminated with noise, and so the observation is possibly perturbed outside the range of $\mathcal{G}$.

The classical remedy involves regularization strategies, the use of which addresses question 4' head on. This class of methods is well-studied for linear inverse problems, but less so for nonlinear inverse problems. Often regularization strategies are thought of as methods based on minimizing penalized least

squares functionals. However, in general, a regularization strategy is a map $\mathcal{R}_\alpha : \mathcal{Y} \to \Gamma$ dependent on a regularization parameter $\alpha > 0$, and a successful one should carry three abilities: $\mathcal{R}_\alpha$ should be a continuous map, so that reconstructions arising from it are stable with respect to the observations. $\mathcal{R}_\alpha$ should converge to $\mathcal{G}^{-1}$ pointwise in the range of $\mathcal{G}$ as $\alpha \to 0$, so that it acts like $\mathcal{G}^{-1}$ for α small enough. Finally, as observed noisy data Y improves in quality, $\mathcal{R}_\alpha(Y)$ should, for a clever choice of α, approach the ground truth. This last property is sometimes known as 'consistency' in the regularization literature [KV87, JM12, DDDM04] and often in the statistics literature [Nic23, Pol02].

The strength of a consistent method is that it accepts observations that are noisy and outside the range of $\mathcal{G}$. It is the mathematical property of a method that *works*, and it is *the* property we are concerned with in this thesis. At the heart of regularization strategies is also the idea that prior information helps recovering γ. This often guides the design of $\mathcal{R}_\alpha$.

A more recently introduced approach, the Bayesian approach, models this idea of prior knowledge in a direct way by probability distributions. Unlike the approach of regularization, the Bayesian approach does not produce a single estimate of γ. Instead, it produces a probability distribution, which in principle can be used to extract all sorts of information on γ. For this reason it is the go-to approach of the inverse problems community for uncertainty quantification of γ. One can also extract a single estimate from this probability distribution. As we shall see the mean can often be thought of as a consistent method.

The Bayesian approach for linear inverse problems is well-studied and shares certain properties with regularization strategies. However, for nonlinear inverse problems the connection is more diffuse and consistency for Bayesian methods are appearing only recently. Such a recent convergence result posed in [MNP21] makes use of a conditional stability estimate of $\mathcal{G}$, i.e. at least a partial answer of question 3': for a subspace $\mathcal{A} \subset \mathcal{X}$ endowed with a norm $\|\cdot\|_\mathcal{A}$ and $\gamma_1, \gamma_2 \in \Gamma$,

$$\|\gamma_1\|_\mathcal{A}, \|\gamma_2\|_\mathcal{A} \leq M \quad \Rightarrow \quad \|\gamma_1 - \gamma_2\|_\mathcal{X} \leq f(\|\mathcal{G}(\gamma_1) - \mathcal{G}(\gamma_2)\|_\mathcal{Y}), \tag{1.1}$$

for some increasing function $f : \mathbb{R} \to \mathbb{R}$, which is continuous at zero with $f(0) = 0$. Conditional stability estimates require an in-depth analysis of the particular inverse problem and serves as a goal for many research projects, here we mention [Ale88, ARRV09, KRS21]. However, such estimates are not directly useful in relation to reconstruction; they only concern perfect observations in the range of $\mathcal{G}$. Their introduction in relation to consistency for Bayesian methods is therefore of great interest and parallels developments in regularization theory, see [dHQS12].

Concisely stated, this thesis investigates the following question:

5'. What prior information and assumptions render a given nonlinear inverse problem solvable by a consistent method?

We shall study this question both from the (statistical) Bayesian and (deterministic) regularization strategy point of view, and come by three different nonlinear inverse problems in the process.

Chapter 2 contains a brief introduction to classical regularization theory for inverse problems in which we motivate the definition of a regularization strategy. We then continue to summarize original research in Paper A that provides a consistent method for the three-dimensional Calderón problem. In Chapter 3 we give an introduction to the Bayesian approach, when $\mathcal{X} = \mathbb{R}^k$ and $\mathcal{Y} = \mathbb{R}^m$. Our emphasis is on consistency and the theory that leads up this property. The finite-dimensional case is significantly easier than the infinite-dimensional case but contains many of the same properties to serve well as motivation. In addition, we highlight some parallels to regularization theory. In Chapter 4, we introduce the Bayesian approach in the infinite-dimensional setting. We focus on posterior consistency and give some general conditions to obtain this. On this base we shall summarize Paper B concerning consistent Bayesian inclusion detection. Here, we shall consider a photoacoustic tomography inverse problem as a suitable test case, although the approach is not limited to this specific problem. Finally, in the summary of Paper C we provide a consistent method for the Bayesian approach applied to an inverse Robin problem. Here, we will focus on two different prior assumptions and will see a significance in how these assumptions are addressed.

We conclude this introductory chapter by introducing the inverse problems under consideration in this thesis, along with relevant literature.

1.1 Examples of nonlinear inverse problems

1.1.1 The Calderón problem

Calderón's paper of 1980 [Cal80] sparked an interest in not only the problem that would be named after him, but PDE-based inverse problems in general. It is the problem of recovering the electrical conductivity distribution of a conductor from surface measurements of currents and voltages. Knowing the conductivity distribution of an object provides insight into what the object is made of. This is utilized in the imaging technique known as electrical impedance tomography (EIT). Applications range from breast cancer detection [CKK+01] and

stroke detection [ACL+20, MJA+14] in medical imaging to subsurface geophysical imaging [BHV03] and industrial testing [HSPG14].

In our case the problem takes its starting point at a smooth and bounded domain $\mathcal{O} \subset \mathbb{R}^d$, $d = 2, 3$ filled with a conductor with conductivity distribution $\gamma \in L^\infty(\mathcal{O})$ with $\gamma > 0$. That is, we let

$$\mathcal{X} = L^\infty(\mathcal{O}) \quad \text{and} \quad \Gamma = \{\gamma \in L^\infty(\mathcal{O}) : \gamma > 0 \text{ a.e.}\}$$

If there are no sinks or sources of current in the domain, applying an electrical surface potential $g \in H^{1/2}(\partial\mathcal{O})$ induces an electrical potential $u \in H^1(\mathcal{O})$, which uniquely solves

$$\begin{aligned} \nabla \cdot (\gamma \nabla u) &= 0 && \text{in } \mathcal{O}, \\ u &= g && \text{on } \partial\mathcal{O}. \end{aligned}$$

In theory we can repeat this experiment for any $g \in H^{1/2}(\partial\mathcal{O})$ and measure the corresponding current normal $\gamma \partial_\nu u|_{\partial\mathcal{O}} \in H^{-1/2}(\partial\mathcal{O})$. This leads to the definition of the Dirichlet-to-Neumann map Λ_γ,

$$\Lambda_\gamma : H^{1/2}(\partial\mathcal{O}) \to H^{-1/2}(\partial\mathcal{O}), \qquad \Lambda_\gamma g = \gamma \partial_\nu u|_{\partial\Omega},$$

which constitutes the observation for the inverse problem. Then we seek to invert the nonlinear map

$$\mathcal{G} : \gamma \mapsto \Lambda_\gamma.$$

In fact, in [Cal80] Calderón asks question 2' and 4' of injectivity and reconstruction for this problem. For $d = 2$ these questions have been answered in the affirmative: [Nac96] answers the injectivity question for twice differentiable conductivities and provides the D-bar reconstruction method. Based on this method [KLMS09] suggests a modified method that is a regularization strategy. This gives an answer to 4'. Finally, [AP06] upgrades the answer to 2' for $\gamma \in L^\infty(\mathcal{O})$, $\gamma \geq c > 0$.

However, the problem is fundamentally different when $d \geq 3$, and theoretical results are further from a definitive conclusion. [SU88] shows injectivity for twice differentiable conductivities. This is relaxed to Lipschitz conductivities in [CR16] and for $3 \leq d \leq 6$ to $W^{1,d}(\mathcal{O})$-conductivities in [Hab15], see also the references therein for a more complete review. A reconstruction method was posed in [Nac88], but any naive numerical realization of this suffers from 'exponential instability'. This is the starting point of the research we lay out in Section 2.1. Here we shall return to the point of exponential instability and discuss a remedy parallel to that of the regularized D-bar method of [KLMS09]. For now, we remark that exponential instability is folklore for this problem. Indeed, answers to question 3' exist in the following form: if $\|\gamma_1\|_{C^2(\overline{\mathcal{O}})}, \|\gamma_1\|_{C^2(\overline{\mathcal{O}})} \leq M$ and $\gamma_1 = \gamma_2 = 1$ near the boundary, then

$$\|\gamma_1 - \gamma_2\|_{L^\infty(\mathcal{O})} \leq f(\|\Lambda_{\gamma_1} - \Lambda_{\gamma_2}\|_{\mathcal{Y}}) \tag{1.2}$$

for a logarithmic type continuous function $f : \mathbb{R} \to \mathbb{R}$ dependent on M and with $f(0) = 0$, and where $\|\cdot\|_{\mathcal{Y}}$ is the operator norm in the space of bounded linear operators mapping $H^{1/2}(\partial\mathcal{O})$ to $H^{-1/2}(\partial\mathcal{O})$, see [Ale88]. This is the property of (1.1) with $\mathcal{A} = C^2(\overline{\mathcal{O}}) \cap \{\gamma : \gamma = 1 \text{ near } \partial\mathcal{O}\}$. This logarithmic stability is shown to be optimal in [Man01]. Note in two dimensions an estimate in L^2-norm is available for $\mathcal{A} \in H^\alpha(\mathcal{O})$ $\alpha > 0$, see [FR13], also of logarithmic kind. This even allows discontinuous parameters.

The Calderón problem has been posed in a Bayesian framework in [KKSV00] and [DS16] in finite and infinite dimensions, respectively. The conditional stability estimate (1.2) and the framework [MNP21] is used in [AN19] to provide a consistent Bayesian method for conductivities that are at least twice differentiable.

1.1.2 Inverse Robin problems and Hadamard

The inverse Robin problem is a problem for an elliptic PDE of determining a Robin coefficient on a hidden part of the boundary from Cauchy data on the observable part.

Let $\mathcal{O} \subset \mathbb{R}^d$, $d = 2, 3$, be a bounded and smooth domain with a partition of its boundary $\partial\mathcal{O} = \overline{\mathcal{M}} \cup \overline{\mathcal{M}_0} \cup \overline{\mathcal{M}_\gamma}$. Then consider the following Laplace equation for a function $u : \mathcal{O} \to \mathbb{R}$, $h \in H^{-1/2}(\mathcal{M})$ and Robin coefficient $\beta(\gamma) \in L^\infty(\mathcal{M}_\gamma)$

$$\begin{aligned} \Delta u &= 0 && \text{in } \mathcal{O}, \\ \partial_\nu u &= h && \text{on } \mathcal{M}, \\ u &= 0 && \text{on } \mathcal{M}_0, \\ \partial_\nu u + \beta(\gamma) u &= 0 && \text{on } \mathcal{M}_\gamma. \end{aligned} \tag{1.3}$$

Here, we let the coefficient $\beta(\gamma)$ be of the form $\beta(\gamma) := m_\beta + e^\gamma$ with $m_\beta > 0$, which is sufficient to ensure existence and uniqueness of solutions to (1.3) using Lax-Milgram theory. This is a convenient form of ensuring positivity of β, especially in a statistical framework. The Robin inverse problem is then to recover γ given $u|_{\mathcal{M}}$, that is, to invert the nonlinear forward map

$$\mathcal{G} : \gamma \mapsto u|_{\mathcal{M}}. \tag{1.4}$$

When $\gamma \in H^{d-1}(\mathcal{O})$, then $u|_{\mathcal{M}}$ is a continuous function up to the boundary, as we will show in Paper C. For this reason we let

$$\mathcal{X} = L^\infty(\mathcal{O}) \quad \text{and} \quad \Gamma = H^{d-1}(\mathcal{O}).$$

In the context of corrosion detection, $\mathcal{O}$ models an electrically conducting body with a constant conductivity coefficient, where the part $\mathcal{M}_0$ is insulated. Injecting a current flux h at $\mathcal{M}$ leads to an electrical potential inside $\mathcal{O}$. The question is then whether we gain any knowledge of the surface impedance on $\mathcal{M}_\gamma$ from measuring the corresponding voltages at $\mathcal{M}$. Knowing γ is equivalent to knowing $\beta(\gamma)$, and this gives information on something we cannot measure directly, the corrosion at $\mathcal{M}_\gamma$. The problem finds similar applications in thermal imaging: with a prescribed heat flux on $\mathcal{M}$, can we determine the heat-exchange function γ on $\mathcal{M}_\gamma$ from measuring the temperature at $\mathcal{M}$?

The problem was first formulated in [Ing97, CJ99] with the goal of recovering β. More recently, the problem has gained renewed interest by glaciology communities for its relation with a problem for a Stokes PDE system of inferring a basal drag coefficient β of ice sheets from only surface observations of ice velocities and stresses [AG10].

The inverse Robin problem has its humble beginnings in the Cauchy problem. Let $\mathcal{O}$ be the square $(0,\pi)\times(0,1)$, and let $\mathcal{M}$ be the bottom line segment, $\mathcal{M}_0$ be the sides and $\mathcal{M}_\gamma$ be the top segment. Say we prescribe and observe the sine-series

$$h=\sum_{j=1}^{\infty} h_j \sin(jx), \qquad \text{and} \qquad u|_{\mathcal{M}}=\sum_{j=1}^{\infty} u_j \sin(jx),$$

at the bottom. Using separation of variables we can determine the unique solution $u:\mathcal{O}\to\mathbb{R}$ that gave rise to the measurement $u|_{\mathcal{M}}$ as

$$u(x,y)=\sum_{j=1}^{\infty}\left[u_j\cosh(jy)-\frac{h_j}{j}\sinh(jy)\right]\sin(jx).$$

In fact, under certain decay condition of h_j, this solution is a classical solution $u\in C^2(\overline{\mathcal{O}})$ [LN17]. So u satisfies the Robin condition on $(0,\pi)\times\{1\}$, and if dividing by $u(x,1)$ is sensible,

$$\beta(\gamma)(x)=-\frac{u_y'(x,1)}{u(x,1)}=-\frac{\sum_{j=1}^{\infty}\left[ju_j\sinh(j)-h_j\cosh(j)\right]\sin(jx)}{\sum_{j=1}^{\infty}\left[u_j\cosh(j)-\frac{h_j}{j}\sinh(j)\right]\sin(jx)}. \tag{1.5}$$

Small perturbations in the observations u_j are perturbed by an exponential factor $\sinh(j)$ and $\cosh(j)$. This ill-posedness in determining $\beta(\gamma)$ comes from the lack of continuity in determining $u(x,1)$ and $u_y'(x,1)$ from h and $u|_{\mathcal{M}}$. This was known by Hadamard in 1923, see [Had53, ARRV09] and the following example.

Example 1.1 *Consider $h=h_n\sin(nx)$ and $u|_{\mathcal{M}}=0$ such that*

$$u(x,y)=\frac{h_n}{n}\sinh(ny)\sin(nx).$$

For example setting $h_n = \frac{1}{n}$*, we note* $h \to 0$ *uniformly at* $\mathcal{M}$ *as* $n \to \infty$*, while*

$$u(x,1) = \frac{1}{n^2}\sinh(n)\sin(nx) \quad \text{and} \quad u'_y(x,1) = \frac{1}{n}\cosh(n)\sin(nx)$$

diverges as $n \to \infty$*, hence there is no continuous dependence of* $u(x,1)$ *and* $u'_y(x,1)$ *on* h*.*

For this example, it is noted in [ARRV09] that an *a priori* bound such as $\|\nabla u\|_{L^2(\mathcal{O})} \leq M$ leads to a different outcome. Indeed, then

$$\|u\|_{L^2((0,\pi)\times(0,1))} \to 0$$

at a logarithmic rate as $n \to \infty$. Essentially, the condition restricts h_n to sequences of fast decay. For $y < 1$, we even have that

$$\|u\|_{L^2((0,\pi)\times(0,1))} \leq |h_n|^\sigma$$

for some $0 < \sigma < 1$. This kind of global logarithmic continuity and interior Hölder continuity under *a priori* conditions on u turns out to hold in the general case as well [ARRV09]. This observation leads to a conditional stability estimate of the form (1.1) for $\mathcal{A} = C^1(\mathcal{M}_\gamma)$ and f of logarithmic type, see [ADPR03]. See also [HY15, LN17] for stability results under the *a priori* condition that γ is real analytic. We remark that the inverse problem has a unique solution, for example when γ is positive and continuous, see [CJ99].

Reconstruction for the inverse Robin problem has been studied using classical regularization methods based on penalized least squares, see [CJ99, LN17, Jin07] and the references therein. [FI99] provides a direct accurate method provided the domain is sufficiently thin. The problem has been posed in a Bayesian framework in [NN22], which determines γ and $\mathcal{M}_\gamma$ simultaneously. The related inverse Robin problem for the Stokes PDE has been considered in the Bayesian framework in [Art15, NPK18, BNVP21], where in the two latter the framework is similar to the general approach in [Stu10].

1.1.3 Inclusion detection and quantitative photoacoustic tomography

An objective in many inverse problems is to recover inhomogeneities or inclusions in a medium; applications range from cancer detection and stroke detection in medical imaging to defect detection in material science. We consider an inclusion detection problem as an inverse problem of recovering parameters of the

form $\gamma = \kappa_1 \mathbb{1}_A + \kappa_2$ for some *a priori* known constants $\kappa_1, \kappa_2 > 0$, and a measurable set $A \subset \mathbb{R}^d$, $d = 2, 3$. In Paper B, we shall generalize this to a sum of multiple indicator functions each with a set A_i and constant κ_i, $i = 1, \dots \mathcal{N}$.

This can be a hard problem as we do not have any regularity of the parameter of interest. One the other hand, it is also strong prior information that the parameter has this form, and this can be utilized. Inclusion detection has been analyzed extensively in the context of the Calderón problem, see for example [Gar16] for an overview. Uniqueness, i.e. an answer to question 2', is proven in [Isa88], stability is analyzed in [ADC05], which gives conditional stability of logarithmic type, the condition being that A is sufficiently regular in a uniform sense. In [DCR03] logarithmic stability was shown to optimal. Monotonocity methods is considered in [HU13], see also the references therein. When the inclusions are also known to be small *a priori*, strong results are available; we have a characterization of the range of the forward map and stability results [CFMV98, BHV03]. Inclusion detection problem are often known as inverse obstacle problems in the context of acoustic or electromagnetic scattering, see [CK19] for an overview of the reconstruction methods involved.

The level set method is a general method tackling this problem across different inverse problems, see [San96] and the references therein. This method is applied in a Bayesian framework in [ILS16, DIS17]. A Bayesian approach for detection of star-shaped inclusions is considered in [BTG14, DS16]. These are the methods we will consider in Paper B.

One class of inverse problems shows promise in addressing inclusion detection with guaranteed success. These are the inverse problems arising in 'hybrid imaging' methods that combine advantages of different imaging techniques coming from the underlying physics, see [Kuc12].

One such example is the inverse problem of quantitative photoacoustic tomography (QPAT). The problem of QPAT is the second part of a two-part technique in photoacoustic tomography. This second part seeks to recover the optical parameters of a biological object from information on the absorbed energy density from a given light source. This absorbed energy density is estimated in the first part of the photoacoustic tomography problem. In the 'diffusion approximation' [BRUZ11] light transport is modelled according to the elliptic equation

$$\begin{aligned} -\nabla \cdot \mu \nabla u + \gamma u &= 0 \quad \text{in } \mathcal{O}, \\ u &= g \quad \text{on } \partial\mathcal{O}, \end{aligned} \tag{1.6}$$

where $\mathcal{O}$ is the bounded domain that models the biological object and $\mu, \gamma \in L^\infty(\mathcal{O})$ with $\mu > 0$ and $\gamma \geq 0$, are the optical parameters. In this thesis, we

find the following choice of normed space and subset useful:

$$\mathcal{X} = L^2(\mathcal{O}) \quad \text{and} \quad \Gamma = L^2_\Lambda(\mathcal{O}) := \{\gamma \in L^2(\mathcal{O}) : \Lambda^{-1} \leq \gamma \leq \Lambda \text{ a.e.}\}$$

for some constant $\Lambda > 0$. Note that Γ is a closed subset of $L^2(\mathcal{O})$, since $L^\infty(\mathcal{O})$-closed balls are closed in $L^2(\mathcal{O})$ as a consequence of the Riesz-Fischer theorem [RF10, Section 7.3].

We call u the light intensity, and the prescribed Dirichlet boundary condition $u = g$ defines the source of incoming light. In this setting, the absorbed energy density $H \in L^\infty(\mathcal{O})$ takes the form

$$H(x) = G(x)\gamma(x)u(x),$$

where the Grüneisen parameter G models the photoacoustic effect. We will assume this to be known and set for simplicity $G = 1$. Note the map

$$(\mu, \gamma) \mapsto H$$

is well-defined, since (1.6) has a unique solution. Likewise, we could consider several illuminations $g_1, g_2, \ldots$ and corresponding data $H_1, H_2, \ldots$. The questions of injectivity and continuity have been considered in a number of papers for two illuminations. We mention here [BU10, BRUZ11, ADCFV17, BCT22, Cho21], which answer such questions under conditions on g_1 and g_2 and γ. The latter concludes Hölder continuity of $H \mapsto (\mu, \gamma)$ given that $\|\mu\|_{C^{1,1}(\overline{\mathcal{O}})}, \|\gamma\|_{C^{0,1}(\overline{\mathcal{O}})} \leq M$.

Our main interest in QPAT stems from the fact that for a fixed and known μ the forward map

$$\mathcal{G} : \gamma \mapsto H \tag{1.7}$$

has favorable properties even for non-regular γ. In this case injectivity and stability can be reduced to choosing g such that u is bounded from above and away from zero. Indeed, then γ is found by solving

$$\begin{aligned} -\nabla \cdot \mu \nabla u + H &= 0 \quad \text{in } \mathcal{O}, \\ u &= g \quad \text{on } \partial\mathcal{O}, \end{aligned}$$

and computing $\gamma = H/u$. As well-posed as this seems, the inverse problem can become harder, when u is close to zero. For example, we do not have uniform continuity of $\mathcal{G}^{-1}$ defined on all of $L^\infty(\mathcal{O})$, as is demonstrated in the following.

Example 1.2 *Consider $\mu = 1$, $\mathcal{O} = (0,1)$ and the boundary condition $u(0) = u(1) = 1$. Then* (1.6) *takes the form:*

$$\begin{aligned} u'' &= \gamma u \quad \text{in } (0,1), \\ u(0) = u(1) &= 1, \end{aligned}$$

Take for $n = 1, 2, \ldots,$

$$u_n = \begin{cases} p_{1,n}(x) & 0 \le x < 1/4, \\ 1/n & 1/4 \le x \le 3/4, \\ p_{2,n}(x) & 3/4 < x \le 1, \end{cases} \quad \textit{with} \quad u_n'' = \begin{cases} 32 - 2/n & 0 \le x < 1/4, \\ 0 & 1/4 \le x \le 3/4, \\ 32 - 2/n & 3/4 < x \le 1, \end{cases}.$$

Here $p_{1,n}, p_{2,n}$ *are the second-order polynomials satisfying* $p_{1,n}(0) = p_{2,n}(1) = 1$, $p_{1,n}(1/4) = p_{2,n}(3/4) = 1/n$ *and* $p'_{1,n}(1/4) = p'_{2,n}(3/4) = 0$. *Consider now the function*

$$\tilde{u}_n = \begin{cases} \tilde{p}_{1,n}(x) & 0 \le x < 1/4, \\ f_n(x) & 1/4 \le x \le 3/4, \\ \tilde{p}_{2,n}(x) & 3/4 < x \le 1, \end{cases},$$

where $f_n(x) = c_{1,n}e^{-nx} + c_{2,n}e^{nx}$ *with* $c_{1,n}, c_{2,n}$ *such that* $f_n(0) = f_n(1) = 1$, *and* $\tilde{p}_{1,n}, \tilde{p}_{2,n}$ *are the second-order polynomials that connects smoothly with* $f_n(x)$ *such that* $\tilde{p}_{1,n}(0) = \tilde{p}_{2,n}(1) = 1$. *Straightforward computations show that*

$$\tilde{u}_n'' = \begin{cases} 32 - 32f_n(1/4) + 8f_n'(1/4) & 0 \le x < 1/4, \\ n^2 f_n(x) & 1/4 \le x \le 3/4, \\ 32 - 32f_n(3/4) - 8f_n'(3/4) & 3/4 < x \le 1, \end{cases}.$$

Note both u_n *and* $\tilde{u}_n$ *are positive, while* $\tilde{H}_n - H_n = \tilde{u}_n'' - u_n''$ *converges uniformly to zero. However,* $\gamma_n = H_n/u_n = 0$ *on* $[1/4, 3/4]$, *whereas* $\tilde{\gamma}_n = \tilde{H}_n/\tilde{u}_n = n^2$ *on* $[1/4, 3/4]$.

In Paper B we show that $\mathcal{G}$ satisfies a conditional stability estimate of the form (1.1) for $f(x) = Cx$ and $\gamma_i \in L^2_\Lambda(\mathcal{O})$, $i = 1, 2$. This makes the QPAT inverse problem a suitable test case for consistent inclusion detection methods in the Bayesian framework. We will return to this topic in the summary of Paper B in Section 4.2.

1.1.4 A spherical gravity anomaly

To introduce concepts in infinite-dimensional spaces we occasionally find it convenient to give a finite-dimensional example. With this purpose in mind we pose the following simple inverse problem in geology, see [TGS90, Section 2.7] for problems of that kind. It is the problem of determining the radius $r > 0$ and depth $z > 0$ of a buried sphere of a known material, given measurements of the gravitational acceleration over it. One can think of it as a simple inclusion detection problem. The gravitational acceleration measured at the surface

at horizontal distance x away from the center of the sphere is, according to Newton's 'Shell' theorem,

$$g(x) = 4G\pi\rho \frac{r^3 z}{(x^2+z^2)^{3/2}}, \tag{1.8}$$

where ρ is the density contrast and G is the gravitational constant. Let us say we measure right above the sphere at $x = 0$ and at some distance away at $x = 100$. We argue that we can always measure right above the sphere, since this is where the signal is the strongest. Then we set $\gamma = (r, z)$ and define the forward map

$$\mathcal{G}(\gamma) := (g(0), g(100)) \in \mathbb{R}^2.$$

Here we let,

$$\mathcal{X} = \mathbb{R}^2 \quad \text{and} \quad \Gamma = \mathbb{R}^2_+ = \{y = (y_1, y_2) \in \mathbb{R}^2 : y_1 > 0, y_2 > 0\}.$$

We claim that γ is uniquely determined by $\mathcal{G}(\gamma)$. Indeed, assume $\mathcal{G}(\gamma_1) = \mathcal{G}(\gamma_2)$. Setting $\gamma_1 = (r_1, z_1)$ and $\gamma_2 = (r_2, z_2)$, two equations follow:

$$\begin{aligned} r_1^3 z_2^2 - r_2^3 z_1^2 &= 0, \\ r_1^3 z_1 (z_2^2 + 100^2)^{3/2} - r_2^3 z_2 (z_1^2 + 100^2)^{3/2} &= 0, \end{aligned}$$

Isolating r_1^3/r_2^3 from both equations gives us

$$\frac{z_1^3}{(z_1^2+100^2)^{3/2}} = \frac{z_2^3}{(z_2^2+100^2)^{3/2}},$$

but $z \mapsto z^3/(z^2+100^2)^{3/2}$ is a strictly increasing function and hence $z_1 = z_2$. Then, it follows from the first equation above that $r_1 = r_2$.

The Jacobian determinant $|J\mathcal{G}| : \mathbb{R}^2 \to \mathbb{R}$ of $\mathcal{G}$ can be computed (using for example a computer algebra system) as

$$|J\mathcal{G}(\gamma)| = C \frac{r^5}{z^2(z^2+100^2)^{5/2}} > 0$$

for all $r, z > 0$. Then $\mathcal{G}$ is an open mapping, see [Apo74, Theorem 13.5], and hence $\mathcal{G}^{-1}$ is continuous on its image $\mathcal{G}(\Gamma)$. Using the same approach one may check that the singular values of $(J\mathcal{G})(\gamma)$ are uniformly bounded when $m < r, z < M$. Hence, for such γ the mean value inequality gives the local Lipschitz continuity

$$\begin{aligned} \|\mathcal{G}(\gamma_1) - \mathcal{G}(\gamma_2)\| &\leq \int_0^1 \|J\mathcal{G}(\gamma_2 + t(\gamma_1 - \gamma_2))\| \|\gamma_1 - \gamma_2\| \, dt, \\ &\leq C(m, M)\|\gamma_1 - \gamma_2\|. \end{aligned} \tag{1.9}$$

denoting both the Euclidean norm and induced operator norm by $\|\cdot\|$ and the fact that this operator norm corresponds to the largest singular value. This estimate implies that $\mathcal{G}$ is continuous in every point $\gamma \in \Gamma$.

Chapter 2

Regularization of inverse problems

Regularization strategies are the classical remedy for noisy data in inverse problems. Its theoretical foundation is solid and has been studied in the last decades, see the monograph [EHN96] for a Hilbert space setting and [KNS08] for the Banach space setting. In this chapter, we consider observing $Y = Y(\varepsilon)$ that is a perturbation of $\mathcal{G}(\gamma_0)$, i.e.

$$Y = \mathcal{G}(\gamma_0) + \varepsilon\xi,$$

where $\xi \in \mathcal{Y}$ with $\|\xi\| \leq 1$ (in the norm $\|\cdot\|$ of $\mathcal{Y}$). We call $\varepsilon > 0$ the noise level. The prospect of a successful regularization strategy is to stably recover information on γ_0 even if $Y \notin \mathcal{R}(\mathcal{G})$. In fact, the strategy should improve recovery when ε decreases. This is the property of consistency. One classical view on such regularization strategies is the following: solve a penalized least-squares problem such as

$$\min_{\gamma\in\Gamma} J(\gamma), \qquad J(\gamma) := \|\mathcal{G}(\gamma) - Y\|^2 + \alpha\|\gamma\|_{\mathcal{X}}^2, \tag{2.1}$$

where $(\mathcal{X}, \|\cdot\|_{\mathcal{X}})$ and $(\mathcal{Y}, \|\cdot\|)$ are suitable function spaces and $\alpha > 0$ is called the regularization parameter. In the Hilbert space setting, a solution exists given that $\mathcal{G}$ is continuous and weakly sequentially closed, see [EHN96, Section 10]. When $\mathcal{G}$ is also linear and compact, solving (2.1) becomes an instructive exercise. Then, a singular system $(\sigma_n, v_n, u_n)_{n=1}^{\infty}$ of $\mathcal{G}$ exists, see [EHN96, Section 2.2],

and the unique minimizer of (2.1) has the form

$$\gamma_{\alpha,\varepsilon} = \sum_{n=1}^{\infty} \frac{\sigma_n}{\sigma_n^2 + \alpha} \langle Y, u_n \rangle v_n. \tag{2.2}$$

for any $Y \in \mathcal{Y}$, see [EHN96, Chapter 5]. Here we denote $\langle \cdot, \cdot \rangle$ the inner product in $\mathcal{Y}$. This minimizer is known as the *Tikhonov* regularizer, see [EHN96, Chapter 5] for a proper treatment. We introduce it to remark upon three classical properties of the map $\mathcal{R}_\alpha : \mathcal{Y} \to \mathcal{X}$ defined by $\mathcal{R}_\alpha Y := \gamma_{\alpha,\varepsilon}$, where we for simplicity assume $\mathcal{G}$ is injective:

1. $\mathcal{R}_\alpha$ is continuous: for any $Y \in \mathcal{Y}$, by Parseval's identity

$$\|\mathcal{R}_\alpha Y\|_{\mathcal{X}}^2 = \sum_{n=1}^{\infty} c_n^2 \langle Y, u_n \rangle^2 \leq \sup_{n \in \mathbb{N}} c_n^2 \|Y\|^2,$$

   and $c_n(\alpha) := \frac{\sigma_n}{\sigma_n^2 + \alpha} \leq \frac{1}{2\sqrt{\alpha}}$, since $2\sqrt{\alpha}\sigma_n \leq \alpha + \sigma_n^2$ for all $\alpha, \sigma_n > 0$.

2. $\mathcal{R}_\alpha \gamma$ converges to $\mathcal{G}^{-1}$ pointwise on $\mathcal{G}(\Gamma)$: see [Kir11, Theorem 2.6].

3. $\mathcal{R}_\alpha Y \to \gamma_0$ in $\mathcal{X}$, when $\varepsilon \to 0$ for a well-chosen $\alpha = \alpha(\varepsilon)$ going to zero: by the triangle inequality

$$\begin{aligned} \|\mathcal{R}_\alpha Y - \gamma_0\|_{\mathcal{X}} &\leq \|\mathcal{R}_\alpha Y - \mathcal{R}_\alpha \mathcal{G} \gamma_0\|_{\mathcal{X}} + \|\mathcal{R}_\alpha \mathcal{G} \gamma_0 - \gamma_0\|_{\mathcal{X}}, \\ &\leq \frac{\varepsilon}{2\sqrt{\alpha}} + \|\mathcal{R}_\alpha \mathcal{G} \gamma_0 - \gamma_0\|_{\mathcal{X}} \to 0, \end{aligned}$$

   as $\varepsilon \to 0$, where we have used 1. and 2. above.

These are the three properties we seek in regularization strategies: continuity as in point 1, convergence as in point 2, and consistency as in point 3. The regularizing nature of (2.1) is intuitive: we should minimize a misfit, while at the same time keep $\|\gamma\|_{\mathcal{X}}$ small. However, it is a little misguided to think that all regularization strategy has the form of penalized least squares. Instead, we define it to be a map $\mathcal{R}_\alpha : \mathcal{Y} \to \mathcal{X}$ that possesses these three properties. This is the definition an admissible regularization strategy in [Kir11, EHN96] also presented in [KLMS09] in the nonlinear setting, which we now give here.

Definition 2.1 A family of continuous mappings $\mathcal{R}_\alpha : Y \to \mathcal{X}$, parametrized by *regularization parameter* $0 < \alpha < \infty$, is called a *regularization strategy* for $\mathcal{G} : \Gamma \to \mathcal{Y}$ in $\mathcal{A} \subset \Gamma$ if

$$\lim_{\alpha \to 0} \|\mathcal{R}_\alpha \mathcal{G}(\gamma) - \gamma\|_{\mathcal{X}} = 0, \tag{2.3}$$

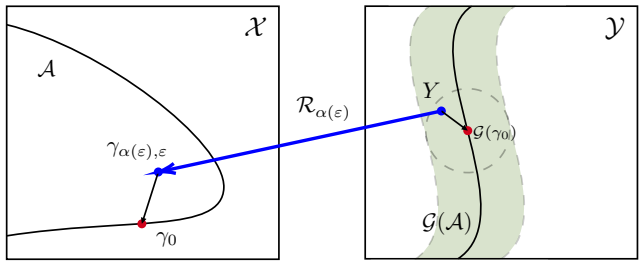

Figure 2.1: Graphical representation of the consistency property (2.4) of admissible regularization strategies.

for each fixed $\gamma \in \mathcal{A}$. Furthermore, a regularization strategy $\mathcal{R}_\alpha$ is called *admissible* if

$$\alpha(\varepsilon) \to 0 \quad \text{as} \quad \varepsilon \to 0,$$

and for any fixed $\gamma_0 \in \mathcal{A}$ we have

$$\sup_{Y \in \mathcal{Y}: \|Y - \mathcal{G}(\gamma_0)\| \le \varepsilon} \|\mathcal{R}_{\alpha(\varepsilon)} Y - \gamma_0\|_{\mathcal{X}} \to 0 \quad \text{as} \quad \varepsilon \to 0. \tag{2.4}$$

The consistency property of (2.4) is visualized in Figure 2.1. For nonlinear problems Tikhonov regularization remains relevant. However, in this case J is not necessarily convex, and so (2.1) does not necessarily have a unique solution. This makes it difficult to define a map $\mathcal{R}_\alpha$ as in the linear case. A related problem in estimation theory has lead statisticians to ask for the measurability properties of $Y \mapsto \hat{\gamma}_{\alpha,\varepsilon}$, where $\hat{\gamma}_{\alpha,\varepsilon}$ is a clever choice among the minimizers of (2.1), see [GN16, Exercise 7.2.3]. This is not a focus in the regularization literature: stability and convergence properties is often proven for any minimizer of (2.1) in [EHN96, KNS08]. The spherical anomaly problem in $\mathbb{R}^2$ is particularly simple in the presence of inverse continuity:

Example 2.1 (Tikhonov for spherical anomaly) *$\mathcal{G} : \mathbb{R}^2_+ \to \mathbb{R}^2$ is continuous by (1.9). Let $\mathcal{A}$ be the closed set of elements $\gamma = (r, z)$ such that $0 < m \le r, z < \infty$. Then there exists a solution $\gamma_{\alpha,\varepsilon}$ to (2.1), see [Ric16, Theorem 4.1]. Any such solution satisfies (for the Euclidean norm $\|\cdot\|$ on $\mathbb{R}^2$)*

$$\|\mathcal{G}(\gamma_{\alpha,\varepsilon}) - Y\|^2 + \alpha \|\gamma_{\alpha,\varepsilon}\|^2 \le \varepsilon^2 + \alpha \|\gamma_0\|^2. \tag{2.5}$$

The triangle inequality implies

$$\begin{aligned}\|\mathcal{G}(\gamma_{\alpha,\varepsilon}) - \mathcal{G}(\gamma_0)\|^2 &\leq 2\|\mathcal{G}(\gamma_{\alpha,\varepsilon}) - Y\|^2 + 2\|Y - \mathcal{G}(\gamma_0)\|^2, \\ &\leq 4\varepsilon^2 + 2\alpha\|\gamma_0\|^2.\end{aligned}$$

So for a suitable choice $\alpha = \alpha(\varepsilon) \to 0$ as $\varepsilon \to 0$, we have

$$\sup_{Y \in \mathbb{R}^2 : \|Y - \mathcal{G}(\gamma_0)\| \leq \varepsilon} \|\mathcal{G}(\gamma_{\alpha,\varepsilon}) - \mathcal{G}(\gamma_0)\| \to 0$$

as $\varepsilon \to 0$. By continuity of $\mathcal{G}^{-1}$ in $\mathcal{G}(\Gamma)$, we conclude $\gamma_{\alpha(\varepsilon),\varepsilon} \to \gamma_0$. The same argument works for Y replaced with $\mathcal{G}(\gamma)$, and $\alpha \to 0$ independent of ε. Continuity of $\gamma_{\alpha,\varepsilon}$ with respect to Y is analyzed in for example [EHN96, 10.2].

In general, it is too much to ask for continuity of $\mathcal{G}^{-1}$ in $\mathcal{G}(\Gamma)$. What is becoming a more standard approach is to understand instead the conditional properties of the inverse problem, as in the questions 2' and 3', and in typical answers of the form (1.1). Here, $\|\cdot\|_{\mathcal{A}}$ is typically a stronger norm than $\|\cdot\|_{\mathcal{X}}$. Penalizing with this norm instead of $\|\cdot\|_{\mathcal{X}}$ in (2.1) and following (2.5), we conclude that

$$\alpha\|\gamma_{\alpha,\varepsilon}\|_{\mathcal{A}}^2 \leq \varepsilon^2 + \alpha\|\gamma_0\|_{\mathcal{A}}^2.$$

Then $\|\gamma_{\alpha(\varepsilon),\varepsilon}\|_{\mathcal{A}}$ is bounded when $\varepsilon^2/\alpha(\varepsilon)$ is bounded as $\varepsilon \to 0$, which permits the use of (1.1), when $\gamma_0 \in \mathcal{A}$. Hence, $\gamma_{\alpha(\varepsilon),\varepsilon} \to \gamma_0$ as $\varepsilon \to 0$ and we can even get a rate. To conclude similar statements on consistency without the use of conditional stability estimates, we often require the stronger condition that $\varepsilon^2/\alpha(\varepsilon) \to 0$ as $\varepsilon \to 0$. This interrelation between ε and the noise dependent regularization parameter $\alpha(\varepsilon)$ is related to our findings in Chapter 4.

2.1 A regularization strategy for the Calderón problem

In the rest of this chapter, we consider a regularization analysis of the three-dimensional Calderón problem as introduced in Section 1.1.1. Despite the widespread practical use of Tikhonov-based methods in the context of the Calderón problem, see for example [Lio04], less is known about their theoretical properties. Examples include [Dob92, Ron08, Ron16, LMP03, JM12], see also references therein. In [JM12] continuity and consistency is provided under assumptions akin to the classical source condition in [EHN96, Theorem 10.4]. Under general conditions of injectivity of $\mathcal{G}$, [Ron08] proves consistency of a generalized Tikhonov method. This includes for example L^1-convergence of a total variation

regularizer to certain discontinuous γ_0. This is provided without a convergence rate. Consistency conditions for iterative regularization methods in the context of the Calderón problem appear in [Kin22, LR08] and seem hard to verify in general.

Interestingly, the existence of stability estimates of the form (1.1) with $f(x) = Cx^\nu$, $\nu > 0$, is enough to conclude convergence to $\gamma_0 \in \mathcal{A}$ of the *Landweber* iteration starting in $\mathcal{A}$. This is exemplified in [dHQS12, Section 5] for the Calderón problem powered by the stability estimate provided in [ADC05]. Furthermore, [dHQS12, Remark 4.4] and [SGG$^+$09] show that if $\nu \geq 1$, then the classical source condition is satisfied.

For these methods, computing $\gamma_{\alpha(\varepsilon),\varepsilon}$ involves iteration. In contrast, direct reconstruction methods for the Calderón problem have been analyzed in [Nac88, Nac96], since Calderón's own contribution [Cal80]. Based on the D-bar method in two dimensions in [Nac96], [KLMS09] suggests a modified method that is an admissible regularization strategy. Not until recently, a regularization analysis of the three-dimensional method of [Nac88] was undertaken. This is the content of Paper A in [KR22b], which we discuss in the following sections.

2.1.1 Nachman's reconstruction algorithm in three dimensions

Intuitively, the first step of the Nachman's reconstruction algorithm is to determine the electrical surface potentials that extract useful information from Λ_{γ_0}. Examples of such surface potentials are those who belong in a family of functions $\psi_\zeta \in H^{1/2}(\partial\mathcal{O})$ called complex geometrical optics (CGO). These were considered in the context of the Calderón problem first by [SU88]. They are indexed by a complex frequency $\zeta \in \mathbb{C}^3$ satisfying $\zeta \cdot \zeta := \sum_{i=1}^3 \zeta_i^2 = 0$ and approximates in a certain sense the harmonic functions $e^{ix\cdot\zeta}$ for $x \in \mathbb{R}^3$. We refer to [Knu02] for a first introduction to the use of these in the Calderón problem.

The crucial use of ψ_ζ in determining $\gamma_0 \in C^2(\mathcal{O})$ with $\gamma_0 = 1$ near $\partial\mathcal{O}$ becomes clear when defining the function $q_0 := \gamma_0^{-1/2}\Delta(\gamma_0^{1/2})$ and the set $\mathcal{V}_z$ for some $z \in \mathbb{R}^3$ characterized by

$$\zeta = -\frac{z}{2} + (\kappa^2 - \frac{|z|^2}{4})^{1/2} k^{\perp\perp} + i\kappa k^\perp,$$

where $\kappa \geq |z|/2$, $\{z, k^\perp, k^{\perp\perp}\}$ is an orthonormal real set of vectors in $\mathbb{R}^3$, and $|\zeta(z)| = \sqrt{2}\kappa$. Indeed, for each $z \in \mathbb{R}^3$ and $\zeta = \zeta(z) \in \mathcal{V}_z \subset \mathbb{C}^3$, [Nac88] shows

that for $|\zeta|$ large enough (see also (11)-(12) [KR22b])

$$\left| \int_{\partial\mathcal{O}} e^{-ix\cdot(z+\zeta)} (\Lambda_{\gamma_0} - \Lambda_1)\psi_\zeta(x)\, \sigma(dx) - \hat{q}_0(z) \right| \leq C|\zeta|^{-1}, \tag{2.6}$$

where σ denotes the surface measure on $\partial\mathcal{O}$, $\hat{q}_0$ is the Fourier transform of q_0 and $C > 0$ is constant depending on q_0. This implies that we can approximate $\hat{q}_0(z)$ well by an integral, if we pick $|\zeta(z)|$ large enough. That is, if we know the trace of the CGO solutions. Note if $|z|$ is large, then

$$|\zeta(z)| = \sqrt{2}\kappa \geq \frac{|z|}{\sqrt{2}}$$

should be large. This integral is also known as the scattering transform $\mathbf{t}(z, \zeta(z))$

$$\mathbf{t}(z, \zeta(z)) = \int_{\partial\mathcal{O}} e^{-ix\cdot(z+\zeta)} (\Lambda_{\gamma_0} - \Lambda_1)\psi_\zeta(x)\, \sigma(dx).$$

After performing an inverse Fourier transform to obtain q_0, a boundary value problem is usually solved to obtain γ_0. To recap, it is a method of three steps:

$$\Lambda_{\gamma_0} \quad \xrightarrow{(1)} \quad \mathbf{t} \quad \xrightarrow{(2)} \quad q_0 \quad \xrightarrow{(3)} \quad \gamma_0$$

However, recovering ψ_ζ on $\partial\mathcal{O}$ for $|\zeta|$ large is unstable. These are usually computed by solving a boundary integral equation involving a kernel that is exponentially growing in $|\zeta|$, and hence we expect that any error in the data Λ_{γ_0} is multiplied by an exponential factor in its contribution to $\psi_\zeta|_{\partial\mathcal{O}}$. Even if $\psi_\zeta|_{\partial\mathcal{O}}$ were recovered perfectly, any error in Λ_{γ_0} is multiplied by $e^{-ix\cdot\zeta}$ in (2.6). It stands to reason that this method needs to be modified, ideally, to a regularization strategy.

2.2 Paper A: Regularized Calderón problem in three dimensions

In Paper A, we address the instability of Nachman's reconstruction algorithm by proposing an admissible regularization strategy. This regularization strategy finds its inspiration in numerical realizations of the ideal method. Such examples count [BKM11, KM11, HIK$^+$21, BKIS09], which approximate $\mathbf{t}$ by replacing ψ_ζ with $e^{ix\cdot\zeta}$, and [DHK12, DK14], which solve approximate boundary integral equations to obtain approximations of $\psi_\zeta|_{\partial\mathcal{O}}$. Common for all is that they seek to recover $\mathbf{t}$ in a bounded domain $|z| < M$ using $|\zeta(z)|$ small. When it comes to

picking $|\zeta(z)|$, two popular choices are

$$|\zeta(z)| = M^p,\ p > 0 \qquad \text{(fixed)},$$
$$|\zeta(z)| = \frac{|z|}{\sqrt{2}} \qquad \text{(minimal)}.$$

While both choices allows admissible $\zeta(z) \in \mathcal{V}_z$, the fixed choice is natural, since it ensures convergence of $\mathbf{t}(z, \zeta(z))$ to $\hat{q}_0(z)$ when $M \to \infty$ by letting $|\zeta(z)| \to \infty$. However, the minimal choice might provide additional stability. For $|z| \geq M$, $\mathbf{t}(z, \zeta(z))$ is set to zero, and so its inverse Fourier transform is smooth. Note the choice of M should depend on the noise level of the observation $Y = \Lambda_{\gamma_0} + \varepsilon\xi$. We summarize the method as follows.

Method 1 *Truncated CGO reconstruction in three dimensions*

Step 1$^\varepsilon$ *Let $M = M(\varepsilon) > 0$ be determined by a sufficiently small ε. For each fixed z with $|z| < M$, take $\zeta(z) \in \mathcal{V}_z$ with an appropriate size determined by M and solve the boundary integral equation (see* (15) *[KR22b]) to recover $\psi^\varepsilon_\zeta|_{\partial\mathcal{O}}$. Compute the truncated scattering transform by*

$$\mathbf{t}^\varepsilon_{M(\varepsilon)}(z, \zeta(z)) := \begin{cases} \int_{\partial\mathcal{O}} e^{-ix\cdot(z+\zeta(z))}(Y - \Lambda_1)\psi^\varepsilon_\zeta(x)d\sigma(x), & |z| < M(\varepsilon), \\ 0, & |z| \geq M(\varepsilon), \end{cases}$$

Step 2$^\varepsilon$ *Set $\widehat{q_\varepsilon}(z) := \mathbf{t}^\varepsilon_{M(\varepsilon)}(z, \zeta(z))$ and compute the inverse Fourier transform to obtain q_ε.*

Step 3$^\varepsilon$ *Solve the boundary value problem*

$$\begin{aligned} (-\Delta + q_\varepsilon)(\gamma_\varepsilon)^{1/2} &= 0 \qquad \text{in } \mathcal{O}, \\ (\gamma_\varepsilon)^{1/2} &= 1 \qquad \text{on } \partial\mathcal{O}. \end{aligned} \tag{2.7}$$

and extract γ_ε.

The boundary integral equation for unperturbed an unperturbed observation is of the form

$$B_\zeta(\psi_\zeta) = e^{ix\cdot\zeta}|_{\partial\mathcal{O}},$$

for a bounded operator $B_\zeta : H^{1/2}(\partial\mathcal{O}) \to H^{1/2}(\partial\mathcal{O})$ in which $\mathcal{G}(\gamma_0) = \Lambda_{\gamma_0}$ enters. When $\varepsilon > 0$ this becomes B^ε_ζ. A number of results in Paper A center around the existence and uniqueness of solutions to equations with B^ε_ζ. Using these we show that Method 1 gives rise to an admissible regularization strategy in the sense of Definition 2.1, where the regularization parameter is M^{-1}. To satisfy the definition, technical modifications are made to Method 1 so that it defines a map $\mathcal{R}_\alpha$ on $\mathcal{Y}$ and not just an ε-neighborhood of $\mathcal{G}(\mathcal{A})$ for sufficiently small $\varepsilon > 0$.

2.2.1 Main result

The main theorem of PAPER A is the following.

THEOREM 2.2 (THEOREM 1.1 IN [KR22B]) *Suppose $\mathcal{A}$ is the set of γ in $C^2(\overline{\mathcal{O}})$ such that $\|\gamma\|_{C^2(\overline{\mathcal{O}})} \leq M$, $\gamma \geq M^{-1}$ and $\gamma(x) \equiv 1$ for $\operatorname{dist}(x, \partial\mathcal{O}) < m$ for some $M, m > 0$. Then there exists $\varepsilon_0 > 0$, dependent only on M and m such that the family $\mathcal{R}_\alpha$ defined by (30) in [KR22b] ($\mathcal{R}_{\alpha(\varepsilon)} Y := \gamma_{\alpha,\varepsilon}$ as defined by Method 1 for $0 < \varepsilon < \varepsilon_0$ and $M(\varepsilon) = \alpha(\varepsilon)^{-1}$) is an admissible regularization strategy with the following choice of regularization parameter:*

$$\alpha(\varepsilon) = \begin{cases} (-1/11 \log(\varepsilon))^{-1/p} & \text{for } 0 < \varepsilon < \varepsilon_0, \\ \frac{\varepsilon}{\varepsilon_0}(-1/11 \log(\varepsilon_0))^{-1/p} & \text{for } \varepsilon \geq \varepsilon_0, \end{cases}$$

with $p > 3/2$.

This theoretical result is derived from a number of steps, which we give an overview of here:

1. The unperturbed boundary integral equation $B_\zeta(\psi_\zeta) = e^{ix\cdot\zeta}$ is uniquely solvable for $|\zeta|$ large enough depending on γ_0, i.e. for $|\zeta| > D_{\gamma_0}$.
2. In this regime, we conclude that B_ζ^{-1} is bounded: an upper bound on its operator norm grows exponentially in $|\zeta|$.
3. A Neumann series argument concludes that also B_ζ^ε has a bounded inverse for ε small enough.
4. If $|\zeta| = -\frac{1}{11}\log(\varepsilon)$, eventually $|\zeta| > D_{\gamma_0}$ for ε small enough. In this case, the distance between the solutions $\psi_\zeta^\varepsilon|_{\partial\mathcal{O}}$ are bounded by a term of order ε^k for some $k > 0$.
5. The triangle inequality implies

   $$|\mathbf{t}^\varepsilon_{M(\varepsilon)}(z, \zeta(z)) - \hat{q}_0(z)| \leq |\mathbf{t}^\varepsilon_{M(\varepsilon)}(z, \zeta(z)) - \mathbf{t}(z, \zeta(z))| + |\mathbf{t}(z, \zeta(z)) - \hat{q}_0(z)|,$$

   where the first term is shown to be of order ε^k for some $k > 0$ using the previous step and the second term is bounded by $|\zeta|^{-1}$ by (2.6).
6. Then also $\|\mathbf{t}^\varepsilon_{M(\varepsilon)} - \hat{q}_0\|_{L^2(\mathbb{R}^3)}$ goes to zero, when $\varepsilon \to 0$, if $|\zeta| = M^p$ for $p > 3/2$.
7. Continuity of the inverse Fourier transform on $L^2(\mathbb{R}^3)$ and stability of the elliptic boundary value problem (2.7) implies that $\gamma_{\alpha,\varepsilon} \to \gamma_0$ in $L^\infty(\mathcal{O})$.

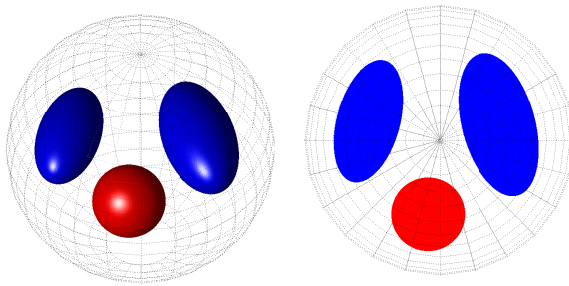

Figure 2.2: Figure 1 in [KR22b]. The piecewise constant heart-lungs phantom in a three-dimensional view (left image), and in the planar cross section $x^3 = 0$ (right image). The conductive ball has conductvity 2, while the resistive ellipsoids have conductivity 0.5

2.2.2 Numerical results

The numerical implementation of Method 1 is largely due to [DHK12, DK14] and can be found on GitHub [DKRH22]. We reconstruct the conductivity from noisy simulated data arising from two different piecewise constant phantoms. One is the heart-lungs phantom considered in [KR22b], see Figure 2.2, the other is a hemorrhagic stroke phantom considered in [KR22a], see Figure 2.3. The method performs well on data from piecewise constant phantoms, despite the missing theoretical foundation.

In Figure 2.4, we see regularized reconstructions for noisy simulated data from the heart-lungs phantom corresponding to approximately 0.1% relative noise ($\varepsilon = 10^{-3}$), 0.01% relative noise ($\varepsilon = 10^{-4}$), 0.001% relative noise ($\varepsilon = 10^{-5}$) and 0.0001% relative noise ($\varepsilon = 10^{-6}$) each for a handpicked choice of M. We clearly see the convergence of the regularized reconstructions to the ground truth as the noise level decreases and the truncation radius increases.

In Figure 2.5, on the other hand, we see regularized reconstructions for noisy simulated data from the hemorrhagic stroke phantom corresponding to 0.1% relative noise. The only parameter that changes between the plots is the truncation radius, which we vary from 7 to 9.25 in steps of 0.25. Also here we see the regularizing effect of the choice of truncation radius.

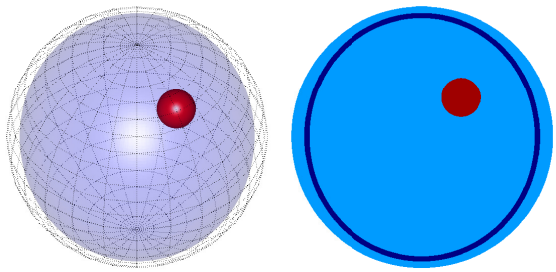

Figure 2.3: The piecewise constant hemorraghic stroke phantom in a three-dimensional view (left image), and in the planar cross section $x^3 = 0$ (right image). The conductive ball has conductvity 3, while the resistive ellipsoidal shell has conductivity 0.2

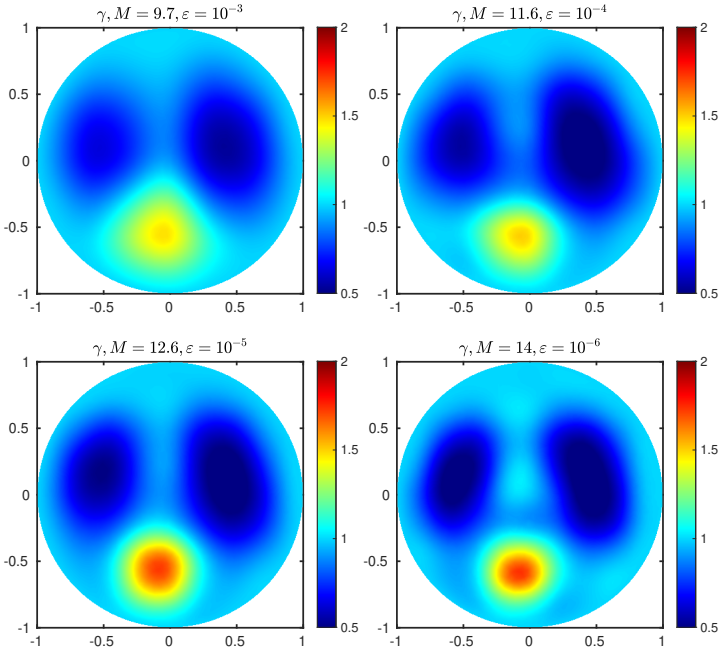

Figure 2.4: Figure 3 in [KR22b]. Cross sections ($x^3 = 0$) of reconstructions using the regularized reconstruction algorithm on noisy Dirichlet-to-Neumann maps. $|\zeta| = \frac{1}{3\sqrt{2}} M^{3/2}$

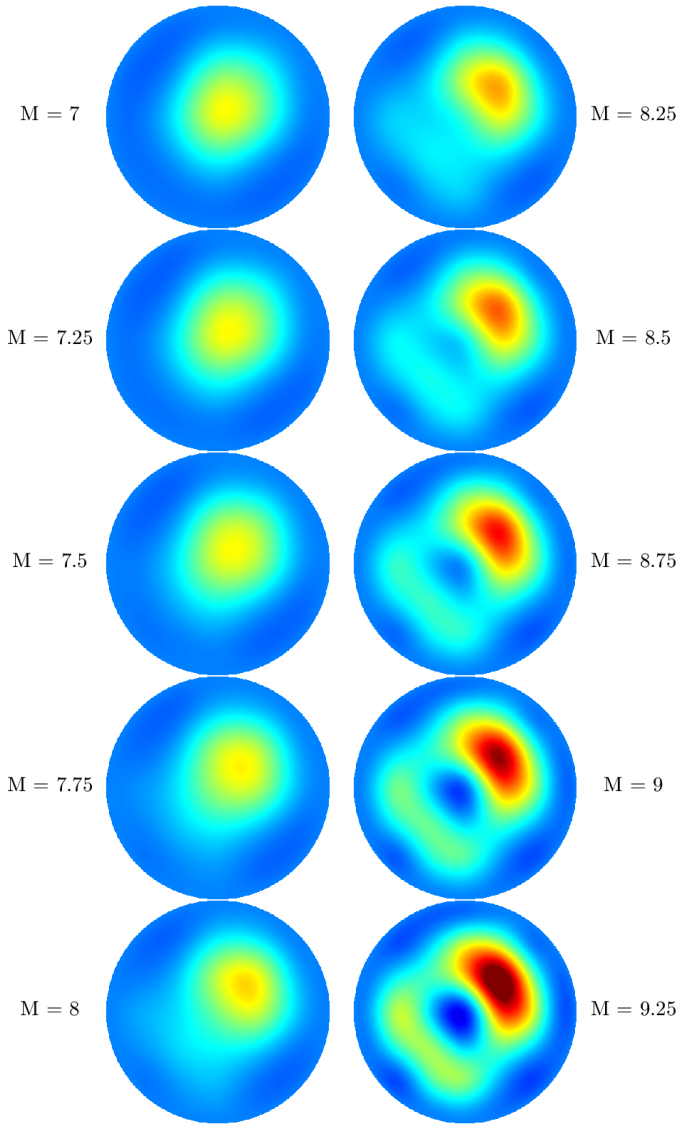

Figure 2.5: Regularized reconstructions of noisy data for the hemorrhagic stroke phantom corresponding to 0.1% relative noise. The truncation radius M varies from 7 to 9.25 in steps of 0.25 and $|\zeta(z)|$ is chosen minimally.

2.2.3 Discussion and outlook

Regularization by truncating high-frequency information is common and related to the truncated singular value decomposition in which one truncates the sum (2.2) and sets $\alpha = 0$. The idea of truncating the scattering transform appears in [KLMS09] in the context of the related two-dimensional D-bar method. Here, boundedness of B_ζ follows in much the same way as in [KLMS09]. However, there are fundamental differences to the two-dimensional reconstruction method: there the admissible set $\mathcal{V}_z \subset \mathbb{C}^2$ for $z \in \mathbb{R}^2$, reduces to a set of two points: $\{-1/2(z+iz^\perp), -1/2(z-iz^\perp)\}$, where $z^\perp \in \mathbb{R}^2$ satisfies $z^\perp \cdot z = 0$ and $|z^\perp| = |z|$. So one does not have the degrees of freedom to approximate $\hat{q}(z)$ for small $|z|$ by taking $|\zeta(z)|$ large. Instead, $\mathbf{t}$ enters in the D-bar equation, where also the small frequency information is utilized, see [KLMS09]. This is viable in two dimensions, since the boundary integral equation have shown to be solvable for all $\zeta \in \mathbb{C}^2 \setminus \{0\}$ with $\zeta \cdot \zeta = 0$, [Nac96]. In dimensions higher than two, this has only been shown for $|\zeta|$ large enough, or when γ is small and close to a constant [CKS06]. So a goal of Paper A is really to ensure $|\zeta|$ can be taken large enough.

Important new steps involves investigating the reconstruction method for real data. This is related to [IMNS04] for the two-dimensional D-bar method and [HIK$^+$21, HMI$^+$22] for the three-dimensional so-called $\mathbf{t}^{\text{exp}}$ approximation. An interesting new direction includes extending the truncation of the scattering transform using prior information, see [AM16] for an approach for the two-dimensional D-bar method. In the case of the case of stroke detection, the introduction of a highly resistive skull hampers the ability of the method [KR22a]. We expect this method could benefit from adding a resistive skull as prior information.

Chapter 3

A Bayesian story in finite dimensions

In this chapter, we motivate many of the key findings in the Bayesian approach to inverse problems in infinite-dimensional spaces by considering the finite dimensional case. That is, we let $\mathcal{X} = \mathbb{R}^k$ and $\mathcal{Y} = \mathbb{R}^m$. We consider observing Y that is a perturbation of $\mathcal{G}(\gamma_0)$ by *random* noise, i.e.

$$Y = \mathcal{G}(\gamma) + \varepsilon\xi, \tag{3.1}$$

where $\gamma = \gamma_0 \in \Gamma \subset \mathbb{R}^k$, $\xi \sim N(0, I)$ and $I : \mathbb{R}^m \to \mathbb{R}^m$ is the identity covariance. We still call $\varepsilon > 0$ the noise level, but to study its effect when it decreases in a countable way, we let $\varepsilon = \varepsilon_n := \sigma/\sqrt{n}$ for $n \in \mathbb{N}$ and some $\sigma > 0$.

The Bayesian approach to inverse problem as advocated for in [KKSV00] centers around a posterior distribution in $\mathbb{R}^k$. This is a conditional probability distribution that involves the *likelihood* function and a *prior* distribution in the famous Bayes' rule

$$\text{posterior} \propto \text{likelihood} \times \text{prior}.$$

Whereas the likelihood function is specified through the measurement process, that is, through our knowledge of the forward map and the noise, the prior distribution models our information on γ_0 *prior* to performing measurements. In this chapter and the next, we will see that the prior often plays the role of regularization in the Bayesian framework.

In the following sections we will underpin the usefulness of the posterior distribution in different settings. We shall see how, much akin to Definition 2.1 of an admissible regularization strategy, the posterior distribution gives rise to a method (the mean of the posterior) that is both continuous and consistent. We do this under the *frequentist* assumption that there is a true parameter $\gamma_0 \in \Gamma$ that gives rise to observed data. We refer to [GvdV17, Chapter 6] for a discussion on the justification of such studies for dogmatic Bayesians.

3.1 The posterior distribution

The posterior distribution is often regarded as *the* solution to an inverse problem in the Bayesian approach. To obtain this probability distribution, we consider the likelihood function arising from (3.1) with γ_0 replaced by some $\gamma \in \Gamma$, where Γ is a Borel subset of $\mathbb{R}^k$ endowed with its Borel σ-algebra $\mathcal{B}(\Gamma)$. Indeed, then $Y \sim N(\mathcal{G}(\gamma), \varepsilon^2 I)$ is a Gaussian random vector in $\mathbb{R}^m$ with density

$$p_n^\gamma(y) := C(\varepsilon_n) \exp\left(-\frac{1}{2\varepsilon_n^2}\|\mathcal{G}(\gamma) - y\|^2\right), \tag{3.2}$$

where $C(\varepsilon_n) = 1/\sqrt{2\pi\varepsilon_n^2}$ is a constant we will not keep track of, and $\|\cdot\|$ is used to denote the Euclidean norm of both $\mathbb{R}^k$ and $\mathbb{R}^m$. We refer to $\gamma \mapsto p_n^\gamma(y)$ as the *likelihood* function and denote the corresponding measure P_n^γ. Given a prior distribution Π in Γ with density π we can construct the *joint* probability density of γ and Y by

$$\pi(\gamma, y) = p_n^\gamma(y)\pi(\gamma),$$

which indeed is a probability density if $(\gamma, y) \mapsto p_n^\gamma(y)$ is jointly measurable, see [Pol02, Theorem 20, Chapter 4]. This is the case, since $\mathcal{G}$ is continuous, see [AB06, Lemma 4.5.1]. The *marginal* density of Y is

$$p_n(y) = \int_\Gamma \pi(\gamma, y)\, d\gamma, \tag{3.3}$$

which satisfies $p_n(y) \leq C(\varepsilon_n)$ by (3.2). Then, Bayes' rule gives the posterior density as a conditional density of γ given $Y = y$, by dividing the marginal density into the joint density:

$$\pi_y(\gamma) = \frac{p_n^\gamma(y)\pi(\gamma)}{p_n(y)}. \tag{3.4}$$

The corresponding conditional distribution, the posterior, then takes the form

$$\Pi(B|y) = \int_B \pi_y(\gamma)\, d\gamma, \quad \forall B \in \mathcal{B}(\Gamma). \tag{3.5}$$

When we write $Y = y$ we mean that we have observed a realization $Y(\omega) = y$ for some $\omega \in \Omega$, and we denote by $\Pi(B|Y)$ the map $\omega \mapsto \Pi(B|Y(\omega))$, which we also call a posterior. The denominator in (3.4) ensures that $\pi_y(\gamma)$ is indeed a probability density that integrates to 1. Practitioners are often not careful when dividing by this quantity, in fact, it is often not needed: For all $\gamma \in \mathbb{R}^k$ and $y \in \mathbb{R}^m$, note that $0 < p_n^\gamma(y) \leq C(\varepsilon_n)$, and so $0 < p_n(y) \leq C(\varepsilon_n)$. Since $z \mapsto 1/z$ is continuous for $z > 0$, in fact $y \mapsto p_n(y)^{-1}$ is measurable and hence $(\gamma, y) \mapsto \pi_y(\gamma)$ is jointly measurable. It follows that $y \mapsto \Pi(B|y)$ is measurable.

In the more general case, where $p_n^\gamma(y)$ takes a different form, we can still ensure a well-defined posterior by the following argument, which we record for future use. Note that the marginal probability of $\{y : p_n(y) = 0\} =: C$ is zero, i.e.,

$$\int_C p_n(y)\, dy = 0.$$

This also means that $\pi_y(\gamma)$ is a well-defined conditional density for almost all y, see [Pol02, Theorem 12, Chapter 5]. We can avoid definitional problems by setting $\pi_y(\gamma) = 0$, when y is such that $p_n(y) = 0$. This is a general trick by 'arbitrary extension' that makes $(\gamma, y) \mapsto \pi_y(\gamma)$ well-defined everywhere and jointly measurable, see Section E.2.1. Then also $y \mapsto \Pi(B|y)$ is measurable for all $B \in \mathcal{B}(\mathbb{R}^k)$, see again [Pol02, Theorem 20, Chapter 4]. [GvdV17, Section 1.3] states that there exists a *regular* version $\tilde{\Pi}(\cdot|Y)$ of the distribution (3.5), i.e.,

1. $\omega \mapsto \tilde{\Pi}(B|Y(\omega))$ is measurable for all $B \in \mathcal{B}(\Gamma)$,
2. $B \mapsto \tilde{\Pi}(B|Y(\omega))$ is a probability measure for all $\omega \in \Omega$, and
3. $\Pr(\tilde{\Pi}(B|Y) = \Pi(B|Y)) = 1$ for all $B \in \mathcal{B}(\Gamma)$.

Then one often talk of *the* posterior $\tilde{\Pi}(\cdot|Y)$ and denote it by $\Pi(\cdot|Y)$. We go to this level of detail, since we want to make precise statements about the posterior: by the second point in the above list, every realization of data gives rise to a probability measure in Γ. Where this measure gives mass is essential to the success of algorithms targeting it. On the other hand, the data we observe is random and our statements on $\Pi(\cdot|Y)$ should take this into account. In fact, $\omega \mapsto \Pi(B|Y(\omega))$ is a $[0, 1]$-valued random variable by the first point of the list. The statement of posterior consistency is exactly such a statement.

3.2 Posterior consistency

Posterior consistency is a statement about the mass the posterior distribution assigns neighborhoods of the ground true parameter γ_0 as the data improves.

Natural neighborhoods of γ_0 are the sets

$$U_n := \{\gamma \in \Gamma : \|\gamma - \gamma_0\| \leq C\delta_n\} \tag{3.6}$$

for some decreasing sequence $\delta_n > 0$ going to zero and some constant $C > 0$. Indeed, posterior consistency is a statement about the convergence of the posterior mass on these sets when $n \to \infty$, i.e. as the noise level goes to zero. This is called posterior consistency in the small noise limit. Alternatively, one can consider posterior consistency in a large data limit. We will return to this in Section 4.1. In any case, if the posterior is consistent at rate δ_n, the mass of the posterior is increasingly concentrated in U_n. Since $\Pi(U_n|Y)$ is a random variable, the sense of convergence must be specified. The sense which seems the most relevant in terms of results, see [GvdV17, Chapter 6] is *convergence in probability*, which we recall now.

For a decreasing sequence $t_n > 0$ going to zero and a sequence of measurable functions $f_n : \mathbb{R}^m \to \mathbb{R}$ we say that the sequence of random variables $\{f_n(Y)\}_{n=1}^{\infty}$ converges to $\upsilon \in \mathbb{R}$ in $P_n^{\gamma_0}$-probability with rate t_n as $n \to \infty$ if

$$\Pr(|f_n(Y) - \upsilon| > t_n) \to 0, \tag{3.7}$$

as $n \to \infty$, or to be precise,

$$P_n^{\gamma_0}(y \in \mathbb{R}^m : |f_n(y) - \upsilon| > t_n) \to 0,$$

as $n \to \infty$. If (3.7) is only satisfied for any arbitrary constant $t > 0$ instead of a specific sequence t_n, we say that $\{f_n(Y)\}_{n=1}^{\infty}$ converges to $\upsilon \in \mathbb{R}$ in $P_n^{\gamma_0}$-probability. Then we use the following definition of posterior consistency, see also [GvdV17, Chapter 6-9] for a general review of posterior consistency and contraction.

Definition 3.1 (Posterior consistency) We say that the posterior distribution *contracts around* or is *consistent in* γ_0 at rate δ_n if

$$\Pi(U_n|Y) \to 1 \quad \text{in } P_n^{\gamma_0}\text{-probability}, \tag{3.8}$$

If (3.8) is only satisfied for all arbitrary constants $\delta > 0$ instead of a specific sequence δ_n in (3.6), we simply say that the posterior distribution is consistent in γ_0.

In the case of a well-posed inverse problem, when $\mathcal{G}^{-1}$ is continuous in $\mathcal{G}(\gamma_0) \in \mathbb{R}^m$, then for all $\delta > 0$, there exists $r_{\delta,\gamma_0} > 0$ such that

$$\begin{gathered}\|\mathcal{G}(\gamma) - \mathcal{G}(\gamma_0)\| \leq r_{\delta,\gamma_0} \quad \text{implies} \quad \|\gamma - \gamma_0\| \leq \delta, \quad \text{i.e.} \\ \{\gamma \in \Gamma : \|\mathcal{G}(\gamma) - \mathcal{G}(\gamma_0)\| \leq r_{\delta,\gamma_0}\} \subset \{\gamma \in \Gamma : \|\gamma - \gamma_0\| \leq \delta\}, \quad \text{and,} \\ \Pi(\gamma : \|\mathcal{G}(\gamma) - \mathcal{G}(\gamma_0)\| \leq r_{\delta,\gamma_0}|Y) \leq \Pi(\gamma : \|\gamma - \gamma_0\| \leq \delta|Y).\end{gathered} \tag{3.9}$$

Then it is sufficient for (3.8) to show that

$$\Pi(\gamma : \|\mathcal{G}(\gamma) - \mathcal{G}(\gamma_0)\| \leq r|Y) \to 1 \quad \text{in } P_n^{\gamma_0}\text{-probability}, \tag{3.10}$$

for all $r > 0$. This is a central idea in the nonlinear posterior consistency theory, considered in function spaces in for example [Vol13, MNP21], since it reduces the analysis from sets of the form (3.6) to sets of the form

$$V := \{\gamma : \|\mathcal{G}(\gamma) - \mathcal{G}(\gamma_0)\| \leq r\}. \tag{3.11}$$

As we shall see, the strength of this approach is that it generalizes posterior consistency with explicit rates for many conditionally well-posed problems, i.e. when conditional stability estimates of the form (1.1) are available. When $\mathcal{G}$ is linear, the posterior is Gaussian, and this makes other approaches available, see [Stu10, Theorem 2.3-2.5]. In the finite-dimensional case, we mention also that posterior contraction often can be concluded by asymptotic Gaussianity of the posterior as is provided by the Bernstein-von-Mises theorem, see [GvdV17, Remark after Example 8.4] and [vdV98, Theorem 10.1].

We take a different approach and show (3.10) for any $r > 0$ with simple techniques. One way is to realize that $\Pr(\|\xi\| > R_n) \to 0$ as $n \to \infty$ for any arbitrarily slowly growing sequence $R_n \to \infty$, see for example the standard inequality [GN16, Theorem 3.1.9]. Then

$$\sup_{y:\|y-\mathcal{G}(\gamma_0)\| \leq \varepsilon_n R_n} \Pi(V^c|y) \to 0 \quad \text{as } n \to \infty \tag{3.12}$$

implies for any $t > 0$ that

$$\begin{aligned}
\Pr(|\Pi(V|Y) - 1| > t) &= \Pr(\Pi(V^c|Y) > t), \\
&\leq \Pr(\Pi(V^c|Y) > t, \|Y - \mathcal{G}(\gamma_0)\| \leq \varepsilon_n R_n) \\
&\quad + \Pr(\Pi(V^c|Y) > t, \|Y - \mathcal{G}(\gamma_0)\| > \varepsilon_n R_n), \\
&\leq \mathbb{1}\{\sup_{y:\|y-\mathcal{G}(\gamma_0)\| \leq \varepsilon_n R_n} \Pi(V^c|y) > t\} \\
&\quad + \Pr(\|\xi\| > R_n) \to 0,
\end{aligned}$$

as $n \to \infty$, and hence (3.10) is satisfied. The property (3.12) can be handled by upper bounding the numerator and lower bounding the denominator of the ratio (3.5), as we do in the following.

Proposition 3.2 *If $\mathcal{G}$ is continuous and $\int_{\gamma:\|\gamma-\gamma_0\| \leq l} \pi(\gamma)\, d\gamma > 0$ for all $l > 0$, then* (3.12) *is satisfied and hence* (3.10) *is satisfied. In particular, if $\mathcal{G}^{-1}$ satisfies* (3.9)*, then the posterior distribution is consistent in γ_0.*

PROOF. As preparation note $y \in \mathbb{R}^m$ that satisfy $\|y - \mathcal{G}(\gamma_0)\| \leq \varepsilon_n R_n$ can be written as $y = \mathcal{G}(\gamma_0) + \varepsilon_n e$ for some $e \in \mathbb{R}^m$ with $\|e\| \leq R_n$. Inserting this into the likelihood (3.2) yields

$$\begin{aligned} p_n^\gamma(y) &= C(\varepsilon_n) \exp\left(-\frac{1}{2\varepsilon_n^2}\|\mathcal{G}(\gamma) - y\|^2\right), \\ &= C(\varepsilon_n) \exp\left(-\frac{1}{2\varepsilon_n^2}\|\mathcal{G}(\gamma) - \mathcal{G}(\gamma_0)\|^2 + \frac{1}{\varepsilon_n}\langle \mathcal{G}(\gamma) - \mathcal{G}(\gamma_0), e\rangle - \frac{1}{2}\|e\|^2\right), \\ &= C(\varepsilon_n, e) \exp\left(-\frac{1}{2\varepsilon_n^2}\|\mathcal{G}(\gamma) - \mathcal{G}(\gamma_0)\|^2 + \frac{1}{\varepsilon_n}\langle \mathcal{G}(\gamma) - \mathcal{G}(\gamma_0), e\rangle\right). \end{aligned}$$

Note by the Cauchy-Schwartz inequality

$$|\langle \mathcal{G}(\gamma) - \mathcal{G}(\gamma_0), e\rangle| \leq \|\mathcal{G}(\gamma) - \mathcal{G}(\gamma_0)\| R_n.$$

The rest of the proof is based on upper bounding the numerator and lower bounding the denominator of the posterior ratio integrated on the set V^c. To upper bound the numerator, note for $y = \mathcal{G}(\gamma_0) + \varepsilon_n e$ and $\gamma \in V^c$ that

$$p_n^\gamma(y) \leq C(\varepsilon_n, e) \sup_{\gamma \in V^c} \exp\left(-\frac{1}{2\varepsilon_n^2}\|\mathcal{G}(\gamma) - \mathcal{G}(\gamma_0)\|^2 + \frac{1}{\varepsilon_n}\|\mathcal{G}(\gamma) - \mathcal{G}(\gamma_0)\| R_n\right),$$

where since $V^c = \{\gamma : \|\mathcal{G}(\gamma) - \mathcal{G}(\gamma_0)\| > r\}$ and $x \mapsto -1/(2\varepsilon_n^2)x^2 + 1/\varepsilon_n R_n x$ is decreasing for $x \in (\varepsilon_n R_n, \infty)$ it is convenient to set R_n such that $r > \varepsilon_n R_n$. Indeed, then $\|\mathcal{G}(\gamma) - \mathcal{G}(\gamma_0)\| = r$ upper bounds the supremum, and

$$p_n^\gamma(y) \leq C(\varepsilon_n, e) \exp\left(-\frac{r^2}{2\varepsilon_n^2} + \frac{r}{\varepsilon_n} R_n\right).$$

Then we have

$$\int_{V^c} p_\varepsilon^\gamma(y)\pi(\gamma)\, d\gamma \leq C(\varepsilon_n, e) \exp\left(-\frac{r^2}{2\varepsilon_n^2} + \frac{r}{\varepsilon_n} R_n\right), \tag{3.13}$$

since π is a probability density integrating to 1. For the lower bound of the denominator, note first that

$$\int_{\gamma : \|\mathcal{G}(\gamma) - \mathcal{G}(\gamma_0)\| \leq l} \pi(\gamma)\, d\gamma > 0$$

for all $l > 0$ by assumption and continuity of $\mathcal{G}$. Then we take a sufficiently slowly decreasing sequence $l_n > 0$ such that

$$\int_{\gamma : \|\mathcal{G}(\gamma) - \mathcal{G}(\gamma_0)\| \leq l_n} \pi(\gamma)\, d\gamma \geq \exp\left(-\frac{1}{4}\frac{r^2}{\varepsilon_n^2}\right). \tag{3.14}$$

This implies

$$\int_\Gamma p_n^\gamma(y)\pi(\gamma)\,d\gamma \geq \int_{\gamma:\|\mathcal{G}(\gamma)-\mathcal{G}(\gamma_0)\|\leq l_n} p_n^\gamma(y)\pi(\gamma)\,d\gamma,$$
$$\geq C(\varepsilon_n, e)\exp\left(-\frac{1}{4}\frac{r^2}{\varepsilon_n^2}\right)\exp\left(-\frac{1}{2\varepsilon_n^2}l_n^2 - \frac{l_n}{\varepsilon_n}R_n\right). \quad (3.15)$$

Collecting the upper bound (3.13) and the lower bound (3.15), we conclude

$$\sup_{y:\|y-\mathcal{G}(\gamma_0)\|\leq\varepsilon_n R_n} \Pi(V^c|y) \leq \exp\left(-\frac{r^2-2l_n^2}{4\varepsilon_n^2} + \frac{r+l_n}{\varepsilon_n}R_n\right) \to 0, \quad (3.16)$$

as $n\to\infty$, since $\exp(-r^2/(4\varepsilon_n^2))$ is the dominant factor, when $n\to\infty$, if we for example set $R_n \propto 1/\sqrt{\varepsilon_n}$. □

The prior condition of Proposition 3.2 is a way of saying that γ_0 is in the support of the prior distribution, see Appendix E.1. This is also a necessary condition: if $\pi(\gamma)=0$ in some neighborhood of γ_0, then the posterior distribution gives mass 0 to this neighborhood, which renders (3.8) impossible. Note that the argument in the proof above is similar to that of [Vol13, Theorem 3.3]. Here, the proof is made so that it is straightforward to extend to an explicit contraction rate. In this case one would replace r with a decreasing sequence $r_n > 0$ satisfying $r_n^2/\varepsilon_n^2 \to 0$. In this case, a stronger condition on the prior is needed: instead of (3.14), it should satisfy

$$\int_{\gamma:\|\mathcal{G}(\gamma)-\mathcal{G}(\gamma_0)\|\leq r_n} \pi(\gamma)\,d\gamma \geq \exp\left(-C\frac{r_n^2}{\varepsilon_n^2}\right), \quad (3.17)$$

for some constant $C>0$. This causes $\exp(-Cr_n^2/\varepsilon_n^2)$ to be the dominant rate of the denominator for some new constant $C>0$, and not something that decays faster. This is often called a 'small ball' condition, and showing this often involves requiring Hölder continuity of $\mathcal{G}$. Going to an infinite-dimensional Hilbert space $\mathcal{Y}$, one can use similar arguments to those above by finding sets S_n such that $\Pr(\xi\in S_n)\to 1$ as $n\to\infty$. In this case $\xi\sim N(0,I)$ needs an interpretation. This approach is used in [Vol13, Theorem 3.3] for 'smooth' noise ξ, and where the contraction rate is dependent on the level of smoothness.

Example 3.1 (Spherical anomaly) *Let $\gamma_0=(r_0,z_0)=(100,1000)$ and π be the prior density arising as the probability density of the random variable*

$$\gamma = (1,1)+\exp(\theta), \quad \theta\sim N\left(\begin{bmatrix}4\\8\end{bmatrix}, \begin{bmatrix}1&0\\0&4\end{bmatrix}\right) =: \Pi_\theta$$

Clearly, there exists $\theta_0\in\mathbb{R}^2$ such that $\Phi(\theta_0) := (1,1)+\exp(\theta_0)=\gamma_0$. Now denote $B(\theta_0,j) := \{\theta\in\mathbb{R}^2 : \|\theta-\theta_0\|\leq j\}$. Since the probability density π_θ

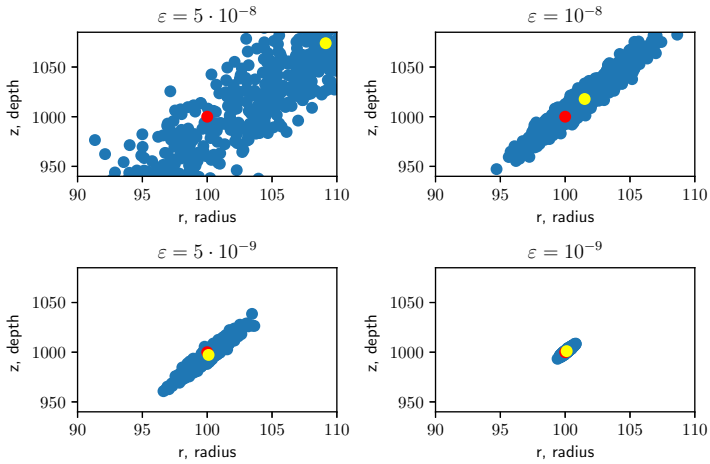

Figure 3.1: Plot of samples from $\Pi(\cdot|y)$ arising for the spherical anomaly inverse problem for four realizations y corresponding to $\varepsilon = 5 \cdot 10^{-8}$, $\varepsilon = 10^{-8}$, $\varepsilon = 5 \cdot 10^{-9}$ and $\varepsilon = 10^{-9}$. These realizations corresponds to approximately 6.93%, 0.87%, 0.72% and 0.06% relative noise. The red dot marks γ_0, whereas the yellow dot marks the sample mean.

corresponding to Π_θ *satisfies* $\pi_\theta(\theta_0) > 0$*, we have that* $\int_{B(\theta_0,j)} \pi_\theta(\theta)\, d\theta > 0$ *for all* $j > 0$*. By continuity of* Φ*, we have for all* $l > 0$

$$\{\theta : \|\Phi(\theta) - \Phi(\theta_0)\| \leq l\} \supset B(\theta_0, j_{l,\theta_0}),$$

for some $j_{l,\theta_0} > 0$*, and hence*

$$\Pr(\gamma \in B(\gamma_0, l)) = \Pr(\theta \in \Phi^{-1}[B(\gamma_0, l)]) \geq \Pr(\theta \in B(\theta_0, j_{l,\theta_0})) > 0,$$

which is to say that the prior condition of Proposition 3.2 is satisfied. Then the corresponding posterior distribution (3.5) *is consistent in* γ_0*. In Figure* (3.1) *this property is demonstrated numerically using the* PYTHON *package* CUQIPY*, see [RAU+23]. Samples from the posterior are computed using an out-of-the-box Metropolis-Hastings sampler implemented in* CUQIPY *as* `MH`*. Note more and more of the samples are contained in a neighborhood of* γ_0*. Not surprisingly radius and depth are correlated variables.*

In Example 3.1 we used the exponential function to construct a prior whose mass is contained in $[1, \infty) \times [1, \infty)$. Such transformations of priors can be useful in guiding the mass to where the user want it to be. Note that the continuity of this transform is essential in satisfying the prior condition, which is key to

controlling the posterior denominator. For an explicit contraction rate, Hölder continuity is sufficient to satisfy (3.17). This is an important point in PAPER B in Section 4.2. In Figure 3.1, we also note that the sample mean seems to converge to γ_0 as $n \to \infty$.

3.3 Computations and convergence of the mean

Results like Proposition 3.2 indicate the usefulness of the posterior distribution in inferring γ_0 in an abstract way. One way to construct concrete methods from the posterior distribution is to consider point estimators, see [KS05]. We will focus on estimators of γ_0. Here, an estimator of γ_0 is any Borel measurable map $\hat{\gamma} : \mathcal{Y} \to \Gamma$. One such popular estimator of γ_0 is the *maximum a posteriori* (MAP) estimator defined by

$$\gamma_{\mathrm{MAP}}(y) := \arg\max_{\gamma \in \Gamma} \pi_y(\gamma).$$

As remarked after Definition 2.1, definitional problems can arise when $\mathcal{G}$ is not linear as in this case the maximization problem does not have a unique solution in general. However, note $(\gamma, y) \mapsto \pi_y(\gamma)$ is continuous in its first argument for all $y \in \mathcal{Y}$ when $\pi(y)$ is continuous, and measurable in its second argument for all $\gamma \in \Gamma$. Then, if Γ is a compact metric space, there exists a Borel measurable function $\gamma_{\mathrm{MAP}} : \mathcal{Y} \to \mathcal{X}$ such that

$$\pi_y(\gamma_{\mathrm{MAP}}(y)) = \max_{\gamma \in \Gamma} \pi_y(\gamma),$$

see [GN16, Exercise 7.2.3]. For a Gaussian prior $\pi(\gamma) \propto \exp(-1/(2\sigma^2)\|\gamma\|^2)$, we have

$$\begin{aligned}
\gamma_{\mathrm{MAP}}(y) &= \arg\max_{\gamma \in \Gamma} p_n^{\gamma}(y)\pi(\gamma), \\
&= \arg\max_{\gamma \in \Gamma} \exp\left(-\frac{1}{2\varepsilon^2}\|\mathcal{G}(\gamma) - y\|^2 - \frac{1}{2\sigma^2}\|\gamma\|^2\right), \\
&= \arg\min_{\gamma \in \Gamma} \left(\|\mathcal{G}(\gamma) - y\|^2 + \frac{\varepsilon^2}{\sigma^2}\|\gamma\|^2\right), \qquad (3.18)
\end{aligned}$$

which is exactly the Tikhonov regularizer of (2.1) with regularization parameter $\alpha = \varepsilon^2/\sigma^2$. This relation has been noted in many works including [KS05]. We also note that the choice of prior decides the penalization term in (3.18), and hence we can see the MAP estimator is a systematic approach to generalized Tikhonov regularization. But this is just one popular estimator, which incidentally faces the issue of non-convex optimization. Consistency can still

be guaranteed theoretically under certain assumptions of $\mathcal{G}$, see [NvdGW20]. Note there are several contributions in consistency of Tikhonov regularizers for random noise both for linear [KLS14] and nonlinear [BHM04] forward maps, see also the references therein.

Another popular estimator is the *posterior* or *conditional mean*

$$E[\gamma|y] = \int_\Gamma \gamma \pi_y(\gamma)\, d\gamma = \int_\Gamma \gamma\, \Pi(d\gamma|y),$$

which is well-defined and measurable in y, when γ is integrable, see Section E.2.2. The posterior mean is integration based and generally computable via *Markov chain Monte Carlo* (MCMC) methods. For independent samples γ_i of the posterior distribution, the averages

$$\bar{\gamma}_N = \frac{1}{N}\sum_{i=1}^{N} \gamma_i$$

converges almost surely to $E[\gamma|y]$ as $N \to \infty$ by the strong law of large numbers [RC04]. If γ is also square integrable, the root mean square error of $\bar{\gamma}_N$ decays to zero as $N^{-1/2}$. As slow as this rate seems, it does not depend on the dimension k and hence even for high-dimensional problems the mean is computable. The trick is then to form a Markov chain whose invariant distribution is the posterior distribution. We refer to the well-known Metropolis-Hastings methods [MRR$^+$53, Has70], among which preconditioned Crank-Nicolson [CRSW13] is a well-performing example, as well as to more general MCMC methods in [RC04, RR04]. Common for these methods is the fact that evaluating $\pi_y(\gamma)$ and/or its gradient up to a constant in γ is sufficient, and hence the denominator in (3.4) is of little importance. Of course these methods are not limited to the posterior mean; any integration based statistic of the form $\int_\Gamma f(\gamma)\, \Pi(d\gamma|y)$ can be approximated in this way.

A second benefit of the posterior mean is that it inherits the convergence properties of the posterior distribution under mild conditions on the prior distribution, see [GvdV17, Theorem 6.8] or [Nic23, Theorem 2.3.2].

Proposition 3.3 *If the assumptions of Proposition 3.2 are satisfied and further if*

$$\int_\Gamma \|\gamma - \gamma_0\| \pi(\gamma)\, d\gamma < \infty, \tag{3.19}$$

then $\|E[\gamma|Y] - \gamma_0\| \to 0$ *in* $P_n^{\gamma_0}$*-probability as* $n \to \infty$.

Proof. We wish to show that for all $t > 0$

$$\Pr(\|E[\gamma|Y] - \gamma_0\| > t) \to 0, \tag{3.20}$$

as $n \to \infty$. By Jensen's inequality for all $y \in \mathcal{Y}$ we have that

$$\|E[\gamma|y] - \gamma_0\| \leq E[\|\gamma - \gamma_0\||y] = \int_\Gamma \|\gamma - \gamma_0\| \pi_y(\gamma)\, d\gamma.$$

Decomposing this integral into $U = \{\gamma : \|\gamma - \gamma_0\| \leq \delta\}$ and U^c for $\delta = t/2$, we find

$$\begin{aligned}\|E[\gamma|y] - \gamma_0\| &\leq \int_U \|\gamma - \gamma_0\| \pi_y(\gamma)\, d\gamma + \int_{U^c} \|\gamma - \gamma_0\| \pi_y(\gamma)\, d\gamma, \\ &\leq t/2 + \int_{U^c} \|\gamma - \gamma_0\| \pi_y(\gamma)\, d\gamma. \end{aligned} \tag{3.21}$$

By (3.9), the property that $\int_{V^c} \|\gamma - \gamma_0\| \pi_y(\gamma)\, d\gamma \to 0$ in $P_n^{\gamma_0}$-probability as $n \to \infty$ for any $r > 0$ implies that the last integral of (3.21) converges to zero in $P_n^{\gamma_0}$-probability as $n \to \infty$, which is enough to conclude (3.20). Following the logic after (3.12), it is sufficient to show that

$$\sup_{y : \|y - \mathcal{G}(\gamma_0)\| \leq \varepsilon_n R_n} \int_{V^c} \|\gamma - \gamma_0\| \pi_y(\gamma)\, d\gamma \to 0,$$

as $n \to \infty$. Copying the argument in the proof of Proposition 3.2, we find that (3.16) is changed to

$$\begin{aligned}\sup_{y : \|y - \mathcal{G}(\gamma_0)\| \leq \varepsilon_n R_n} &\int_{V^c} \|\gamma - \gamma_0\| \pi_y(\gamma)\, d\gamma \\ &\leq C(n) \exp(-r^2/(4\varepsilon_n^2)) \int_\Gamma \|\gamma - \gamma_0\| \pi(\gamma)\, d\gamma, \end{aligned} \tag{3.22}$$

for some large enough constant $C(n)$. This goes to zero as $n \to \infty$ by (3.19). □

Note that (3.19) is generally not a strong condition. It is trivially satisfied for any prior densities that are supported on a bounded subset of Γ, but also for example for Gaussian densities.

Example 3.2 (Spherical anomaly) *For the prior given in Example 3.1 note that*

$$\begin{aligned}\int_\Gamma \|\gamma\|\, \Pi(d\gamma) &= \int_{\mathbb{R}^2} \|\Phi(\theta)\|\, \Pi_\theta(d\theta), \\ &\leq C + C \int_{\mathbb{R}^2} (e^{\theta_1} + e^{\theta_2}) \pi_\theta(\theta)\, d\theta, \\ &\leq C + C \sum_{i=1}^{2} E[e^{e_i \theta}], \end{aligned}$$

using a change of variables and denoting $e_1 = (1, 0)$ and $e_2 = (0, 1)$. Since θ is a Gaussian vector, $e_i\theta$ is a Gaussian random variable and hence the term above is a sum of the moment generating functions of Gaussian random variables, which is finite. It follows from Proposition 3.3 that $\|E[\gamma|Y] - \gamma_0\| \to 0$ in $P_n^{\gamma_0}$-probability as $n \to \infty$. This behavior can be seen numerically in Figure 3.1

3.4 Well-posedness

For a successful algorithm we should not only be concerned with consistency, but also continuity as in the definition of an admissible regularization strategy, Definition 2.1. Results of this kind have been considered in [DS17, Stu10] under the term *well-posedness*. This is of course a reference to Hadamard: the posterior exists, is unique (up to null sets of the marginal distribution of Y), and turns out to be continuous in a suitable sense. This continuity quantifies the effect of changes in y on the posterior distribution. To measure the effect most commonly the Hellinger distance is used. This is defined as

$$d_H(\pi_y, \pi_{y'}) = \left(\frac{1}{2} \int_\Gamma \left[\sqrt{\pi_y} - \sqrt{\pi_{y'}} \right]^2 \right)^{1/2}.$$

One can also define this distance between measures, in which case the Lebesgue densities are replaced by densities with respect to a common reference measure, see [DS17]. Then well-posedness of the posterior is a result like the following.

Proposition 3.4 *Assume $\int_\Gamma \|\mathcal{G}(\gamma)\|^2 \pi(\gamma)\, d\gamma < \infty$. Then there exists a constant $C = C(R) > 0$ such that for all $y, y' \in \mathcal{Y}$ with $\|y\|, \|y\| \le R$*

$$d_H(\pi_y, \pi_{y'}) \le C\|y - y'\|.$$

Proof. This is due to [DS17, Theorem 16], which is straightforward to apply. Indeed, let $\varepsilon = \varepsilon_n$ and note $(\gamma, y) \mapsto \ell(\gamma, y) := 1/(2\varepsilon^2)\|\mathcal{G}(\gamma) - y\|^2$ is continuous, since $\gamma \mapsto \mathcal{G}(\gamma)$ is continuous. Furthermore, using the Cauchy-Schwarz inequality

$$\begin{aligned} |\ell(\gamma, y) - \ell(\gamma, y')| &= 1/(2\varepsilon^2)|\langle 2\mathcal{G}(\gamma) - y - y', y' - y\rangle|, \\ &\le \varepsilon^{-2}(\|\mathcal{G}(\gamma)\| + R)\|y - y'\|. \end{aligned}$$

Then the assumption of the proposition implies

$$\int_\Gamma 1 + [\varepsilon^{-2}(\|\mathcal{G}(\gamma)\| + R)]^2 \pi(\gamma)\, d\gamma < \infty,$$

which shows that the conditions of Theorem 16 in [DS17] are satisfied. □

Other metrics have been considered as well, see for example [Lat20]. Convenient for the Hellinger distance is the following result. Lemma 21 in [DS17] states that

$$\|E[\gamma|y] - E[\gamma|y']\| \leq 2\left(\int_\Gamma \|\gamma\|^2 \,\Pi(d\gamma|y) + \int_\Gamma \|\gamma\|^2 \,\Pi(d\gamma|y')\right)^{1/2} d_H(\pi_y, \pi_{y'}).$$

When $\|y\| \leq R$ we can upper bound $\int_\Gamma \|\gamma\|^2 \,\Pi(d\gamma|y)$ if $\int_\Gamma \|\gamma\|^2 \,\Pi(d\gamma) < \infty$. This is a consequence of a lower bound of $p_n(y)$ in Proposition E.1, which we have already seen in some variant of in the proof of Proposition 3.2. As mentioned earlier, this condition is satisfied for many reasonable priors including Gaussian priors. If also the assumption of Proposition (3.4) is satisfied, then the posterior mean is locally Lipschitz with respect to y.

Example 3.3 (Spherical anomaly) *For $\gamma = (r, z)$ satisfying $r, z > m$ it is clear from* (1.8) *that*

$$\|\mathcal{G}(\gamma)\|^2 \leq g(0)^2 + g(100)^2 \leq C(m) r^6 \leq C(m)\|\gamma\|^6$$

Since $\pi(\gamma) = 0$ for all $\gamma = (r, z)$ satisfying $r, z < 1$, we have

$$\int_\Gamma \|\mathcal{G}(\gamma)\|^2 \pi(\gamma)\, d\gamma \leq C \int_\Gamma \|\gamma\|^6 \pi(\gamma)\, d\gamma,$$

which is finite using the same argument as in Example 3.2. Then Proposition 3.4 applies to the effect that $y \mapsto E[\gamma|y]$ is locally Lipschitz continuous.

Forward maps that arise in inverse problems for PDEs naturally satisfy a condition like $\|\mathcal{G}(\gamma)\| \leq C(1 + \|\gamma\|)$ typically for a subset of Γ in which the prior should concentrate. Well-posedness is considered in infinite-dimensional Hilbert spaces in [DS17, Stu10] and here enters an additional benefit: well-posedness guarentees robustness of the posterior distribution to finite-dimensional approximations of the likelihood function.

To make a connection with the usual definition of admissible regularization strategies, Definition 2.1, we consider the map $y \mapsto E_\alpha[\gamma|y] = E[\gamma|y]$ indexed by $\alpha = \varepsilon_n$ appearing in the likelihood function. For y that are not realizations of (3.1), we may still use this map. Of admissible regularization strategies we required three things: continuity, approximation of $\mathcal{G}^{-1}$ and consistency.

As we noted in the previous setting $y \mapsto E[\gamma|y]$ is often continuous. Moreover, under the conditions of Proposition 3.2 and 3.3 and for a fixed γ_0 in the support

of the prior which gives rise to Y, $E[\gamma|Y]$ is a consistent estimator. We can see this as a modification of (2.4) to allow random perturbations. Finally, the condition that $y \mapsto E[\gamma|y]$ approximates $\mathcal{G}^{-1}$ in the sense of (2.3) follows in much the same way as the consistency condition, in fact, it is easier. Under the conditions of Proposition 3.2 and 3.3, equation (3.16) and continuity of $\mathcal{G}^{-1}$ implies for all $\delta > 0$

$$\Pi(\gamma : \|\gamma - \gamma_0\| > \delta|\mathcal{G}(\gamma_0)) \to 0,$$

as $\alpha \to 0$. Equation (3.22) implies $\int_\Gamma \|\gamma - \gamma_0\| \pi_{\mathcal{G}(\gamma_0)}(\gamma)\, d\gamma \to 0$, as $\alpha \to 0$, and hence by (3.21)

$$\|E_\alpha[\gamma|\mathcal{G}(\gamma_0)] - \gamma_0\| \to 0,$$

as $\alpha \to 0$.

We conclude that with sufficient alteration of Definition 2.1 and under favorable conditions of the inverse problem and prior, the Bayesian approach provides an admissible regularization strategy in the form of the posterior mean. Furthermore, recent theoretical results state that the posterior mean is computable in polynomial time using gradient-based MCMC [NW22]. We have also seen that the Bayesian approach provides a MAP estimator, which can be seen as a generalized Tikhonov regularizer. These results strengthen the foundation of the Bayesian approach. Adding the versatility of different point estimates in relation to uncertainty quantification, the attractiveness of the Bayesian approach becomes clear.

Chapter 4

The Bayesian approach to inverse problems in function spaces

This chapter details some of the key elements in the Bayesian approach to inverse problems in infinite-dimensional function spaces, as is motivated in [Stu10, DS17, Nic23]. This is the case where $\mathcal{X}$ or $\mathcal{Y}$ are infinite-dimensional function spaces. The message is to discretize at the latest possible time for at least three reasons: avoid a prior that is dependent on discretization, see also [LSS09], gain mathematical insight and gain computational advantages of algorithms that are well-defined in infinite dimensions. An example of valuable mathematical insight is understanding the contribution of algorithmic parameters to the convergence of a method. It is also a first step in understanding the computational influence of the dimension in discretizations, see [NW22]. Following [Stu10] several MCMC methods have been proposed in the infinite-dimensional setting and show promise in high-dimensional discretizations, see for example [CRSW13, CLM16]. In this sense, the infinite-dimensional framework is also a step towards high-dimensional computational estimation and uncertainty quantification.

The analysis and development of methods in the infinite-dimensional Bayesian approach to inverse problems is still in its early stages, but it is a natural and necessary progression that has seen its parallel in, for example, regularization theory for inverse problems. One of the key points in this chapter is that the choice of prior is a choice of regularization. As we shall see, it is great tool for

giving weight at the subset of Γ, where ill-posed inverse problem are well-posed. The hope is that this allows reliable recovery if γ_0 is in fact in this subset. In addition, a prior distribution if often chosen for its computational performance. We shall return to this point in PAPER B in Section 4.2.

The results and logic of the previous section generalize for the most part to Banach spaces $\mathcal{X}$ and $\mathcal{Y}$, see [Stu10, DS17, Nic23]. However, the analysis is more technically demanding for a number of reasons. For example, there is no Lebesgue measure. Instead, densities (Radon-Nikodym derivatives, see also Appendix E.1) with respect to a reference measure appear. These can be harder to intuit with. Furthermore, properties of the prior distributions are harder to verify. Mostly Gaussian priors have been considered as these are well-understood, but also 'uniform' priors [Vol13] and 'Besov-type' priors have been considered, see [AW21, ADH21, DS17].

In this chapter, we consider a setting in which $\mathcal{G}^{-1}$ is not continuous on all of $\mathcal{Y}$, but instead satisfy an estimate of the form (1.1). As promised, the framework we present permits consistency in this setting in a natural way with Gaussian priors; this is largely due to [Vol13, MNP21]. We then continue by discussing the application and extension of this framework to the setting of inclusion detection for the QPAT problem initially discussed in Section 1.1.3 and the recovery of a Robin coefficient initially discussed in Section 1.1.2.

4.1 Models and posterior consistency

Two convenient observation models for which the aforementioned framework is well-developed are the *white noise* model in a small noise limit and the *random design regression* model in a large data limit. The former is the most direct generalization of the setting considered in Chapter 3. Indeed, it provides an interpretation for $\xi \sim N(0, I)$ in a separable Hilbert space and consider also the posterior as $\varepsilon_n \to 0$. However, the latter is perhaps easier to understand, since it contains elements of the finite-dimensional case. This is where we begin.

Model 1: Random design regression

Let $\Gamma \subset \mathcal{X}$ be a closed subset of a separable Banach space $\mathcal{X}$. It inherits its metric from $\mathcal{X}$ and is hence endowed with a Borel σ-algebra $\mathcal{B}(\Gamma)$. We let $\mathcal{Y} = L^2(\mathcal{V})$ for some bounded subset $\mathcal{V}$ of $\mathbb{R}^m$, $m \in \mathbb{N}$, endowed with a Borel σ-algebra $\mathcal{B}(\mathcal{V})$. The random design regression model considers observations of

the form

$$Y_i = \mathcal{G}(\gamma)(X_i) + \varepsilon\xi_i, \quad i = 1, \dots, n, \tag{4.1}$$

where $\xi_i \overset{\text{i.i.d.}}{\sim} N(0,1)$ independently of X_i that are uniformly distributed on $\mathcal{V}$. That is, $X_i \overset{\text{i.i.d.}}{\sim} \mu$, where $\mu(B) = \text{vol}(B)/\text{vol}(\mathcal{V})$ and $\text{vol}(B) = \int_B dx$ for all $B \in \mathcal{B}(\mathcal{V})$. This means we observe $\mathcal{G}(\gamma)$ in random locations at $\mathcal{V}$ and with added Gaussian noise. Unlike the observation setting of Chapter 3, the noise level $\varepsilon > 0$ is fixed. However, the number of observations n is not. The random vectors (Y_i, X_i) are identically and independently distributed, and we denote their distribution P_γ with corresponding density

$$p^\gamma(y,x) \equiv \frac{dP^\gamma}{d\nu}(y,x) = C(\varepsilon)\exp\left(-\frac{1}{2\varepsilon^2}|\mathcal{G}(\gamma)(x) - y|^2\right), \quad y \in \mathbb{R}, x \in \mathcal{V},$$

with respect to $d\nu = d\lambda \times d\mu$, where λ is the Lebesgue measure in $\mathbb{R}$, see [Nic23]. Then the joint distribution of $D_n = D := (Y_i, X_i)_{i=1}^n$ is the product measure $P^\gamma \times \ldots \times P^\gamma$ on $\mathcal{D}^n := (\mathbb{R} \times \mathcal{V})^n$. We denote this product measure P_n^γ and note it has a density p_n^γ with respect to ν^n,

$$p_n^\gamma(d) := C\exp\left(-\frac{1}{2\varepsilon^2}\sum_{i=1}^n |\mathcal{G}(\gamma)(x_i) - y_i|^2\right), \quad d = (y_i, x_i)_{i=1}^n.$$

We denote the data generating measure P_n^γ in this way, since we wish to study the posterior when Y_i, $i = 1, \dots, N$, are generated by $\gamma = \gamma_0$ and $n \to \infty$. Now assume that $\mathcal{G} : \Gamma \to C(\overline{\mathcal{V}})$ is continuous. Then $(\gamma, x) \mapsto \mathcal{G}(\gamma)(x)$ is jointly $\mathcal{B}(\Gamma) \otimes \mathcal{B}(\mathcal{V}) - \mathcal{B}(\mathbb{R})$ measurable by [AB06, Lemma 4.5.1]. Then, also $(\gamma, d) \mapsto p_n^\gamma(d)$ is jointly $\mathcal{B}(\Gamma) \otimes \mathcal{B}(\mathcal{D}^n) - \mathcal{B}(\mathbb{R})$ measurable.

Given a prior distribution Π on Γ, we form then the product measure in $\Gamma \times \mathcal{D}^n$

$$Q(A \times B) = \int_A P_n^\gamma(B)\,\Pi(d\gamma) = \int_A \int_B p_n^\gamma(y)\,\nu(dy)\,\Pi(d\gamma). \tag{4.2}$$

By Tonelli's theorem (4.2) is to say that Q has a density with respect to the product measure $\nu \times \Pi$. We can think of Q as the joint distribution of (γ, D). Consider the coordinate projection $T : (\gamma, d) \mapsto d$. The push-forward measure TQ is then the marginal distribution, the distribution of $D = T(\gamma, D)$, and Theorem 12 in [Pol02, Chapter 5] states that it has a density with respect to ν as

$$p_n(d) := \frac{dTQ}{d\nu}(d) = \int_\Gamma p_n^\gamma(d)\,\Pi(d\gamma).$$

This matches the finite-dimensional case (3.3) of the 'marginal'. The theorem also states that the joint density divided by the marginal,

$$\pi_d(\gamma) = \frac{p_n^\gamma(d)}{p_n(d)},$$

defines a probability measure $\Pi(\cdot|d)$ on Γ by

$$\Pi(A|d) := \int_A \pi_d(\gamma)\,\Pi(d\gamma), \quad A \in \mathcal{B}(\Gamma),$$

that is the conditional probability distribution of γ given $D = d$. As in Chapter 3 we will also use the notation $\Pi(\cdot|D)$ for $\omega \mapsto \Pi(\cdot|D(\omega))$. The essential condition of this version of Bayes' rule is that $(\gamma, d) \mapsto p_n^\gamma(d)$ is jointly measurable. Note that $0 \leq |y - \mathcal{G}(\gamma)(x)|^2 < \infty$ for all $(y, x) \in \mathbb{R} \times \mathcal{V}$ and $\gamma \in \Gamma$ by assumption, and hence the normalization constant satisfies

$$0 < \int_\Gamma e^{-\frac{1}{2}\sum_{i=1}^n |y_i - \mathcal{G}(\gamma)(x_i)|^2}\,\Pi(d\gamma) \leq C(\varepsilon)$$

for all $(y_i, x_i)_{i=1}^n \in \mathcal{D}^n$. It follows that $A \mapsto \Pi(A|d)$ is a measure for each $d \in (\mathbb{R} \times \mathcal{V})^n$ and that $\omega \mapsto \Pi(A|D(\omega))$ is measurable for every $A \in \mathcal{B}(\Gamma)$, as in the finite-dimensional case. In particular, $\omega \mapsto \Pi(A|D(\omega))$ is a $[0, 1]$-valued random variable.

Convenience motivates this observation model. Indeed, a main feature is the following equivalence result in [Nic23, Proposition 1.3.1]: suppose

$$\sup_{\gamma \in \Gamma'} \|\mathcal{G}(\gamma)\|_{C(\overline{\mathcal{V}})} \leq U$$

for some constant $U > 0$ and subset $\Gamma' \subset \Gamma$. Then for all $\gamma_1, \gamma_2 \in \Gamma'$

$$C\|\mathcal{G}(\gamma_1) - \mathcal{G}(\gamma_2)\|_{L^2(\mathcal{V})} \leq d_H(p^{\gamma_1}, p^{\gamma_2}) \leq C\|\mathcal{G}(\gamma_1) - \mathcal{G}(\gamma_2)\|_{L^2(\mathcal{V})}, \tag{4.3}$$

where $C = C(U, \varepsilon)$ and $C = C(\varepsilon)$. This relates p^γ to analytical aspects of $\mathcal{G}$, even though only point evaluations of $\mathcal{G}(\gamma)$ appear in (4.1). This fact replaces the need for ideas in approximation theory and conditions on the empirical distribution of x_i in a model where $X_i = x_i$ are deterministic and fixed. One could also consider a different distribution than uniform, which has a density π_X with respect to the Lebesgue measure. Then (4.3) would hold for a π_X-weighted $L^2(\mathcal{V})$-norm instead, which could be more or less convenient than (4.3). We refer to [Nic23] for further discussion on this model.

Model 2: White noise

Let $\mathcal{Y}$ be a separable Hilbert space with norm $\|\cdot\|$ and inner product $\langle\cdot,\cdot\rangle$. Again we let $\Gamma \subset \mathcal{X}$ denote a closed subset of a separable Banach space $\mathcal{X}$. We consider a white noise model with observations of the form

$$Y = \mathcal{G}(\gamma) + \varepsilon_n \xi, \tag{4.4}$$

where $\varepsilon_n > 0$ is the usual n-dependent noise level and ξ is a Gaussian random element of distribution $N(0, I)$. This notion requires an interpretation, which we give in the following. We refer also to [Nic20, Section 7.4] for more details. Let $\{e_\ell\}_{\ell=1}^\infty$ be an orthonormal basis of $\mathcal{Y}$ and define

$$\xi := \sum_{\ell=1}^\infty \xi_\ell e_\ell, \quad \xi_\ell \overset{i.i.d.}{\sim} N(0,1).$$

Define also the weighted Hilbert space $\mathcal{Y}_-$,

$$\mathcal{Y}_- := \left\{ f = \sum_{\ell=1}^\infty f_\ell e_\ell : \|f\|_-^2 := \sum_{\ell=1}^\infty \lambda_\ell^2 f_\ell^2 < \infty \right\},$$

for $\lambda_\ell > 0$ and $\{\lambda_\ell\}_{\ell=1}^\infty \in \ell^2(\mathbb{N})$. Note ξ is a $\mathcal{Y}_-$-valued Gaussian random element, in the usual sense of [GGvdV00], since it is the Karhunen-Loeve expansion corresponding to a covariance operator $K : \mathcal{Y}_- \to \mathcal{Y}_-$ defined by $Ke_\ell = \lambda_\ell^2 e_\ell$, see Proposition 4.1 below. Note also that ξ converges in $\mathcal{Y}_-$ almost surely. Indeed, the deterministic series $\sum_{\ell=1}^\infty f_\ell e_\ell$ converges in $\mathcal{Y}_-$ if and only if $\sum_{\ell=1}^\infty \lambda_\ell^2 f_\ell^2 < \infty$, and since Tonelli's theorem provides us with

$$E\left[\sum_{\ell=1}^\infty \lambda_\ell^2 \xi_\ell^2\right] = \sum_{k=1}^\infty \lambda_\ell^2 E[\xi_\ell^2] = \sum_{k=1}^\infty \lambda_\ell^2 < \infty, \tag{4.5}$$

we conclude $\Pr(\sum_{k=1}^\infty \lambda_\ell^2 \xi_\ell^2 < \infty) = 1$. Also Y is a $\mathcal{Y}_-$-valued Gaussian random element, since it is a translation of $\varepsilon_n \xi$ by an element in $\mathcal{Y}$. We denote the distributions of $\varepsilon_n \xi$ and Y in $\mathcal{Y}_-$ by P_n and P_n^γ respectively. The likelihood function arises as the density of P_n^γ with respect to P_n. This is a consequence of the Cameron-Martin theorem in the Hilbert space $\mathcal{Y}$. The theorem gives the likelihood function as

$$p_n^\gamma(Y) := \frac{dP_n^\gamma}{dP_n}(Y) = \exp\left(\frac{1}{\varepsilon_n^2}\langle Y, \mathcal{G}(\gamma)\rangle - \frac{1}{2\varepsilon_n^2}\|\mathcal{G}(\gamma)\|^2\right),$$

here evaluated in Y, see [GN16][Proposition 6.1.5] and also [Nic20, Section 7.4]. For $y \in \mathcal{Y}$, $\langle Y, y\rangle$ is the Gaussian random variable defined by

$$\langle Y, y\rangle := \langle \mathcal{G}(\gamma), y\rangle + \varepsilon_n W(y),$$

where W is Gaussian process on $\mathcal{Y}$ satisfying $E[W(y)] = 0$ and $E[W(y)W(y')] = \langle y, y'\rangle$. This is process is also known as 'white noise' from where this observation model derives its name, see [GN16][Example 2.1.11]. Since $\langle y, \mathcal{G}(\gamma)\rangle$ is not well-defined for all $y \in \mathcal{Y}_-$ it is convenient instead to consider $(\gamma, \omega) \mapsto p_n^\gamma(Y(\omega))$ as a function on $\Gamma \times \Omega$. Indeed, as argued in [Nic20, Section 7.4], it is jointly Borel measurable, when $\mathcal{G} : \Gamma \to \mathcal{Y}$ is continuous. Naturally, we then form the product measure Q on $\Gamma \times \Omega$ defined by

$$Q(A \times B) = \int_A \int_B p_n^\gamma(Y(\omega)) \Pr(d\omega)\, \Pi(d\gamma).$$

In this setting, Bayes' rule, see [Pol02, Theorem 12] gives a posterior distribution of γ given $Y(\omega)$

$$\Pi(B|Y(\omega)) = \frac{\int_B p_n^\gamma(Y(\omega))\,\Pi(d\gamma)}{\int_\Gamma p_n^\gamma(Y(\omega))\,\Pi(d\gamma)}, \quad B \in \mathcal{B}(\Gamma).$$

Similar to the trick in Section 3.1, we can set $p_n^\gamma(Y(\omega)) = 0$, when the denominator is zero, so that $\Pi(\cdot|Y(\omega))$ is well-defined everywhere. Since Γ is a closed subset of a separable Banach space, in particular a Polish space, there exists a regular version of the posterior distribution, which we denote the same way, see [GvdV17, Section 1.3].

4.1.1 Prior modelling

The posterior gives no mass to sets that are given no mass by the prior. For this reason we can at least give an upper bound of the support of the posterior. Making use of conditional stability estimates of the form (1.1) it then becomes instrumental to control the regularity properties of samples from the prior. To construct prior distributions on Γ with such control, we consider Gaussian priors and push-forwards here of. One of the simplest constructions of Gaussian elements of function spaces is to consider random expansions, such as Karhunen-Loeve expansions. These are considered in the separable Hilbert space setting in [DS17, Section 2.4], which also considers uniform- and Besov-type priors.

For now we will consider priors on $\mathcal{X} = L^2(\mathcal{U})$ of real-valued function defined on $\mathcal{U}$. We will take either a bounded Lipschitz domain $\mathcal{U} \subset \mathbb{R}^k$ or a k-dimensional torus $\mathcal{U} = \mathbb{T}^k := \mathbb{R}^k/\mathbb{Z}^k$ and take an orthonormal basis $\{\phi_\ell\}_{\ell\in\mathbb{Z}^k}$. Then one typically maps the prior through a smooth regularity-preserving map $\Phi : \mathcal{X} \to \Gamma$, see for example [NvdGW20]. Consider the joint distribution of the infinite sequence of independent random variables $\{\lambda_\ell\xi_\ell\}_{\ell\in\mathbb{Z}^k}$ for a positive sequence $\lambda_\ell \in \ell^2(\mathbb{Z}^k)$ and $\xi_\ell \overset{i.i.d.}{\sim} N(0,1)$. This distribution exists on $(\ell^2(\mathbb{Z}^k), B(\ell^2(\mathbb{Z}^k)))$ as the product measure $\times_{\ell\in\mathbb{Z}^k} N(0,\lambda_\ell^2)$, as shown in [DP06, Section 1.5] for the indexing set $\mathbb{N}$. The isomorphism from $\ell^2(\mathbb{Z}^k)$ to $L^2(\mathcal{U})$ defined by,

$$F : \{\tilde{\gamma}_\ell\}_{\ell\in\mathbb{Z}^k} \mapsto \sum_{\ell\in\mathbb{Z}^k} \tilde{\gamma}_\ell\phi_\ell$$

provides a random element u of $L^2(\mathcal{U})$ by

$$\tilde{\gamma} := F(\{\lambda_\ell\xi_\ell\}_{\ell\in\mathbb{Z}^k}) = \sum_{\ell\in\mathbb{Z}^k} \lambda_\ell\xi_\ell\phi_\ell, \tag{4.6}$$

and the corresponding push-forward distribution is a Borel measure, since $F : \ell^2(\mathbb{Z}^k) \to L^2(\mathcal{U})$ is measurable. The following result states that this is indeed a Gaussian random element of $L^2(\mathcal{U})$.

Proposition 4.1 *Let $K : L^2(\mathcal{U}) \to L^2(\mathcal{U})$ be the positive, symmetric and trace-class operator such that $K\phi_\ell = \lambda_\ell^2 \phi_\ell$. Then $\tilde{\gamma}$ in (4.6) is a Gaussian random element of $L^2(\mathcal{U})$ with distribution $N(0, K)$. Moreover, $\tilde{\gamma}$ converges in $L^2(\mathcal{U})$ almost surely.*

Proof. The first assertion follows as in [DPZ14, Proposition 2.18], and the second assertion follows as in (4.5). □

Note this result holds for any separable Hilbert space as is considered in [DPZ14, Proposition 2.18]. We have the following example of a Gaussian random element for a popular choice of K.

Example 4.1 *One could for example consider on $\mathbb{T}^k$ an orthonormal basis $\{\phi_\ell\}_{\ell \in \mathbb{Z}^k}$ of trigonometric functions and K the covariance operator defined by $K\phi_\ell = \lambda_\ell^2 \phi_\ell$ for $\lambda_\ell = (1+|\ell|^2)^{-\delta/2}$ with $\delta > k/2$. By an integral test and change of variables,*

$$\sum_{\ell \in \mathbb{Z}^k} \lambda_\ell^2 \leq C \int_{\mathbb{R}^k} (1+|x|^2)^{-\delta}\, dx = C \int_0^\infty (1+r^2)^{-\delta} r^{k-1}\, dr < \infty,$$

and hence $\lambda_\ell \in \ell^2(\mathbb{Z}^k)$. We can think of $K : L^2(\mathbb{T}^k) \to L^2(\mathbb{T}^k)$ as the spectrally defined operator $(1-\Delta)^{-\delta}$. This covariance operator is often called a Matérn covariance, see for example [RHL14]. It has the benefit that it provides samples that are Sobolev regular. Indeed, by the characterization of Sobolev spaces defined on $\mathbb{T}^k$ in [Tay11] and Tonelli's theorem

$$E[\|\tilde{\gamma}\|^2_{H^\beta(\mathbb{T}^k)}] = E[\sum_{\ell \in \mathbb{Z}^k} (1+|\ell|^2)^\beta \lambda_\ell^2 \xi_\ell^2] = \sum_{\ell \in \mathbb{Z}^k} (1+|\ell|^2)^{\beta-\delta} < \infty$$

for $\beta < \delta - k/2$. Hence, $\tilde{\gamma}$ converges in $H^\beta(\mathbb{T}^k)$ a.s., i.e. $\Pr(\tilde{\gamma} \in H^\beta(\mathbb{T}^k)) = 1$.

To avoid confusion of regularity β with the Robin coefficient we use α as regularity index in the summary of Paper C. We end this part with some remarks.

1. Associated with any Gaussian distribution is a Hilbert space called the reproducing kernel Hilbert space (RKHS). It is determined by the covariance operator and is essential in many properties of Gaussian distributions. In the separable Hilbert space setting that $L^2(\mathcal{U})$ provides, the RKHS associated with a $N(0, K)$ random element is nothing but $K^{1/2}(L^2(\mathcal{U}))$, i.e. the elements of the form $\sum_{\ell \in \mathbb{Z}^k} \lambda_\ell \tilde{\gamma}_\ell \phi_\ell$ for $\tilde{\gamma}_\ell \in \ell^2(\mathbb{Z}^k)$, see [Hai09, Exercise 3.34]. In the case of Example 4.1 above, the RKHS is $H^\delta(\mathbb{T}^k)$. We will not

pursue this topic further here, but refer instead to [GvdV17, GN16, Hai09] for a relevant treatment in Gaussian measure theory.

2. A particularly useful result in Gaussian measure theory is the following. If $\mathcal{X}' \subset \mathcal{X}$ is a continuously embedded Banach space and $\mathcal{X}$ is endowed with a Gaussian measure $\tilde{\Pi}$ such that $\tilde{\Pi}(\mathcal{X}') = 1$, then the restriction of $\tilde{\Pi}$ to $\mathcal{X}'$ is again a Gaussian measure, see [Hai09, Exercise 3.39]. For example, the continuous Sobolev embedding $H^\beta(\mathcal{U}) \subset C(\overline{\mathcal{U}})$ for $\beta > k/2$ renders distribution of $\tilde{\gamma}$ in Example 4.1 a Gaussian measure in $C(\overline{\mathcal{U}})$. Since this embedding is also injective, the associated RKHS remains the same, see [GvdV17, Lemma I.16-I.17].

3. The following argument in the proof of [Nic23, Theorem 2.2.2] makes the regularity of $\tilde{\gamma}$ more quantitative in the general case: Fernique's theorem [GN16, 2.1.20] states that $E[\|\tilde{\gamma}\|_{H^\beta(\mathcal{U})}] < U$ for some $U > 0$, and gives

$$\begin{aligned}\Pr(\|\tilde{\gamma}\|_{H^\beta(\mathcal{U})} > M) &= \Pr(\|\tilde{\gamma}\|_{H^\beta(\mathcal{U})} - E[\|\tilde{\gamma}\|_{H^\beta(\mathcal{U})}] > M - E[\|\tilde{\gamma}\|_{H^\beta(\mathcal{U})}]),\\ &\leq \Pr(|\tilde{\gamma} - E[\|\tilde{\gamma}\|_{H^\beta(\mathcal{U})}]| > M/2),\\ &\leq e^{-CM^2}, \end{aligned} \tag{4.7}$$

for $M > 2E[\|\tilde{\gamma}\|_{H^\beta(\mathcal{U})}]$. Here C is a constant only dependent on the distribution of $\tilde{\gamma}$.

4. A different and perhaps more general viewpoint than that of random series is the viewpoint of Gaussian processes. Here, the task is to pick a covariance kernel that brings the right properties to the process. For Gaussian processes with a continuous covariance kernel, there is also an associated Hilbert space called the (process-)RKHS. See for example [GvdV17, Lemma 11.14] for a correspondence between the two notions. One can construct an orthonormal basis of this Hilbert space by solving an eigenvalue problem involving the covariance kernel, and then decompose the process in this basis, see [AT07, Chapter 3]. One arrives at something of the form of the right-hand side of (4.6). There are several ways to characterize the almost sure regularity properties of the Gaussian process directly. Here we refer to [AT07, Chapter 1] and [DS17, Section 2.5].

4.1.2 Posterior consistency

Definition 3.1 of posterior consistency remains the same, only with Y replaced by D in the case of the random design regression model. Now, however, the posterior is defined on Γ, a closed subset of a separable Banach space.

In this infinite-dimensional setting, posterior consistency for inverse problems was initially considered in the linear forward map case. Here we mention [ALS13, FS12, KvdVvZ11, KLS16, Ray13], where all but the last benefits from Gaussianity of the posterior arising from a Gaussian prior. For nonlinear forward maps we mention [GN20, Kek22, MNP21] in the random design regression model and [AN19, Nic20, AW21, ASK22] in the white noise model, see also [Vol13] for posterior consistency for nonlinear inverse problems in a fixed design regression model.

Early contributions in posterior consistency outside the context of inverse problems concern identifying the data-generating distribution P_n^γ from noisy samples. This is comparable to an inverse problem setting for the identity forward map, and is in fact the first step in nonlinear inverse problems. For a general treatment of posterior consistency and also examples of inconsistency, see [GvdV17, Chapter 6-9]. In the following, we are concerned with consistency at an explicit rate, i.e. posterior contraction, but discuss not the optimality of the rate. This is the subject of, for example, [AN19].

In Section 3.2 we saw how, for $V_n = V$ as in (3.11),

$$\Pi(V_n|Y) \to 1 \qquad \text{in } P_n^{\gamma_0}\text{-probability}, \tag{4.8}$$

as $n \to \infty$, implies posterior consistency by virtue of the continuity of $\mathcal{G}^{-1}$. In contrast, in this section we consider conditional stability estimates. To this end define the semimetric $d_{\mathcal{G}}(\gamma_1, \gamma_2) := \|\mathcal{G}(\gamma_1) - \mathcal{G}(\gamma_2)\|$ on Γ and take V_n of the form

$$V_n := \{\gamma \in \Gamma : d_{\mathcal{G}}(\gamma, \gamma_0) \leq C_0 r_n\} \cap \{\gamma \in \Gamma : \|\gamma\|_{\mathcal{A}} \leq M\}, \tag{4.9}$$

for some constant $C_0 > 0$, some linear subspace $\mathcal{A} \subset \mathcal{X}$ endowed with a norm stronger than the norm in $\mathcal{X}$, and a sequence

$$r_n = n^{-a}, \quad \text{with} \quad 0 < a < 1/2.$$

The case $a = 1/2$ is, in a certain sense, optimal and more than we can hope for, see [GvdV17, Chapter 8]. The sets in (4.9) have this form for two reasons:

1. It is the contribution of [GGvdV00] to give general conditions for a posterior contraction in distance $d_{\mathcal{G}}$. Then [MNP21] succeeded in applying this to conditionally stable nonlinear inverse problems for Gaussian priors in the manner we repeat here. Among these conditions, which we shall make concrete below, is the condition that the prior gives most of its mass to a totally bounded set with respect to $d_{\mathcal{G}}$. Convenient candidates for such sets are of the form $\{\gamma \in \Gamma : \|\gamma\|_{\mathcal{A}} \leq M\}$ for Sobolev or Hölder spaces $\mathcal{A}$, see [GN16, Section 4.3.7]. When the prior distribution puts most of its mass on such sets, so does the posterior. It is therefore natural to intersect with these sets in (4.9).

2. This combines well with the second reason, which is that the conditional stability estimate of the form (1.1) implies

$$V_n \subset \{\gamma \in \Gamma : \|\gamma - \gamma_0\|_{\mathcal{X}} \leq f(C_0 r_n)\} =: U_n. \tag{4.10}$$

This implies posterior consistency in γ_0 at rate $f(C_0 r_n)$, if (4.8) holds.

The conditions for a result like (4.8) can be formulated as follows, where we recall the notion of covering numbers N in Appendix E.1.

Condition A *Let $\mathcal{G} : \Gamma \to \mathcal{Y}$ be a forward map producing noisy observations as in Model 1 or Model 2, and denote Π, the prior distribution. Suppose the following:*

A.1 *The prior gives enough mass to contracting neighborhoods $B_{\mathcal{G}}(\gamma_0, r_n)$ of γ_0*

$$\Pi(B_{\mathcal{G}}(\gamma_0, r_n)) \geq e^{-C_1 n r_n^2}, \quad C_1 > 0,$$

where for Model i we let

$$B_{\mathcal{G}}(\gamma_0, r_n) := \begin{cases} \{\gamma : d_{\mathcal{G}}(\gamma, \gamma_0) \leq r_n\} \cap \{\gamma : \|\mathcal{G}(\gamma)\|_{C(\overline{\mathcal{V}})} \leq U\}, & i = 1, \\ \{\gamma : d_{\mathcal{G}}(\gamma, \gamma_0) \leq r_n\}, & i = 2, \end{cases}$$

for some $U > 0$. In the case of Model 1, we suppose $\|\mathcal{G}(\gamma_0)\|_{C(\overline{\mathcal{V}})} \leq U$ in addition.

A.2 *There exist sets A_n that are almost the support of Π in the sense that*

$$\Pi(\Gamma \setminus A_n) \leq e^{-C_2 n r_n^2}, \quad C_2 > C_1 + 4,$$

A.3 *and that there exists a constant $m_0 > 0$ such that*

$$\log N(A_n, d_{\mathcal{G}}, m_0 r_n) \leq C_3 n r_n^2, \quad C_3 > 0.$$

In the case of Model 1, we suppose $\sup_{\gamma \in A_n} \|\mathcal{G}(\gamma)\|_{C(\overline{\mathcal{V}})} \leq U$ in addition.

The conditions should hold for all n large enough.

Note Condition A enter in [Nic23, Theorem 1.3.2] in the setting of Model 1. A slight modification of this appear for Model 2 in for example [Nic20, Abr20]. There, additional motivation can be found for the conditions. The extra conditions in the case of Model 2 originates from (4.3), since it allows exchanging $d_{\mathcal{G}}$ with d_H.

The aforementioned modification pertains to the third condition, the *metric entropy* condition. This condition implies the existence of certain measurable functions that takes data (either in $\mathcal{D}^n$ or $\mathcal{Y}$ depending on the model) and outputs either 0 or 1. These functions, also known as statistical tests, can distinguish to a high degree between data arising from $\gamma = \gamma_0$, in which case the test outputs 0, and γ that are in A_n and sufficiently $d_{\mathcal{G}}$-distant from γ_0, in which case it maps to 1. These tests play a critical role in upper bounding the numerator of the posterior ratio, which, as we saw in the proof of Proposition 3.2, is a key step. While Condition **A.3** implies the existence of such tests, it is not always necessary. There are some examples of that in [GGvdV00]. However, it is sufficient for the cases we consider here.

The difficulty in finding sets A_n that satisfy Condition **A.3** is *only* that they should satisfy **A.2** at the same time, which is clearly an opposing condition; the better cover A_n provides of the support of the prior, the larger its covering number is.

The *small ball* condition **A.1** we have already seen in (3.17). Similar to its role in the proof of Proposition 3.2, it provides a lower bound of the posterior denominator. The proof of this relies on tools in Gaussian measure theory, although we mention it has been generalized to Laplace-type priors in [AW21, ADH21] corresponding to when ξ_ℓ are distributed according to a Laplace-type distribution in (4.6).

Under these conditions an analog of Proposition 3.2 is as follows:

Theorem 4.2 *Let $\Pi(\cdot|Z)$ be a sequence of posterior distributions, where we write $Z = D$ and $Z = Y$ for Model 1 and Model 2, respectively. Let $\gamma_0 \in \Gamma$, $\mathcal{G}$ and the prior distributions $\Pi = \Pi_n$ satisfy Condition A for some rate r_n. Then, there exists $C_0 = C_0(C_2, C_3, m_0, \varepsilon)$ such that*

$$\Pi(\{\gamma : \|\mathcal{G}(\gamma) - \mathcal{G}(\gamma_0)\| \leq C_0 r_n\} \cap A_n | Z) \to 1 \quad \text{in } P_n^{\gamma_0}\text{-probability},$$

with rate $e^{-bnr_n^2}$ for all $0 < b < C_2 - C_1 - 4$ as $n \to \infty$. In particular, if $A_n \subset \{\gamma : \|\gamma\|_{\mathcal{A}} \leq M\}$, and (4.10) holds, then $\Pi(\cdot|Z)$ is consistent in γ_0 at rate $f(C_0 r_n)$.

Proof. The case of Model 1 is considered in Theorem 1.3.2 in [Nic23]. For Model 2, the covering argument that leads to tests of favorable properties is standard and included in [AKRT23, Appendix B], see also [GvdV17, Appendix D]. Then Theorem 28 in [Nic20] and the modification in [Nic23, Theorem 1.3.2] of intersection with A_n give the claim. The final claim follows from (4.10) and Definition 3.1. Here, we mean that C_0 depends on ε only in the case that we consider Model 1. □

4.1.3 Rescaling the prior

One apparent choice for A_n is $A_n = \{\gamma : \|\gamma\|_{\mathcal{A}} \leq M\}$ as we have already mentioned. In this case either $\Pi(A_n) = 1$ or the prior cannot be fixed with respect to n to satisfy Condition **A.2**. In fact, in the Gaussian case it must depend on n for this choice of A_n. Let for example $\Gamma = L^2(\mathcal{U})$ and $\mathcal{A} = H^\beta(\mathcal{U})$ for some $\beta > 0$ and $\tilde{\Pi}$ be some prior such that $\tilde{\Pi}(H^\beta(\mathcal{U})) = 1$. Example 4.1 provides an example of such a prior. Then by (4.7) for $\tilde{\gamma} \sim \tilde{\Pi}$,

$$\Pr(\|\tilde{\gamma}\|_{\mathcal{A}} > M) \leq e^{-CM^2},$$

which is clearly not enough for Condition **A.2**. Instead, we define a prior that does depend on the observation setting through n. Indeed, take Π as the distribution of

$$\gamma = n^{a-1/2}\tilde{\gamma}, \quad \tilde{\gamma} \sim \tilde{\Pi}.$$

Then

$$\begin{aligned}\Pi(\Gamma \setminus A_n) &= \Pr(\|n^{a-1/2}\tilde{\gamma}\|_{\mathcal{A}} > M), \\ &= \Pr(\|\tilde{\gamma}\|_{\mathcal{A}} > Mn^{1/2-a}), \\ &= e^{-CM^2 n^{1-2a}} = e^{-C(M)nr_n^2},\end{aligned}$$

which is sufficient for Condition **A.2**. There is nothing strange in this rescaling. In fact, we have seen this type of condition in the discussion after Example 2.1. For $\mathcal{X} = \mathbb{R}^k$ and the probability density of $\tilde{\Pi}$ of the form $\tilde{\pi}(\tilde{\gamma}) \propto \exp\left(-\frac{1}{2}\tilde{\gamma}^T C^{-1}\tilde{\gamma}\right)$ for a covariance matrix $C : \mathbb{R}^k \to \mathbb{R}^k$, we can write the resulting posterior probability density function under the rescaling as

$$\begin{aligned}\pi_Y(\tilde{\gamma}) &\propto \exp\left(-\frac{1}{2\varepsilon_n^2}\|\mathcal{G}(\tilde{\gamma}) - Y\|^2 - \frac{1}{2n^{2a-1}}\tilde{\gamma}C^{-1}\tilde{\gamma}\right), \\ &\propto \exp\left(\|\mathcal{G}(\tilde{\gamma}) - Y\|^2 - \frac{\varepsilon_n^2}{n^{2a-1}}\tilde{\gamma}C^{-1}\tilde{\gamma}\right),\end{aligned}$$

hence for MAP estimation $\alpha(\varepsilon_n) = \varepsilon_n^2/n^{2a-1} \propto n^{-2a}$ is the regularization parameter. Clearly $\alpha(\varepsilon_n) \to 0$ as $n \to \infty$ and $\varepsilon_n^2/\alpha = n^{2a-1}$, which converges to zero as $n \to \infty$. In this sense the rescaling enforces the prior to go slower to zero as $n \to \infty$.

4.1.4 Remarks on the infinite-dimensional setting

We conclude this part of the chapter with remarks on the infinite-dimensional setting before entering in a summary and discussion of Paper B and C. These

remarks concern the generalization of the concepts in posterior computation and well-posedness considered in Chapter 3.

1. To recap, we have already seen one natural choice of Π, $\mathcal{A}$, A_n and $\mathcal{G}$ that gives rise to posterior consistency. This is the choice of a rescaled Gaussian prior as Π with support in $\mathcal{A} = H^\beta(\mathcal{U})$ for some $t > 0$, $A_n = \{\gamma : \|\gamma\|_{\mathcal{A}} \leq M\}$ and a Hölder continuous and conditionally stable $\mathcal{G}$ defined on $\mathcal{A}$. In Paper B we shall see a different choice arising for push-forward priors.

2. Upon concluding posterior consistency, a common corollary is convergence in probability of the posterior mean, see [Nic23, Theorem 2.3.2]. Here, the posterior mean is defined in the sense of a Bochner integral

$$E[\gamma|Z] = \int_\Gamma \gamma \, \Pi(d\gamma|Z)$$

given that $\gamma \mapsto \gamma$ is Bochner integrable. Also in this setting a sum of samples γ_i of the posterior distribution $\bar{\gamma}_N = \frac{1}{N}\sum_{i=1}^N \gamma_i$ converges in the mean square sense to $E[\gamma|Z]$ if $\gamma \mapsto \gamma$ is also square-integrable in the Bochner sense, see [KS23]. We refer to Appendix E.2.2 for a definition and a measurability argument of $\omega \mapsto E[\gamma|Z(\omega)]$.

3. The MCMC method pCN is well-defined for a posterior distribution in a separable Hilbert space, see [DS17, Section 5]. However, it is vulnerable to correlated samples and yields slow exploration of the posterior, when the discretization is high-dimensional [CLM16]. Remedies, see [CLM16], take as starting point the Langevin-type algorithms that are also considered in [NW22] and for which posterior mean estimation is guaranteed in a time polynomially depending on the discretization size.

4. Well-posedness of the posterior as in Section 3.4 is considered in [DS17]. However, in the case of the white noise model, note [DS17, Theorem 16] only provides well-posedness of the posterior with respect to $y \in \mathcal{Y}$.

We will now consider the application of Theorem 4.2 in the inclusion detection and inverse Robin problem settings.

4.2 Paper B: Consistent Bayesian reconstruction of inclusions

In Paper B, we consider a Bayesian approach to the inverse problem of inclusion detection for conditionally well-posed inverse problems with observations

in the white noise model, i.e. Model 2. We give a Bayesian reconstruction algorithm (the posterior mean), which is provably consistent. The approach takes advantage of the fact that indicator functions of regular sets form a subset of $\Gamma = L^2_\Lambda(\mathcal{O})$ that has lower 'complexity' than arbitrary bounded subsets of $L^2_\Lambda(\mathcal{O})$. Here, we mean complexity in the sense of covering numbers as in Condition **A.3**. Using Gaussian or Laplace-type priors this parameter set is typically a closed Sobolev or Hölder norm ball, see [Nic23, Theorem 2.2.2], [MNP21] or [AW21], but such priors do not give sufficient mass to discontinuous parameters to conclude consistency.

We address this by parametrizing the set of discontinuous parameters from sets of functions that are sufficiently smooth. More precisely, we aim to recover a parameter γ in sets of the form $\Phi(\Theta)$ for some linear space Θ and a continuous map $\Phi : \Theta \to L^2_\Lambda(D)$ that we call the parametrization, see Figure 4.1. If this map is Hölder continuous, then we can transfer the metric entropy condition, Condition **A.3**, from subsets of $L^2_\Lambda(D)$ to subsets of Θ and see a convergence rate that reflects this reduction. To obtain posterior consistency with an explicit rate, we aim to construct a setting that satisfies Condition A, since Theorem 4.2 provides consistency when estimates like (1.1) exist.

4.2.1 Main results

Initially, we consider the general case $\Theta = H^\beta(\mathcal{U})$, where $\mathcal{U}$ is either the k-dimensional torus or a bounded Lipschitz domain $\mathcal{U} \subset \mathbb{R}^k$, $k \geq 1$ and $\beta > k/2$. We include here the torus in our considerations, since it is a numerically convenient setting. The following three conditions, which are given in Paper B, characterizes a setting in which posterior consistency is guaranteed.

Condition 1 *For any θ_i satisfying $\|\theta_i\|_{H^\beta(\mathcal{U})} \leq M$ for some $M > 0$, $i = 1, 2$, let*

$$\|\Phi(\theta_1) - \Phi(\theta_2)\|_{L^2(\mathcal{O})} \leq C_\Phi \|\theta_1 - \theta_2\|^\zeta_{L^\infty(\mathcal{U})}$$

for some constant $C_\Phi(M) > 0$ and $0 < \zeta < \infty$.

Condition 2 *For any γ_i of the form $\gamma_i = \Phi(\theta_i)$ with $\|\theta_i\|_{H^\beta(\mathcal{U})} \leq M$ for some $M > 0$, $i = 1, 2$, let*

$$\|\mathcal{G}(\gamma_1) - \mathcal{G}(\gamma_2)\| \leq C_\mathcal{G} \|\gamma_1 - \gamma_2\|^\eta_{L^2(\mathcal{O})}$$

for some constants $C_\mathcal{G}(M) > 0$ and $0 < \eta < \infty$. In addition, let

$$\|\gamma_1 - \gamma_2\|_{L^2(\mathcal{O})} \leq f(\|\mathcal{G}(\gamma_1) - \mathcal{G}(\gamma_2)\|), \tag{4.11}$$

for some modulus of continuity $f : \mathbb{R} \to \mathbb{R}$, which is continuous at zero with $f(0) = 0$.

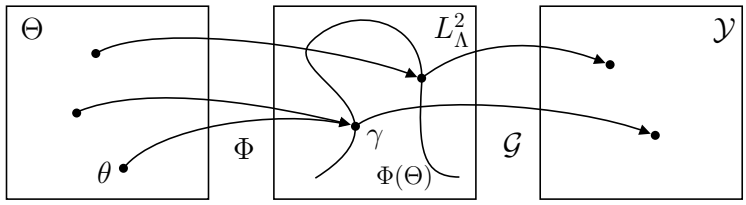

Figure 4.1: Figure 1 in [AKRT23]. The setup of the parametrization $\Phi : \Theta \to L^2_\Lambda(\mathcal{O})$ and forward map $\mathcal{G} : L^2_\Lambda(\mathcal{O}) \to \mathcal{Y}$

Condition 3 *Let Π'_θ be a centred Gaussian probability measure on $H^\beta(\mathcal{U})$, $\beta > \dim(\mathcal{U})/2$, with $\Pi'_\theta(H^\beta(\mathcal{U})) = 1$. Let the RKHS $(\mathcal{H}, \|\cdot\|_{\mathcal{H}})$ of Π'_θ be continuously embedded into $H^\delta(\mathcal{U})$ for some $\delta > \beta$. Then let Π_θ be the distribution of*

$$\theta = n^{a-\frac{1}{2}}\theta', \quad \theta' \sim \Pi'_\theta \tag{4.12}$$

for a as in Condition A and let $\Pi = \Phi\Pi_\theta$.

Here, (4.11) plays the role of the conditional stability estimate of (1.1), and we already note that (1.7), i.e. the QPAT problem, satisfies this condition for any Φ mapping into $L^2_\Lambda(\mathcal{O})$. Note we have considered a prior like Π'_θ in Example 4.1 and argued why the rescaling (4.12) is natural in Section 4.1.3. In this setting, we have the following general result, which makes use of key ideas found in the proof of Theorem 2.2.2. of [Nic23] to prove that Condition A is satisfied. See Section 4.2.3 for a discussion on how the theorem below differs.

Theorem 4.3 (Theorem 3.1 in [AKRT23]) *Suppose that the Condition 1, 2 and 3 are satisfied for $\beta > k/2$, and $\gamma_0 \in \Phi(\mathcal{H})$. Let $\Pi(\cdot|Y)$ be the corresponding sequence of posterior distributions arising for the model* (4.4). *Then there exists $C_0 > 0$ such that*

$$\Pi(\|\gamma - \gamma_0\|_{L^2(\mathcal{O})} \leq f(C_0 r_n)|Y) \to 1 \quad \text{in } P_n^{\gamma_0}\text{-probability},$$

where $r_n = n^{-a}$ with

$$a = \frac{\eta\zeta\delta}{2\eta\zeta\delta + k}. \tag{4.13}$$

The corresponding posterior mean $E[\gamma|Y]$ in $L^2(D)$ satisfies for some constant $C > 0$ large enough

$$\|E[\gamma|Y] - \gamma_0\|_{L^2(\mathcal{O})} \to 0 \quad \text{in } P_n^{\gamma_0}\text{-probability}$$

with rate $f(Cr_n)$ as $n \to \infty$.

In Paper B we apply this to two parametrizations used in inclusion detection.

Case 1: The star-shaped set parametrization

First we consider star-shaped inclusions in the plane. More precisely, we consider $\Theta = H^\beta(\mathbb{T})$, i.e. $\mathcal{U} = \mathbb{T}$ and $k = 1$, where $\mathbb{T}$ is the one-dimensional torus and $\beta > 3/2$. We then define the parametrization

$$\Phi_{\text{star}}(\theta) := \kappa_1 \mathbb{1}_{A(\theta)} + \kappa_2. \tag{4.14}$$

with $\Lambda^{-1} \leq \kappa_1, \kappa_2 \leq \Lambda/2$ and where $A(\theta)$ is the star-shaped set characterized by

$$\partial A(\theta) = x + \{\exp(\theta(\vartheta))v(\vartheta),\ 0 \leq \vartheta \leq 2\pi\}, \quad v(\vartheta) := (\cos\vartheta, \sin\vartheta).$$

for some fixed point $x \in \mathcal{O}$, which we assume to be given. We can think of $A(\theta)$ as a deformed disk centered in x. Since Φ should map into $L^2_\Lambda(\mathcal{O})$, we implicitly always consider $\Phi = \Phi_{\text{star}}$ as the restriction to $\mathcal{O}$ of the right-hand side in (4.14).

For certain inverse problems, which allows the unique identification of elements in the range of Φ_{star} with stability as in Condition 2, we then have the following result.

Theorem 4.4 (Theorem 4.1 in [AKRT23]) *Suppose that Condition 2 is satisfied for $\beta > 3/2$ and $\Phi = \Phi_{\text{star}}$. Let $\gamma_0 = \Phi_{\text{star}}(\theta_0)$ for $\theta_0 \in \mathcal{H}$. Let $\Pi(\cdot|Y)$ be the corresponding sequence of posterior distributions arising for the model (4.4) and prior $\Pi = \Phi_{\text{star}}\Pi_\theta$ satisfying Condition 3. Then there exists a constant $C > 0$ such that*

$$\|E[\gamma|Y] - \gamma_0\|_{L^2(\mathcal{O})} \to 0 \quad \text{in } P_n^{\gamma_0}\text{-probability}$$

with rate $f(Cn^{-a})$ as $n \to \infty$, where

$$a = \frac{\eta\delta}{2\eta\delta + 2}. \tag{4.15}$$

The proof is a straight-forward application of Theorem 4.3, once one has shown Φ_{star} satisfies Condition 1 for $\zeta = 1/2$. Note by (4.13) that (4.15) corresponds to the rate of detecting γ_0 in $\mathcal{H}$ directly using the identity map $I : H^\beta(\mathcal{U}) \to H^\beta(\mathcal{O})$ for $\mathcal{U} = \mathcal{O}$. The difference is of course that we detect something that is piecewise constant with the star-shaped set parametrization.

Case 2: The level set parametrization

Next, we consider inclusions arising from level sets of continuous functions $\theta : \mathcal{U} \to \mathbb{R}$ defined on $\mathcal{U} = \mathcal{O}$, i.e. $k = \dim(\mathcal{O})$. One possibility is the following

parametrization:

$$\Phi_{\text{level},\epsilon}(\theta) = \kappa_1 H_\epsilon(\theta) + \kappa_2,$$

where $H_\epsilon : \mathbb{R} \to \mathbb{R}$ is a continuous approximation of the usual Heaviside function

$$H_\epsilon(z) = \begin{cases} 0 & \text{if } z < -\epsilon, \\ \frac{1}{2\epsilon} z + \frac{1}{2} & \text{if } -\epsilon \leq z < \epsilon, \\ 1 & \text{if } \epsilon \leq z, \end{cases}$$

for some $\epsilon > 0$. With somewhat loose notation we mean by $H_\epsilon(\theta)$ the function that satisfies $H_\epsilon(\theta)(x) = H_\epsilon(\theta(x))$. For $\epsilon = 0$, H_ϵ coincides with the usual Heaviside function and in this case we denote $\Phi_{\text{level},0} = \Phi_{\text{level}}$. To maintain nice properties of Φ_{level} we restrict it to functions in the subset

$$H^\beta_\diamond(\mathcal{O}) := H^\beta(\mathcal{O}) \cap T,$$

where $\beta > 2 + k/2$ and $T := \{\theta \in C^2(\overline{\mathcal{O}}) : \exists x \in \mathcal{O}, \theta(x) = 0, |(\nabla\theta)(x)| = 0\}^c$. Note that $H^\beta(\mathcal{O})$ embeds continuously into $C^2(\mathcal{O})$ by a Sobolev embedding, see for example [Gri85, Theorem 1.4.4.1]. T is the set of functions that do not attain critical values on their zero level set. This restriction will be essential in studying the approximation of $\Phi_{\text{level},\epsilon}$ to Φ_{level}.

However, the level set parametrization Φ_{level} does not satisfy Condition 1, see Example 3 in Paper B. The intuition is that if θ flattens out near the set $\{x : \theta(x) = 0\}$, then the level set can change rapidly. This is why we make use of a continuous modification H_ϵ of H. Then the approximation properties of $\Phi_{\text{level},\epsilon}$ to Φ_{level} allows a consistent reconstruction of $\gamma_0 = \Phi_{\text{level}}(\theta_0)$ in a small noise limit, if ϵ is chosen to dependent on n in the right way.

Theorem 4.5 (Theorem 4.6 in [AKRT23]) *Suppose that Condition 2 is satisfied for $\theta_i \in H^\beta_\diamond(\mathcal{O})$ for $f(x) = Cx^\nu$, $\nu > 0$, and for $\Phi = \Phi_{\text{level},n^{-l}}$ for a well-chosen $l > 0$, and where C and $C_\mathcal{G}$ are independent of n. Let $\gamma_0 = \Phi_{\text{level}}(\theta_0)$ for $\theta_0 \in \mathcal{H} \cap H^\beta_\diamond(\mathcal{O})$. Let $\Pi(\cdot|Y)$ be the corresponding sequence of posterior distributions arising for the model* (4.4) *and prior $\Pi = \Phi_{\text{level},n^{-k}}\Pi_\theta$ as above. Then,*

$$\|E[\gamma|Y] - \gamma_0\|_{L^2(\mathcal{O})} \to 0 \quad \text{in } P_n^{\gamma_0}\text{-probability}$$

with rate $n^{-a\nu}$ as $n \to \infty$ for

$$a = \frac{\eta\delta}{2k\nu\eta + 2\eta\delta + k}.$$

See [AKRT23, Section 5] for a result that permits the use of the QPAT problem in these results. This is also the problem we consider as a test case of the Bayesian approach for inclusion detection. In Paper B, we have generalized Theorem 4.4 and Theorem 4.5 to include the case of multiple inclusions, which is the numerical case we consider.

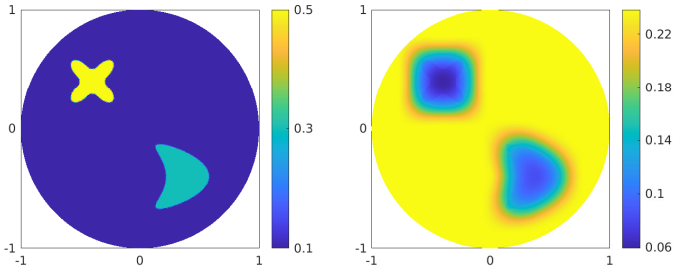

Figure 4.2: Figure 2 in [AKRT23] Simulated absorption γ_0 (left image) and diffusion μ (right image) distributions.

4.2.2 Numerical results

In PAPER B, we test the Bayesian approach for the two priors arising from Φ_{star} and $\Phi_{\text{level},\epsilon}$ generalized to two inclusions. The following is implemented in MATLAB and available at GITHUB [Ras23]. As an approximation to the continuous observation model (4.4), for the numerical experiments we consider observing

$$Y_k = \langle \mathcal{G}(\gamma), e_k \rangle_{L^2(\mathcal{O})} + \varepsilon \xi_k, \qquad k = 1, \dots, N_d \tag{4.16}$$

for $N_d = 351$. This observation model approximates (4.4) as $N_d \to \infty$ in a suitable sense, see [AN19]. As the ground truth we consider two inclusions depicted in Figure 4.2 of the form

$$\gamma_0 = \kappa_1 + \kappa_2 \mathbb{1}_{A_1} + \kappa_3 \mathbb{1}_{A_2},$$

where $(\kappa_1, \kappa_2, \kappa_3) = (0.1, 0.4, 0.2)$. The corresponding observation, the projection of $H = \mathcal{G}(\gamma)$ onto $\{e_k\}_{k=1}^{N_d}$, next to a noise realization can be seen in Figure 4.3. To approximate a prior satisfying Condition 3 for $\Phi = \Phi_{\text{star}}$, we consider Π as the distribution of

$$\gamma = \Phi_{\text{star}}(\theta_1, \theta_2) := \kappa_1 + \kappa_2 \mathbb{1}_{A(x_1,\theta_1)} + \kappa_3 \mathbb{1}_{A(x_2,\theta_2)},$$

for $x_1 = (0.37, -0.43)$, $x_2 = (-0.44, 0.36)$, and

$$\theta_i = \bar{\theta} + \sum_{|\ell| \le 12} g_{\ell,i} w_\ell \phi_\ell, \qquad g_{\ell,1}, g_{\ell,2} \overset{i.i.d.}{\sim} N(0,1),$$

for $i = 1, 2$. Here $\{\phi_\ell\}_{\ell \in \mathbb{Z}}$ is the usual real orthonormal basis of trigonometric functions on $L^2(\mathbb{T})$, $\bar{\theta} = -2$ and $w_\ell = q(\tau^2 + |\ell|^2)^{-\delta/2}$ with $\delta = 5/2$, $\tau = 4$. We handpick $q > 0$ for each noise level instead of the rescaling (4.12). This is comparable to handpicking the regularization parameter in regularization

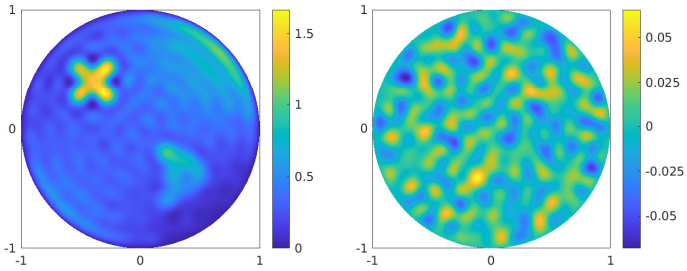

Figure 4.3: Figure 2 in [AKRT23] Projection of absorbed optical energy density H corresponding to (μ, γ_0) (left image) and of the white noise expansion (right image) projected onto the span of $\{e_k\}_{k=1}^{N_d}$ and scaled to 4% relative noise compared to H in $L^2(\mathcal{O})$-norm.

strategies, see (3.18). In the case of the level set parametrization, we choose Π as the distribution of

$$\gamma = \Phi_\epsilon(\theta) = \sum_{i=1}^{3} \kappa_i [H_\epsilon(\theta - c_{i-1}) - H_\epsilon(\theta - c_i)]$$

restricted to $\mathcal{O}$, with $(c_0, c_1, c_2, c_3) = (-\infty, -1, 1, \infty)$ and

$$\theta = \sum_{|\ell_1| \leq 4, |\ell_2| \leq 4} g_\ell w_\ell \phi_\ell, \qquad g_\ell \overset{i.i.d.}{\sim} N(0,1).$$

Here $\{\phi_\ell\}_{\ell \in \mathbb{Z}^2}$ is the usual real orthonormal basis of trigonometric functions on $L^2([-1.1, 1.1]^2)$ and $w_\ell = q(\tau^2 + |\ell|^2)^{-\delta/2}$ with $\delta = 1.2$ and $\tau = 10$. We choose $q > 0$ and $\epsilon > 0$ for each noise level. Note also that we set $H_\epsilon(\theta - \infty) = 0$ and $H_\epsilon(\theta + \infty) = 1$.

We use MCMC methods to approximate the posterior mean for the two choices of prior distributions and refer to [AKRT23] for more details. In Figure 4.4 we see the posterior mean estimates arising for the star-shaped set parametrization and data realizations of different noise levels. Note the posterior mean converges to the ground truth as the noise level goes to zero. Since the posterior means are based on averages of piecewise constant functions, the lack of smooth features in the mean indicates a small posterior variance. This is what we see in Figure 4.4. We interpret this as a consequence of the fast contraction rate provided by conditional stability estimate of the QPAT problem, see [AKRT23, Lemma 5.2], and the star-shaped set parametrization. In Figure 4.5, we see the posterior mean arising for the smoothened level set parametrization and different noise levels. Also here, we see some convergence towards the ground truth. Note,

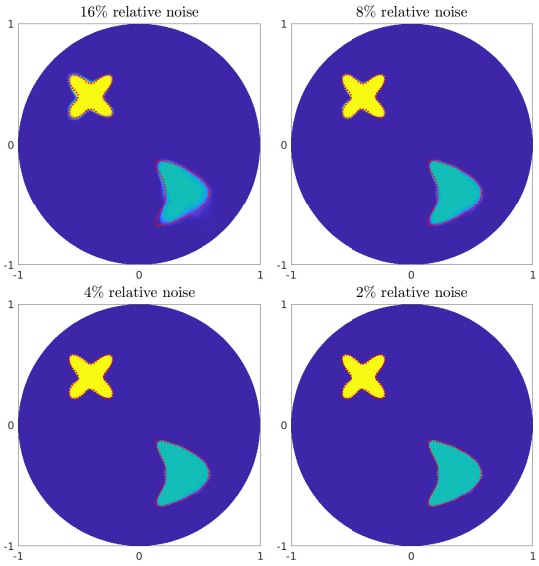

Figure 4.4: Figure 5 in [AKRT23]. Posterior mean estimates of the absorption parameter using the star-shaped set parametrization in different noise regimes. The dotted red line indicates the location of γ_0.

in this case, the smoothness of the mean is also provided by the smoothened level set parametrization. In Paper B, we note that the convergence is not exact, and it does not match the theoretical rate either. This is also too much to expect from the projected observation (4.16), since it does not match the idealized white noise model (4.4).

4.2.3 Discussion and outlook

Theorem 4.4 and 4.5 give theoretical foundation to two Bayesian inclusion detection methods used in literature, see the references in [AKRT23]. Moreover, the results quantifies the convergence in form of a convergence rate that depends on the dimension k of $\mathcal{U}$, the Hölder exponent of $\mathcal{G} \circ \Phi$ and the (conditional) modulus of continuity f of $\mathcal{G}^{-1}$.

Theorem 2.2.2 in [Nic23] differs from Theorem 4.3 in that it considers a single (conditional) Lipschitz map $\mathcal{G}$. In our case, $\mathcal{G} \circ \Phi$ is Hölder continuous. Furthermore, we can drop an assumption on the uniform boundedness of $\mathcal{G} \circ \Phi$, which plays a role in [Nic23] in the equivalence (4.3) for the random design regression

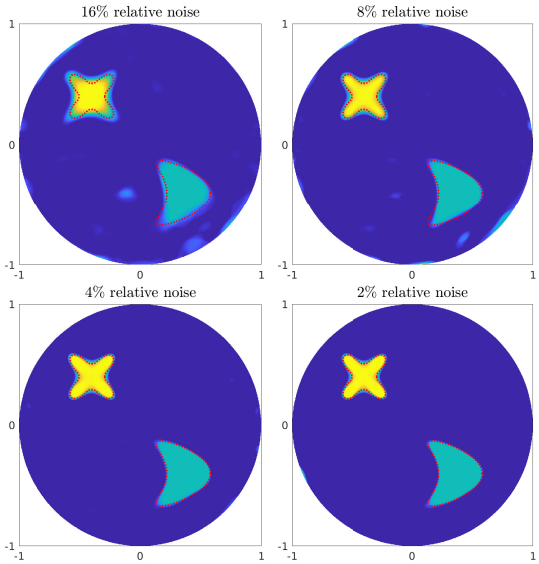

Figure 4.5: Figure 6 in [AKRT23]. Posterior mean estimates of the absorption parameter using the level set parametrization in different noise regimes. The dotted red line indicates the location of γ_0.

model. Finally, compared to Theorem 2.2.3 of [Nic23] we consider conditional continuity only of $\mathcal{G}^{-1}$ and not of $(\mathcal{G} \circ \Phi)^{-1}$. The novelty of Paper B is to show that this extension has relevance in the form of $\Phi_{\text{level},\epsilon}$ and Φ_{star}.

There are several new directions that this research could continue in. Theorem 4.4 and 4.5 and their generalizations to multiple inclusions hold for any forward map satisfying Condition 2. Examples of compatible inverse problems include the Calderón problem in two dimensions, where [CFR10] provides a stability estimate that is permitted for the star-shaped set parametrization, see also [AKRT23, Section 7]. In three dimensions and higher, conditional stability for inclusion detection in the context of the Calderón problem has been considered and shown to be logarithmic at best [ADC05]. The generalization to three dimensions and more complex phantoms is left for future work.

In Paper B, we report that the level set parametrization yields sampling diagnostics that are under performing compared to the star shaped set parametrization. An important direction in the numerical optimization of this approach is to consider gradient based sampling methods. It is also possible that the star-shaped set method could benefit from a layer potential approach to solving the governing PDE for precise computations. This is left for future work.

4.3 Paper C: A Bayesian approach to inverse Robin problems

In Paper C, we consider the Bayesian approach for two nonlinear inverse Robin problems in the random design regression model, i.e. Model 1. We are already familiar with one of them; this is the problem of inverting (1.4). The other is a similar problem arising in a Stokes PDE system. Solving the latter problem plays an important role in initializing large-scale ice sheet models used for sea level predictions, see [AG10]. Further, addressing this problem in a Bayesian framework that allows uncertainty quantification should be of great interest, as it would ultimately lead to sea level predictions with 'error bars'.

In this paper, we aim to show convergence of the posterior mean as the number of observations increase. We will achieve this through posterior consistency in a way that will justify and motivate the choice of prior. Our approach will be to make use of Theorem 4.2. We will restrict ourselves to the prototypical example of the scalar Laplace equation (1.3) and the forward map (1.4), since it is the simpler case. Although it is not straightforward to generalize this to other inverse Robin problems, as we will discuss in Section 4.3.3, we will use these results to motivate the Bayesian approach for inverse Robin problems in general. Indeed, it is not uncommon that results and approaches for the inverse Robin problem for the scalar Laplace equation has been used to motivate an approach for the inverse Robin problem for the Stokes model, see [AG10]. In Paper C, we show that the posterior distribution is well-defined for the Stokes model and thereby show that the Bayesian methodology is at least admissible.

We begin with some assumptions that specifies the setting. These are mostly needed to obtain conditional stability estimates of the form (1.1), as is needed for the effective application of Theorem 4.2. Let $\mathcal{O} \subset \mathbb{R}^2$ and consider in addition the following assumptions.

Assumption 1 (Domain) *We assume $\mathcal{M}_\gamma = (0,1) \times \{0\}$ and define the set $\mathcal{M}_{\gamma,\epsilon} := (\epsilon, 1-\epsilon) \times \{0\}$ for some $0 < \epsilon < 1$. Furthermore, we assume $\partial\mathcal{O}$ is a simple closed curve decomposed into four subarcs oriented as $\mathcal{M}_\gamma$, $\mathcal{M}_0^1$, $\mathcal{M}$, $\mathcal{M}_0^2$, and where $\mathcal{M}_0 = \mathcal{M}_0^1 \cup \mathcal{M}_0^2$.*

We assume $\mathcal{M}_\gamma = (0,1) \times \{0\}$, since we want to avoid defining Gaussian processes on manifolds. Occasionally, we identify $\mathcal{M}_\gamma$ with $(0,1) \subset \mathbb{R}$. The following positivity condition of h might be avoided as in [ADPR03] and is only needed for the second part of Theorem 4.7 below.

Assumption 2 *We assume that h is not identical to a constant and that $h \in H_1 := \{h \in H^{1/2}(\mathcal{M}) : h \geq 0, \|h\|_{H^{1/2}(\mathcal{M})} \leq M_h\}$ for some $M_h > 0$.*

Conditional stability

Under these assumptions the story of Paper C is that different *a priori* insights lead to different convergence properties if we use the right prior distribution. We consider two different *a priori* insights: first, we consider a $\beta(\gamma)$ that has Sobolev regularity. This the case if $\gamma \in \Gamma = H^1(\mathcal{M}_\gamma)$. Second, we consider $\beta = \beta(\gamma)$ that are real analytic on $\mathcal{M}_\gamma$. We make this concrete by defining the following subsets of Γ defined for some $M > 0$:

$$\mathcal{A}_1(M) := \{\gamma \in H^1(\mathcal{M}_\gamma) : \|\gamma\|_{H^1(\mathcal{M}_\gamma)} \leq M\},$$
$$\mathcal{A}_2(M) := \{\gamma \in C^\infty(\overline{\mathcal{M}}_\gamma) : \|\gamma\|_{C(\overline{\mathcal{M}}_\gamma)} \leq M, \sup_{x \in \overline{\mathcal{M}}_\gamma} |(\partial^k \beta)(x)| \leq M(k!)M^k\}.$$

Note that β is real analytic on $\overline{\mathcal{M}}_\gamma$ if and only if $\beta \in C^\infty(\overline{\mathcal{M}}_\gamma)$ with

$$\sup_{x \in \overline{\mathcal{M}}_\gamma} |(\partial^k \beta)(x)| \leq M_\beta (k!) M_\beta^k$$

for some $M_\beta > 0$, see [KP02, Chapter 1]. We can think of $\mathcal{A}_2(M)$ as functions that are 'uniformly' analytic with the added condition $\|\gamma\|_{C(\overline{\mathcal{M}}_\gamma)} \leq M$ to ensure $\gamma \mapsto \beta(\gamma)$ is (locally) Lipschitz continuous in both directions. Under the condition that $\gamma \in \mathcal{A}_j(M)$, $j = 1, 2$, we have the following stability estimates.

Lemma 4.6 (Conditional stability, Lemma 2.4 in [KRS23]) *Let $\mathcal{O}$ satisfy Assumption 1 and h satisfy Assumption 2.*

(i) If $\gamma_i \in \mathcal{A}_1(M)$, $i = 1, 2$, then there exists constants $K_1 > 0$ and $0 < \sigma_1 < 1$ such that

$$\|\gamma_1 - \gamma_2\|_{L^\infty(\mathcal{M}_{\gamma,\epsilon})} \leq K_1 |\log(\|\mathcal{G}(\gamma_1) - \mathcal{G}(\gamma_2)\|_{L^2(\mathcal{M})})|^{-\sigma_1},$$

where K_1 and σ_1 depend only on $\mathcal{O}$, h, m_β, M and ϵ.

(ii) If $\gamma_i \in \mathcal{A}_2(M)$, $i = 1, 2$, then there exists constants $K_2 > 0$ and $0 < \sigma_2 < 1$ such that

$$\|\gamma_1 - \gamma_2\|_{L^2(\mathcal{M}_{\gamma,\epsilon})} \leq K_2 \|\mathcal{G}(\gamma_1) - \mathcal{G}(\gamma_2)\|_{L^2(\mathcal{M})}^{\sigma_2},$$

where K_2 and σ_2 depend $\mathcal{O}$, M_h, M and ϵ.

The first estimate is of the form (1.1) for $\mathcal{A} = H^1(\mathcal{M}_\gamma)$ and is due to [ADPR03]. We can also think of the second estimate is being of the form (1.1) for $\mathcal{A} =$ 'real analytic functions on $\overline{\mathcal{M}}_\gamma$'. This estimate is a modified version of an estimate in [HY15, Theorem 3.1].

Prior distributions

Our next goal is to design prior distributions in Γ that target these two stability regimes. To this end, we consider the $[-\pi, \pi)$-torus $\mathbb{T}$ and a real orthonormal basis $\{\phi_\ell\}_{\ell\in\mathbb{Z}}$ of $L^2(\mathbb{T})$ consisting of $\phi_\ell(x) = 1/\sqrt{\pi}\cos(\ell x)$ for $\ell > 0$, $\phi_\ell(x) = 1/\sqrt{\pi}\sin(\ell x)$ for $\ell < 0$ and $\phi_0 = 1/\sqrt{2\pi}$. Then the random series

$$\tilde{\gamma}_1 = \sum_{\ell\in\mathbb{Z}} g_\ell(1+\ell^2)^{-\delta/2}\phi_\ell, \qquad g_\ell \overset{i.i.d.}{\sim} N(0,1), \tag{4.17}$$

$$\tilde{\gamma}_2 = \sum_{\ell\in\mathbb{Z}} g_\ell e^{-\frac{\delta}{2}\ell^2}\phi_\ell, \qquad g_\ell \overset{i.i.d.}{\sim} N(0,1), \tag{4.18}$$

define Gaussian priors in $L^2(\mathbb{T})$ for the right choice of $\delta > 0$. We have already seen this form of $\tilde{\gamma}_1$ before in Example 4.1 and know it as a Gaussian prior for the Matérn covariance. Then $\tilde{\gamma}_1|_{\mathcal{M}_\gamma} \in H^\alpha(\mathcal{M}_\gamma)$ almost surely for all $\alpha < \delta - 1/2$. Similarly, $\tilde{\gamma}_2|_{\mathcal{M}_\gamma}$ is almost surely an element of the space

$$A_\alpha(\mathcal{M}_\gamma) := \{f = g|_{\mathcal{M}_\gamma} : g \in A_\alpha(\mathbb{T})\},$$

with

$$A_\alpha(\mathbb{T}) := \{f \in L^2(\mathbb{T}) : \|f\|^2_{\alpha,\mathbb{T}} := \sum_{\ell\in\mathbb{Z}} |f_\ell|^2 e^{\alpha\ell^2} < \infty\},$$

for $\alpha < \delta$, where we denote $f_\ell := \langle f, \phi_\ell\rangle_{L^2(\mathbb{T})}$. In Paper C, we establish a relationship between norm balls in $A_\delta(\mathcal{M}_\gamma)$ and the set $\mathcal{A}_2(M)$. This relationship, as part of the lore in Fourier analysis, is well-known as a Paley-Wiener theorem. This allows the use of Lemma 4.6 (ii) in consistency proofs.

We then let Π_1 and Π_2 be the rescaled Gaussian distributions defined by

$$\Pi_1 := \mathcal{L}\left(n^{-1/(4\delta+2)}\tilde{\gamma}_1\right),$$
$$\Pi_2 := \mathcal{L}\left(\log(n)^{-1}\tilde{\gamma}_2\right),$$

which in the first case is simply the rescaling considered in Section 4.1.3 for $a = \delta/(2\delta+1)$.

4.3.1 Main results

In Paper C, we prove the following theorem as the main result.

Theorem 4.7 (Theorem 3.1 in [KRS23]) *Consider the posterior distribution $\Pi_j(\cdot|D_n)$ arising from observations (4.1) in the model (1.4) and prior distributions Π_j, $j = 1, 2$, which are dependent on $\delta > 0$.*

(i) If $\gamma_0 \in H^\delta(\mathcal{M}_\gamma)$, $\delta > 3/2$, then

$$\|E_1[\gamma|D_n] - \gamma_0\|_{L^\infty(\mathcal{M}_{\gamma,\epsilon})} \to 0 \qquad \text{in } P^n_{\gamma_0}\text{-probability}$$

with rate $|\log(Cn^{-\delta/(2\delta+1)})|^{-\sigma}$ for some $0 < \sigma < 1$ and constant $C > 0$ as $n \to \infty$.

(ii) If $\gamma_0 \in A_\delta(\mathcal{M}_\gamma)$, $\delta > 0$, then

$$\|E_2[\gamma|D_n] - \gamma_0\|_{L^2(\mathcal{M}_{\gamma,\epsilon})} \to 0 \qquad \text{in } P^n_{\gamma_0}\text{-probability}$$

with rate $n^{-\sigma/2}\log(n)^\sigma$ for some $0 < \sigma < 1$ as $n \to \infty$.

Note the logarithmic convergence rate of (i) above matches the logarithmic stability of Lemma 4.6 (i), whereas the algebraic rate of (ii) corresponds to the Hölder estimate of Lemma 4.6 (ii). Both parts of Theorem 4.7 are based on Theorem 4.2 and therefore on satisfying Condition A. The first result is an application of a more general result in [MNP21] and [Nic23, Theorem 2.3.2]. They give conditions for the forward map and choice of prior similar to Condition 2 and 3 of Paper B so that Condition A is satisfied. The second result requires new results, which we provide, see [KRS23, Lemma C.4]. These are based on [Nic23, Theorem 2.2.2], but for the rate $n^{-1/2}$ up to a log-factor.

4.3.2 Numerical results

To test the Bayesian approach, we have the following preliminary numerical results. Note these are not included in the current version of Paper C. We consider $\mathcal{O} = (0,1) \times (0, 0.2)$ with $\mathcal{M}_0 = \{0\} \times (0, 0.2) \cup \{1\} \times (0, 0.2)$ and $\mathcal{M} = (0,1) \times \{0.2\}$. Here, we consider a prescribed Neumann condition $h = 10(\sin(12\pi x) + 1)$. Given $\gamma \in L^\infty(\mathcal{M}_\gamma)$, we approximate $u|_\mathcal{M}$ using Fenics [LL16]. We consider two triangular finite element meshes: a fine mesh consisting

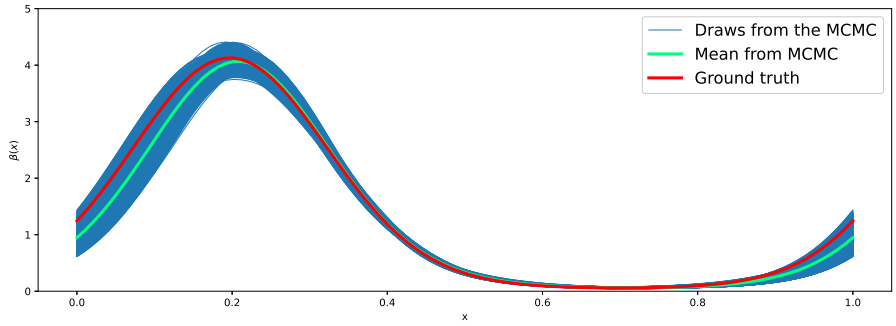

Figure 4.6: Ground truth $\beta(\gamma_0)$ together with the posterior mean and 10^3 posterior samples from a posterior based on the truncated Matérn prior.

of $3.2 \cdot 10^5$ elements, and a coarse mesh consisting $4.5 \cdot 10^3$ elements. We aim at recovering $\beta(\gamma_0) = m_\beta + e^{\gamma_0}$ for

$$\gamma_0 = \sum_{|\ell| \leq 2} \gamma_{0,\ell} \tilde{\phi}_\ell,$$

for $m_\beta = 0$, $\tilde{\phi}_\ell = \sqrt{2}\cos(2\pi\ell x)$ for $\ell > 0$, $\tilde{\phi}_\ell = \sqrt{2}\sin(2\pi\ell x)$ for $\ell < 0$, $\tilde{\phi}_0 = 1$, and

$$(\gamma_{0,0}, \gamma_{0,1}, \gamma_{0,-1}, \gamma_{0,2}, \gamma_{0,-2}) = (-0.57496, 0.68064, 2.01914, 0.11381, -0.07831),$$

which we picked at random.

We deviate from the theoretical setting by considering truncated priors $\tilde{\Pi}_j$, $j = 1, 2$, on the $[0, 1)$-torus, i.e. (4.17) and (4.18), but with ϕ_ℓ replaced by $\tilde{\phi}_\ell$ which is set to zero for $|\ell| > 2$. We note that this is a favorable setting to consider this inverse problem in.

We consider observations of the form (4.1) with $n = 1000$ observations in uniformly random locations at $\mathcal{M}$ and $\varepsilon = 5 \cdot 10^{-2}$. We consider a multilevel MCMC method, Algorithm 2 in [LMS+20], based on the pCN proposal distribution with the step size chosen as $b = \sqrt{2} \cdot 10^{-3}$, see [CRSW13]. After a burn-in of $5 \cdot 10^4$ samples we consider $2.4 \cdot 10^5$ samples in total. Then we base the posterior mean Monte Carlo approximation on 10^3 equidistant samples from this pool.

The resulting posterior mean approximation and samples can be seen in Figure 4.6 and 4.7. Both choices seem to capture the ground truth well. One can

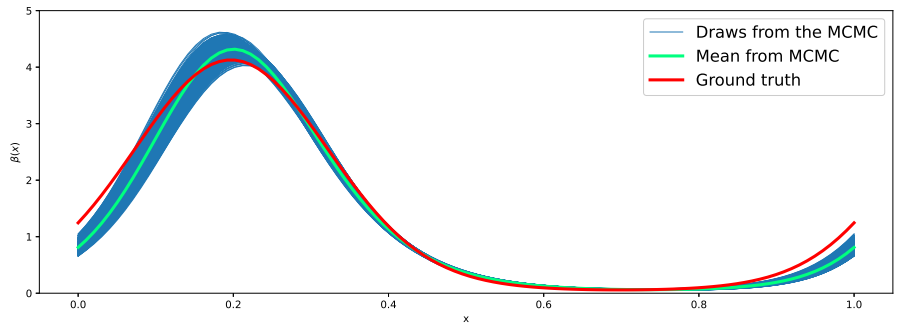

Figure 4.7: Ground truth $\beta(\gamma_0)$ together with the posterior mean and 10^3 posterior samples from a posterior based on the truncated squared exponential prior.

even argue that the posterior samples corresponding to the squared exponential prior are slightly more concentrated than for the Matérn prior. We also note the increased uncertainty near the end points of the interval, which is due to Dirichlet condition at $\mathcal{M}_0$. We believe this numerical example suggests the feasibility of the Bayesian approach to inverse Robin problems.

4.3.3 Discussion and outlook

Theorem 4.7 justifies and quantifies, in the form of a convergence rate, the use of Matérn and squared exponential Gaussian prior distributions in the context of inverse Robin problems. This is a first step in addressing the inverse Robin problems in a Bayesian framework with theoretical guarantees.

Yet, the main theorem does not generalize straightforwardly to the Stokes system of PDEs, see [AG10], which is often used to model ice dynamics. This would require new conditional stability estimates of the form (1.1). The current closest candidate of [BEG13] lacks two things: the right-hand side of the estimate depends on the velocity $u|_{\mathcal{M}}$, but also on the pressure p and its normal derivative at $\mathcal{M}$. This only entails conditional stability if we observe both the velocity and the pressure. The second problem enters in the idea (1.5), where one writes $\beta = -u^{-1}\partial_\nu u$ on $\mathcal{M}_\gamma$ to recover β. Maximum principles for the scalar Laplace equation can be used to conclude $u > 0$ on this set. However, the problem of finding boundary conditions for which this is true for the Stokes system remains, to our knowledge, open, see also [BEG13]. This is why the stability of β in [BEG13] is concluded only on a set $K \subset\subset \mathcal{M}_\gamma$ on which u does

not vanish. This set is not *a priori* known. Whether this estimate can be made independent of the pressure p and its normal derivative $\partial_\nu p|_{\mathcal{M}}$ at $\mathcal{M}$, we leave as a future challenge.

The use of rescaled Gaussian priors targeting analytic functions in the context of posterior consistency for nonlinear inverse problems is new. The theoretical backbone, [KRS23, Lemma C.4], extends straightforwardly to domains $\mathcal{M}_\gamma$ that are subsets $[0,1)^2 \times \{0\}$. Therefore, this result may be of interest in posterior consistency analyses for other inverse problems involving analytic functions. Another direction left for future work is to generalize this to a larger class of analytic functions on $\mathcal{M}_\gamma$ using Gaussian processes and a continuous version of the Paley-Wiener theorem. For ideas in this direction we refer to [vdVvZ09]. Also, in [vdVvZ09] the time-scale parameter of the prior process is adjusted by a 'hyperprior' providing a consistent method, which achieves the optimal rate for a given smoothness of γ_0. Whether this hierarchical approach is compatible with consistency in a nonlinear inverse problem setting remains an interesting question. There are some results in this direction, see [GN20], where the truncation of the prior series (for example (4.17)) is chosen as a random variable.

Finally, completing a numerical example in a less favorable setting and for different choices of n for both the problem in the scalar Laplace model and the Stokes model is left for future work. We expect to see a difference in the convergence properties of the posterior distributions corresponding to the two different priors, if we try to infer a larger number of coefficients and consider a prior truncated at a higher level.

Chapter 5

Concluding remarks

This thesis begins with the presentation of nonlinear ill-posed inverse problems. We have posed question 5′ on what prior information would give rise to consistent reconstruction methods for a given nonlinear inverse problem. This question has been addressed in three different settings and from two perspectives: the perspective of regularization theory and the Bayesian perspective.

1. In the context of the three-dimensional Calderón problem, the prior information of knowing that γ_0 is lower bounded away from zero, has a bounded C^2-norm and is 1 near the boundary, is enough to reconstruct it with a consistent method. In fact, the direct method based on the truncated CGO reconstruction (Method 1) is an admissible regularization strategy. Future work includes incorporating additional prior information in this method.

2. For a given nonlinear inverse problem, the problem of detecting inclusions can be addressed in a Bayesian framework. The prior information that the inclusions are regular is often enough to reconstruct them with a consistent and stable method arising as the posterior mean. For success, we require that the given inverse problem is conditionally well-posed for inclusions that are sufficiently smooth. This is the case for a number of inverse problems including a quantitative photoacoustic tomography problem and Calderón's problem, where the former was considered in Paper

B. Future work includes generalizing the setting of Paper B to other parametrizations and inverse problems.

3. In the Bayesian approach to inverse Robin problems that we consider in this thesis, we distinguish between two pieces of prior information. For real analytic Robin coefficients, the posterior mean is consistent with a fast convergence rate given that a prior distribution that targets analyticity is used. This rate is better than the logarithmic rate, which is obtained for Sobolev smooth coefficients. Also, the approach for recovering real analytic parameters generalize to other inverse problems.

In this thesis, we have noted parallels between the regularization theory perspective and the Bayesian perspective. There is the classical relationship of MAP estimation and generalized Tikhonov regularization. Also, we can often consider the posterior mean as an admissible regularization strategy. Conditional stability estimates become relevant in consistency with explicit rates in both worlds as we have noted in Section 2.1. Studying further the relationship between theoretical conditions for posterior consistency and computation, see [NW22], and classical conditions for convergence of regularization strategies, such as [EHN96, Theorem 10.4], pose a great challenge for future work.

Constructing consistent methods that 'adapts', see [vdVvZ09], to the smoothness of γ_0 in convergence rate is a formidable new challenge in consistency analysis for nonlinear inverse problems. It is possible that a hierarchical Bayesian approach in the direction of [vdVvZ09] and [GN20] can achieve this. This would bridge a gap between theory and the popular use of hierarchical Bayesian methods in practice.

The development of consistency analysis in nonlinear Bayesian inverse problems is still in its early stages. Yet, great strides have been made towards general and 'easily' verifiable conditions for consistency. Continuing this progress towards prior distributions and models used by the inverse problems community continue to be a worthy and important objective.

Bibliography

[AB06] Charalambos D. Aliprantis and Kim C. Border. *Infinite dimensional analysis*. Springer, Berlin, third edition, 2006. A hitchhiker's guide.

[Abr20] Luke Kweku William Abraham. *Consistency of nonparametric Bayesian methods for two statistical inverse problems arising from partial differential equations*. PhD thesis, University of Cambridge, 2020.

[ACL+20] J. P. Agnelli, A. Cöl, M. Lassas, R. Murthy, M. Santacesaria, and S. Siltanen. Classification of stroke using neural networks in electrical impedance tomography. *Inverse Problems*, 36(11):115008, 2020.

[ADC05] G. Alessandrini and M. Di Cristo. Stable determination of an inclusion by boundary measurements. *SIAM J. Math. Anal.*, 37(1):200–217, 2005.

[ADCFV17] Giovanni Alessandrini, Michele Di Cristo, Elisa Francini, and Sergio Vessella. Stability for quantitative photoacoustic tomography with well-chosen illuminations. *Ann. Mat. Pura Appl. (4)*, 196(2):395–406, 2017.

[ADH21] Sergios Agapiou, Masoumeh Dashti, and Tapio Helin. Rates of contraction of posterior distributions based on p-exponential priors. *Bernoulli*, 27(3):1616–1642, 2021.

[ADPR03] G. Alessandrini, L. Del Piero, and L. Rondi. Stable determination of corrosion by a single electrostatic boundary measurement. *Inverse Problems*, 19(4):973–984, 2003.

[AG10] Robert J. Arthern and G. Hilmar Gudmundsson. Initialization of ice-sheet forecasts viewed as an inverse Robin problem. *Journal of Glaciology*, 56(197):527–533, 8 2010.

[AKRT23] Babak Maboudi Afkham, Kim Knudsen, Aksel Kaastrup Rasmussen, and Tanja Tarvainen. A Bayesian approach for consistent reconstruction of inclusions. *arXiv preprint arXiv:2308.13673*, 2023. In submission.

[Ale88] Giovanni Alessandrini. Stable determination of conductivity by boundary measurements. *Appl. Anal.*, 27(1-3):153–172, 1988.

[ALS13] Sergios Agapiou, Stig Larsson, and Andrew M. Stuart. Posterior contraction rates for the Bayesian approach to linear ill-posed inverse problems. *Stochastic Process. Appl.*, 123(10):3828–3860, 2013.

[AM16] Melody Alsaker and Jennifer L. Mueller. A D-bar algorithm with a priori information for 2-dimensional electrical impedance tomography. *SIAM J. Imaging Sci.*, 9(4):1619–1654, 2016.

[AN19] Kweku Abraham and Richard Nickl. On statistical Calderón problems. *Math. Stat. Learn.*, 2(2):165–216, 2019.

[AP06] Kari Astala and Lassi Päivärinta. Calderón's inverse conductivity problem in the plane. *Ann. of Math. (2)*, 163(1):265–299, 2006.

[Apo74] Tom M Apostol. *Mathematical analysis; 2nd ed.* Addison-Wesley series in mathematics. Addison-Wesley, Reading, MA, 1974.

[ARRV09] Giovanni Alessandrini, Luca Rondi, Edi Rosset, and Sergio Vessella. The stability for the Cauchy problem for elliptic equations. *Inverse Problems*, 25(12):123004, 47, 2009.

[Art15] Robert J. Arthern. Exploring the use of transformation group priors and the method of maximum relative entropy for bayesian glaciological inversions. *Journal of Glaciology*, 61(229):947–962, 2015.

[ASK22] Anuj Abhishek, Thilo Strauss, and Taufiquar Khan. An optimal Bayesian estimator for absorption coefficient in diffuse optical tomography. *SIAM J. Imaging Sci.*, 15(2):797–821, 2022.

[AT07] Robert J. Adler and Jonathan E. Taylor. *Random fields and geometry*. Springer Monographs in Mathematics. Springer, New York, 2007.

[AW21] Sergios Agapiou and Sven Wang. Laplace priors and spatial inhomogeneity in Bayesian inverse problems. *arXiv preprint arXiv:2112.05679*, 2021.

[BCT22] Eric Bonnetier, Mourad Choulli, and Faouzi Triki. Stability for quantitative photoacoustic tomography revisited. *Res. Math. Sci.*, 9(2):Paper No. 24, 30, 2022.

[BEG13] Muriel Boulakia, Anne Claire Egloffe, and Céline Grandmont. Stability estimates for the unique continuation property of the Stokes system and for an inverse boundary coefficient problem. *Inverse Problems*, 29(11), 11 2013.

[BHM04] Nicolai Bissantz, Thorsten Hohage, and Axel Munk. Consistency and rates of convergence of nonlinear Tikhonov regularization with random noise. *Inverse Problems*, 20(6):1773–1789, 2004.

[BHV03] Martin Brühl, Martin Hanke, and Michael S. Vogelius. A direct impedance tomography algorithm for locating small inhomogeneities. *Numer. Math.*, 93(4):635–654, 2003.

[BKIS09] Gregory Boverman, Tzu Jen Kao, David Isaacson, and Gary J. Saulnier. An implementation of Calderón's method for 3-D Limited-View EIT. *IEEE Transactions on Medical Imaging*, 28(7), 2009.

[BKM11] Jutta Bikowski, Kim Knudsen, and Jennifer L. Mueller. Direct numerical reconstruction of conductivities in three dimensions using scattering transforms. *Inverse Problems*, 27(1):015002, 19, 2011.

[BNVP21] O. Babaniyi, R. Nicholson, U. Villa, and N. Petra. Inferring the basal sliding coefficient field for the stokes ice sheet model under rheological uncertainty. *The Cryosphere*, 15(4):1731–1750, 2021.

[BRUZ11] Guillaume Bal, Kui Ren, Gunther Uhlmann, and Ting Zhou. Quantitative thermo-acoustics and related problems. *Inverse Problems*, 27(5):055007, 15, 2011.

[BTG14] Tan Bui-Thanh and Omar Ghattas. An analysis of infinite dimensional bayesian inverse shape acoustic scattering and its numerical approximation. *SIAM/ASA Journal on Uncertainty Quantification*, 2(1):203–222, 2014.

[BU10] Guillaume Bal and Gunther Uhlmann. Inverse diffusion theory of photoacoustics. *Inverse Problems*, 26(8):085010, 20, 2010.

[Cal80] A. P. Calderón. On an inverse boundary value problem. In *Seminar on Numerical Analysis and its Applications to Continuum Physics*, pages 65–73. Soc. Brasileira de Matematica, Rio de Janeiro, 1980.

[CFMV98] D. J. Cedio-Fengya, S. Moskow, and M. S. Vogelius. Identification of conductivity imperfections of small diameter by boundary measurements. Continuous dependence and computational reconstruction. *Inverse Problems*, 14(3):553–595, 1998.

[CFR10] Albert Clop, Daniel Faraco, and Alberto Ruiz. Stability of Calderón's inverse conductivity problem in the plane for discontinuous conductivities. *Inverse Probl. Imaging*, 4(1):49–91, 2010.

[Cho21] Mourad Choulli. Some stability inequalities for hybrid inverse problems. *C. R. Math. Acad. Sci. Paris*, 359:1251–1265, 2021.

[CJ99] Slim Chaabane and Mohamed Jaoua. Identification of Robin coefficients by the means of boundary measurements. *Inverse Problems*, 15(6):1425–1438, 1999.

[CK19] David Colton and Rainer Kress. *Inverse acoustic and electromagnetic scattering theory*, volume 93 of *Applied Mathematical Sciences*. Springer, Cham, fourth edition, 2019.

[CKK+01] V Cherepenin, A Karpov, A Korjenevsky, V Kornienko, A Mazaletskaya, D Mazourov, and D Meister. A 3d electrical impedance tomography (EIT) system for breast cancer detection. *Physiological Measurement*, 22(1):9–18, feb 2001.

[CKS06] H. Cornean, K. Knudsen, and S. Siltanen. Towards a d-bar reconstruction method for three-dimensional EIT. *J. Inverse Ill-Posed Probl.*, 14(2):111–134, 2006.

[CLM16] Tiangang Cui, Kody J. H. Law, and Youssef M. Marzouk. Dimension-independent likelihood-informed MCMC. *J. Comput. Phys.*, 304:109–137, 2016.

[CR16] Pedro Caro and Keith M. Rogers. Global uniqueness for the Calderón problem with Lipschitz conductivities. *Forum Math. Pi*, 4:e2, 28, 2016.

[CRSW13] S. L. Cotter, G. O. Roberts, A. M. Stuart, and D. White. MCMC methods for functions: modifying old algorithms to make them faster. *Statist. Sci.*, 28(3):424–446, 2013.

[DCR03] Michele Di Cristo and Luca Rondi. Examples of exponential instability for inverse inclusion and scattering problems. *Inverse Problems*, 19(3):685–701, 2003.

[DDDM04] Ingrid Daubechies, Michel Defrise, and Christine De Mol. An iterative thresholding algorithm for linear inverse problems with a sparsity constraint. *Comm. Pure Appl. Math.*, 57(11):1413–1457, 2004.

[DHK12] Fabrice Delbary, Per Christian Hansen, and Kim Knudsen. Electrical impedance tomography: 3D reconstructions using scattering transforms. *Applicable Analysis*, 91(4):737–755, 2012.

[dHQS12] Maarten V. de Hoop, Lingyun Qiu, and Otmar Scherzer. Local analysis of inverse problems: Hölder stability and iterative reconstruction. *Inverse Problems*, 28(4):045001, 16, 2012.

[DIS17] Matthew M. Dunlop, Marco A. Iglesias, and Andrew M. Stuart. Hierarchical Bayesian level set inversion. *Stat. Comput.*, 27(6):1555–1584, 2017.

[DK14] Fabrice Delbary and Kim Knudsen. Numerical nonlinear complex geometrical optics algorithm for the 3D Calderón problem. *Inverse Probl. Imaging*, 8(4):991–1012, 2014.

[DKRH22] Fabrice Delbary, Kim Knudsen, Aksel Kaastrup Rasmussen, and Per Christian Hansen. crEITive. `https://github.com/akselkaastras/crEITive`, 2022.

[Dob92] David C. Dobson. Convergence of a reconstruction method for the inverse conductivity problem. *SIAM J. Appl. Math.*, 52(2):442–458, 1992.

[DP06] Giuseppe Da Prato. *An introduction to infinite-dimensional analysis*. Universitext. Springer-Verlag, Berlin, 2006. Revised and extended from the 2001 original by Da Prato.

[DPZ14] Giuseppe Da Prato and Jerzy Zabczyk. *Stochastic equations in infinite dimensions*, volume 152 of *Encyclopedia of Mathematics and its Applications*. Cambridge University Press, Cambridge, second edition, 2014.

[DS16] Matthew M. Dunlop and Andrew M. Stuart. The Bayesian formulation of EIT: analysis and algorithms. *Inverse Probl. Imaging*, 10(4):1007–1036, 2016.

[DS17] Masoumeh Dashti and Andrew M. Stuart. The Bayesian approach to inverse problems. In *Handbook of uncertainty quantification. Vol. 1, 2, 3*, pages 311–428. Springer, Cham, 2017.

[DU77] J. Diestel and J. J. Uhl, Jr. *Vector measures*. Mathematical Surveys, No. 15. American Mathematical Society, Providence, R.I., 1977. With a foreword by B. J. Pettis.

[Dud02] R. M. Dudley. *Real analysis and probability*, volume 74 of *Cambridge Studies in Advanced Mathematics*. Cambridge University Press, Cambridge, 2002. Revised reprint of the 1989 original.

[EHN96] Heinz W. Engl, Martin Hanke, and Andreas Neubauer. *Regularization of inverse problems*, volume 375 of *Mathematics and its Applications*. Kluwer Academic Publishers Group, Dordrecht, 1996.

[FI99] Dario Fasino and Gabriele Inglese. An inverse Robin problem for Laplace's equation: theoretical results and numerical methods. *Inverse Problems*, 15(1):41–48, 1999. Conference on Inverse Problems, Control and Shape Optimization (Carthage, 1998).

[FR13] Daniel Faraco and Keith M. Rogers. The Sobolev norm of characteristic functions with applications to the Calderón inverse problem. *Q. J. Math.*, 64(1):133–147, 2013.

[FS12] Jean-Pierre Florens and Anna Simoni. Regularized posteriors in linear ill-posed inverse problems. *Scand. J. Stat.*, 39(2):214–235, 2012.

[Gar16] Henrik Garde. *Prior Information in Inverse Boundary Problems*. PhD thesis, Technical University of Denmark, 2016.

[GGvdV00] Subhashis Ghosal, Jayanta K. Ghosh, and Aad W. van der Vaart. Convergence rates of posterior distributions. *The Annals of Statistics*, 28(2):500 – 531, 2000.

[GN16] Evarist Giné and Richard Nickl. *Mathematical foundations of infinite-dimensional statistical models*. Cambridge Series in Statistical and Probabilistic Mathematics. Cambridge University Press, New York, 2016.

[GN20] Matteo Giordano and Richard Nickl. Consistency of Bayesian inference with Gaussian process priors in an elliptic inverse problem. *Inverse Problems*, 36(8):085001, 35, 2020.

[Gri85] P. Grisvard. *Elliptic problems in nonsmooth domains*, volume 24 of *Monographs and Studies in Mathematics*. Pitman (Advanced Publishing Program), Boston, MA, 1985.

[GvdV17] Subhashis Ghosal and Aad van der Vaart. *Fundamentals of nonparametric Bayesian inference*, volume 44 of *Cambridge Series in Statistical and Probabilistic Mathematics*. Cambridge University Press, Cambridge, 2017.

[Hab15] Boaz Haberman. Uniqueness in Calderón's problem for conductivities with unbounded gradient. *Comm. Math. Phys.*, 340(2):639–659, 2015.

[Had53] Jacques Hadamard. *Lectures on Cauchy's problem in linear partial differential equations*. Dover Publications, New York, 1953.

[Hai09] Martin Hairer. An introduction to stochastic pdes. *arXiv preprint arXiv:0907.4178*, 2009.

[Has70] W. K. Hastings. Monte carlo sampling methods using Markov chains and their applications. *Biometrika*, 57(1):97–109, 1970.

[HIK+21] Sarah J. Hamilton, David Isaacson, Ville Kolehmainen, Peter A. Muller, Jussi Toivainen, and Patrick F. Bray. 3D electrical impedance tomography reconstructions from simulated electrode data using direct inversion t^{exp} and Calderón methods. *Inverse Probl. Imaging*, 15(5):1135–1169, 2021.

[HMI+22] S J Hamilton, P A Muller, D Isaacson, V Kolehmainen, J Newell, O Rajabi Shishvan, G Saulnier, and J Toivanen. Fast absolute 3d cgo-based electrical impedance tomography on experimental tank data. *Physiological Measurement*, 43(12):124001, dec 2022.

[HSPG14] Milad Hallaji, Aku Seppänen, and Mohammad Pour-Ghaz. Electrical impedance tomography-based sensing skin for quantitative imaging of damage in concrete. *Smart Materials and Structures*, 23(8):085001, jun 2014.

[HU13] Bastian Harrach and Marcel Ullrich. Monotonicity-based shape reconstruction in electrical impedance tomography. *SIAM J. Math. Anal.*, 45(6):3382–3403, 2013.

[HY15] Guanghui Hu and Masahiro Yamamoto. Hölder stability estimate of Robin coefficient in corrosion detection with a single boundary measurement. *Inverse Problems*, 31(11):115009, 20, 2015.

[ILS16] Marco A. Iglesias, Yulong Lu, and Andrew Stuart. A Bayesian level set method for geometric inverse problems. *Interfaces Free Bound.*, 18(2):181–217, 2016.

[IMNS04] D. Isaacson, J.L. Mueller, J.C. Newell, and S. Siltanen. Reconstructions of chest phantoms by the D-bar method for electrical impedance tomography. *IEEE Transactions on Medical Imaging*, 23(7):821–828, 2004.

[Ing97] Gabriele Inglese. An inverse problem in corrosion detection. *Inverse Problems*, 13(4):977–994, 1997.

[Isa88] Victor Isakov. On uniqueness of recovery of a discontinuous conductivity coefficient. *Comm. Pure Appl. Math.*, 41(7):865–877, 1988.

[Jin07] Bangti Jin. Conjugate gradient method for the Robin inverse problem associated with the Laplace equation. *Internat. J. Numer. Methods Engrg.*, 71(4):433–453, 2007.

[JM12] Bangti Jin and Peter Maass. An analysis of electrical impedance tomography with applications to Tikhonov regularization. *ESAIM Control Optim. Calc. Var.*, 18(4):1027–1048, 2012.

[Kah85] Jean-Pierre Kahane. *Some random series of functions*, volume 5 of *Cambridge Studies in Advanced Mathematics*. Cambridge University Press, Cambridge, second edition, 1985.

[Kek22] Hanne Kekkonen. Consistency of Bayesian inference with Gaussian process priors for a parabolic inverse problem. *Inverse Problems*, 38(3):035002, 29, 2022.

[Kin22] Stefan Kindermann. On the tangential cone condition for electrical impedance tomography. *Electron. Trans. Numer. Anal.*, 57:17–34, 2022.

[Kir11] Andreas Kirsch. *An introduction to the mathematical theory of inverse problems*, volume 120 of *Applied Mathematical Sciences*. Springer, New York, second edition, 2011.

[KKSV00] Jari P. Kaipio, Ville Kolehmainen, Erkki Somersalo, and Marko Vauhkonen. Statistical inversion and Monte Carlo sampling methods in electrical impedance tomography. *Inverse Problems*, 16(5):1487–1522, 2000.

[KLMS09] Kim Knudsen, Matti Lassas, Jennifer L. Mueller, and Samuli Siltanen. Regularized D-bar method for the inverse conductivity problem. *Inverse Probl. Imaging*, 3(4):599–624, 2009.

[KLS14] Hanne Kekkonen, Matti Lassas, and Samuli Siltanen. Analysis of regularized inversion of data corrupted by white Gaussian noise. *Inverse Problems*, 30(4):045009, 18, 2014.

[KLS16] Hanne Kekkonen, Matti Lassas, and Samuli Siltanen. Posterior consistency and convergence rates for Bayesian inversion with hypoelliptic operators. *Inverse Problems*, 32(8):085005, 31, 2016.

[KM11] Kim Knudsen and Jennifer L. Mueller. The Born approximation and Calderón's method for reconstruction of conductivities in 3-D. *Discrete Contin. Dyn. Syst.*, pages 844–853, 2011.

[KNS08] Barbara Kaltenbacher, Andreas Neubauer, and Otmar Scherzer. *Iterative regularization methods for nonlinear ill-posed problems*, volume 6 of *Radon Series on Computational and Applied Mathematics*. Walter de Gruyter GmbH & Co. KG, Berlin, 2008.

[Knu02] Kim Knudsen. *On the inverse conductivity problem*. PhD thesis, Aalborg Universitet, 2002.

[KP02] Steven G. Krantz and Harold R. Parks. *A primer of real analytic functions*. Birkhäuser Advanced Texts: Basler Lehrbücher. [Birkhäuser Advanced Texts: Basel Textbooks]. Birkhäuser Boston, Inc., Boston, MA, second edition, 2002.

[KR22a] Kim Knudsen and Aksel Kaastrup Rasmussen. Direct method for stroke detection with electrical impedance tomography in three dimensions. Technical report, Department of Applied Mathematics and Computer Science, Technical University of Denmark, 2022.

[KR22b] Kim Knudsen and Aksel Kaastrup Rasmussen. Direct regularized reconstruction for the three-dimensional Calderón problem. *Inverse Probl. Imaging*, 16(4):871–894, 2022.

[KRS21] Herbert Koch, Angkana Rüland, and Mikko Salo. On instability mechanisms for inverse problems. *Ars Inven. Anal.*, pages Paper No. 7, 93, 2021.

[KRS23] Ieva Kazlauskaite, Aksel Kaastrup Rasmussen, and Fanny Seizilles. The Bayesian approach to inverse Robin problems. In preparation, 2023.

[KS05] Jari Kaipio and Erkki Somersalo. *Statistical and computational inverse problems*, volume 160 of *Applied Mathematical Sciences*. Springer-Verlag, New York, 2005.

[KS23] Kristin Kirchner and Christoph Schwab. Monte Carlo convergence rates for kth moments in Banach spaces. *arXiv preprint arXiv:2212.03797*, 2023.

[Kuc12] Peter Kuchment. Mathematics of hybrid imaging: A brief review. In Irene Sabadini and Daniele C Struppa, editors, *The Mathematical Legacy of Leon Ehrenpreis*, pages 183–208, Milano, 2012. Springer Milan.

[KV87] Robert V. Kohn and Michael Vogelius. Relaxation of a variational method for impedance computed tomography. *Comm. Pure Appl. Math.*, 40(6):745–777, 1987.

[KvdVvZ11] B. T. Knapik, A. W. van der Vaart, and J. H. van Zanten. Bayesian inverse problems with Gaussian priors. *The Annals of Statistics*, 39(5):2626 – 2657, 2011.

[Lat20] Jonas Latz. On the well-posedness of Bayesian inverse problems. *SIAM/ASA J. Uncertain. Quantif.*, 8(1):451–482, 2020.

[Lio04] William R B Lionheart. EIT reconstruction algorithms: pitfalls, challenges and recent developments. *Physiological Measurement*, 25(1):125, feb 2004.

[LL16] Hans Petter Langtangen and Anders Logg. *Solving PDEs in Python*, volume 3 of *Simula SpringerBriefs on Computing*. Springer, Cham, 2016. The FEniCS tutorial I.

[LMP03] Michael Lukaschewitsch, Peter Maass, and Michael Pidcock. Tikhonov regularization for electrical impedance tomography on unbounded domains. *Inverse Problems*, 19(3):585–610, 2003.

[LMS+20] Mikkel B. Lykkegaard, Grigorios Mingas, Robert Scheichl, Colin Fox, and Tim J. Dodwell. Multilevel delayed acceptance MCMC with an adaptive error model in PyMC3. *arXiv preprint arXiv:2012.0566*, 2020.

[LN17] Jijun Liu and Gen Nakamura. Recovering the boundary corrosion from electrical potential distribution using partial boundary data. *Inverse Probl. Imaging*, 11(3):521–538, 2017.

[LR08] A. Lechleiter and A. Rieder. Newton regularizations for impedance tomography: Convergence by local injectivity. *Inverse Problems*, 24(6):065009, 18, 2008.

[LSS09] Matti Lassas, Eero Saksman, and Samuli Siltanen. Discretization-invariant Bayesian inversion and Besov space priors. *Inverse Probl. Imaging*, 3(1):87–122, 2009.

[Man01] Niculae Mandache. Exponential instability in an inverse problem for the Schrödinger equation. *Inverse Problems*, 17(5):1435–1444, 2001.

[MJA+14] Emma Malone, Markus Jehl, Simon Arridge, Timo Betcke, and David Holder. Stroke type differentiation using spectrally constrained multifrequency EIT: Evaluation of feasibility in a realistic head model. *Physiological Measurement*, 35(6):1051–1066, 2014.

[MNP21] François Monard, Richard Nickl, and Gabriel P. Paternain. Consistent inversion of noisy non-Abelian X-ray transforms. *Comm. Pure Appl. Math.*, 74(5):1045–1099, 2021.

[MRR+53] Nicholas Metropolis, Arianna W. Rosenbluth, Marshall N. Rosenbluth, Augusta H. Teller, and Edward Teller. Equation of state calculations by fast computing machines. *The Journal of Chemical Physics*, 21(6):1087–1092, 1953.

[Nac88] Adrian I. Nachman. Reconstructions from boundary measurements. *Ann. of Math. (2)*, 128(3):531–576, 1988.

[Nac96] Adrian I. Nachman. Global uniqueness for a two-dimensional inverse boundary value problem. *Ann. of Math. (2)*, 143(1):71–96, 1996.

[Nic20] Richard Nickl. Bernstein–von Mises theorems for statistical inverse problems I: Schrödinger equation. *J. Eur. Math. Soc. (JEMS)*, 22(8):2697–2750, 2020.

[Nic23] Richard Nickl. *Bayesian non-linear statistical inverse problems*. Zurich Lectures in Advanced Mathematics. EMS Press, Berlin, 2023.

[NN22] Ruanui Nicholson and Matti Niskanen. Joint estimation of Robin coefficient and domain boundary for the Poisson problem. *Inverse Problems*, 38(1):015008, 23, 2022.

[NPK18] Ruanui Nicholson, Noémi Petra, and Jari P. Kaipio. Estimation of the Robin coefficient field in a Poisson problem with uncertain conductivity field. *Inverse Problems*, 34(11):115005, 26, 2018.

[NvdGW20] Richard Nickl, Sara van de Geer, and Sven Wang. Convergence rates for penalized least squares estimators in PDE constrained regression problems. *SIAM/ASA J. Uncertain. Quantif.*, 8(1):374–413, 2020.

[NW22] Richard Nickl and Sven Wang. On polynomial-time computation of high-dimensional posterior measures by langevin-type algorithms. *J. Eur. Math. Soc.*, December 2022.

[Pol02] David Pollard. *A user's guide to measure theoretic probability*, volume 8 of *Cambridge Series in Statistical and Probabilistic Mathematics*. Cambridge University Press, Cambridge, 2002.

[Ras23] Aksel Kaastrup Rasmussen. Bayesian inclusion detection for quantitative photoacoustic tomography. `https://github.com/akselkaastras/inclusion-qPAT`, 2023.

[RAU+23] Nicolai Riis, Amal Alghamdi, Felipe Uribe, Silja Christensen, Babak Afkham, Per Christian Hansen, and Jakob Jorgensen. CUQIpy – Part I: Computational uncertainty quantification for

inverse problems in Python. *arXiv preprint arXiv:2305.16949*, 05 2023.

[Ray13] Kolyan Ray. Bayesian inverse problems with non-conjugate priors. *Electron. J. Stat.*, 7:2516–2549, 2013.

[RC04] Christian P. Robert and George Casella. *Monte Carlo statistical methods*. Springer Texts in Statistics. Springer-Verlag, New York, second edition, 2004.

[RF10] H.L. Royden and P. Fitzpatrick. *Real analysis*. Prentice Hall, Boston, fourth edition, 2010.

[RHL14] Lassi Roininen, Janne M. J. Huttunen, and Sari Lasanen. Whittle-Matérn priors for Bayesian statistical inversion with applications in electrical impedance tomography. *Inverse Probl. Imaging*, 8(2):561–586, 2014.

[Ric16] Mathias Richter. *Inverse problems—basics, theory and applications in geophysics*. Lecture Notes in Geosystems Mathematics and Computing. Birkhäuser/Springer, Cham, 2016.

[Ron08] L. Rondi. On the regularization of the inverse conductivity problem with discontinuous conductivities. *Inverse Problems and Imaging*, 2(3):397–409, 2008.

[Ron16] L. Rondi. Discrete approximation and regularisation for the inverse conductivity problem. *Rend. Istit. Mat. Univ. Trieste*, 48:315–352, 2016.

[RR04] Gareth O. Roberts and Jeffrey S. Rosenthal. General state space Markov chains and MCMC algorithms. *Probab. Surv.*, 1:20–71, 2004.

[San96] Fadil Santosa. A level-set approach for inverse problems involving obstacles. *ESAIM Contrôle Optim. Calc. Var.*, 1:17–33, 1995/96.

[SGG+09] Otmar Scherzer, Markus Grasmair, Harald Grossauer, Markus Haltmeier, and Frank Lenzen. *Variational methods in imaging*, volume 167 of *Applied Mathematical Sciences*. Springer, New York, 2009.

[Stu10] A. M. Stuart. Inverse problems: a Bayesian perspective. *Acta Numer.*, 19:451–559, 2010.

[SU88] J Sylvester and G Uhlmann. Inverse boundary-value problems at the boundary - continuous dependence. *Communications on Pure and Applied Mathematics*, 41(2):197–219, 1988.

[Tay11] Michael E. Taylor. *Partial differential equations I. Basic theory*, volume 115 of *Applied Mathematical Sciences*. Springer, New York, second edition, 2011.

[TGS90] W.M. Telford, L.P. Geldart, and R.E. Sheriff. *Applied Geophysics*. Cambridge University Press, Cambridge, 2nd ed. edition, 1990.

[vdV98] A. W. van der Vaart. *Asymptotic statistics*, volume 3 of *Cambridge Series in Statistical and Probabilistic Mathematics*. Cambridge University Press, Cambridge, 1998.

[vdVvZ09] A. W. van der Vaart and J. H. van Zanten. Adaptive Bayesian estimation using a Gaussian random field with inverse gamma bandwidth. *Ann. Statist.*, 37(5B):2655–2675, 2009.

[Vol13] Sebastian J. Vollmer. Posterior consistency for Bayesian inverse problems through stability and regression results. *Inverse Problems*, 29(12):125011, 32, 2013.

Appendix A

Paper A

The following is an exact reproduction of the paper titled *Direct regularized reconstruction for the three-dimensional Calderón problem* by Kim Knudsen and Aksel Kaastrup Rasmussen, published in Inverse Problems and Imaging, 16(4):871–894, 2022.

Inverse Problems and Imaging
Vol. 16, No. 4, August 2022, pp. 871–894
doi:10.3934/ipi.2022002

DIRECT REGULARIZED RECONSTRUCTION FOR THE THREE-DIMENSIONAL CALDERÓN PROBLEM

Kim Knudsen and Aksel Kaastrup Rasmussen*

Technical University of Denmark
Department of Applied Mathematics and Computer Science
DK-2800 Kgs. Lyngby, Denmark

(Communicated by Mikko Salo)

Abstract. Electrical Impedance Tomography gives rise to the severely ill-posed Calderón problem of determining the electrical conductivity distribution in a bounded domain from knowledge of the associated Dirichlet-to-Neumann map for the governing equation. The uniqueness and stability questions for the three-dimensional problem were largely answered in the affirmative in the 1980's using complex geometrical optics solutions, and this led further to a direct reconstruction method relying on a non-physical scattering transform. In this paper, the reconstruction problem is taken one step further towards practical applications by considering data contaminated by noise. Indeed, a regularization strategy for the three-dimensional Calderón problem is presented based on a suitable and explicit truncation of the scattering transform. This gives a certified, stable and direct reconstruction method that is robust to small perturbations of the data. Numerical tests on simulated noisy data illustrate the feasibility and regularizing effect of the method, and suggest that the numerical implementation performs better than predicted by theory.

1. **Introduction.** Electrical Impedance Tomography (EIT) provides a noninvasive method of obtaining information on the electrical conductivity distribution of electric conductive media from exterior electrostatic measurements of currents and voltages. There are many applications in medical imaging including early detection of breast cancer [13, 58], hemorrhagic stroke detection [40, 24], pulmonary function monitoring [2, 22, 38] and targeting control in transcranial brain stimulation [52]. Applications also include industrial testing, for example, crack damage detection in cementitious structures [28, 25], and subsurface geophysical imaging [57]. The mathematical problem of EIT is called the Calderón problem and was first formulated by A.P. Calderón in 1980 [10] as follows: Consider a bounded Lipschitz domain $\Omega \subset \mathbb{R}^3$ filled with a conductor with a distribution $\gamma \in L^\infty(\Omega)$, $\gamma \geq c > 0$. Under the assumption of no sinks or sources of current in the domain, applying an electrical surface potential $f \in H^{1/2}(\partial\Omega)$ induces an electrical potential $u \in H^1(\Omega)$,

2020 *Mathematics Subject Classification.* Primary: 35R30, 65J20; Secondary: 65N21.
Key words and phrases. Calderón problem, ill-posed problem, electrical impedance tomography, regularization, direct reconstruction algorithm.
* Corresponding author.

which uniquely solves the conductivity equation

$$\begin{aligned} \nabla \cdot (\gamma \nabla u) &= 0 \quad \text{in } \Omega, \\ u &= f \quad \text{on } \partial\Omega. \end{aligned} \tag{1}$$

The Dirichlet-to-Neumann map $\Lambda_\gamma : H^{1/2}(\partial\Omega) \to H^{-1/2}(\partial\Omega)$ is defined as

$$\Lambda_\gamma f = \gamma \partial_\nu u|_{\partial\Omega},$$

and associates a voltage potential on the boundary with a corresponding normal current flux. All pairs $(f, \gamma\partial_\nu u|_{\partial\Omega})$, or equivalently the Dirichlet-to-Neumann map, constitute the available data.

The forward problem is the problem of determining the Dirichlet-to-Neumann map given the conductivity, and it amounts to solving the boundary value problem (1) for all possible f. The Calderón problem now asks whether γ is uniquely determined by Λ_γ, and how to stably reconstruct γ from Λ_γ, if possible. Uniqueness and reconstruction were considered and solved for sufficiently regular conductivity distributions in dimension $n \geq 3$ in a series of papers [46, 44, 47, 56, 12]. The results are based on complex geometrical optics (CGO) solutions to a Schrödinger equation derived from (1). The first step of the reconstruction method is to recover the CGO solutions on $\partial\Omega$ by solving a weakly singular boundary integral equation with an exponentially growing kernel. The second step is obtaining the so-called non-physical scattering transform, which approximates in a large complex frequency limit the Fourier transform of $\gamma^{-1/2}\Delta\gamma^{1/2}$. Applying the inverse Fourier transform and solving a boundary value problem yields γ in the third step. Numerical algorithms following the scattering transform approach in dimension $n \geq 3$ have been developed by approximating the scattering transform [7, 36, 26, 8], by approximating the boundary integral equations [16], and for the full theoretical reconstruction algorithm [17]. A reconstruction algorithm for conductivity distributions close to a constant has been suggested, but not implemented [15].

A similar scattering transform approach combined with tools from complex analysis enables uniqueness and reconstruction [45] for the two-dimensional Calderón problem. More recently, a final affirmative answer was given to the question of uniqueness for a general bounded conductivity distribution in two dimensions [6]. Numerical algorithms and implementation for the two-dimensional problem have been considered [33, 34, 42, 43, 53, 54] and a regularization analysis and full implementation was given in [35]. We stress that in any practical case the Calderón problem is three-dimensional, since applying potentials on the boundary of a planar cross section of Ω leads to current flow leaving the plane.

The Calderón problem is known to be severely ill posed. Conditional stability estimates exist [3, 4] of the form

$$\|\gamma_1 - \gamma_2\|_{L^\infty(\Omega)} \leq f(\|\Lambda_{\gamma_1} - \Lambda_{\gamma_2}\|_Z),$$

for an appropriate function space Z and continuous function f with $f(0) = 0$ of logarithmic type. Furthermore, logarithmic stability is optimal [41]. While this is relevant for the theoretical reconstruction, there is no guarantee that a practically measured $\Lambda_\gamma^\varepsilon$ of a perturbed Dirichlet-to-Neumann map is the Dirichlet-to-Neumann map of any conductivity. We emphasize that in any practical case we can not have infinite-precision data, but rather a noisy finite approximation. Consequently, any computational algorithm for the problem needs regularization.

Classical regularization theory for inverse problems is given in [20, 32] with a focus on least squares formulations. A common approach to regularization for the

Calderón problem is based on iterative regularized least-squares, and convergence of such methods is analyzed in [18, 49, 50, 37, 30] in the context of EIT. A quantitative comparison of CGO-based methods and iterative regularized methods is given in [26]. Reconstruction by statistical inversion is developed in [31, 19], where in the latter, the problem is posed in an infinite-dimensional Bayesian framework. A different statistical approach to the Calderón problem shows stable reconstruction of the surface conductivity on a domain given noisy data [11]. Convergence estimates in probability of a statistical estimator (posterior mean) to the true conductivity given noisy data with a sufficiently small noise level are considered in [1].

In this paper we provide a direct CGO-based regularization strategy with an admissible parameter choice rule for reconstruction in the three-dimensional Calderón problem under the following assumptions:

Assumption 1. *For simplicity of exposition, we assume the domain of interest Ω is embedded in the unit ball in $\mathbb{R}^3$. Furthermore, we assume $\partial\Omega$ is smooth.*

Assumption 2 (Parameter and data space)**.** *We consider the forward map $F : D(F) \subset L^\infty(\Omega) \to Y$, $\gamma \mapsto \Lambda_\gamma$ with the following definition of $D(F)$. Let $\Pi > 0$ and $0 < \rho < 1$, then $\gamma \in D(F) \subset L^\infty(\Omega)$ satisfies*

$$\begin{aligned} \|\gamma\|_{C^2(\overline{\Omega})} &\le \Pi, \\ \gamma(x) &\ge \Pi^{-1} \quad \text{for all } x \in \Omega, \\ \gamma(x) &\equiv 1 \qquad \text{for } \operatorname{dist}(x, \partial\Omega) < \rho, \end{aligned}$$

where we assume knowledge of Π and ρ. We continuously extend $\gamma \equiv 1$ outside Ω. The data space $Y \subset \mathcal{L}(H^{1/2}(\partial\Omega), H^{-1/2}(\partial\Omega))$ consists of bounded linear operators $\Lambda : H^{1/2}(\partial\Omega) \to H^{-1/2}(\partial\Omega)$ that are Dirichlet-to-Neumann alike in the sense

$$\Lambda(1) = 0,$$

$$\int_{\partial\Omega} (\Lambda f)(x)\, d\sigma(x) = 0 \quad \text{for every } f \in H^{1/2}(\partial\Omega).$$

We equip $D(F)$ and Y with the inherited norms $\|\cdot\|_{D(F)} = \|\cdot\|_{L^\infty(\Omega)}$ and $\|\cdot\|_Y = \|\cdot\|_{H^{1/2}(\partial\Omega)\to H^{-1/2}(\partial\Omega)}$.

There is no reason to believe that the regularity assumptions of γ is optimal, in fact, we expect that the strategy generalizes to the less regular setting of [12]. We recall the adaptation of the definitions in [20, 32] presented in [35] of a regularization strategy in the nonlinear setting. A family of continuous mappings $\mathcal{R}_\alpha : Y \to L^\infty(\Omega)$, parametrized by *regularization parameter* $0 < \alpha < \infty$, is called a *regularization strategy* for F if

$$\lim_{\alpha\to 0} \|\mathcal{R}_\alpha \Lambda_\gamma - \gamma\|_{L^\infty(\Omega)} = 0, \tag{2}$$

for each fixed $\gamma \in D(F)$. We define the perturbed Dirichlet-to-Neumann map as

$$\Lambda_\gamma^\varepsilon = \Lambda_\gamma + \mathcal{E},$$

with $\mathcal{E} \in Y$ and $\|\mathcal{E}\|_Y \le \varepsilon$ for some $\varepsilon > 0$. We call ε the noise level, since we eventually simulate perturbations $\mathcal{E}$ as random noise. Furthermore, a regularization strategy $\mathcal{R}_\alpha : Y \to L^\infty(\Omega)$, $0 < \alpha < \infty$, is called *admissible* if

$$\alpha(\varepsilon) \to 0 \quad \text{as} \quad \varepsilon \to 0, \tag{3}$$

and for any fixed $\gamma \in \mathcal{D}(F)$ we have

$$\sup_{\Lambda_\gamma^\varepsilon \in Y} \{\|\mathcal{R}_{\alpha(\varepsilon)}\Lambda_\gamma^\varepsilon - \gamma\|_{L^\infty(\Omega)} \mid \|\Lambda_\gamma^\varepsilon - \Lambda_\gamma\|_Y \leq \varepsilon\} \to 0 \quad \text{as} \quad \varepsilon \to 0. \tag{4}$$

The topology in which we require convergence is essential; we require convergence in strong operator topology, but not in norm topology. The main result of this paper is then as follows.

Theorem 1.1. *Suppose $\Pi > 0$ and $0 < \rho < 1$ are given and let $D(F)$ be as in Assumption 2. Then there exists $\varepsilon_0 > 0$, dependent only on Π and ρ such that the family $\mathcal{R}_\alpha$ defined by (30) is an admissible regularization strategy for F with the following choice of regularization parameter:*

$$\alpha(\varepsilon) = \begin{cases} (-1/11\log(\varepsilon))^{-1/p} & \text{for } 0 < \varepsilon < \varepsilon_0, \\ \frac{\varepsilon}{\varepsilon_0}(-1/11\log(\varepsilon_0))^{-1/p} & \text{for } \varepsilon \geq \varepsilon_0, \end{cases} \tag{5}$$

with $p > 3/2$.

This gives theoretical justification for practical reconstruction of the Calderón problem in three dimensions. This is the first deterministic regularization analysis for the three-dimensional Calderón problem known to the authors. Similar results have been shown for the related two-dimensional D-bar reconstruction [35], and we will in fact adopt the spectral truncation from there to our setting. This extension is non-trivial in part because there are no existence and uniqueness guarantees for the CGO solutions that are independent of the magnitude of the complex frequency in the three-dimensional case. In addition, while the two-dimensional D-bar method enjoys the continuous dependence of the solution to the D-bar equation on the scattering transform, it is not obvious when the frequency information of γ is stably recovered from the scattering transform corresponding to a perturbed Dirichlet-to-Neumann map in the three-dimensional case.

We denote the set of bounded linear operators between Banach spaces X and Y by $\mathcal{L}(X, Y)$ and use $\mathcal{L}(X) := \mathcal{L}(X, X)$. We denote the Euclidean matrix operator norm by $\|\cdot\|_N := \|\cdot\|_{\mathbb{C}^{(N+1)^2} \to \mathbb{C}^{(N+1)^2}}$. The operator norm of $A : H^s(\partial\Omega) \to H^t(\partial\Omega)$ is denoted by $\|A\|_{s,t}$. We reserve C for generic constants and $C_1, C_2, \ldots$ for constants of specific value. Finally, exponential functions of the form $e^{ix\cdot\zeta}$, $x \in \mathbb{R}^3$, $\zeta \in \mathbb{C}^3$, is denoted $e_\zeta(x)$.

In Section 2, the full non-linear reconstruction algorithm for the three-dimensional Calderón problem is given. Section 3 gives technical estimates regarding the boundary integral equation and the scattering transform and provides a regularizing method for perturbed data with ε sufficiently small. Then Section 4 extends continuously the method to a regularization strategy $\mathcal{R}_\alpha$ defined on Y and proves Theorem 1.1. In Section 5, the necessary numerical details concerning the representation of the Dirichlet-to-Neumann map and computation of the relevant norm are given. In addition, a noise model is given. Section 6 presents and discusses numerical results of noise tests with a piecewise constant conductivity distribution using an implementation given in [17], which is available from the corresponding author by request.

2. The full non-linear reconstruction method.

Let $v = \gamma^{1/2}u$, then v is a solution to the Schrödinger equation

$$\begin{aligned} (-\Delta + q)v &= 0 \quad \text{in } \Omega, \\ v &= g \quad \text{on } \partial\Omega, \end{aligned} \tag{6}$$

with $q = \gamma^{-1/2}\Delta\gamma^{1/2}$ if and only if u is a solution to (1) with $f = \gamma^{-1/2}g$. Note in our setting $q = 0$ near $\partial\Omega$ and $q \equiv 0$ is extended continuously outside Ω and further $\Lambda_q g = \partial_\nu v = \Lambda_\gamma f$. The reconstruction method considered here is based on CGO solutions ψ_ζ to (6), which take the form

$$(-\Delta + q)\psi_\zeta = 0 \quad \text{in } \mathbb{R}^3, \tag{7}$$

satisfying $\psi_\zeta(x) = e^{ix\cdot\zeta}(1 + r_\zeta(x))$. Here the complex frequency $\zeta \in \mathbb{C}^3$ satisfies $\zeta\cdot\zeta = 0$ making $e^{ix\cdot\zeta}$ harmonic, and the remainder r_ζ belongs to certain weighted L^2 spaces. In the three-dimensional case, existence and uniqueness of CGO solutions have been shown for large complex frequencies,

$$|\zeta| > C_0\|q\|_{L^\infty(\Omega)} =: D_q \tag{8}$$

for some constant $C_0 > 0$, or alternatively for $|\zeta|$ small [56, 15]. The analysis involves the Faddeev Green's function

$$G_\zeta(x) := e^{i\zeta\cdot x}g_\zeta(x) \qquad g_\zeta(x) := \frac{1}{(2\pi)^3}\int_{\mathbb{R}^3}\frac{e^{ix\cdot\xi}}{|\xi|^2 + 2\xi\cdot\zeta}\,d\xi,$$

where g_ζ is defined in the sense of the inverse Fourier transform of a tempered distribution and interpretable as a fundamental solution of $(-\Delta - 2i\zeta\cdot\nabla)$. Boundedness of convolution by g_ζ on Ω is well known [56, 9, 51]:

$$\|g_\zeta * f\|_{L^2(\Omega)} \le C|\zeta|^{s-1}\|f\|_{L^2(\Omega)}, \quad s \in \{0, 1, 2\}, \tag{9}$$

where $|\zeta|$ is bounded away from zero, and C is independent of ζ and f.

The non-physical scattering transform is defined for all those ζ that give rise to a unique CGO solution ψ_ζ as

$$\mathbf{t}(\xi, \zeta) = \int_{\mathbb{R}^3} e^{-ix\cdot(\xi+\zeta)}\psi_\zeta(x)q(x)\,dx, \quad \xi \in \mathbb{R}^3. \tag{10}$$

It is useful to see the scattering transform as a non-linear Fourier transform of the potential q. Indeed, for $|\zeta| > D_q$ we have

$$|\mathbf{t}(\xi, \zeta) - \hat{q}(\xi)| \le C\|q\|^2_{L^\infty(\Omega)}|\zeta|^{-1}, \tag{11}$$

for all $\xi \in \mathbb{R}^3$, where C is independent of ζ and q. Whenever $(\zeta + \xi)\cdot(\zeta + \xi) = 0$, integration by parts in (10) yields

$$\mathbf{t}(\xi, \zeta) = \int_{\partial\Omega} e^{-ix\cdot(\xi+\zeta)}(\Lambda_\gamma - \Lambda_1)\psi_\zeta(x)\,d\sigma(x), \tag{12}$$

where $d\sigma$ denotes the surface measure on $\partial\Omega$. For fixed $\xi \in \mathbb{R}^3$ this gives rise to the set $\mathcal{V}_\xi = \{\zeta \in \mathbb{C}^3 \setminus \{0\} \mid \zeta\cdot\zeta = 0,\ (\zeta + \xi)\cdot(\zeta + \xi) = 0\}$ parametrized by

$$\zeta(\xi) = \left(-\frac{\xi}{2} + \left(\kappa^2 - \frac{|\xi|^2}{4}\right)^{1/2} k^{\perp\perp}\right) + i\kappa k^\perp, \tag{13}$$

with $\kappa \ge \frac{|\xi|}{2}$ and $k^\perp, k^{\perp\perp} \in \mathbb{R}^3$ are unit vectors and $\{\xi, k^\perp, k^{\perp\perp}\}$ is an orthogonal set [17]. Note that for $\zeta(\xi) \in \mathcal{V}_\xi$ and $k \ge \frac{|\xi|}{2}$ we have $|\zeta(\xi)| = \sqrt{2}\kappa$; consequently $\lim_{\kappa\to\infty}|\zeta(\xi)| = \infty$.

For each fixed ζ the trace of the CGO solution $\psi_\zeta|_{\partial\Omega}$ is recoverable from the boundary integral equation

$$\psi_\zeta|_{\partial\Omega} + \mathcal{S}_\zeta\left(\Lambda_\gamma - \Lambda_1\right)\left(\psi_\zeta|_{\partial\Omega}\right) = e_\zeta|_{\partial\Omega}, \tag{14}$$

where $\mathcal{S}_\zeta : H^{-1/2}(\partial\Omega) \to H^{1/2}(\partial\Omega)$ is the boundary single layer operator defined by

$$(\mathcal{S}_\zeta\varphi)(x) = \int_{\partial\Omega} G_\zeta(x-y)\varphi(y)d\sigma(y), \quad x \in \partial\Omega.$$

With $\mathcal{S}_0$ we denote the boundary single layer operator corresponding to the usual Green's function G_0 for the Laplacian. Occasionally we use the same notation when $x \in \mathbb{R}^3 \setminus \partial\Omega$ and note it is well known that $\mathcal{S}_0\varphi$ and hence $\mathcal{S}_\zeta\varphi$ is continuous in $\mathbb{R}^3$ [14]. We let

$$B_\zeta := [I + \mathcal{S}_\zeta(\Lambda_\gamma - \Lambda_1)],$$

denote the boundary integral operator and we note the boundary integral equation (14) is a uniquely solvable Fredholm equation of the second kind for $|\zeta| > D_q$ [45]. This gives a method of recovering the Fourier transform of q in every frequency through the scattering transform (12) as $|\zeta| \to \infty$. This method of reconstruction for the Calderón problem in three dimensions was first explicitly given in [44, 47]. We summarize the method in three steps.

Method 1. CGO reconstruction in three dimensions

Step 1: Fix $\xi \in \mathbb{R}^3$ and solve the boundary integral equation (14) for all $\zeta(\xi) \in \mathcal{V}_\xi$. Compute $\mathbf{t}(\xi, \zeta(\xi))$ by (12).

Step 2: Compute $\hat{q}(\xi)$ by

$$\lim_{|\zeta(\xi)|\to\infty} \mathbf{t}(\xi, \zeta(\xi)) = \hat{q}(\xi), \quad \xi \in \mathbb{R}^3,$$

and $q(x)$ by the inverse Fourier transform.

Step 3: Solve the boundary value problem

$$\begin{aligned}(-\Delta + q)\gamma^{1/2} &= 0 \quad \text{in } \Omega,\\ \gamma^{1/2} &= 1 \quad \text{on } \partial\Omega,\end{aligned}$$

and extract γ.

We remark that it is sufficient to solve the boundary integral equation in step 1 for a sequence $\{\zeta_k(\xi)\}_{k=1}^\infty$ of complex frequencies in $\mathcal{V}_\xi$ that tends to infinity.

3. **Regularized reconstruction by truncation.** We continue by mimicking Method 1 with Λ_γ replaced by $\Lambda_\gamma^\varepsilon$ with ε small. We note that, in any case, using ψ_ζ with $|\zeta|$ large is impractical. Indeed, when using perturbed measurements naively in (12), the propagated perturbation of $\mathbf{t}$ is ε multiplied with a factor exponentially growing in $|\zeta|$. This factor originates from the solution of the perturbed boundary integral equation

$$B_\zeta^\varepsilon(\psi_\zeta^\varepsilon|_{\partial\Omega}) := \psi_\zeta^\varepsilon|_{\partial\Omega} + \mathcal{S}_\zeta\left(\Lambda_\gamma^\varepsilon - \Lambda_1\right)(\psi_\zeta^\varepsilon|_{\partial\Omega}) = e_\zeta|_{\partial\Omega}, \tag{15}$$

and in multiplication with $e^{-ix\cdot(\xi+\zeta(\xi))}$, see Lemma 3.3. We will show below that (15) is solvable for sufficiently small ε. To mitigate this exponential behavior we propose a reconstruction method that makes use of two coupled truncations: one of the complex frequency ζ and one of the real frequency of the signal q^ε, the perturbed analog of q. As we shall see, an upper bound of the magnitude $|\zeta(\xi)|$ determines an upper bound of the proximity of $\mathbf{t}$ to $\hat{q}$, when using perturbed data. From (13) we have

$$|\zeta(\xi)| \geq \frac{|\xi|}{\sqrt{2}},$$

and hence fixing $|\zeta(\xi)|$ gives a bounded region in $\mathbb{R}^3$, $|\xi| < M$ for some $M > 0$, in which $\mathbf{t}$ can be computed. This gives the following method.

Method 2. Truncated CGO reconstruction in three dimensions

Step 1$^\varepsilon$: Let $M = M(\varepsilon) > 0$ be determined by a sufficiently small ε. For each fixed ξ with $|\xi| < M$, take $\zeta(\xi) \in \mathcal{V}_\xi$ with an appropriate size determined by M and solve (15) to recover $\psi^\varepsilon_\zeta|_{\partial\Omega}$. Compute the truncated scattering transform by

$$\mathbf{t}^\varepsilon_{M(\varepsilon)}(\xi, \zeta(\xi)) := \begin{cases} \int_{\partial\Omega} e^{-ix\cdot(\xi+\zeta(\xi))}(\Lambda^\varepsilon_\gamma - \Lambda_1)\psi^\varepsilon_\zeta(x)d\sigma(x), & |\xi| < M(\varepsilon), \\ 0, & |\xi| \geq M(\varepsilon), \end{cases}$$

Step 2$^\varepsilon$: Set $\widehat{q^\varepsilon}(\xi) := \mathbf{t}^\varepsilon_{M(\varepsilon)}(\xi, \zeta(\xi))$ and compute the inverse Fourier transform to obtain q^ε.

Step 3$^\varepsilon$: Solve the boundary value problem

$$\begin{aligned} (-\Delta + q^\varepsilon)(\gamma^\varepsilon)^{1/2} &= 0 \qquad \text{in } \Omega, \\ (\gamma^\varepsilon)^{1/2} &= 1 \qquad \text{on } \partial\Omega. \end{aligned}$$

and extract γ^ε.

We call M the truncation radius and note it should depend on ε. Truncation of the scattering transform with truncation radius M is well known in regularization theory for the two-dimensional D-bar reconstruction method [35]. We can see the real truncation as a low-pass filtering in the frequency domain; this leads to additional smoothing in the spatial domain. Note that M determines the level of regularization and poses as a regularization parameter $\alpha = M^{-1}$ in the sense of (4).

In the following section we derive the required properties of $\mathcal{S}_\zeta$, B_ζ^{-1} and $(B^\varepsilon_\zeta)^{-1}$. The invertibility of B^ε_ζ depends on the invertibility of the unperturbed boundary integral operator B_ζ, which is well known due to the mapping properties of $\mathcal{S}_\zeta$. Although boundedness of $\mathcal{S}_\zeta$ and B_ζ^{-1} in the three-dimensional case follows by similar arguments to that of the two-dimensional [35], it is not immediately clear when $(B^\varepsilon_\zeta)^{-1}$ exists in the absence of existence and uniqueness guarantees of ψ_ζ for small $|\zeta|$. Neither is it clear under which circumstances q^ε approximates q as the noise level goes to zero. This is dealt with in Lemma 3.4 below by choosing a suitable rate, at which $|\zeta|$ and M goes to infinity as ε goes to zero.

3.1. **The perturbed boundary integral equation.** When $|\zeta|$ is bounded away from zero we can bound $\mathcal{S}_\zeta$ using the mapping properties (9) of convolution with g_ζ between Sobolev spaces defined on Ω. We note that one can give better bounds for arbitrarily small $|\zeta| < 1$ than the following result by considering the integral operator $\mathcal{S}_\zeta - \mathcal{S}_0$ with a smooth kernel, see [15, 35].

Lemma 3.1. *Let $\varphi \in H^{-1/2}(\partial\Omega)$ such that $\int_{\partial\Omega} \varphi(x)\, d\sigma(x) = 0$ and let $\zeta \in \mathbb{C}^3$ with $\zeta \cdot \zeta = 0$ and $|\zeta| > \beta > 0$. Then for the boundary single layer operator, $\mathcal{S}_\zeta$, we have that*

$$\|\mathcal{S}_\zeta\varphi\|_{H^{1/2}(\partial\Omega)} \leq C_1(1 + |\zeta|)e^{2|\zeta|}\|\varphi\|_{H^{-1/2}(\partial\Omega)},$$

where the constant C_1 is independent of ζ.

Proof. We follow [35]. Letting $x \in \mathbb{R}^3 \setminus \overline{\Omega}$ and introducing $u \in H^1(\Omega)$ with $\Delta u = 0$ and $\partial_\nu u = \varphi$ we write

$$\begin{aligned}(\mathcal{S}_\zeta\varphi)(x) &= \int_{\partial\Omega} G_\zeta(x-y)\varphi(y)\,d\sigma(y),\\ &= \int_\Omega \nabla_y G_\zeta(x-y)\cdot\nabla u(y)dy,\\ &= -\nabla\cdot\left(G_\zeta * (\nabla u)\right)(x),\\ &= -\nabla\cdot\left[e^{ix\cdot\zeta}\left(g_\zeta * (e^{-iy\cdot\zeta}\nabla u)\right)\right](x),\end{aligned}$$

using integration by parts, the chain rule and the fact that $G_\zeta(x-\cdot)$ is smooth in Ω. By the continuity of $\mathcal{S}_\zeta$ the above holds for $x\in\partial\Omega$ as well. Note from (9) and Leibniz' rule that

$$\|\nabla\cdot\left[e^{ix\cdot\zeta}\left(g_\zeta * (e^{-iy\cdot\zeta}\nabla u)\right)\right]\|_{L^2(\Omega)} \le Ce^{2|\zeta|}\|\nabla u\|_{L^2(\Omega)},$$

and

$$\|\partial_{x_i}\nabla\cdot\left[e^{ix\cdot\zeta}\left(g_\zeta * (e^{-iy\cdot\zeta}\nabla u)\right)\right]\|_{L^2(\Omega)} \le C|\zeta|e^{2|\zeta|}\|\nabla u\|_{L^2(\Omega)},$$

for $i=1,2,3$. This yields

$$\begin{aligned}\|\mathcal{S}_\zeta\varphi\|_{H^{1/2}(\partial\Omega)} &\le \|\nabla\cdot\left[e^{ix\cdot\zeta}\left(g_\zeta * (e^{-iy\cdot\zeta}\nabla u)\right)\right]\|_{H^1(\Omega)},\\ &\le C(1+|\zeta|)e^{2|\zeta|}\|\nabla u\|_{L^2(\Omega)},\\ &\le C(1+|\zeta|)e^{2|\zeta|}\|\varphi\|_{H^{-1/2}(\partial\Omega)},\end{aligned}$$

using the trace theorem and stability of the Neumann problem for u. Here C is dependent on β since $|\zeta|>\beta$. □

We have the following estimate of B_ζ^{-1}. The main idea of the proof is to consider a solution $f\in H^{1/2}(\partial\Omega)$ to $B_\zeta f = h$ for some $h\in H^{1/2}(\partial\Omega)$ and then control the exponential component of f by creating a link to the CGO solutions of the Schrödinger equation.

Lemma 3.2. *For $\zeta\in\mathbb{C}^3\backslash\{0\}$ with $\zeta\cdot\zeta=0$ and $|\zeta|>D_q$ as in (8), the operator B_ζ is invertible with*

$$\|B_\zeta^{-1}\|_{1/2} \le C_2(1+|\zeta|)e^{2|\zeta|}, \tag{16}$$

where C_2 is a constant depending only on the a priori knowledge Π and ρ.

Proof. We follow [35]. Using integration by parts note that $B_\zeta f = f + G_\zeta * (qv_f)$ on $\partial\Omega$, where $v_f\in H^1(\Omega)$ is the unique solution to

$$\begin{aligned}(-\Delta+q)v_f &= 0 \qquad &&\text{in } \Omega,\\ v_f &= f \qquad &&\text{on } \partial\Omega.\end{aligned}$$

To bound f we bound v_f by writing $v_f = v - u^{\exp}$ with

$$\begin{aligned}\Delta v &= 0 \qquad &&\text{in } \Omega,\\ v &= B_\zeta f \qquad &&\text{on } \partial\Omega,\end{aligned}$$

and $u^{\exp} := G_\zeta * (qv_f)$. From the stability property of the Dirichlet problem it is sufficient to bound $u^{\exp}$ in terms of v. Note $(-\Delta+q)u^{\exp} = qv$ and hence conjugating with exponentials yields the equation in $\mathbb{R}^3$,

$$(-\Delta - 2i\zeta\cdot\nabla + q)u = qve^{-ix\cdot\zeta}, \tag{17}$$

where we set $u = e^{-ix\cdot\zeta}u^{\exp}$. It is well known that u is the unique solution among functions in certain weighted $L^2(\mathbb{R}^3)$-spaces satisfying

$$\|u\|_{L^2(\Omega)} \leq C\|q\|_{L^\infty}\frac{e^{|\zeta|}}{|\zeta|}\|v\|_{L^2(\Omega)},$$

whenever $|\zeta| > D_q$, see [56]. Indeed, convolution with g_ζ on both sides of (17) gives

$$u = g_\zeta * (-qu + qve^{-ix\cdot\zeta}),$$

which upgrades the estimate to

$$\|u\|_{H^1(\Omega)} \leq C\|q\|_{L^\infty}e^{|\zeta|}\|v\|_{L^2(\Omega)},$$

using (9). Now the estimate (16) follows straightforwardly from the trace theorem. □

We note that a main difference between the boundary integral equation in two dimensions and three dimensions is the possible existence of a certain ζ for which there exists no unique CGO solutions to (7). The next result shows that Lemma 3.1 and Lemma 3.2 implies solvability of the perturbed boundary integral equation using a Neumann series argument on the form

$$B_\zeta^\varepsilon = I + \mathcal{S}_\zeta(\Lambda_\gamma^\varepsilon - \Lambda_\gamma) + \mathcal{S}_\zeta(\Lambda_\gamma - \Lambda_1) = [I + A_\zeta^\varepsilon]B_\zeta,$$

where $A_\zeta^\varepsilon := \mathcal{S}_\zeta\mathcal{E}B_\zeta^{-1}$ is a bounded operator in $H^{1/2}(\partial\Omega)$. It is clear from Lemma 3.2 that q fixes a lower bound for $|\zeta|$, for which B_ζ is certain to be invertible. When the noise level is sufficiently small such that $D_q < |\zeta| < R(\varepsilon)$, for some R, we may invert B_ζ^ε. We have the following result.

Lemma 3.3. *Let $R = R(\varepsilon) := -\frac{1}{6}\log\varepsilon$, and suppose $D_q < |\zeta| < R(\varepsilon_1)$ for some $0 < \varepsilon_1 < 1$. Then there exists $0 < \varepsilon_2 \leq \varepsilon_1$ for which B_ζ^ε is invertible whenever $0 < \varepsilon < \varepsilon_2$. Furthermore we have the estimate*

$$\|\psi_\zeta^\varepsilon - \psi_\zeta\|_{H^{1/2}(\partial\Omega)} \leq C_3\varepsilon(1+R)^4e^{7R},$$

where C_3 is a constant depending only on the a priori knowledge of Π and ρ.

Proof. Since $\mathcal{E} \in Y$, it maps onto trace functions that have zero mean on the boundary. Then from Lemma 3.1 and Lemma 3.2 we find

$$\begin{aligned}\|A_\zeta^\varepsilon\|_{1/2} = \|\mathcal{S}_\zeta\mathcal{E}B_\zeta^{-1}\|_{1/2} &\leq C_1C_2\varepsilon(1+R)^2e^{4R},\\ &\leq C\varepsilon e^{5R}, \qquad (18)\end{aligned}$$

where we have absorbed the polynomial in R into the exponential and thereby obtained a new constant. By the definition of R, we note the right-hand side of (18) goes to zero as ε goes to zero, and hence there exists a $0 < \varepsilon_2 \leq \varepsilon_1$ such that $\|A_\zeta^\varepsilon\|_{1/2} < \frac{1}{2}$. Then by a Neumann series argument, $I + A_\zeta^\varepsilon$ is invertible with $\|(I + A_\zeta^\varepsilon)^{-1}\|_{1/2} < 2$, and $(B_\zeta^\varepsilon)^{-1} = B_\zeta^{-1}[I + A_\zeta^\varepsilon]^{-1}$. From the boundary integral equations we have $\psi_\zeta = B_\zeta^{-1}(e_\zeta|_{\partial\Omega})$ and $\psi_\zeta^\varepsilon = (B_\zeta^\varepsilon)^{-1}(e_\zeta|_{\partial\Omega})$. Then with the use of Lemma 3.2 we have for $0 < \varepsilon < \varepsilon_2$

$$\begin{aligned}\|\psi_\zeta^\varepsilon\|_{H^{1/2}(\partial\Omega)} &\leq \|(B_\zeta^\varepsilon)^{-1}(e_\zeta|_{\partial\Omega})\|_{H^{1/2}(\partial\Omega)},\\ &\leq 2\|B_\zeta^{-1}\|_{1/2}\|e^{ix\cdot\zeta}\|_{H^{1/2}(\partial\Omega)}, \qquad (19)\\ &\leq C(1+|\zeta|)^2e^{3|\zeta|}. \qquad (20)\end{aligned}$$

With the use of Lemma 3.2 we have for $0 < \varepsilon < \varepsilon_2$

$$\begin{aligned}\|(B_\zeta^\varepsilon)^{-1} - B_\zeta^{-1}\|_{1/2} &= \|B_\zeta^{-1}[(I + A_\zeta^\varepsilon)^{-1} - I]\|_{1/2},\\ &\leq \|B_\zeta^{-1}\|_{1/2}\|(I + A_\zeta^\varepsilon)^{-1}[I - (I + A_\zeta^\varepsilon)]\|_{1/2},\\ &\leq \|B_\zeta^{-1}\|_{1/2}\|(I + A_\zeta^\varepsilon)^{-1}\|_{1/2}\|A_\zeta^\varepsilon\|_{1/2},\\ &\leq 2C_1C_2^2\varepsilon(1+R)^3e^{6R}.\end{aligned}$$

Finally we obtain

$$\begin{aligned}\|\psi_\zeta^\varepsilon - \psi_\zeta\|_{H^{1/2}(\partial\Omega)} &= \|[(B_\zeta^\varepsilon)^{-1} - B_\zeta^{-1}]e_\zeta\|_{H^{1/2}(\partial\Omega)},\\ &\leq \|(B_\zeta^\varepsilon)^{-1} - B_\zeta^{-1}\|_{1/2}\|e^{ix\cdot\zeta}\|_{H^{1/2}(\partial\Omega)},\\ &\leq 2C_1C_2^2\varepsilon(1+R)^4e^{7R},\end{aligned} \tag{21}$$

for $0 < \varepsilon < \varepsilon_2$. □

3.2. **Truncation of the scattering transform.** We now show that fixing the magnitude of the complex frequency $|\zeta(\xi)| = (M(\varepsilon))^p$ with $p > 3/2$, enables control over the proximity of the truncated scattering transform $\mathbf{t}_M^\varepsilon(\cdot,\zeta)$ to $\hat{q}$ for small noise levels. This choice is justified from the following result.

Lemma 3.4. *Let $M(\varepsilon) = (-1/11\log(\varepsilon))^{1/p}$ be a truncation radius depending on ε and some exponent $p > 3/2$. Fix $\xi \in \mathbb{R}^3$ with $|\xi| < M(\varepsilon)$, suppose $\zeta(\xi) \in \mathcal{V}_\xi$ with*

$$|\zeta(\xi)| = (M(\varepsilon))^p = -\frac{1}{11}\log(\varepsilon)$$

and let ε_2 be defined as in the proof of Lemma 3.3. Further fix $q \in L^\infty(\Omega)$ corresponding to a $\gamma \in D(F)$. Then $\mathbf{t}_M^\varepsilon$ is well defined by (29) for $0 < \varepsilon < \varepsilon_2$ and

$$\lim_{\varepsilon\to 0}\|\mathbf{t}_{M(\varepsilon)}^\varepsilon - \hat{q}\|_{L^2(\mathbb{R}^3)} = 0.$$

Proof. For *(i)* fix first $|\xi| < M(\varepsilon)$ and note first by the triangle inequality that

$$|\mathbf{t}_{M(\varepsilon)}^\varepsilon(\xi,\zeta(\xi)) - \hat{q}(\xi)| \leq |\mathbf{t}_{M(\varepsilon)}^\varepsilon(\xi,\zeta(\xi)) - \mathbf{t}(\xi,\zeta(\xi))| + |\mathbf{t}(\xi,\zeta(\xi)) - \hat{q}(\xi)|. \tag{22}$$

By Lemma 3.3 there exists a unique solution ψ_ζ^ε to the perturbed boundary integral equation and hence $\mathbf{t}_M^\varepsilon$ is well defined. Using (20) and (21), we find the following, in which we set $R = R(\varepsilon)$, $M = M(\varepsilon)$ and $\zeta = \zeta(\xi)$ for simplicity of exposition,

$$\begin{aligned}|\mathbf{t}_M^\varepsilon(\xi,\zeta) - \mathbf{t}(\xi,\zeta)| &= \left|\int_{\partial\Omega} e^{-ix\cdot(\xi+\zeta)}[(\Lambda_\gamma^\varepsilon - \Lambda_1)\psi_\zeta^\varepsilon(x) - (\Lambda_\gamma - \Lambda_1)\psi_\zeta(x)]d\sigma(x)\right|,\\ &\leq \|e^{-ix\cdot(\xi+\zeta)}\|_{H^{1/2}(\partial\Omega)}\|\Lambda_\gamma - \Lambda_1\|_Y\|\psi_\zeta^\varepsilon - \psi_\zeta\|_{H^{1/2}(\partial\Omega)}\\ &\quad + \|e^{-ix\cdot(\xi+\zeta)}\|_{H^{1/2}(\partial\Omega)}\|\Lambda_\gamma^\varepsilon - \Lambda_\gamma\|_Y\|\psi_\zeta^\varepsilon\|_{H^{1/2}(\partial\Omega)},\\ &\leq C(1+|\zeta|)e^{|\zeta|}\left[\varepsilon(1+|\zeta|)^4e^{7|\zeta|} + \varepsilon(1+|\zeta|)^2e^{3|\zeta|}\right],\end{aligned} \tag{23}$$

where we use the fact that $\|\Lambda_\gamma - \Lambda_1\|_Y \leq C$, where C depends only on Π by the continuity of the forward map $\gamma \mapsto \Lambda_\gamma$. Then,

$$|\mathbf{t}_M^\varepsilon(\xi,\zeta) - \mathbf{t}(\xi,\zeta)| \leq C\varepsilon e^{9|\zeta|}.$$

Using (22) and the property (11) we conclude for $|\xi| < M(\varepsilon)$ that

$$|\mathbf{t}_M^\varepsilon(\xi,\zeta) - \hat{q}(\xi)| \leq C\varepsilon e^{9|\zeta|} + C|\zeta|^{-1}. \tag{24}$$

Then for *(ii)*, using the triangle inequality and (24) we find

$$\begin{aligned}\|\mathbf{t}_M^\varepsilon - \hat{q}\|_{L^2(\mathbb{R}^3)} &\le \|\mathbf{t}_M^\varepsilon - \hat{q}\|_{L^2(|\xi|<M)} + \|\hat{q}\|_{L^2(|\xi|\ge M)},\\ &\le C(\varepsilon e^{9|\zeta|} + M^{-p})\left(\int_0^M r^2\,dr\right)^{1/2} + \|\hat{q}\|_{L^2(|\xi|\ge M)},\\ &\le C(\varepsilon e^{10|\zeta|} + M^{3/2-p}) + \|\hat{q}\|_{L^2(|\xi|\ge M)},\\ &\le C\varepsilon^{1/11} + C(-1/11\log(\varepsilon))^{3/2-p} + \|\hat{q}\|_{L^2(|\xi|\ge M)},\end{aligned}$$

for $0<\varepsilon<\varepsilon_2$. Since $q\in L^\infty(\Omega)$ is compactly supported in Ω, we have $q\in L^2(\mathbb{R}^3)$, and hence the energy of the tail of $\hat{q}$ converges to zero as $M(\varepsilon)$ goes to infinity. The result follows as $p>3/2$. □

One may obtain an explicit decay of $\hat{q}$ by assuming a certain regularity of q. Notice the proof above works fine with the choice $|\zeta| = K_1M^p + K_2$ for some $0<K_1<1$, $K_2>0$ and $p>3/2$. A user may choose among such $|\zeta|$ freely, with $p=3/2$ being the critical choice. We now prove that γ^ε exists and is unique and that the propagated reconstruction error tends to zero if $\varepsilon\to 0$, given $\|q^\varepsilon - q\|_{L^2(\Omega)}$ is sufficiently small. This is possible in $H^2(\Omega)$ by a Neumann series argument and elliptic regularity. For the boundary value problem

$$\begin{aligned}(-\Delta + q^\varepsilon)u &= f \qquad \text{in } \Omega,\\ u &= 0 \qquad \text{on } \partial\Omega,\end{aligned}$$

with $f\in L^2(\Omega)$, we introduce the notation $L^\varepsilon : H_0^1(\Omega)\cap H^2(\Omega)\to L^2(\Omega)$, $L^\varepsilon : u\mapsto f$, defined for any $q^\varepsilon\in L^2(\Omega)$ and then note

$$\gamma^\varepsilon = [(L^\varepsilon)^{-1}(-q^\varepsilon)+1]^2,$$

whenever $(L^\varepsilon)^{-1}$ exists.

Lemma 3.5. *Let $q=\Delta\gamma^{1/2}\gamma^{-1/2}$ be a potential with $\gamma\in D(F)$. Then there exists a $0<\varepsilon_3<1$ such that for $0<\varepsilon<\min(\varepsilon_2,\varepsilon_3)=:\varepsilon_0$ the boundary value problem*

$$\begin{aligned}(-\Delta + q^\varepsilon)(\gamma^\varepsilon)^{1/2} &= 0 \qquad \text{in } \Omega,\\ (\gamma^\varepsilon)^{1/2} &= 1 \qquad \text{on } \partial\Omega,\end{aligned} \tag{25}$$

has a unique solution in $H^2(\Omega)$. Furthermore the following inequality holds

$$\|\gamma^{1/2} - (\gamma^\varepsilon)^{1/2}\|_{H^2(\Omega)} \le C_4\|q - q^\varepsilon\|_{L^2(\Omega)}, \tag{26}$$

where C_4 is dependent only on Π and ρ.

Proof. Note $(-\Delta+q)^{-1}$ exists and is bounded for $L^2(\Omega)$ into $H_0^1(\Omega)\cap H^2(\Omega)$ with

$$\|u\|_{H^2(\Omega)} \le C\|f\|_{L^2(\Omega)}, \tag{27}$$

by elliptic regularity [21]. Here C is dependent only on Π. We construct

$$L^\varepsilon u = (-\Delta+q)[I + (-\Delta+q)^{-1}(q^\varepsilon - q)]u,$$

and seek boundedness of $(-\Delta+q)^{-1}(q^\varepsilon - q)$ in $H^2(\Omega)$ as our goal. For any $u\in H^2(\Omega)$

$$\|(-\Delta+q)^{-1}(q^\varepsilon - q)u\|_{H^2(\Omega)} \le C\|q^\varepsilon - q\|_{L^2(\Omega)}\|u\|_{H^2(\Omega)},$$

using (27) and Sobolev embedding theory. By Lemma 3.4, there exists a $0<\varepsilon_3<1$ such that for all $0<\varepsilon<\min(\varepsilon_2,\varepsilon_3)$

$$\|(-\Delta+q)^{-1}(q^\varepsilon - q)\|_{H^2(\Omega)\to H^2(\Omega)} \le C\|q^\varepsilon - q\|_{L^2(\Omega)} < \frac{1}{2}.$$

Hence $(L^\varepsilon)^{-1}$ exists and is uniformly bounded with respect to $0 < \varepsilon \leq \varepsilon_0$. Finally, since $\gamma \in L^\infty(\Omega)$ we have $(q^\varepsilon - q)\gamma^{1/2} \in L^2(\Omega)$, and by solving

$$\begin{aligned} L^\varepsilon(\gamma^{1/2} - (\gamma^\varepsilon)^{1/2}) &= (q^\varepsilon - q)\gamma^{1/2} \quad && \text{in } \Omega \\ \gamma^{1/2} - (\gamma^\varepsilon)^{1/2} &= 0 && \text{on } \partial\Omega, \end{aligned}$$

we obtain the estimate (26). □

We conclude that γ^ε of Method 2 exists uniquely and approximates γ in the $H^2(\Omega)$-norm, whenever $\varepsilon < \varepsilon_0$.

4. **Extending the method to a regularization strategy.** From the definition of an admissible regularization strategy it is clear $\mathcal{R}_\alpha$ must be defined on Y and not only an ε_0-neighborhood of $F(\mathcal{D}(F))$. However, $(B_\zeta^\varepsilon)^{-1}$ and $(L^\varepsilon)^{-1}$ exists only for small enough ε. We confront this by extending these operators to $(B_\zeta^\varepsilon)_\alpha^\dagger$ and $(L^\varepsilon)_\alpha^\dagger$ coinciding with $(B_\zeta^\varepsilon)^{-1}$ and $(L^\varepsilon)^{-1}$ for $\varepsilon < \varepsilon_0$, such that $\mathcal{R}_\alpha$ is continuous and well defined on Y. There are several ways to obtain such extensions, however we will follow [35] and construct explicit pseudoinverses by means of functional calculus. Define the normal operator

$$S_\zeta^\varepsilon := (B_\zeta^\varepsilon)^*(B_\zeta^\varepsilon) \in \mathcal{L}(H^{1/2}(\partial\Omega)),$$

where $(B_\zeta^\varepsilon)^*$ is the adjoint operator of $(B_\zeta^\varepsilon) \in \mathcal{L}(H^{1/2}(\partial\Omega))$. Similarly we define

$$T_\zeta^\varepsilon := (L^\varepsilon)^*(L^\varepsilon) \in \mathcal{L}(L^2(\Omega)).$$

Let h_α^1 and h_α^2 be two real functions defined for $0 < \alpha < \infty$ as

$$h_\alpha^i(t) := \begin{cases} t^{-1} & \text{for } t > \kappa_i(\alpha), \\ \kappa_i(\alpha)^{-1} & \text{for } t \leq \kappa_i(\alpha), \end{cases}$$

for $i = 1, 2$ with $\kappa_i(\alpha) = \frac{1}{4} r_i(\alpha)^2$, where we will see below the estimates (26) and (31) motivates the definition

$$r_i(\alpha) := \begin{cases} \frac{1}{C_2(1+\alpha^{-p})e^{2\alpha^{-p}}} & \text{for } i = 1, \\ \frac{1}{C_4} & \text{for } i = 2, \end{cases}$$

with $p > 3/2$. We define the α-pseudoinverses $(B_\zeta^\varepsilon)_\alpha^\dagger$ of B_ζ^ε and $(L^\varepsilon)_\alpha^\dagger$ of L^ε for any $0 < \alpha < \infty$ as

$$\begin{aligned} (B_\zeta^\varepsilon)_\alpha^\dagger &:= h_\alpha^1(S_\zeta^\varepsilon)(B_\zeta^\varepsilon)^*, \\ (L^\varepsilon)_\alpha^\dagger &:= h_\alpha^2(T^\varepsilon)(L^\varepsilon)^*, \end{aligned}$$

where the operators $h_\alpha^1(S_\zeta^\varepsilon)$ in $\mathcal{L}(H^{1/2}(\partial\Omega))$ and $h_\alpha^2(T^\varepsilon)$ in $\mathcal{L}(L^2(\Omega))$ are defined in the sense of continuous functional calculus (see for example [48, 55]) and depend continuously on S_ζ^ε and T^ε, respectively (see for example [35, Lemma 3.1]). This implies $\Lambda_\gamma^\varepsilon \mapsto (B_\zeta^\varepsilon)_\alpha^\dagger$ and $q^\varepsilon \mapsto (L^\varepsilon)_\alpha^\dagger$ are continuous mappings. Explicitly, for a self-adjoint operator $S : \mathcal{H} \to \mathcal{H}$ for a Hilbert space $\mathcal{H}$ we set

$$h_\alpha^i(S) = \int_{\sigma(S)} h_\alpha^i(\lambda)\, dP(\lambda), \tag{28}$$

where $\sigma(S) \subset \mathbb{C}$ denotes the spectrum of S, and P is a spectral measure on $\sigma(S)$.

Method 3. Regularized CGO reconstruction in three dimensions

Step 1$_\alpha$: Given $\alpha > 0$, set $M = \alpha^{-1}$. For each $|\xi| < M$ take $\zeta(\xi) \in \mathcal{V}_\xi$ with $|\zeta(\xi)| = M^p$ for $p > 3/2$ and define

$$\tilde{\psi}_\alpha := (B_\zeta^\varepsilon)_\alpha^\dagger(e_\zeta|_{\partial\Omega})$$

and compute the truncated scattering transform $\mathbf{t}_\alpha(\xi, \zeta(\xi))$ for $\zeta(\xi)$ in $\mathcal{V}_\xi$ by

$$\tilde{\mathbf{t}}_\alpha(\xi, \zeta(\xi)) = \begin{cases} \int_{\partial\Omega} e^{-ix\cdot(\xi+\zeta(\xi))}(\Lambda_\gamma^\varepsilon - \Lambda_1)\tilde{\psi}_\alpha(x)d\sigma(x) & |\xi| < M, \\ 0 & |\xi| \geq M \end{cases} \tag{29}$$

Step 2$_\alpha$: Define $\widehat{q_\alpha}(\xi) := \tilde{\mathbf{t}}_\alpha(\xi, \zeta(\xi))$ and compute the inverse Fourier transform to obtain q_α.

Step 3$_\alpha$: Solve the boundary value problem (25) by computing $(L^\varepsilon)_\alpha^\dagger(-q_\alpha)$ and set

$$\mathcal{R}_\alpha\Lambda_\gamma^\varepsilon := [(L^\varepsilon)_\alpha^\dagger(-q_\alpha) + 1]^2 \tag{30}$$

Proof of Theorem 1.1. Given $\Lambda_\gamma^\varepsilon$ in Y we have

$$\begin{aligned} |\tilde{\mathbf{t}}_\alpha(\xi, \zeta(\xi))| &\leq \left| \int_{\partial\Omega} e^{-ix\cdot(\xi+\zeta)}[(\Lambda_\gamma^\varepsilon - \Lambda_\gamma)\tilde{\psi}_\alpha(x) + (\Lambda_\gamma - \Lambda_1)\tilde{\psi}_\alpha(x)]d\sigma(x) \right|, \\ &\leq \|e^{-ix\cdot(\xi+\zeta)}\|_{H^{1/2}(\partial\Omega)}\|\Lambda_\gamma^\varepsilon - \Lambda_\gamma\|_Y\|\tilde{\psi}_\alpha\|_{H^{1/2}(\partial\Omega)} \\ &\quad \|e^{-ix\cdot(\xi+\zeta)}\|_{H^{1/2}(\partial\Omega)}\|\Lambda_\gamma - \Lambda_1\|_Y\|\tilde{\psi}_\alpha\|_{H^{1/2}(\partial\Omega)}, \\ &< \infty, \end{aligned}$$

for all $\xi \in \mathbb{R}^3$, since $(B_\zeta^\varepsilon)_\alpha^\dagger$ is bounded in $H^{1/2}(\partial\Omega)$. Then by compact support $\tilde{\mathbf{t}}_\alpha \in L^2(\mathbb{R}^3)$. It follows the inverse Fourier transform of this object is well defined and hence the family of operators $\mathcal{R}_\alpha$ is well defined. Using the continuity of the maps $\Lambda_\gamma^\varepsilon \mapsto (B_\zeta^\varepsilon)_\alpha^\dagger$ and $q_\alpha \mapsto (L^\varepsilon)_\alpha^\dagger$, a parallel estimation to (23) and the linearity and boundedness of the inverse Fourier transform in $L^2(\mathbb{R}^3)$, it is clear that $\mathcal{R}_\alpha$ is a family of continuous mappings. Now recall from Lemma 3.2 and (19) that for $0 < \varepsilon < \varepsilon_0$ we have that

$$\|(B_\zeta^\varepsilon)\|_{1/2}^{-1} \leq \|(B_\zeta^\varepsilon)^{-1}\|_{1/2} \leq 2C_2(1 + |\zeta|)e^{2|\zeta|}. \tag{31}$$

Set $|\zeta| = \alpha^{-p}$ and note

$$S_\zeta^\varepsilon \geq \frac{1}{4}r_1(\alpha)^2 I.$$

By definition of the α-pseudoinverse and (28) we have that $(B_\zeta^\varepsilon)_\alpha^\dagger = (B_\zeta^\varepsilon)^{-1}$ for $0 < \varepsilon < \varepsilon_0$, and hence $\tilde{\psi}_\alpha = \psi_\zeta^\varepsilon$ is unique. It follows by Lemma 3.4 that $\tilde{\mathbf{t}}(\cdot, \zeta(\cdot))$ is well defined and $q_\alpha = q^\varepsilon$ converges to q as ε goes to zero. Conversely, for $0 < \varepsilon < \varepsilon_0$ we have $(L^\varepsilon)_\alpha^\dagger = (L^\varepsilon)^{-1}$, and hence by Lemma 3.5 and the Sobolev embedding $H^2(\Omega) \subset C^0(\overline{\Omega})$, (4) is satisfied. Note also the weaker requirement (2) follows analogously. The property (3) is satisfied by (5). □

A direct consequence of the truncation of the scattering transform is the following property of the reconstruction $\mathcal{R}_\alpha(\varepsilon)\Lambda_\gamma^\varepsilon$ for sufficiently small ε. The regularized reconstructions are as regular as Ω.

Proposition 1. *Suppose $\Lambda_\gamma^\varepsilon = \Lambda_\gamma + \mathcal{E}$ with $\|\mathcal{E}\|_Y \leq \varepsilon < \varepsilon_0$. Then $\mathcal{R}_\alpha(\varepsilon)\Lambda_\gamma^\varepsilon \in C^\infty(\overline{\Omega})$.*

Proof. Since $\tilde{\mathbf{t}}_\alpha(\cdot, \zeta(\cdot)) \in L^1(\mathbb{R}^3)$ has compact support, it follows q_α is smooth. Since $\partial\Omega$ is smooth, it follows $\mathcal{R}_\alpha\Lambda_\gamma^\varepsilon \in C^\infty(\overline{\Omega})$ by elliptic regularity [21]. □

5. **Computational methods.** In this section we outline methods of representing and computing the Dirichlet-to-Neumann map numerically and consider the discretization of the boundary integral equations. We assume $\Omega = B(0,1)$ in order to utilize spherical harmonics in representation of functions on $\partial\Omega$.

5.1. **Representation and computation of the Dirichlet-to-Neumann map.** We consider the Hilbert space $H^s(\partial\Omega)$, $s > 0$, defined as the space of all functions f in $L^2(\partial\Omega)$ that satisfy

$$\|f\|^2_{L^2(\partial\Omega)} + \|(-\Delta_S)^{s/2} f\|^2_{L^2(\partial\Omega)} < \infty, \tag{32}$$

where $(-\Delta_S)^{s/2}$ is the fractional order spherical Laplace operator on the unit sphere. Since spherical harmonics, say $\{Y_n^m\}_{n\in\mathbb{N}_0, |m|\le n}$, constitute an orthonormal basis of $L^2(\partial\Omega)$ (see for example [14]), we may expand $f \in L^2(\partial\Omega)$ as

$$f = \sum_{n=0}^{\infty} \sum_{m=-n}^{n} \langle f, Y_n^m\rangle Y_n^m, \qquad \langle f, Y_n^m\rangle = \int_{\partial\Omega} f(x)\overline{Y_n^m(x)}\, d\sigma(x).$$

The spherical harmonics are eigenvectors of $(-\Delta_S)$, in particular,

$$(-\Delta_S)^{s/2} Y = (n(n+1))^{s/2} Y,$$

for any spherical harmonic Y of degree n. Then the requirement (32) gives rise to a characterization of $H^s(\partial\Omega)$ suitable for $s \in \mathbb{R}$ as those functions $f \in L^2(\partial\Omega)$ that satisfy

$$\sum_{n=0}^{\infty} \sum_{m=-n}^{n} (1+n^2)^s |\langle f, Y_n^m\rangle|^2 < \infty.$$

See [39, Chapter 1.7] for a more general treatment and the case $s < 0$. Thus we define the $H^s(\partial\Omega)$ inner products as

$$\langle f, g\rangle_s := \langle f, g\rangle_{H^s(\partial\Omega)} = \sum_{n=0}^{\infty} \sum_{m=-n}^{n} w_s(n) \langle f, Y_n^m\rangle \overline{w_s(n)\langle g, Y_n^m\rangle},$$

where the multiplier functions are defined as

$$w_s(n) := (1+n^2)^{s/2}, \qquad \text{for } n \in \mathbb{N}_0,\ s \in \mathbb{R},$$

and hence $\|f\|_{H^s(\partial\Omega)} = \langle f, f\rangle_s^{1/2}$. We build an orthonormal basis $\{\phi^s_{n,m}\}_{n\in\mathbb{N}_0, |m|\le n}$ of $H^s(\partial\Omega)$ with

$$\phi^s_{n,m} = w_{-s}(n) Y_n^m.$$

and hence any $g \in H^s(\partial\Omega)$ has the expansion

$$g = \sum_{n=0}^{\infty} \sum_{m=-n}^{n} \langle g, \phi^s_{n,m}\rangle_s \phi^s_{n,m}.$$

Consider the $L^2(\partial\Omega)$ orthogonal projection P_N to the space spanned by spherical harmonics of degree less than or equal to N, as

$$P_N g = \sum_{n=0}^{N} \sum_{m=-n}^{n} \langle g, Y_n^m\rangle Y_n^m.$$

Note $\langle g, Y_n^m \rangle$ as an integral over the unit sphere may be approximated by coefficients $c_{n,m}(\underline{g})$ using Gauss-Legendre quadrature in $2(N+1)^2$ appropriately chosen quadrature points $\{x_k\}_{k=1}^{2(N+1)^2}$ on the unit sphere as in [17]. Here we denote $\underline{g} = (g(x_1), \ldots, g(x_{2(N+1)^2}))$. Define

$$L_N g := \sum_{n=0}^{N} \sum_{m=-n}^{n} c_{n,m}(\underline{g}) Y_n^m.$$

We may approximate any operator $\Lambda : H^s(\partial\Omega) \to H^{-s}(\partial\Omega)$ using Q, a matrix in $\mathbb{C}^{2(N+1)^2 \times 2(N+1)^2}$ defined by

$$(\Lambda g)(x_k) \simeq [Q\underline{g}]_k := \sum_{n=0}^{N} \sum_{m=-n}^{n} c_{n,m}(\underline{g})(\Lambda Y_n^m)(x_k), \quad k = 1, \ldots, 2(N+1)^2. \tag{33}$$

From here it is clear we can write Q as

$$Q = \widetilde{Q} A, \tag{34}$$

where $A : \underline{g} \mapsto (c_{0,0}(\underline{g}), \ldots, c_{N,N}(\underline{g}))$, and $[\widetilde{Q}]_{k\ell} = \Lambda Y_\ell(x_k)$, where Y_ℓ is the ℓ'th spherical harmonic in the natural order. We can think of A as the matrix that takes a point-cloud representation of a function on $\partial\Omega$ and gives the spherical harmonic representation.

Similarly to [35], an approximation of the operator norm then takes the form

$$\|\Lambda\|_{s,-s} \simeq \sup_f \frac{\|\mathcal{Q} f\|_{\mathbb{C}^{(N+1)^2}}}{\|f\|_{\mathbb{C}^{(N+1)^2}}} = \|\mathcal{Q}\|_N, \tag{35}$$

where $[\mathcal{Q}]_{ij} = \langle \Lambda \phi_{n,m}^s, \phi_{n',m'}^{-s} \rangle_{-s}$ with $i = n'^2 + n' + m' + 1$ and $j = n^2 + n + m + 1$. We may approximate

$$\begin{aligned} \langle \Lambda \phi_{n,m}^s, \phi_{n',m'}^{-s} \rangle_{-s} &= w_{-s}(n) w_{-s}(n') \langle \Lambda Y_n^m, Y_{n'}^{m'} \rangle, \\ &\simeq w_{-s}(n) w_{-s}(n') c_{n',m'}(\underline{\Lambda Y_n^m}). \end{aligned} \tag{36}$$

With $\mathcal{B}$ we denote the map that takes the matrix Q and gives the approximation of $\mathcal{Q}$ defined by (36). For $\Lambda = \Lambda_\gamma$ we denote the approximation (33), Q_γ.

From (33) it is clear that to represent Λ_γ we need only to compute $(\Lambda_\gamma Y_n^m)(x_k)$ in the quadrature points x_k. In this paper we compute $(\Lambda_\gamma Y_n^m)(x_k)$ efficiently by the boundary integral approach for piecewise constant conductivities given in [17], an approach which despite the lack of reconstruction theory has shown to perform well.

5.2. **Noise model.** We simulate a perturbation of the Dirichlet-to-Neumann map by adding Gaussian noise to Q_γ. We let

$$Q_\gamma^\varepsilon = Q_\gamma + \delta E, \tag{37}$$

where $\delta > 0$ and the elements of the $2(N+1)^2 \times 2(N+1)^2$ matrix E are independent Gaussian random variables with zero mean and unit variance. We modify E such that $\mathcal{B}E$ has a first row and column as zeros, such that we may consider $\mathcal{B}E$ as an approximation of a linear and bounded operator $\mathcal{E} \in Y$. Furthermore, we approximate $\|\mathcal{E}\|_Y$ using (35) and (36) and note we can specify an absolute level of noise $\|\mathcal{E}\|_Y \approx \varepsilon$ by choosing δ appropriately. The relative noise level is then

$$\delta \frac{\|\mathcal{E}\|_Y}{\|\Lambda_\gamma\|_Y} \approx \delta \frac{\|\mathcal{B}E\|_N}{\|\mathcal{B}Q_\gamma\|_N}.$$

Note the noise model in [17] scales each element of E with the corresponding element of Q_γ. Noise models for electrode data simulation typically takes the form

$$V_j^\varepsilon = V_j + \delta_j E_j,$$

as in [26], where V_j is the voltage vector corresponding to the j'th current pattern, $\delta_j > 0$ is a scaling parameter dependent on V_j and E_j is a Gaussian vector independent of $E_{j'}$ for $j \neq j'$. For our case such a noise model corresponds best to adding to $\widetilde{Q}_\gamma$ in (34) a matrix $\widetilde{E}$ whose columns are $\delta_j E_j$. One may check by vectorizing $A^T\widetilde{E}^T$ that the corresponding E of (37) consists of independent and identically distributed Gaussian vectors as rows. However, the elements of each row are now correlated with covariance matrix $A^T\mathrm{diag}(\delta)A$.

Finally, we define the signal-to-noise ratio as

$$\mathrm{SNR} = \frac{1}{(N+1)^2}\sum_{n=0}^{N}\sum_{m=-n}^{n}\frac{\|Q_\gamma \underline{Y_n^m}\|_{\mathbb{C}^{2(N+1)^2}}}{\delta\|E\underline{Y_n^m}\|_{\mathbb{C}^{2(N+1)^2}}}.$$

5.3. **Solving the boundary integral equations.** Following [17] we discretize the perturbed boundary integral equations (15) by

$$\left[I + (\mathcal{S}_0 L_N + \mathcal{H}_\zeta^N)(\Lambda_\gamma^\varepsilon - \Lambda_1)L_N\right]((\psi_\zeta^N)^\varepsilon|_{\partial\Omega}) = e_\zeta|_{\partial\Omega}, \tag{38}$$

where $\mathcal{H}_\zeta^N$ is the approximation of the integral operator $\mathcal{S}_\zeta - \mathcal{S}_0$ using the Gauss-Legendre quadrature rule of order $N+1$ on the unit sphere in the aforementioned quadrature points $\{x_k\}_{k=1}^{2(N+1)^2}$. We find the following result regarding the convergence of the perturbed solutions $(\psi_\zeta^N)^\varepsilon$ of (38) analogously to [16, 17].

Theorem 5.1. *Suppose $D < |\zeta(\xi)| < -\frac{1}{6}\log\varepsilon_2$ and $\mathcal{E}$ is a linear bounded operator from $H^s(\partial\Omega)$ to $H^t(\partial\Omega)$ for all $s \geq 1/2$ and $t > s$. Then for all $s > 3/2$, there exists $N_0 \in \mathbb{N}$ such that for all $N \geq N_0$ the operator $I + (\mathcal{S}_0 L_N + \mathcal{H}_\zeta^N)(\Lambda_\gamma^\varepsilon - \Lambda_1)L_N$ is invertible in $H^s(\partial\Omega)$. Furthermore we have,*

$$\|(\psi_\zeta^N)^\varepsilon - \psi_\zeta^\varepsilon\|_{H^s(\partial\Omega)} \leq \frac{C}{N^{s-3/2}}\|e_\zeta\|_{H^s(\partial\Omega)}.$$

Proof. The result follows from a Neumann series argument as in Lemma 3.1 and Theorem 3.2 of [17] as for $D < |\zeta(\xi)| < -\frac{1}{6}\log\varepsilon_2$, there exists a bounded inverse $(B_\zeta^\varepsilon)^{-1}$ by Lemma 3.3. □

This result ensures that the solutions of the discretized perturbed boundary integral equations are unique and converge to the solutions of (15).

5.4. **Choice of $|\zeta(\xi)|$ and truncation radius.** It is clear from Method 3 that we should set $|\zeta(\xi)| = M^p$ for some exponent $p > 3/2$. Due to the high sensitivity of the CGO solutions with respect to $|\zeta(\xi)|$, we may choose $|\zeta(\xi)|$ differently in practice, although we will not necessarily have a regularization strategy in theory. One idea of [16] is to set $|\zeta(\xi)|$ minimal in the admissible set (13), that is

$$|\zeta(\xi)| = \frac{M}{\sqrt{2}}.$$

A different idea is to choose $|\zeta(\xi)|$ independently for each ξ such that $|\zeta(\xi)|$ is minimal with $|\zeta(\xi)| = \frac{|\xi|}{\sqrt{2}}$. We take the critical choice $|\zeta(\xi)| = K_1 M^{3/2}$ for some constant $0 < K_1 < 1$ to maintain the smallest $|\zeta|$ within the boundaries of the theory.

In practice we compute $\mathbf{t}_{M(\varepsilon)}(\xi, \zeta(\xi))$ in a ξ-grid of points $|\xi| \leq M$ as in [17]. The Shannon sampling theorem ensures we can recover uniquely the inverse Fourier transform if we sample densely enough. We use the discrete Fourier transform in equidistant ξ- and x-grids in three dimensions.

$$\xi_k^j = -M + k\frac{2M}{K-1} \quad \text{and} \quad x_n^j = -x_{\max} + n\frac{2x_{\max}}{K-1},$$

for $n, k = 0, \ldots, K-1$, $j = 1, 2, 3$ and some $x_{\max}$ determined by K and M. Indeed the discrete Fourier transform requires

$$M = \frac{\pi(K-1)^2}{2Kx_{\max}}.$$

to recover $q^\varepsilon(x_n^j)$ for all $n = 0, \ldots, K-1$, $j = 1, 2, 3$. In practical applications, we do not know the noise level, in which case we choose M and K and consequently determine $x_{\max}$. Then we recover q^ε in an appropriate finite element mesh of the unit ball using trilinear interpolation. The discrete Fourier transform is computed efficiently with the use of FFT [23] with complexity $\mathcal{O}(K^3 \log K^3)$.

The problem of finding the optimal truncation radius given noisy data $\Lambda_\gamma^\varepsilon$ is largely open and is related to the problem of systematically choosing a regularization parameter of regularized reconstruction for an inverse problem. In this paper, we choose the truncation radius by inspection for the simulated data. For further details on the implementation of the reconstruction algorithm we refer to [16, 17].

6. **Numerical results.**

We test Method 2 as a regularization strategy. We are interested in whether the reconstruction converges to the true conductivity distribution as the noise level goes to zero, and likewise as the regularization parameter α goes to zero for a non-noisy Dirichlet-to-Neumann map. To this end, we simulate a Dirichlet-to-Neumann map for a well-known phantom.

6.1. **Test phantom.**

The piecewise constant heart-lungs phantom consists of two spheroidal inclusions and a ball inclusion embedded in the unit sphere with a background conductivity of 1. The phantom is summarized in Table 1. We compute and represent the Dirichlet-to-Neumann map and noisy counterparts as described in Section 5.1. In particular, the forward map is computed using $2(N+1)^2$ boundary points on the unit sphere and using maximal degree N of spherical harmonics with $N = 25$.

Inclusion	Center	Radii	Axes	Conductivity
Ball	$(-0.09, -0.55, 0)$	$r = 0.273$		2
Left spheroid	$0.55(-\sin(\frac{5\pi}{12}), \cos(\frac{5\pi}{12}), 0)$	$r_1 = 0.468$, $r_2 = 0.234$, $r_3 = 0.234$	$(\cos(\frac{5\pi}{12}), \sin(\frac{5\pi}{12}), 0)$, $(-\sin(\frac{5\pi}{12}), \cos\frac{5\pi}{12}), 0)$, $(0, 0, 1)$	0.5
Right spheroid	$0.45(\sin(\frac{5\pi}{12}), \cos(\frac{5\pi}{12}), 0)$	$r_1 = 0.546$, $r_2 = 0.273$, $r_3 = 0.273$	$(\cos(\frac{5\pi}{12}), -\sin(\frac{5\pi}{12}), 0)$, $(\sin(\frac{5\pi}{12}), \cos(\frac{5\pi}{12}), 0)$, $(0, 0, 1)$	0.5

TABLE 1. Summary of piecewise constant heart-lungs phantom consisting of three inclusions

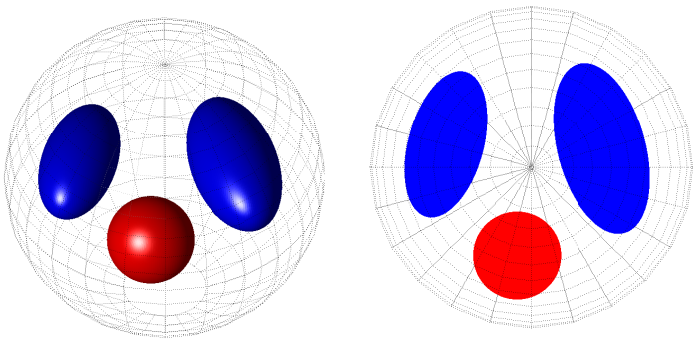

(A) (B)

FIGURE 1. The piecewise constant heart-lungs phantom in a three-dimensional view (A), and in the planar cross section $x^3 = 0$ (B).

6.2. **Regularization in practice.** We now consider the regularization strategy, Method 2, in practice. Alluding to (2), we test the reconstruction algorithm by keeping the test data fixed and varying the regularization parameter. In Figure 2, we see cross-sectional plots of reconstructed conductivities for different truncation radii $M = \alpha^{-1}$. We use $|\zeta(\xi)| = \frac{1}{4}M^{3/2}$ as the critical choice such that $\zeta(\xi) \in \mathcal{V}_\xi$ for $M \geq 8$, and use the accurate Dirichlet-to-Neumann map with no added noise. The figure shows increasing accuracy and contrast for increasing truncation radii. Similar to the findings of [17], we experience failing reconstructions for large enough truncation radii as the frequency data is dominated by exponentially amplified noise inherent to the finite-precision representation of Λ_γ. This happens since there is noise present in the representation of the Dirichlet-to-Neumann map, no matter how accurately it represents the true infinite-precision data. We see the effect of truncation in practice: low resolution, smaller dynamical range and more smoothness caused by the missing high frequency data. Though not immediately clear from this figure, the reconstructions slightly overshoot the conductivity of the resistive spheroidal inclusions with conductivities as small as 0.38. In addition, the reconstruction algorithm seems to work well in practice on piecewise constant conductivity distributions.

In Figure 3, we see cross-sectional plots of reconstructed conductivities using Dirichlet-to-Neumann maps with added noise and for fixed $|\zeta(\xi)| = \frac{1}{3\sqrt{2}}M^{3/2}$. Here, K_1 is chosen such that $\zeta(\xi)$ is small and admissible for $M \geq 9$. The truncation radii are chosen optimally by visual inspection. The figure shows reconstructions in the presence of noise of levels ranging from $\varepsilon = 10^{-6}$ to $\varepsilon = 10^{-3}$ in the Dirichlet-to-Neumann map. We see improving quality of reconstruction as the noise level decreases in accordance with Definition 1. Beyond noise levels of 10^{-3}, reconstruction is still feasible without the corruption of unstable noise, although, they need heavy regularization and start to lack visible features of the phantom. In Figure 4, we see the conductivity reconstruction using noisy data with $\varepsilon = 10^{-2}$ corresponding to approximately 1% relative noise. The resistive spheroidal inclusions start to connect and the conductive spherical inclusion is not as accurately placed. The

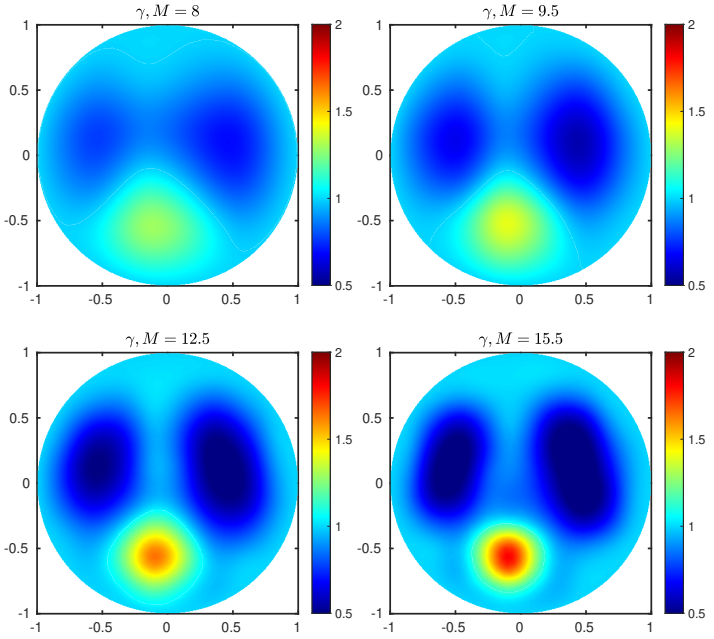

FIGURE 2. Cross sections ($x^3 = 0$) of reconstructions using the regularized reconstruction algorithm with different choices of truncation radius M, $K = 12$ and $|\zeta(\xi)| = \frac{1}{4}M^{3/2}$. There is no added noise.

remaining intensity in the signal compared to the case $M = 9.7$ in Figure 4 could suggest that additional regularization is needed.

The truncation radii of reconstructions in Figure 3 and 4 chosen by visual inspection are plotted and compared to the theoretically predicted truncation radius in Figure 5. This comparison suggests the prediction is somewhat pessimistic and that the practical algorithm allows for lighter regularization in comparison to what the theoretical estimates portend. However, the prediction and practical reconstructions are not directly comparable, since we should pick $|\zeta(\xi)| = K_1 M^p$ with p strictly larger than $3/2$ according to theory. Finally, we note the noise model utilized by [17] and [26] give somewhat different results compared to our unnormalized perturbation. The results also raise the question of how practical the reconstruction method is for more realistic data. Had we decreased the resolution of the basis of spherical harmonics to which voltages and currents are projected, the approximation error of highly oscillatory functions would increase. In this case we can expect to pick the truncation radius smaller to get a stable reconstruction. Investigating the reconstruction method for electrode data is subject to further study and is related to [29] for the two-dimensional D-bar method and [26] for the three-dimensional so-called $\mathbf{t}^{\exp}$ approximation. Possible improvements to the truncation strategy

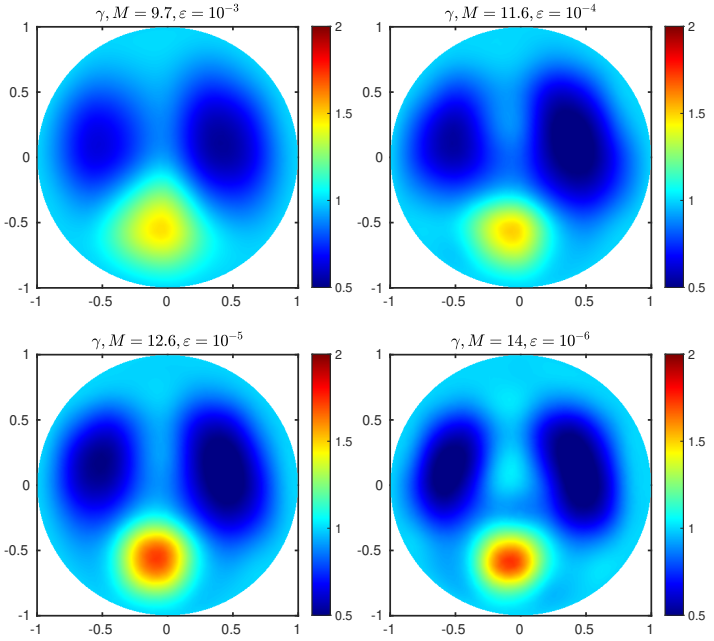

FIGURE 3. Cross sections ($x^3 = 0$) of reconstructions using the regularized reconstruction algorithm on noisy Dirichlet-to-Neumann maps. The noise levels correspond to relative noise levels $\varepsilon \approx 0.1\%$ with SNR $= 12 \cdot 10^3$ (top left), $\varepsilon \approx 0.01\%$ with SNR $= 123 \cdot 10^3$ (top right), $\varepsilon \approx 0.001\%$ with SNR $= 1172 \cdot 10^3$ (bottom left) and $\varepsilon \approx 0.0001\%$ with SNR $= 11299 \cdot 10^3$ (bottom right). The parameters used are $K = 11$ and $|\zeta(\xi)| = \frac{1}{3\sqrt{2}} M^{3/2}$.

include extending the support of $\mathbf{t}$ with prior information using the forward map as in [5]. In addition, one could experiment with a truncation by thresholding as in [27].

7. **Conclusions.** In this paper we provide and investigate a regularization strategy for the Calderón problem in three dimensions. The main result of the paper is Theorem 1.1, which shows that the algorithm defined by Method 3 yields reconstructions approximating the true conductivity, when using data corrupted by a sufficiently small perturbation. The proof relies on a gap of the magnitude of the complex frequency in which the existence of unique CGO solutions is guaranteed and the noise level allows a stable and unique solution to the boundary integral equation. The reconstructions from this strategy are regular as a result of the spectral filtering. Numerical results show the regularizing behavior of the reconstruction algorithm in practice and suggests one can utilize higher frequency information in

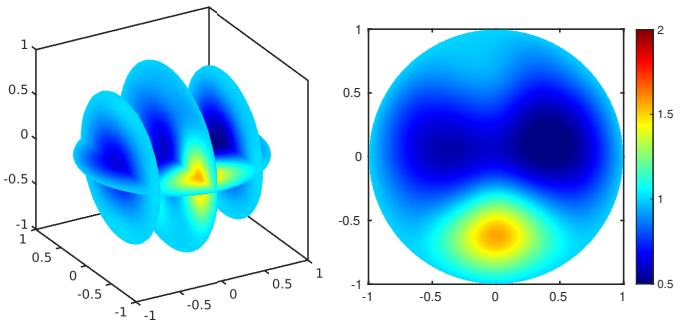

(A) (B)

FIGURE 4. Regularized reconstruction using noisy Dirichlet-to-Neumann maps with $\varepsilon = 10^{-2}$, which corresponds to approximately 1% relative noise and SNR $= 1.17 \cdot 10^3$. Plot (A) shows the cross sections $x^3 = 0$, $x^2 = -0.6$, $x^2 = -0.05$ and $x^2 = 0.6$, whereas plot (B) shows the plane corresponding to $x^3 = 0$. The parameters used are $M = 9$, $K = 11$ and $|\zeta(\xi)| = \frac{1}{3\sqrt{2}} M^{3/2}$.

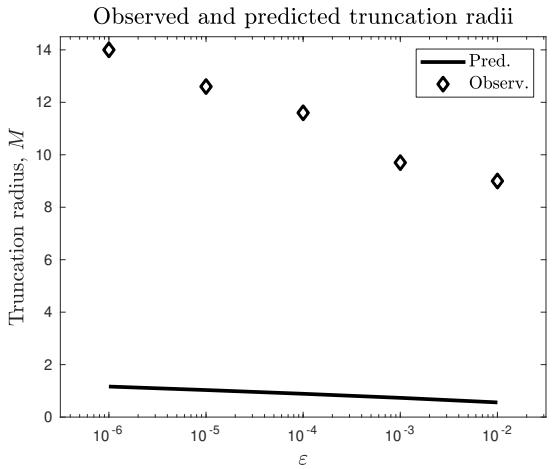

FIGURE 5. The truncation radii as predicted by theory $M = (-1/11 \log(\varepsilon))^{-1/p}$ for $p = 3/2$, and the chosen truncation radii for the noisy reconstructions of Figure 3 and 4.

the data than suggested by the theory. The reconstructions of piecewise constant conductivity data show promise even in the case of 1% relative noise.

Acknowledgments. AKR and KK were supported by The Villum Foundation (grant no. 25893).

REFERENCES

[1] K. Abraham and R. Nickl, On statistical Calderón problems, *Math. Stat. Learn.*, **2** (2019), 165–216.
[2] A. Adler, R. Amyot, R. Guardo, J. Bates and Y. Berthiaume, Monitoring changes in lung air and liquid volumes with electrical impedance tomography, *Journal of Applied Physiology*, **83** (1997), 1762–1767.
[3] G. Alessandrini, Stable determination of conductivity by boundary measurements, *Appl. Anal.*, **27** (1988), 153–172.
[4] G. Alessandrini, Singular solutions of elliptic equations and the determination of conductivity by boundary measurements, *J. Differential Equations*, **84** (1990), 252–272.
[5] M. Alsaker and J. L. Mueller, A D-bar algorithm with a priori information for 2-dimensional electrical impedance tomography, *SIAM J. Imaging Sci.*, **9** (2016), 1619–1654.
[6] K. Astala and L. Päivärinta, Calderón's inverse conductivity problem in the plane, *Ann. of Math. (2)*, **163** (2006), 265–299.
[7] J. Bikowski, K. Knudsen and J. L. Mueller, Direct numerical reconstruction of conductivities in three dimensions using scattering transforms, *Inverse Problems*, **27** (2011), 015002, 19 pp.
[8] G. Boverman, T.-J. Kao, D. Isaacson and G. J. Saulnier, An implementation of Calderón's method for 3-D Limited-View EIT, *IEEE Transactions on Medical Imaging*, **28** (2009), 1073–82.
[9] R. M. Brown, Global uniqueness in the impedance-imaging problem for less regular conductivities, *SIAM J. Math. Anal.*, **27** (1996), 1049–1056.
[10] A.-P. Calderón, On an inverse boundary value problem, in *Seminar on Numerical Analysis and its Applications to Continuum Physics (Rio de Janeiro, 1980)*, Soc. Brasil. Mat., Rio de Janeiro, 1980, 65–73.
[11] P. Caro and A. Garcia, The Calderón problem with corrupted data, *Inverse Problems*, **33** (2017), 085001, 17 pp.
[12] P. Caro and K. M. Rogers, Global uniqueness for the Calderón problem with Lipschitz conductivities, *Forum. Math. Pi*, **4** (2016), e2, 28 pp.
[13] V. Cherepenin, A. Karpov, A. Korjenevsky, V. Kornienko, Y. Kultiasov, M. Ochapkin, O. Trochanova and J. Meister, Three-dimensional EIT imaging of breast tissues: System design and clinical testing, *IEEE Transactions on Medical Imaging*, **21** (2002), 662–667.
[14] D. Colton and R. Kress, *Inverse Acoustic and Electromagnetic Scattering Theory*, vol. 93 of Applied Mathematical Sciences, Springer-Verlag, Berlin, 1992.
[15] H. Cornean, K. Knudsen and S. Siltanen, Towards a d-bar reconstruction method for three-dimensional EIT, *J. Inverse Ill-Posed Probl.*, **14** (2006), 111–134.
[16] F. Delbary, P. C. Hansen and K. Knudsen, Electrical impedance tomography: 3D reconstructions using scattering transforms, *Appl. Anal.*, **91** (2012), 737–755.
[17] F. Delbary and K. Knudsen, Numerical nonlinear complex geometrical optics algorithm for the 3D Calderón problem, *Inverse Probl. Imaging*, **8** (2014), 991–1012.
[18] D. C. Dobson, Convergence of a reconstruction method for the inverse conductivity problem, *SIAM J. Appl. Math.*, **52** (1992), 442–458.
[19] M. Dunlop and A. Stuart, The Bayesian formulation of EIT: Analysis and algorithms, *Inverse Probl. Imaging*, **10** (2016), 1007–1036.
[20] H. W. Engl, M. Hanke and A. Neubauer, *Regularization of Inverse Problems*, vol. 375 of Mathematics and its Applications, Kluwer Academic Publishers Group, Dordrecht, 1996.
[21] L. C. Evans, *Partial Differential Equations*, vol. 19, American Mathematical Society, 2010.
[22] I. Frerichs and T. Becher, Chest electrical impedance tomography measures in neonatology and paediatrics - a survey on clinical usefulness, *Physiological Measurement*, **40** (2019), 054001.
[23] M. Frigo and S. G. Johnson, The design and implementation of FFTW3, *Proceedings of the IEEE*, **93** (2005), 216–231.
[24] N. Goren, J. Avery, T. Dowrick, E. Mackle, A. Witkowska-Wrobel, D. Werring and D. Holder, Multi-frequency electrical impedance tomography and neuroimaging data in stroke patients, *Scientific Data*, **5** (2018), 180112, 10 pp.

[25] M. Hallaji, A. Seppänen and M. Pour-Ghaz, Electrical impedance tomography-based sensing skin for quantitative imaging of damage in concrete, *Smart Materials and Structures*, **23** (2014), 085001.
[26] S. J. Hamilton, D. Isaacson, V. Kolehmainen, P. A. Muller, J. Toivainen and P. F. Bray, 3D electrical impedance tomography reconstructions from simulated electrode data using direct inversion t^{exp} and Calderón methods, *Inverse Probl. Imaging*, **15** (2021), 1135–1169.
[27] A. Hauptmann, M. Santacesaria and S. Siltanen, Direct inversion from partial-boundary data in electrical impedance tomography, *Inverse Problems*, **33** (2017), 025009, 26 pp.
[28] T. C. Hou and J. P. Lynch, Electrical impedance tomographic methods for sensing strain fields and crack damage in cementitious structures, *Journal of Intelligent Material Systems and Structures*, **20** (2009), 1363–1379.
[29] D. Isaacson, J. Mueller, J. Newell and S. Siltanen, Reconstructions of chest phantoms by the d-bar method for electrical impedance tomography, *IEEE Transactions on Medical Imaging*, **23** (2004), 821–828.
[30] B. Jin and P. Maass, An analysis of electrical impedance tomography with applications to Tikhonov regularization, *ESAIM Control Optim. Calc. Var.*, **18** (2012), 1027–1048.
[31] J. P. Kaipio, V. Kolehmainen, E. Somersalo and M. Vauhkonen, Statistical inversion and Monte Carlo sampling methods in electrical impedance tomography, *Inverse Problems*, **16** (2000), 1487–1522.
[32] A. Kirsch, *An Introduction to the Mathematical Theory of Inverse Problems*, vol. 120 of Applied Mathematical Sciences, 2nd edition, Springer, New York, 2011.
[33] K. Knudsen, A new direct method for reconstructing isotropic conductivities in the plane, *Physiological Measurement*, **24** (2003), 391–401.
[34] K. Knudsen, M. Lassas, J. L. Mueller and S. Siltanen, D-bar method for electrical impedance tomography with discontinuous conductivities, *SIAM J. Appl. Math.*, **67** (2007), 893–913.
[35] K. Knudsen, M. Lassas, J. L. Mueller and S. Siltanen, Regularized D-bar method for the inverse conductivity problem, *Inverse Probl. Imaging*, **3** (2009), 599–624.
[36] K. Knudsen and J. L. Mueller, The Born approximation and Calderón's method for reconstruction of conductivities in 3-D, *Discrete Contin. Dyn. Syst.*, 8th AIMS Conference. Suppl. Vol. II, 2011, 844–853.
[37] A. Lechleiter and A. Rieder, Newton regularizations for impedance tomography: Convergence by local injectivity, *Inverse Problems*, **24** (2008), 065009, 18 pp.
[38] S. Leonhardt and B. Lachmann, Electrical impedance tomography: The holy grail of ventilation and perfusion monitoring?, *Intensive Care Medicine*, **38** (2012), 1917–1929.
[39] J.-L. Lions and E. Magenes, *Non-Homogeneous Boundary Value Problems and Applications. Vol. I*, Springer-Verlag, New York-Heidelberg, 1972, Translated from the French by P. Kenneth, Die Grundlehren der mathematischen Wissenschaften, Band 181.
[40] E. Malone, M. Jehl, S. Arridge, T. Betcke and D. Holder, Stroke type differentiation using spectrally constrained multifrequency EIT: Evaluation of feasibility in a realistic head model, *Physiological Measurement*, **35** (2014), 1051–1066.
[41] N. Mandache, Exponential instability in an inverse problem for the Schrödinger equation, *Inverse Problems*, **17** (2001), 1435–1444.
[42] J. L. Mueller and S. Siltanen, Direct reconstructions of conductivities from boundary measurements, *SIAM J. Sci. Comput.*, **24** (2003), 1232–1266.
[43] J. L. Mueller, S. Siltanen and D. Isaacson, A direct reconstruction algorithm for electrical impedance tomography, *IEEE Transactions on Medical Imaging*, **21** (2002), 555–559.
[44] A. I. Nachman, Reconstructions from boundary measurements, *Ann. of Math. (2)*, **128** (1988), 531–576.
[45] A. I. Nachman, Global uniqueness for a two-dimensional inverse boundary value problem, *Ann. of Math. (2)*, **143** (1996), 71–96.
[46] A. Nachman, J. Sylvester and G. Uhlmann, An n-dimensional Borg-Levinson theorem, *Comm. Math. Phys.*, **115** (1988), 595–605.
[47] R. G. Novikov, Multidimensional inverse spectral problem for the equation $-\Delta\psi + (v(x) - Eu(x))\psi = 0$, *Functional Analysis and its Applications*, **22** (1988), 263–272.
[48] M. Reed and B. Simon, *Methods of Modern Mathematical Physics 1, Functional Analysis*, Academic Press, 1980.
[49] L. Rondi, On the regularization of the inverse conductivity problem with discontinuous conductivities, *Inverse Probl. Imaging*, **2** (2008), 397–409.

[50] L. Rondi, Discrete approximation and regularisation for the inverse conductivity problem, *Rend. Istit. Mat. Univ. Trieste*, **48** (2016), 315–352.
[51] M. Salo, Semiclassical pseudodifferential calculus and the reconstruction of a magnetic field, *Comm. Partial Differential Equations*, **31** (2006), 1639–1666.
[52] C. Schmidt, S. Wagner, M. Burger, U. V. Rienen and C. H. Wolters, Impact of uncertain head tissue conductivity in the optimization of transcranial direct current stimulation for an auditory target, *Journal of Neural Engineering*, **12** (2015), 046028.
[53] S. Siltanen, J. Mueller and D. Isaacson, Erratum: "An implementation of the reconstruction algorithm of A. Nachman for the 2D inverse conductivity problem" [Inverse Problems **16** (2000), 681–699], *Inverse Problems*, **17** (2001), 1561–1563.
[54] S. Siltanen, J. Mueller and D. Isaacson, An implementation of the reconstruction algorithm of A. Nachman for the 2D inverse conductivity problem, *Inverse Problems*, **16** (2000), 681–699.
[55] P. Sołtan, *A Primer on Hilbert Space Operators*, Springer International Publishing, 2018.
[56] J. Sylvester and G. Uhlmann, A global uniqueness theorem for an inverse boundary value problem, *Ann. of Math. (2)*, **125** (1987), 153–169.
[57] Y. Zhao, E. Zimmermann, J. A. Huisman, A. Treichel, B. Wolters, S. Van Waasen and A. Kemna, Broadband EIT borehole measurements with high phase accuracy using numerical corrections of electromagnetic coupling effects, *Measurement Science and Technology*, **24** (2013), 085005.
[58] Y. Zou and Z. Guo, A review of electrical impedance techniques for breast cancer detection, *Medical Engineering and Physics*, **25** (2003), 79–90.

Received June 2021; revised November 2021; early access January 2022.

E-mail address: kiknu@dtu.dk
E-mail address: akara@dtu.dk

Appendix B

Paper B

The following appendix is a paper titled *A Bayesian approach for consistent reconstruction of inclusions* by Babak Maboudi Afkham, Kim Knudsen, Aksel Kaastrup Rasmussen and Tanja Tarvainen, currently in submission and available on arXiv, arXiv:2308.13673, 2023.

A Bayesian approach for consistent reconstruction of inclusions

B M Afkham[1], K Knudsen[1], A K Rasmussen[1]‡ and T Tarvainen[2]

[1] Department of Applied Mathematics and Computer Science, Technical University of Denmark, DK-2800 Kgs. Lyngby, Denmark
[2] Department of Technical Physics, University of Eastern Finland, Kuopio 70210, Finland

E-mail: akara@dtu.dk

Abstract. This paper considers a Bayesian approach for inclusion detection in nonlinear inverse problems using two known and popular push-forward prior distributions: the star-shaped and level set prior distributions. We analyze the convergence of the corresponding posterior distributions in a small measurement noise limit. The methodology is general; it works for priors arising from any Hölder continuous transformation of Gaussian random fields and is applicable to a range of inverse problems. The level set and star-shaped prior distributions are examples of push-forward priors under Hölder continuous transformations that take advantage of the structure of inclusion detection problems. We show that the corresponding posterior mean converges to the ground truth in a proper probabilistic sense. Numerical tests on a two-dimensional quantitative photoacoustic tomography problem showcase the approach. The results highlight the convergence properties of the posterior distributions and the ability of the methodology to detect inclusions with sufficiently regular boundaries.

Keywords: inverse problems, Bayesian inference, inclusion detection, Gaussian prior, posterior consistency

1. Introduction

The Bayesian approach to inverse problems has in recent decades generated considerable interest due to its ability to incorporate prior knowledge and quantify uncertainty in solutions to inverse problems, see [1, 2]. A commonly recurring objective in inverse problems for imaging science is to recover inhomogeneities or inclusions, i.e. piecewise constant features, in a medium; applications range from cancer detection in medical imaging [3, 4] to defect detection in material science [5, 6]. In a Bayesian framework, this can be tackled by designing a prior distribution that favors images with these features.

An optimization-based approach can address this by parametrizing the relevant subset of the image space and minimizing a functional over the preimage of this parametrization, see for example [7]. This is visualized in Figure 1, where we consider

‡ Corresponding author

the parametrization Φ defined on a linear space Θ and giving rise to the subset $\Phi(\Theta)$ of the image space

$$L^2_\Lambda(D) = \{\gamma \in L^2(D) : \Lambda^{-1} \leq \gamma \leq \Lambda \text{ a.e.}\},$$

where D is a bounded and smooth domain in $\mathbb{R}^d$, $d = 2, 3$ and $\Lambda > 0$ is a constant. Such approaches benefit computationally from the fact that the set of images with inclusions, i.e. $\Phi(\Theta)$, form a low-dimensional subset of the image space $L^2_\Lambda(D)$. In the Bayesian framework, a related approach makes use of a push-forward distribution as the prior distribution, i.e. the distribution of a transformed random element of Θ. This often leads to strong *a priori* assumptions, as the prior only gives mass to the range of the parametrization. More classical prior distributions including Laplace-type priors, see for example [8], and other heavy-tailed distributions often fail to take advantage of the low dimension of such images.

In this paper, we consider a Bayesian approach that captures this idea for two parametrizations used in detection of inclusions for nonlinear inverse problems: the star-shaped set and level set parametrizations. These parametrizations are studied rigorously in [9, 10, 11] and remain popular to Bayesian practitioners: we mention [1, 12, 13, 14, 15, 16] in the case of the star-shaped inclusions and [17, 18, 19, 20, 12, 21] for the level set inclusions, see also references therein.

The solution to the inverse problem in the Bayesian setting is the conditional distribution of the unknown given data, referred to as the posterior distribution. The posterior distribution has proved to be well-posed in the sense of [2] for such parametrizations. This means that the posterior distribution continuously depends on the data in some metric for distributions. This property implies, for example, that the posterior mean and variance are continuous with respect to the data, see [8]. However, such results give no guarantee as to where the posterior distribution puts its mass.

A more recent framework provided in [22] using ideas from [23], see also [24], gives tools to analyze the convergence of the posterior distribution for nonlinear inverse problems. Such results, known as 'posterior consistency', address whether the sequence of posterior distributions arising from improving data (in a small noise or large sample size limit) gives mass approximating 1 to balls centered in the ground true parameter γ_0 generating the data. Nonlinearity in the forward map and parametrization makes consistency results for Gaussian posterior distributions, as in [25], inapplicable. Currently, the setting of [22] and similar approaches require smoothness of the parameter of interest. A crucial condition is that the parameter set that is given most of the mass by the prior, has small 'complexity' in the sense of covering numbers, see [23, Theorem 2.1] or [24, Theorem 1.3.2]. Using Gaussian priors, this parameter set is typically a closed Sobolev or Hölder norm ball, see [24, Theorem 2.2.2] or [22]. However, such priors do not give sufficient mass to discontinuous parameters to conclude consistency. In this paper, we aim to address this, at least partially, by parametrizing the set of discontinuous parameters from a linear space Θ of sufficiently smooth functions.

We aim to recover an element γ, which we call the *image* or the *physical parameter*, in a subset $\Phi(\Theta)$ of $L^2_\Lambda(D)$ for some continuous map $\Phi : \Theta \to L^2_\Lambda(D)$. We consider a nonlinear forward map $\mathcal{G} : L^2_\Lambda(D) \to \mathcal{Y}$ mapping into a real separable Hilbert space

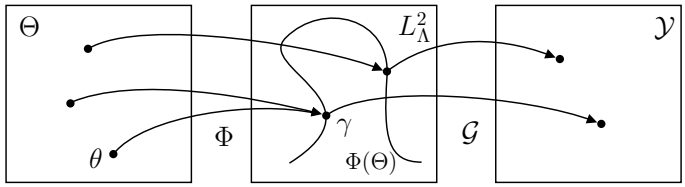

Figure 1: A visiualization of the parametrization $\Phi : \Theta \to L^2_\Lambda(D)$ and forward map $\mathcal{G} : L^2_\Lambda(D) \to \mathcal{Y}$.

$\mathcal{Y}$ with inner product $\langle \cdot, \cdot \rangle$ and norm $\|\cdot\|$. We refer again to Figure 1 for an overview of this setup. This setting allows us to make use of the framework provided in [22], but transfer the complexity condition from subsets of $L^2_\Lambda(D)$ to subsets of Θ, see Section 3.2. In the context of inclusion detection, this means we can detect inclusions with sufficiently smooth boundaries.

Our contributions can be summarized as follows:

- We present a posterior consistency result for the general setting mentioned above, when the parametrization Φ satisfies mild conditions in regularity. We use the framework provided by [22] extending to Hölder continuous $\mathcal{G}$ and push-forward priors. In particular, this gives an estimator, the posterior mean, which converges in probability to the true physical parameter in the small noise limit. Formally, this means there is an algorithm $\hat{\gamma}$ defined for noisy measurements Y depending on the noise level $\varepsilon > 0$ such that
$$\|\hat{\gamma}(Y) - \gamma_0\|_{L^2(D)} \to 0$$
in probability as $\varepsilon \to 0$. This statement will be made precise in Section 2. Furthermore, the rate of convergence is determined in part by the smoothness of elements in Θ and the regularity of the parametrization.
- We show that two parametrizations for inclusion detection, a star-shaped set parametrization and a smoothened level set parametrization, satisfy the conditions for this setup. This verifies and quantifies the use of such parametrizations.
- We numerically verify the approach based on the two parametrizations in a small noise limit for a nonlinear PDE-based inverse problem using Markov chain Monte Carlo (MCMC) methods. We consider a two-dimensional quantitative photoacoustic (QPAT) problem of detecting an absorption coefficient. We derive a new stability estimate following [26, 27].

We note that the framework of [22] in e.g. [28] and [29] shows consistency for 'regular link functions' Φ (defined in [30]), which are smooth and bijective. The archetypal example is $\Phi = \exp$ or a smoothened version to ensure positivity of the physical parameter γ. As we shall see, injectivity and inverse continuity are not necessary for the proofs when we want to show consistency in $L^2_\Lambda(D)$. One novelty of our work is to show that this observation has relevance: we seek to recover the physical parameter γ instead of a non-physical parameter in Θ that generated it. As we shall see, a natural parametrization for star-shaped inclusions is Hölder continuous from a suitable space

Θ to $L^2_\Lambda(D)$. The same holds true for a smoothened level set parametrization, which we will encounter in Section 4.2.

The structure of the paper can be summarized as follows. In Section 2, we recall a few key elements of the Bayesian framework in a 'white noise' model as outlined in [2] and [31, Section 7.4], including the notion of posterior consistency with a rate. In Section 3, we show that Hölder continuity of Φ, some smoothness of elements in $\Phi(\Theta)$ and conditional continuity of $\mathcal{G}^{-1}$, suffice to show that the posterior mean converges to the ground truth γ_0 in $L^2(D)$ as the noise goes to zero. Section 4 considers these conditions for the level set and star-shaped set parametrizations, which are well-known in the literature. In Section 5, we consider the two-dimensional quantitative photoacoustic tomography problem suited for piecewise constant parameter inference. Then, Section 6 gives background to our numerical tests and results that emulate the theoretical setting of Section 3. We present conclusive remarks in Section 7.

In the following, we let random variables be defined on a probability space $(\Omega, \mathcal{F}, \Pr)$. For a metric space $\mathcal{Z}_1$ the Borel σ-algebra is denoted by $\mathcal{B}(\mathcal{Z}_1)$. If $F : \mathcal{Z}_1 \to \mathcal{Z}_2$ is a measurable map between the measure space $(\mathcal{Z}_1, \mathcal{B}(\mathcal{Z}_1), m)$ and the measurable space $(\mathcal{Z}_2, \mathcal{B}(\mathcal{Z}_2))$, then Fm denotes the push-forward measure defined by $Fm(B) = m(F^{-1}(B))$ for all $B \in \mathcal{B}(\mathcal{Z}_1)$. We denote by $L^2(\Omega, \Pr)$ the space of real-valued square integrable measurable functions from $(\Omega, \mathcal{F}, \Pr)$ to $(\mathbb{R}, \mathcal{B}(\mathbb{R}))$. When Pr is the Lesbegue measure on $\mathbb{R}$, we simply write $L^2(\Omega)$. We call probability measures defined on $\mathcal{B}(\mathcal{Z}_1)$ Borel distributions.

2. The Bayesian approach to inverse problems

Bayesian inference in inverse problems centers around a posterior distribution. This is formulated by Bayes' rule once a prior distribution in $L^2_\Lambda(D)$ has been specified and the likelihood function has been determined by the measurement process. In this paper, we consider a 'continuous' model of indirect observations

$$Y = \mathcal{G}(\gamma) + \varepsilon_n \xi, \tag{1}$$

for a continuous forward map $\mathcal{G} : L^2_\Lambda(D) \to \mathcal{Y}$, where the separable Hilbert space $\mathcal{Y}$ has an orthonormal basis $\{e_k\}_{k=1}^\infty$. Here ξ is 'white noise' in $\mathcal{Y}$ defined below in (4). We denote the noise level by $\varepsilon_n := \frac{\sigma}{\sqrt{n}}$ for some $\sigma > 0$ and $n \in \mathbb{N}$, which has this convenient form to study a countable sequence of posterior distributions in decreasing noise, i.e. for growing n. When we write Y, it is understood that this depends on n and γ. The rate $n^{-1/2}$ is natural: if $\mathcal{Y}$ is a subspace of Hölder continuous functions on a bounded domain, this observation model is equivalent to observing n discrete point evaluations of $\mathcal{G}(\gamma)$ with added standard normal noise as $n \to \infty$, see [31] and [32, Section 1.2.3].

Given a Borel prior distribution Π on $L^2_\Lambda(D)$, the posterior distribution $\Pi(\cdot|Y)$ is proportional to the product of the likelihood and prior. Indeed, according to Bayes' rule, if $\mathcal{Y}$ is finite-dimensional, the posterior distribution has a density (Radon-Nikodym derivative) of the form

$$\frac{d\Pi(\cdot|y)}{d\Pi}(\gamma) = \frac{1}{Z} \exp\left(-\frac{1}{2\varepsilon_n^2}\|\mathcal{G}(\gamma) - y\|^2\right), \quad \forall y \in \mathcal{Y}$$

where $Z > 0$ is a constant, see for example [8, 33]. This is well-defined for almost all y under the marginal distribution of Y. The relevance of this object emerges, when evaluating it in a realization $Y(\omega) = y$. Using inner product rules we can rewrite this as

$$\Pi(B|Y) = \frac{1}{Z}\int_B \exp\left(\frac{1}{\varepsilon_n^2}\langle Y, \mathcal{G}(\gamma)\rangle - \frac{1}{2\varepsilon_n^2}\|\mathcal{G}(\gamma)\|^2\right)\Pi(d\gamma), \quad B \in \mathcal{B}(L^2_\Lambda(D)), \tag{2}$$

where the contribution of Y is absorbed in the constant $Z > 0$. The purpose of the following paragraphs is to argue that this formula remains valid, when $\mathcal{Y}$ is infinite-dimensional with the interpretation that $\langle Y, \mathcal{G}(\gamma)\rangle$ is a Gaussian random variable defined by

$$\langle Y, y\rangle := \langle \mathcal{G}(\gamma), y\rangle + \varepsilon_n W(y), \tag{3}$$

where W is a white noise process on $\mathcal{Y}$ satisfying $\mathbb{E}[W(y)] = 0$ and $\mathbb{E}[W(y)W(y')] = \langle y, y'\rangle$, see [32][Example 2.1.11]. To this end, let

$$\xi := \sum_{k=1}^{\infty} \xi_k e_k, \qquad \xi_k \overset{i.i.d.}{\sim} N(0,1), \tag{4}$$

which is convergent in $\mathcal{Y}_-$ in the mean square sense, see [8, Section 2.4], where $\mathcal{Y}_-$ is the Hilbert space $\mathcal{Y}_-$, see also [31, Section 7.4], defined by

$$\mathcal{Y}_- := \left\{ f = \sum_{k=1}^{\infty} f_k e_k : \|f\|_-^2 := \sum_{k=1}^{\infty} \lambda_k^2 f_k^2 < \infty \right\}$$

for $\lambda_k > 0$ and $\{\lambda_k\}_{k=1}^{\infty} \in \ell^2$. Note ξ is a Gaussian random element of $\mathcal{Y}_-$, since it is the Karhunen-Loeve expansion of a mean zero Gaussian random element with covariance operator $K : \mathcal{Y}_- \to \mathcal{Y}_-$ defined by $Ke_k = \lambda_k^2 e_k$, see [8]. Then Y is also a $\mathcal{Y}_-$-valued Gaussian random element, since it is a translation of $\varepsilon_n\xi$ by an element in $\mathcal{Y}$. We denote the distributions of $\varepsilon_n\xi$ and Y in $\mathcal{Y}_-$ by P_n and P_n^γ, respectively. We can think of P_n^γ as the data-generating distribution indexed by γ, the physical parameter generating the data, and n, which controls the noise regime.

The likelihood function arises as the density (Radon-Nikodym derivative) of P_n^γ with respect to P_n. This is a consequence of the Cameron-Martin theorem in the Hilbert space $\mathcal{Y}$. The theorem gives the likelihood function as

$$p_n^\gamma(Y) := \frac{dP_n^\gamma}{dP_n}(Y) = \exp\left(\frac{1}{\varepsilon_n^2}\langle Y, \mathcal{G}(\gamma)\rangle - \frac{1}{2\varepsilon_n^2}\|\mathcal{G}(\gamma)\|^2\right),$$

here evaluated in Y, see [32][Proposition 6.1.5]. See also a derivation in [31, Section 7.4], for which it suffices that $\gamma \mapsto \mathcal{G}(\gamma)$ is continuous from (the standard Borel space) $L^2_\Lambda(D)$ with the $L^2(D)$-topology into $\mathcal{Y}$.

Then Bayes' rule [33, p. 7] formulates *a* posterior distribution as a measure in $L^2_\Lambda(D)$ as in the right-hand side of (2), well-defined for almost all Y. According to [33], this equals almost surely a Markov kernel, which we will call *the* posterior distribution and also denote it by $\Pi(\cdot|Y)$. That is to say that $B \mapsto \Pi(B|Y(\omega))$ is a measure for every $\omega \in \Omega$ and $\omega \mapsto \Pi(B|Y(\omega))$ is measurable for every $B \in \mathcal{B}(L^2_\Lambda(D))$. In particular, $\omega \mapsto \Pi(B|Y(\omega))$ is a $[0,1]$-valued random variable.

Convergence in probability In preparation for the subsequent section, we recall the notion of convergence in probability. Let $t_n > 0$ be a decreasing sequence going to zero. For a fixed $\gamma_0 \in L^2_\Lambda(D)$ and a sequence of measurable functions $f_n : \mathcal{Y}_- \to \mathbb{R}$ we say that the sequence of random variables $\{f_n(Y)\}_{n=1}^\infty$ converges to $\upsilon \in \mathbb{R}$ in $P_n^{\gamma_0}$-probability with rate t_n as $n \to \infty$ if there exists a constant $C > 0$ such that

$$P_n^{\gamma_0}(y \in \mathcal{Y}_- : |f_n(y) - \upsilon| \leq Ct_n) \to 1, \tag{5}$$

as $n \to \infty$. We consider the following two cases, where we recall that both the posterior distribution and Y depend tacitly on n.

(i) For a sequence of sets $\{B_n\}_{n=1}^\infty$ in $\mathcal{B}(L^2_\Lambda(D))$, we could claim that

$$\Pi(B_n|Y) \to 1 \quad \text{in } P_n^{\gamma_0}\text{-probability},$$

with rate t_n as $n \to \infty$. That is, $f_n(Y) = \Pi(B_n|Y)$ and $\upsilon = 1$. If this is the case for $B_n := \{\gamma : \|\gamma - \gamma_0\|_{L^2(D)} \leq C_0 r_n\}$ for some decreasing sequence $r_n > 0$ going to zero and constant $C_0 > 0$, we say that the posterior distribution *contracts around* or is *consistent in* γ_0 at rate r_n.

(ii) Denote by $E[\gamma|Y]$ the mean ('posterior mean') with respect to $\Pi(\cdot|Y)$. This is defined in the sense of a Bochner integral,

$$E[\gamma|Y] := \int_{L^2_\Lambda(D)} \gamma \, \Pi(d\gamma|Y),$$

which is well-defined by [34, Theorem 2], since for all $\omega \in \Omega$

$$\int_{L^2_\Lambda(D)} \|\gamma\|_{L^2(D)} \, d\Pi(d\gamma|Y(\omega)) \leq \Lambda\sqrt{\mathrm{vol}(D)} < \infty.$$

Then $\omega \mapsto E[\gamma|Y(\omega)]$ is an $L^2(D)$-valued random element by the definition of the Bochner integral and by the measurability of pointwise limits of measurable functions, see [35, Theorem 4.2.2]. We could claim that

$$\|E[\gamma|Y] - \gamma_0\|_{L^2(D)} \to 0 \quad \text{in } P_n^{\gamma_0}\text{-probability},$$

with rate t_n as $n \to \infty$. That is, $f_n(Y) = \|E[\gamma|Y] - \gamma_0\|_{L^2(D)}$ and $\upsilon = 0$.

2.1. Posterior consistency

In this section we recall sufficient conditions posed in [22], see also [24], such that the posterior distribution in our specific setup is consistent. More specifically, we recall for which ground truths $\gamma_0 \in L^2_\Lambda(D)$, forward models $\mathcal{G}$ and prior distributions Π

$$\Pi(\gamma : \|\gamma - \gamma_0\|_{L^2(D)} \leq C\tilde{r}_n|Y) \to 1 \quad \text{in } P_n^{\gamma_0}\text{-probability}, \tag{6}$$

as $n \to \infty$ for some positive decreasing sequence $\tilde{r}_n$ going to zero. A consequence of this result, under additional assumptions on the prior, is that the posterior mean converges to γ_0 in $P_n^{\gamma_0}$-probability, see [24, Theorem 2.3.2] or [33, Theorem 8.8],

$$\|E[\gamma|Y] - \gamma_0\|_{L^2(D)} \to 0 \quad \text{in } P_n^{\gamma_0}\text{-probability}, \tag{7}$$

with rate r_n as $n \to \infty$. This is the case of (ii) above. In the nonlinear inverse problem setting, posterior consistency in the sense of (6) follows from a two-step procedure with the use of conditional stability estimates.

Step 1 The first step reduces convergence of $\{\Pi(\tilde{B}_n|Y)\}_{n=1}^{\infty}$ from sets of the form

$$\tilde{B}_n = \{\gamma \in L^2_\Lambda(D) : \|\gamma - \gamma_0\|_{L^2(D)} \leq C\tilde{r}_n\}$$

to sets of the form

$$B_n = \{\gamma \in L^2_\Lambda(D) : \|\mathcal{G}(\gamma) - \mathcal{G}(\gamma_0)\| \leq Cr_n, \gamma \in A_n\}.$$

Indeed, for specially chosen subsets $A_n \subset L^2_\Lambda(D)$ which may depend on n, assume we have the estimate

$$\|\gamma_1 - \gamma_2\|_{L^2(D)} \leq \|\mathcal{G}(\gamma_1) - \mathcal{G}(\gamma_2)\|^\nu, \tag{8}$$

for all $\gamma_1, \gamma_2 \in A_n$ and some $\nu > 0$. Then $B_n \subset \tilde{B}_n$ and hence

$$\Pi(B_n|Y) \leq \Pi(\tilde{B}_n|Y), \tag{9}$$

where $\tilde{r}_n = r_n^\nu$.

Step 2 The second step involves showing that $\Pi(B_n|Y)$ converges to 1 in $P_n^{\gamma_0}$-probability as $n \to \infty$. This is posterior consistency on the 'forward level'.

Combining **Step 1** and **Step 2**, we find that $\Pi(\tilde{B}_n|Y)$ converges to 1 in $P_n^{\gamma_0}$-probability as $n \to \infty$. The 'conditional' stability estimate of the first step is of independent interest for many inverse problems in literature and usually requires an in-depth analysis of the inverse problem at hand. In this paper we treat first (8) as an assumption, see Condition 2. Although any modulus of continuity will do for the first step in this two-step procedure, for our concrete example in photoacoustic tomography we will show a Lipschitz stability estimate that holds for all $\gamma \in L^2_\Lambda(D)$, see Section 5. Our main motivation for including A_n in the analysis is to keep the exposition generally applicable.

One of the contributions of [22, 24] is to address **Step 2** for a random design regression observation model using Theorem 2.1 in [23] and the equivalence between the distance (semi-metric)

$$d_{\mathcal{G}}(\gamma_1, \gamma_2) := \|\mathcal{G}(\gamma_1) - \mathcal{G}(\gamma_2)\|$$

and the Hellinger distance, see [24], of the data-generating distributions (corresponding to our p_n^γ). Theorem 28 in [31], see also [32, Theorem 7.3.5], adapts the proof to the observation model (1), which is what we will use. One can see this second step as showing posterior consistency in $\mathcal{G}(\gamma_0)$ at rate r_n for the push-forward $\mathcal{G}\Pi(\cdot|Y)$ as in [36]. Below, we use the covering number $N(A, d, \rho)$ for a semimetric d, which denotes the minimum number of closed d-balls of radius $\rho > 0$ needed to cover A, see Appendix A for a precise definition. Then the condition to complete **Step 2** is as follows.

Condition A. *Let $\Pi = \Pi_n$ be a sequence of prior distributions in $L^2_\Lambda(D)$. Let $\mathcal{G}$ be the forward model $\mathcal{G} : L^2_\Lambda(D) \to \mathcal{Y}$ and $\gamma_0 \in L^2_\Lambda(D)$ the ground truth. Let r_n satisfy $r_n = n^{-a}$ for some $0 < a < 1/2$. Suppose that,*

A.1 *the prior gives enough mass to contracting balls $B_{\mathcal{G}}(\gamma_0, r_n) := \{\gamma : d_{\mathcal{G}}(\gamma, \gamma_0) \leq r_n\}$.*

$$\Pi(B_{\mathcal{G}}(\gamma_0, r_n)) \geq e^{-C_1 n r_n^2}, \quad C_1 > 0, \tag{10}$$

A.2 *there exist sets A_n that are almost the support of Π in the sense that*

$$\Pi(L^2_\Lambda(D) \setminus A_n) \leq e^{-C_2 n r_n^2}, \quad C_2 > C_1 + 4, \tag{11}$$

A.3 *and that there exists a constant $m_0 > 0$ such that*

$$\log N(A_n, d_{\mathcal{G}}, m_0 r_n) \leq C_3 n r_n^2, \quad C_3 > 0, \tag{12}$$

all for n large enough.

Condition **A.1** is a sufficient condition such that the denominator of the posterior distribution cannot decay too fast as $n \to \infty$. This is helpful when showing $\Pi(B_n^c|Y) \to 0$ in $P_n^{\gamma_0}$-probability as $n \to \infty$. On the other hand Condition **A.2** and **A.3** are conditions that give control over the numerator in a sense that is made precise in the proof of Theorem 2.1 in [23] (or for example Theorem 28 in [31]). It is also a trade-off; the sets A_n should be large enough such that they are almost the support of the prior, but small enough such that the covering number increases sufficiently slowly when $n \to \infty$. In the general case, **Step 2** is completed by the following result proved in Appendix B.

Theorem 2.1. *Let $\Pi(\cdot|Y)$ be the sequence of posterior distributions arising for the model (1) with $\gamma_0 \in L^2_\Lambda(D)$, $\mathcal{G}$ and prior distributions $\Pi = \Pi_n$ satisfying Condition A for some rate r_n. Then, there exists $C_0 = C_0(C_2, C_3, m_0, \sigma)$ such that*

$$\Pi(B_{\mathcal{G}}(\gamma_0, C_0 r_n) \cap A_n|Y) \to 1 \quad \text{in } P_n^{\gamma_0}\text{-probability}, \tag{13}$$

with rate $e^{-bnr_n^2}$ for all $0 < b < C_2 - C_1 - 4$ as $n \to \infty$.

Given the preceding result, we can conclude posterior consistency in γ_0 at rate $\tilde{r}_n$ as in **Step 1**, if we have a conditional stability estimate as (8).

2.2. Markov chain Monte Carlo

While Section 2.1 concludes in an abstract way the usefulness of the posterior distribution, in this section we briefly recall methods to approximate it. We consider MCMC methods that approximate $E[\gamma|Y]$ (or other statistics) from averages of samples from a Markov chain that has the posterior distribution as its stationary distribution. Since the composition $\mathcal{G} \circ \Phi$ maps Θ into $\mathcal{Y}$ continuously by assumption, given a prior distribution Π_θ in Θ, there exists a posterior distribution $\Pi_\theta(\cdot|Y)$ in Θ of the form

$$\Pi_\theta(B|Y) := \frac{1}{Z} \int_B \exp\left(\frac{1}{\varepsilon_n^2} \langle Y, \mathcal{G}(\Phi(\theta)) \rangle - \frac{1}{2\varepsilon_n^2} \|\mathcal{G}(\Phi(\theta))\|^2 \right) \Pi_\theta(d\theta), \quad B \in \mathcal{B}(\Theta). \tag{14}$$

Naturally, if $\Pi = \Phi\Pi_\theta$, then by a change of variables

$$\Pi(\cdot|Y) = \Phi\Pi_\theta(\cdot|Y),$$

see for example [36, Theorem B.1], i.e. $\theta \sim \Pi_\theta(\cdot|Y)$ implies $\Phi(\theta) \sim \Pi(\cdot|Y)$. This gives rise to the following 'high-level' algorithm: given a realization $y \in \mathcal{Y}_-$ of Y,

1. choose $\theta^{(0)} \in \Theta$ and $K > 0$,
2. generate $\{\theta^{(k)}\}_{k=1}^K$ in Θ using $\theta^{(0)}$ as initial condition with an MCMC method targeting $\Pi_\theta(\cdot|y)$, and
3. return $\{\Phi(\theta^{(k)})\}_{k=1}^K$.

For our numerical examples, we use the preconditioned Crank-Nicolson (pCN) MCMC method, see [37]. This method uses only single evaluation of the log-likelihood function every iteration and is hence attractive for expensive PDE-based forward maps. It is well-defined when Θ is a Hilbert space and possesses favorable theoretical properties, see [37, 38]. The idea to generate samples from $\Pi(\cdot|y)$ by pushing forward samples also appears in certain reparametrizations of posterior distributions for the use of hyperparameters, see [39].

3. Posterior consistency using parametrizations

In this section, we follow [22, 24] in their approach to satisfy Condition A. In the case where $\Pi = \Phi\Pi_\theta$ for Π_θ Gaussian and $\mathcal{G} \circ \Phi$ Lipschitz continuous, the approach is the same. We give a brief recap for the case where $\mathcal{G} \circ \Phi$ is Hölder continuous for the convenience of the reader. We tackle this by introducing three new conditions convenient for an inverse problem setting. We oppose this to Condition A, which is general and applicable in many statistical inference problems. As our base case, we assume $\Theta = H^\beta(\mathcal{X})$, where $\mathcal{X}$ is either the d'-dimensional torus or a bounded Lipschitz domain $\mathcal{X} \subset \mathbb{R}^{d'}$, $d' \geq 1$ and $\beta > d'/2$. We include here the torus in our considerations, since it is a numerically convenient setting. For more general parametrizations for inclusion detection, we shall need small deviations from this setting. However, these cases will take the same starting point of $H^\beta(\mathcal{X})$ in Section 4. We begin by stating conditions on Φ, $\mathcal{G}$ and Π so that Condition A is satisfied. To do this, we introduce the following subset of Θ.

$$\mathcal{S}_\beta(M) = \{\theta \in \Theta : \|\theta\|_{H^\beta(\mathcal{X})} < M\}.$$

We then require the following conditions of Φ.

Condition 1 (On the parametrization Φ)**.** *For any $\theta_1, \theta_2 \in \mathcal{S}_\beta(M)$ for some $M > 0$, let*

$$\|\Phi(\theta_1) - \Phi(\theta_2)\|_{L^2(D)} \leq C_\Phi \|\theta_1 - \theta_2\|^\zeta_{L^\infty(\mathcal{X})} \tag{15}$$

for some constant $C_\Phi(M) > 0$ and $0 < \zeta < \infty$.

That is, we require at least conditional Hölder continuity of the parametrization map Φ. The $L^\infty(\mathcal{X})$ topology is not necessary for what follows and can be generalized to any L^p, $p \geq 1$ or H^s-norm, $s < \beta$. Similarly, we require conditional forward and inverse Hölder continuity of the forward map $\mathcal{G}$.

Condition 2 (On the forward map $\mathcal{G}$)**.** *For any $\gamma_1, \gamma_2 \in \Phi(\mathcal{S}_\beta(M))$, let*

$$\|\mathcal{G}(\gamma_1) - \mathcal{G}(\gamma_2)\| \leq C_\mathcal{G} \|\gamma_1 - \gamma_2\|^\eta_{L^2(D)}$$

for some constants $C_\mathcal{G}(M) > 0$ and $0 < \eta < \infty$. In addition, let

$$\|\gamma_1 - \gamma_2\|_{L^2(D)} \leq f(\|\mathcal{G}(\gamma_1) - \mathcal{G}(\gamma_2)\|),$$

for some increasing function $f : \mathbb{R} \to \mathbb{R}$, which is continuous at zero with $f(0) = 0$.

We have the following condition on the prior distributions Π we consider. They should be push-forward distributions of a scaled Gaussian prior distribution in Θ.

Condition 3 (Prior Π)**.** *Let Π'_θ be a centred Gaussian probability measure on $H^\beta(\mathcal{X})$, $\beta > d'/2$, with $\Pi'_\theta(H^\beta(\mathcal{X})) = 1$. Let the reproducing kernel Hilbert space (RKHS), see [33], $(\mathcal{H}, \|\cdot\|_\mathcal{H})$ of Π'_θ be continuously embedded into $H^\delta(\mathcal{X})$ for some $\delta > \beta$. Then Π_θ is the distribution of*

$$\theta = n^{a-\frac{1}{2}}\theta', \quad \theta' \sim \Pi'_\theta \tag{16}$$

for a as in Condition A. Then let $\Pi = \Phi\Pi_\theta$.

This gives the following structure

$$\mathcal{H} \subset H^\delta(\mathcal{X}) \subset H^\beta(\mathcal{X}) = \Theta. \tag{17}$$

If one chooses for example a Matérn covariance, see [40], such that $\Pi'_\theta(H^\beta(\mathcal{X})) = 1$, then $\mathcal{H} = H^\delta(\mathcal{X})$ with $\delta = \beta + d'/2$, see Example 11.8 and Lemma 11.35 in [33] or

[24, Theorem 6.2.3]. The scaling in (16) essentially updates the weight of the prior term to go slower to zero. Indeed, dividing through by the factor ε_n^{-2} appearing in the data-misfit term, the prior term scales as $\varepsilon_n^2 n^{1-2a} \sim r_n^2$. This term play the role of the 'regularization parameter' in [41]. Note that $\lim_{n\to\infty} r_n = 0$ and $\lim_{n\to\infty} \varepsilon_n^2/r_n^2 = 0$, as is needed for the convergence of Tikhonov regularizers for example, see [41, Theorem 5.2]. The scaling (16) is also common in the consistency literature, see for example [22]. In our setting, it ensures that samples are with high probability in a totally bounded set A_n, as was called for in Condition **A.2** and **A.3**. We note for $\beta > d'/2$ that Π'_θ is also a Gaussian measure on the separable Banach space $C(\overline{\mathcal{X}})$ endowed with the usual supremum norm $\|f\|_\infty := \sup_{x\in\overline{\mathcal{X}}} |f(x)|$. This is a consequence of a continuous Sobolev embedding and [42, Exercise 3.39].

Under Condition 1, 2 and 3, the lemmas in the subsequent sections ensure that Condition A is satisfied. Then we have the following theorem for posterior consistency at $\gamma_0 \in \Phi(\mathcal{H})$ using the push-forward prior $\Pi = \Phi\Pi_\theta$ for Π_θ a Gaussian distribution satisfying Condition 3.

Theorem 3.1. *Suppose Condition 1, 2 and 3 are satisfied for $\beta > d'/2$, and $\gamma_0 \in \Phi(\mathcal{H})$. Let $\Pi(\cdot|Y)$ be the corresponding sequence of posterior distributions arising for the model (1). Then there exists $C_0 > 0$ such that*

$$\Pi(\|\gamma - \gamma_0\|_{L^2(D)} \leq f(C_0 r_n)|Y) \to 1 \quad \text{in } P_n^{\gamma_0}\text{-probability},$$

where $r_n = n^{-a}$ with

$$a = \frac{\eta\zeta\delta}{2\eta\zeta\delta + d'}. \tag{18}$$

The rate of convergence in probability is $e^{-bnr_n^2}$ for any $b > 0$ choosing $C_0 > 0$ large enough.

Proof. Note first that Lemma 3.4 shows that Condition **A.1** is satisfied for some $C_1 = C_1(C_\Phi, C_\mathcal{G}, \zeta, \eta, d', \delta, \theta_0, \Pi'_\theta)$. Given $b > 0$, Lemma 3.2 states that we can choose $M > C(C_2, \Pi'_\theta, \delta, d')$ such that Condition **A.2** is satisfied and $0 < b < C_2 - C_1 - 4$. For this choice of M, Lemma 3.3 gives $m_0 = m_0(C_\Phi, C_\mathcal{G}, \zeta, \eta, M)$ and $C_3 = C_3(\delta, M, d', \mathcal{X})$ such that Condition **A.3** is satisfied. Then, by Theorem 2.1, there exists $C_0(C_2, C_3, m_0)$

$$\Pi(B_\mathcal{G}(\gamma_0, C_0 r_n) \cap A_n|Y) \to 1 \quad \text{in } P_n^{\gamma_0}\text{-probability},$$

with rate $e^{-bnr_n^2}$ as $n \to \infty$. Then the wanted result is a consequence of (9). □

Posterior consistency with a rate as in the preceding theorem often leads to the convergence of related estimators with the same rate, see [33]. Here, we repeat an argument found in [24] to conclude that the posterior mean converges in $P_n^{\gamma_0}$-probability to γ_0 as $n \to \infty$.

Corollary 1. *Under the assumptions of Theorem 3.1, the posterior mean $E[\gamma|Y]$ in $L^2(D)$ satisfies for some constant $C > 0$ large enough*

$$\|E[\gamma|Y] - \gamma_0\|_{L^2(D)} \to 0 \quad \text{in } P_n^{\gamma_0}\text{-probability}$$

with rate $f(Cr_n)$ as $n \to \infty$.

Proof. The proof of Theorem 2.3.2 in [24] applies here, since Φ maps into $L^2_\Lambda(D)$ by assumption and hence

$$\int_{L^2_\Lambda(D)} \|\gamma-\gamma_0\|^2_{L^2(D)}\,\Pi(d\gamma) = \int_\Theta \|\Phi(\theta)-\Phi(\theta_0)\|^2_{L^2(D)}\,\Pi_\theta(d\theta) \le 4\Lambda^2|D|.$$

□

3.1. Excess mass condition ***A.2***

To motivate more precisely the scaling of the prior and the form of A_n, we recall [22, Lemma 5.17]:

$$\Pi'_\theta(\|\theta'\|_{H^\beta(\mathcal{X})} > M) \le e^{-CM^2},$$

for all M large enough and some fixed $C>0$ depending on Π'_θ. Then

$$\Pi_\theta(\|\theta\|_{H^\beta(\mathcal{X})} > M) = \Pi'_\theta(\|\theta'\|_{H^\beta(\mathcal{X})} > Mn^{1/2-a}) \le e^{-CM^2n^{1-2a}} = e^{-CM^2nr_n^2}. \quad (19)$$

Hence, Π_θ charges $\mathcal{S}_\beta(M)$ with sufficient mass in relation to Condition **A.2**. However, we can consider a smaller set with the same property. Define

$$A_n := \Phi(\Theta_n), \qquad \Theta_n := \{\theta=\theta_1+\theta_2 : \|\theta_1\|_\infty \le M\bar r_n, \|\theta_2\|_{\mathcal{H}} \le M\} \cap \mathcal{S}_\beta(M), \quad (20)$$

for $\bar r_n := r_n^{\frac{1}{\eta\zeta}}$.

Lemma 3.2. *If Condition 3 is satisfied and $r_n = n^{-a}$ for*

$$a = \frac{\eta\zeta\delta}{2\eta\zeta\delta + d'}, \quad (21)$$

then condition ***A.2*** *is satisfied for A_n defined by (20).*

Proof. [24, Theorem 2.2.2 and exercise 2.4.4] shows that for $M > C(C_2, \Pi'_\theta, \delta, d')$

$$\Pi_\theta(\Theta\setminus\Theta_n) \le e^{-C_2nr_n^2},$$

for any given $C_2>0$, since $(\bar r_n n^{1/2-a})^{-b} = nr_n^2$ for $b = 2d'/(2\delta-d')$. Then,

$$\begin{aligned}\Pi(L^2_\Lambda(D)\setminus A_n) &= \Pi_\theta(\Phi^{-1}(L^2_\Lambda(D)\setminus A_n)),\\ &= \Pi_\theta(\Theta\setminus\Theta_n) \le e^{-C_2nr_n^2}, \end{aligned} \quad (22)$$

as follows from (19). □

3.2. Metric entropy condition ***A.3***

Now we show that the sets on the form A_n defined by (20) satisfy Condition **A.3**. This is straight-forward, when Φ is Hölder continuous by Lemma A.1. We also recall that an upper bound on the covering number of Sobolev norm balls is well-known, see Lemma A.2.

Lemma 3.3. *Suppose Condition 1 and 2 are satisfied. Then Condition* ***A.3*** *is satisfied for A_n as in (20) and a as in (21).*

Proof. Define for $\theta' \in C(\overline{\mathcal{X}})$ and $\rho > 0$ the norm ball $B_\infty(\theta', \rho) := \{\theta \in C(\overline{\mathcal{X}}) : \|\theta - \theta'\|_\infty \leq \rho\}$ and denote by $B_\infty(\rho)$ the ball centered in $\theta' = 0$. Recall (20), for which we note $\Theta_n \subset (B_\infty(M\bar{r}_n) + \mathcal{S}_\delta(CM)) \cap \mathcal{S}_\beta(M)$ for some constant $C > 0$ by Condition 3. Then applying Lemma A.3 for $\rho = \bar{r}_n$

$$N(\Theta_n, \|\cdot\|_\infty, 2M\bar{r}_n) \leq N(\mathcal{S}_\delta(CM), \|\cdot\|_\infty, M\bar{r}_n),$$

Now using Lemma A.1 (i) and the Hölder continuity of $\mathcal{G} \circ \Phi$ on $\mathcal{S}_\delta(M)$, there exists a constant $m_0 = m_0(\eta, \zeta, C_\Phi, C_\mathcal{G}, M)$ such that for any $n > 0$ large enough,

$$\begin{aligned}\log N(A_n, d_\mathcal{G}, m_0 r_n) &\leq \log N(\Theta_n, \|\cdot\|_\infty, 2M\bar{r}_n),\\ &\leq \log N(\mathcal{S}_\delta(CM), \|\cdot\|_\infty, M\bar{r}_n),\\ &\leq C_3 \bar{r}_n^{-\frac{d'}{\delta}} = C_3 n r_n^2, \end{aligned} \tag{23}$$

where $C_3 = C_3(\delta, M, d', C, \mathcal{X})$ and where we used Lemma A.2 and (21). □

3.3. Small ball condition ***A.1***

In this section, we consider the strong assumption that $\gamma_0 \in \Phi(\mathcal{H})$. We refer the reader to [43] for a more general case where θ_0 is only in the closure of $\mathcal{H}$ in Θ. However, this extension is not immediately compatible with the scaling (16). What follows in this section is based on the work [24]. We extend this to the case of Hölder continuous maps $\mathcal{G} \circ \Phi$ in a straight-forward manner. Below we need the scaled RKHS $\mathcal{H}_n := n^{a-1/2}\mathcal{H} = \{n^{a-1/2}h : h \in \mathcal{H}\}$, see Condition 3, with norm

$$\|h\|_{\mathcal{H}_n} = n^{1/2-a}\|h\|_\mathcal{H}.$$

This is the RKHS associated with Π_θ, see [42] or [32, Exercise 2.6.5].

Lemma 3.4. *Let Π satisfy Condition 3 and let $\gamma_0 = \Phi(\theta_0)$ for some $\theta_0 \in \mathcal{H}$. If Condition 1 and 2 are satisfied, then Condition* ***A.1*** *is satisfied for a as in (21).*

Proof. For $R > 0$ large enough depending on θ_0 and Π'_θ, we have by Condition 1 and 2,

$$\begin{aligned}\{\theta \in \Theta : d_\mathcal{G}(\Phi(\theta), \Phi(\theta_0)) \leq r_n\}&\\ &\supset \{\theta \in \Theta : d_\mathcal{G}(\Phi(\theta), \Phi(\theta_0)) \leq r_n\} \cap \mathcal{S}_\beta(R),\\ &\supset \{\theta \in \Theta : \|\Phi(\theta) - \Phi(\theta_0)\|_{L^2(D)} \leq C r_n^{1/\eta}, \|\theta\|_{H^\beta(\mathcal{X})} \leq R\}\\ &\supset \{\theta \in \Theta : \|\theta - \theta_0\|_\infty \leq C\bar{r}_n, \|\theta - \theta_0\|_{H^\beta(\mathcal{X})} \leq \tilde{R}\},\end{aligned} \tag{24}$$

where $C = C(\eta, \zeta, C_\mathcal{G}, C_\Phi, R)$ and $\tilde{R} = R - \|\theta_0\|_{H^\beta(\mathcal{X})}$, and where we used the triangle inequality. Note also $\tilde{\Pi}_\theta(\cdot) = \Pi_\theta(\cdot + \theta_0)$ is a Gaussian measure in the separable Hilbert space $H^\beta(\mathcal{X})$. In addition, a closed norm ball in $H^\beta(\mathcal{X})$ is a closed subset of $H^\beta(\mathcal{X})$ and so is $\{\theta \in H^\beta(\mathcal{X}) : \|\theta\|_\infty \leq C\bar{r}_n\}$ by a Sobolev embedding. Then we can apply the Gaussian correlation inequality [24, Theorem 6.2.2] to (24) so that

$$\begin{aligned}\Pi_\theta(d_\mathcal{G}(\Phi(\theta), \Phi(\theta_0)) \leq r_n) &\geq \Pi_\theta(\|\theta - \theta_0\|_\infty \leq C\bar{r}_n, \|\theta - \theta_0\|_{H^\beta(\mathcal{X})} \leq \tilde{R}),\\ &= \tilde{\Pi}_\theta(\|\theta\|_\infty \leq C\bar{r}_n, \|\theta\|_{H^\beta(\mathcal{X})} \leq \tilde{R}),\\ &\geq \tilde{\Pi}_\theta(\|\theta\|_\infty \leq C\bar{r}_n)\tilde{\Pi}_\theta(\|\theta\|_{H^\beta(\mathcal{X})} \leq \tilde{R}).\end{aligned} \tag{25}$$

To each of the factors in the right-hand side of (25) we apply [32, Corrollary 2.6.18] to the effect that for large n

$$\begin{aligned}\Pi_\theta(d_{\mathcal{G}}(\Phi(\theta),\Phi(\theta_0)) \le r_n) \\ &\ge e^{-\|\theta_0\|^2_{\mathcal{H}_n}}\Pi_\theta(\|\theta\|_\infty \le C\bar{r}_n)\Pi_\theta(\|\theta\|_{H^\beta(\mathcal{X})} \le \tilde{R}), \\ &\ge e^{-C'n^{1-2a}}\Pi'_\theta(\|\theta'\|_\infty \le C\bar{r}_n n^{1/2-a}),\end{aligned}$$

for $C' = C'(\theta_0, \Pi'_\theta)$ using also that $\Pi_\theta(\|\theta\|_{H^\beta(\mathcal{X})} \le \tilde{R}) \le 1/2$ for R large enough as follows from (19). The rest of the argument follows [28, Lemma 11] and uses [44, Theorem 1.2], see also Lemma A.2, and the continuous embedding $\mathcal{H} \subset H^\delta(\mathcal{X})$ to conclude

$$\begin{aligned}\Pi'_\theta(\|\theta'\|_\infty \le C\bar{r}_n n^{1/2-a}) &\ge e^{-C''(\bar{r}_n n^{1/2-a})^{-b}}, \\ &= e^{-C''nr_n^2}\end{aligned}$$

with $C'' = C''(C, C')$ and $b = \frac{2d'}{2\delta - d'}$, which fits the choice (21) of a. □

4. Parametrizations for inclusions

In this section, we make use of Theorem 3.1 for two specific parametrizations suited for inclusion detection: a star-shaped set parametrization and a level set parametrization. These are parametrizations on the form

$$\Phi(\theta) = \sum_{i=1}^{\mathcal{N}} \kappa_i \mathbb{1}_{A_i(\theta)} \tag{26}$$

for some Lebesgue measurable subsets $A_i(\theta)$ of $\mathbb{R}^d$ and constants $\kappa_i > 0$ for $i = 1, \ldots, \mathcal{N}$, which we denote collectively as $\kappa = \{\kappa_i\}_{i=1}^{\mathcal{N}}$. Since we consider parametrizations that map into $L^2_\Lambda(D)$, we will implicitly consider $\Phi(\theta)$ as the restriction of the right-hand side of (26) to D. Note that recovering parameters on this form requires that we know *a priori* the parameter values κ_i. However, this could further be modelled into the prior. In the following, we construct $A_i(\theta)$ as star-shaped sets and level sets.

4.1. Star-shaped set parametrization

We start by considering the parametrization for a single inclusion, i.e. $\mathcal{N} = 1$. For simplicity of exposition, we consider the star-shaped sets in the plane, although it is straight-forward to generalize to higher dimensions. Let φ be a continuously differentiable 2π-periodic function. We can think of $\theta : \mathbb{T} \to \mathbb{R}$ as a function defined on the 1-dimensional torus $\mathbb{T} := \mathbb{R}/2\pi\mathbb{Z}$. The boundary of the star-shaped set is a deformed unit circle: for a point x in D it takes for $v(\vartheta) := (\cos\vartheta, \sin\vartheta)$ the form

$$\partial A(\theta) = x + \{\exp(\theta(\vartheta))v(\vartheta),\ 0 \le \vartheta \le 2\pi\},$$

Then we write

$$A(\theta) = x + \{s\exp(\theta(\vartheta))v(\vartheta), 0 \le s \le 1, 0 \le \vartheta \le 2\pi\}. \tag{27}$$

Let $\kappa_1, \kappa_2 > 0$ and define

$$\Phi(\theta) := \kappa_1 \mathbb{1}_{A(\theta)} + \kappa_2. \tag{28}$$

We have the following conditional continuity result, where we for simplicity fix $x \in D$.

Lemma 4.1. *Let $\theta_1, \theta_2 \in H^\beta(\mathbb{T})$ and $\|\theta_i\|_{H^\beta(\mathbb{T})} \leq M$ with $\beta > 3/2$ for $i = 1, 2$. Then*

$$\|\Phi(\theta_1) - \Phi(\theta_2)\|_{L^2(D)} \leq C\|\theta_1 - \theta_2\|_{L^\infty(\mathbb{T})}^{1/2},$$

where C only depends on M and κ_1.

Proof. By the translation invariance of the Lebesgue measure, it is sufficient to bound the area of the symmetric difference $A(\theta_1)\Delta A(\theta_2) := (A(\theta_1) \setminus A(\theta_2)) \cup (A(\theta_2) \setminus A(\theta_1))$ for $x = 0$. We parameterize this planar set using $K : [0, 1] \times [0, 2\pi] \to \mathbb{R}^2$, defined by

$$K(s, \vartheta) = [s \exp(\theta_1(\vartheta)) + (1 - s) \exp(\theta_2(\vartheta))]v(\vartheta).$$

Note that $\|\theta_i\|_{H^\beta(\mathbb{T})} \leq M$ implies $\|\theta_i\|_{C^1(\mathbb{T})} \leq CM$ by a continuous Sobolev embedding. We have

$$\begin{aligned} \frac{\partial K}{\partial s}(s, \vartheta) &= [\exp(\theta_1(\vartheta)) - \exp(\theta_2(\vartheta))]v(\vartheta), \\ \left|\frac{\partial K}{\partial \vartheta}(s, \vartheta)\right| &\leq C(M), \end{aligned}$$

and the well-known change of variables formula,

$$\begin{aligned} \mathrm{vol}(A(\theta_1)\Delta A(\theta_2)) &= \int_0^1 \int_0^{2\pi} |JK(s, \vartheta)| \, d\vartheta \, ds, \\ &\leq C(|(\partial_s K(s, \vartheta))_1||(\partial_\vartheta K(s, \vartheta))_2| + |(\partial_s K(s, \vartheta))_2||(\partial_\vartheta K(s, \vartheta))_1|), \\ &\leq C(M)|e^{\theta_1(\vartheta)} - e^{\theta_2(\vartheta)}|, \\ &\leq C(M)\|\theta_1 - \theta_2\|_{L^\infty(\mathbb{T})}, \end{aligned}$$

where $|JK(s, \vartheta)|$ is the determinant of the Jacobian of the map K. In the last line, we used that $z \mapsto \exp(z)$ is locally Lipschitz as follows from the mean value theorem. □

Using the triangle inequality for the symmetric difference and the main result of [45], we would also have an estimate on the continuity of Φ as defined on $D \times H^\beta(\mathbb{T})$, i.e. on elements (x, θ). We could then endow $D \times H^\beta(\mathbb{T})$ with a product prior which straight-forwardly satisfies Condition **A.1**. For simplicity we skip this extension. Instead, we gather the following conclusion that follows directly from Theorem 3.1 and Corollary 1.

Theorem 4.2. *Suppose Condition 2 is satisfied for $\beta > 3/2$. Let $\gamma_0 = \Phi(\theta_0)$ for $\theta_0 \in \mathcal{H}$. Let $\Pi(\cdot|Y)$ be the corresponding sequence of posterior distributions arising for the model (1) and prior $\Pi = \Phi\Pi_\theta$ satisfying Condition 3. Then there exists $C > 0$ such that*

$$\|E[\gamma|Y] - \gamma_0\|_{L^2(D)} \to 0 \quad \text{in } P_n^{\gamma_0}\text{-probability} \tag{29}$$

with rate $f(Cn^{-a})$ as $n \to \infty$, where

$$a = \frac{\eta\delta}{2\eta\delta + 2}.$$

Note that this is the rate of (18) with $\zeta = 1/2$ and $d' = 1$. Clearly this convergence rate takes into account that a smooth star-shaped inclusion belongs to a low-dimensional subset of $L^2_\Lambda(D)$. One can think of this fast convergence rate (compared to Gaussian priors directly in $L^2(D)$) as an expression of uncertainty reduction. Parameters $\gamma \in L^2_\Lambda(D)$ on the form (28) carry some regularity. Indeed, using results in [46, 47] showing α-Sobolev regularity for $0 < \alpha < 1/2$ reduces to giving

an upper bound of the area of the ε-tubular neighborhood of $\partial A(\theta)$ with respect to ε. This is provided by Steiner's inequality, see [48], for $d = 2$, or more generally by Weyl's tube formula, see [49], when $d \geq 2$. Then $\|\Phi(\theta)\|_{H^\alpha(D)} \leq C(M, D, \alpha)$ for $\|\theta\|_{H^\beta(\mathbb{T})} \leq M$.

Multiple inclusions The case of multiple star-shaped inclusions is a straight-forward generalization using the triangle inequality. We consider for $\mathcal{N} \geq 1$, the map

$$\Phi : (H^\beta(\mathbb{T}))^{\mathcal{N}} \to L^2_\Lambda(D)$$

as in (26) with $A_i(\theta) = A(\theta_i) + x_i$ from A in (27) with $x = 0$, $x_i \in D$, and where we set $\theta = (\theta_1, \dots, \theta_{\mathcal{N}})$. We denote $\|\cdot\|_{\mathcal{N}}$ the direct product norm associated with the norm on $L^\infty(\mathbb{T})$, i.e.

$$\|\theta\|_{\mathcal{N}} = \max\left(\|\theta_1\|_{L^\infty(\mathbb{T})}, \dots, \|\theta_{\mathcal{N}}\|_{L^\infty(\mathbb{T})}\right).$$

We have the following continuity result.

Lemma 4.3. *Let $\theta_i, \tilde{\theta}_i \in H^\beta(\mathbb{T})$ with $\|\theta_i\|_{H^\beta(\mathbb{T})} \leq M$, $\|\tilde{\theta}_i\|_{H^\beta(\mathbb{T})} \leq M$ for $i = 1, \dots, \mathcal{N}$. For $\theta = (\theta_1, \dots, \theta_{\mathcal{N}})$ and $\tilde{\theta} = (\tilde{\theta}_1, \dots, \tilde{\theta}_{\mathcal{N}})$ we have*

$$\|\Phi(\theta) - \Phi(\tilde{\theta})\|_{L^2(D)} \leq C\|\theta - \tilde{\theta}\|_{\mathcal{N}}^{1/2},$$

where C only depends on M, κ and $\mathcal{N}$.

Proof. Using the triangle inequality and Lemma 4.1,

$$\begin{aligned}
\|\Phi(\theta) - \Phi(\tilde{\theta})\|^2_{L^2(D)} &= \left\| \sum_{i=1}^{\mathcal{N}} \kappa_i (\mathbb{1}_{A_i(\theta)} - \mathbb{1}_{A_i(\tilde{\theta})}) \right\|^2_{L^2(D)}, \\
&\leq C \left(\sum_{i=1}^{\mathcal{N}} \|\mathbb{1}_{A_i(\theta)} - \mathbb{1}_{A_i(\tilde{\theta})}\|_{L^2(D)} \right)^2, \\
&\leq C \left(\sum_{i=1}^{\mathcal{N}} \|\theta_i - \tilde{\theta}_i\|^{1/2}_{L^\infty(\mathbb{T})} \right)^2, \\
&\leq C\|\theta - \tilde{\theta}\|_{\mathcal{N}},
\end{aligned}$$

by the equivalence of the p-norms $p > 0$ on $\mathbb{R}^{\mathcal{N}}$. □

Parallel to the remark before Lemma 4.1, we mention that a statement similar to Lemma 4.3 holds true for a map Φ defined on $(D \times H^\beta(\mathbb{T}))^{\mathcal{N}}$, if we in addition wish to infer $x_1, \dots, x_{\mathcal{N}}$. In preparation for the main result of this section let us change notation to suit the current setting. Let

$$\Theta = H^\beta(\mathbb{T})^{\mathcal{N}} \quad \text{and} \quad \mathcal{S}_\beta(M) = \{\theta \in \Theta : \|\theta_i\|_{H^\beta(\mathbb{T})} < M, i = 1, \dots, \mathcal{N}\}. \tag{30}$$

We then endow Θ with a (product) prior distribution of Π_θ satisfying Condition 3:

$$\tilde{\Pi}_\theta = \otimes_{i=1}^{\mathcal{N}} \Pi_\theta \quad \text{satisfying} \quad \tilde{\Pi}_\theta(B) = \Pi_\theta(B_1) \dots \Pi_\theta(B_{\mathcal{N}}), \tag{31}$$

for $B = B_1 \times \dots \times B_{\mathcal{N}} \in \mathcal{B}(H^\beta(\mathbb{T}))^{\mathcal{N}} = \mathcal{B}(H^\beta(\mathbb{T})^{\mathcal{N}})$. The last equality is found in for example [50, Lemma 1.2]. For this prior, we have the following result, which is accounted for in Appendix C.

Theorem 4.4. *Suppose Condition 2 is satisfied for $\mathcal{S}_\beta(M)$ as in (30) for $\beta > 3/2$. Let $\gamma_0 = \Phi(\theta_0) = \Phi(\theta_{0,1}, \dots, \theta_{0,\mathcal{N}})$ for $\theta_{0,i} \in \mathcal{H}$, $i = 1, \dots, \mathcal{N}$. Let $\Pi(\cdot|Y)$ be the corresponding sequence of posterior distributions arising for the model (1) and prior $\Pi = \Phi\tilde{\Pi}_\theta$ for (31). Then there exists $C > 0$ such that*

$$\|E[\gamma|Y] - \gamma_0\|_{L^2(D)} \to 0 \quad \text{in } P_n^{\gamma_0}\text{-probability} \tag{32}$$

with rate $f(Cn^{-a})$ as $n \to \infty$, where

$$a = \frac{\eta\delta}{2\eta\delta + 2}.$$

Note that this is the rate as of Theorem 4.2, i.e. the rate does not depend on the number of inclusions; this dependence appears in the constant C.

4.2. Level set parametrization

In this section, we consider the level set parametrization of piecewise constant functions. The simplest case is to compose a given continuous function $\theta : \mathcal{X} \to \mathbb{R}$, for $\mathcal{X} \supset D$, i.e. $d = d' = 2, 3$, with the Heaviside function $H(z) = \mathbb{1}_{z \geq 0}(z)$ as

$$\gamma(x) = \Phi(\theta)(x) = \kappa_1 H(\theta(x)) + \kappa_2,$$

for $\kappa_1, \kappa_2 > 0$. However, $\Phi : H^\beta(\mathcal{X}) \to L^2_\Lambda(D)$ is not uniformly Hölder continuous on $\mathcal{S}_\beta(M)$ for any $\beta, M > 0$ and hence does not satisfy Condition 1. Indeed, if $|\nabla\theta|$ is small near the set $\{x : \theta(x) = 0\}$, small changes in θ can lead to big changes in γ. A lower bound on $|\nabla\theta|$ near this set suffices, as can be seen from the implicit function theorem, see Lemma C.1. This type of condition also appears in level set estimation of probability densities, see [51]. We illustrate this phenomenon by the following two-dimensional example.

Example 1. *Let $\mathcal{X} = D = B(0, 1/2)$ the two-dimensional disc of radius $1/2$. Take as $\theta_{(n)}$ the radially symmetric functions $\theta_{(n)}(r, \vartheta) = \frac{1}{n} + r^{2n}$ and $\tilde{\theta}_{(n)} = -\theta_{(n)}$ for $0 \leq r \leq 1$ and $0 \leq \vartheta \leq 2\pi$. It is clear that $\theta_{(n)}, \tilde{\theta}_{(n)} \in \mathcal{S}_1(M)$ for all $n \in \mathbb{N}$, and that*

$$\begin{aligned}\|\theta_{(n)} - \tilde{\theta}_{(n)}\|_{L^\infty(\mathcal{X})} &\leq 2\|n^{-1}\|_{L^\infty(\mathcal{X})} + 2\|r^{2n}\|_{L^\infty((0,1/2))}, \\ &\leq 2n^{-1} + 2^{1-2n} \to 0\end{aligned}$$

as $n \to \infty$. However $\Phi(\theta_{(n)}) = \kappa_1$ and $\Phi(\tilde{\theta}_{(n)}) = \kappa_2$ so $\|\Phi(\theta_{(n)}) - \Phi(\tilde{\theta}_{(n)})\|_{L^2(D)} = |\kappa_2 - \kappa_1|$.

The example is easy to extend to the more general case where the L^∞-norm is replaced with the C^k-norm. Note also that for fixed $\theta_{(n)} = \theta$, we have continuity of Φ in this particular example. This fact generalizes to continuity of Φ in functions θ that do not have critical points on $\{x : \theta(x) = 0\}$. However, for the stronger Condition 1, it is not obvious how much mass Gaussian distributions give to functions whose gradient is lower bounded away from zero near $\{x : \theta(x) = 0\}$. For this reason, we take a different approach. We define an approximation Φ_ϵ of Φ for which Condition 1 is satisfied. This gives an approximate posterior distribution that contracts around $\gamma_0^\epsilon = \Phi_\epsilon(\theta_0)$. We shall see that if we take $\epsilon = n^{-k}$ for some $k \in (0, 1)$, then the approximation properties of Φ_ϵ to Φ and a triangle inequality argument ensure we have consistency at $\gamma_0 = \Phi(\theta_0)$. To this end, consider the continuous approximation H_ϵ of the Heaviside function

$$H_\epsilon(z) := \begin{cases} 0 & \text{if } z < -\epsilon, \\ \dfrac{1}{2\epsilon}z + \dfrac{1}{2} & \text{if } -\epsilon \leq z < \epsilon, \\ 1 & \text{if } \epsilon \leq z. \end{cases} \tag{33}$$

We want to note two straight-forward properties of H_ϵ:

$$|H_\epsilon(z) - H_\epsilon(\tilde{z})| \leq \frac{1}{2\epsilon}|z - \tilde{z}|, \quad \text{for all } z, \tilde{z} \in \mathbb{R}, \tag{34}$$

and

$$|H_\epsilon(z) - H(z)| \leq \frac{1}{2}\mathbb{1}_{(-\epsilon,\epsilon)}(z), \quad \text{for all } z \in \mathbb{R}. \tag{35}$$

We could even consider a smooth approximation for H_ϵ, as in [21], but this is not necessary for our case. To construct the continuous level set parametrization, take constants $\mathbf{c} = \{c_i\}_{i=1}^{\mathcal{N}}$ satisfying

$$-\infty = c_0 < c_1 < \ldots < c_{\mathcal{N}} = \infty$$

for some $\mathcal{N} \in \mathbb{N}$. Given a continuous function $\theta : D \to \mathbb{R}$ define

$$A_i(\theta) := \{x \in D : c_{i-1} \leq \theta(x) < c_i\}, \quad i = 1, \ldots, \mathcal{N},$$

and let Φ be of the form (26). The corresponding approximate level set parametrization is then

$$\Phi_\epsilon(\theta) := \sum_{i=1}^{\mathcal{N}} \kappa_i [H_\epsilon(\theta - c_{i-1}) - H_\epsilon(\theta - c_i)], \tag{36}$$

where we define $H_\epsilon(z - c_0) = 1$ and $H_\epsilon(z - c_{\mathcal{N}}) = 0$ for any $z \in \mathbb{R}$. One can check that Φ_ϵ coincides with Φ, when $\epsilon = 0$. Motivated by Example 1 and the property that stationary Gaussian random fields have almost surely no critical points on their level sets, we define the admissible level set functions as

$$H_\diamond^\beta(\mathcal{X}) := H^\beta(\mathcal{X}) \cap \bigcap_{i=1}^{\mathcal{N}-1} T_{c_i}, \quad \beta > 2 + \frac{d'}{2},$$

where

$$T_c := \{\theta \in C^2(\overline{\mathcal{X}}) : \exists x \in \mathcal{X}, \theta(x) = c, |(\nabla\theta)(x)| = 0\}^{\complement}.$$

Indeed, according to [52, Proposition 6.12], for each fixed $c \in \mathbb{R}$ we have

$$\Pi'_\theta(T_c) = 1 \quad \text{and hence} \quad \Pi'_\theta(H_\diamond^\beta(\mathcal{X})) = 1 \tag{37}$$

if $\Pi'_\theta(C^2(\overline{\mathcal{X}})) = 1$ and the covariance function associated with $(\theta(x) : x \in \mathcal{X})$ for $\theta \sim \Pi'_\theta$ is stationary. This is permitted since $((\theta(x), \partial_1\theta(x), \ldots, \partial_{d'}\theta(x)) : x \in \mathcal{X})$ is a Gaussian process, see for example [53, Section 9.4]. Note also that it is known that $T_c \in \mathcal{B}(C^2(\overline{D}))$ since $\{\theta \in C^2(\overline{D}) : |\theta(x) - c| + |(\nabla\theta)(x)| \geq 1/n, \forall x \in D\}$ is a Borel set.

Lemma 4.5. *We have the following:*

(i) If $\theta_0 \in H_\diamond^\beta(\mathcal{X})$, then for $\beta > 1 + d'/2$ and $\epsilon > 0$ sufficiently small

$$\|\Phi_\epsilon(\theta_0) - \Phi(\theta_0)\|_{L^2(D)} \leq C(\theta_0, \mathcal{X}, D, \mathbf{c})\epsilon^{1/2}.$$

(ii) For any $\theta, \tilde{\theta} \in H^2(\mathcal{X})$,

$$\|\Phi_\epsilon(\theta) - \Phi_\epsilon(\tilde{\theta})\|_{L^2(D)} \leq C(\kappa, \mathcal{N}, D)\epsilon^{-1}\|\theta - \tilde{\theta}\|_{L^\infty(D)}.$$

Proof. (i) Note first

$$\Phi_\epsilon(\theta_0) - \Phi(\theta_0) = \sum_{i=1}^{\mathcal{N}} \kappa_i [(H_\epsilon(\theta_0 - c_{i-1}) - H(\theta_0 - c_{i-1})) - (H_\epsilon(\theta_0 - c_i) - H(\theta_0 - c_i))].$$

By the triangle inequality and (35)

$$\|\Phi_\epsilon(\theta_0) - \Phi(\theta_0)\|_{L^2(D)} \leq \sum_{i=1}^{\mathcal{N}} \kappa_i (\|\mathbb{1}_{(-\epsilon,\epsilon)}(\theta_0 - c_{i-1})\|_{L^2(D)} + \|\mathbb{1}_{(-\epsilon,\epsilon)}(\theta_0 - c_i)\|_{L^2(D)})$$

It is clear that $\mathbb{1}_{(-\epsilon,\epsilon)}(\theta_0(x) - c_{i-1}) = \mathbb{1}_{V_\epsilon}(x)$ with

$$V_\epsilon := \{x \in \mathcal{X} : |\theta_0(x) - c_{i-1}| < \epsilon\}. \tag{38}$$

By Lemma C.1 $|V_\epsilon| \leq C(\theta_0, c_{i-1}, \mathcal{X})\epsilon$, and hence the wanted result follows by repeated application.
(ii) Again by the triangle inequality and now (34) we have

$$\begin{aligned}
\|\Phi_\epsilon(\theta) - \Phi_\epsilon(\tilde{\theta})\|_{L^2(D)} &= \sum_{i=1}^{\mathcal{N}} \kappa_i \|H_\epsilon(\theta - c_{i-1}) - H_\epsilon(\tilde{\theta} - c_{i-1})\|_{L^2(D)} \\
&\quad + \sum_{i=1}^{\mathcal{N}} \kappa_i \|H_\epsilon(\theta - c_i) - H_\epsilon(\tilde{\theta} - c_i)\|_{L^2(D)}, \\
&\leq \epsilon^{-1} \sum_{i=1}^{\mathcal{N}} \kappa_i \|\theta - \tilde{\theta}\|_{L^2(D)}, \\
&\leq C(\kappa, \mathcal{N}, D)\epsilon^{-1} \|\theta - \tilde{\theta}\|_{L^\infty(D)}.
\end{aligned}$$

□

For the following consistency result we let

$$\Theta = H^\beta_\diamond(\mathcal{X}), \qquad \mathcal{S}_\beta(M) := \{\theta \in H^\beta_\diamond(\mathcal{X}) : \|\theta\|_{H^\beta(\mathcal{X})} \leq M\}. \tag{39}$$

We endow Θ with a prior distribution Π_θ that satisfies Condition 3 for $\beta > 2 + d'/2$ such that the covariance kernel associated with the random field is stationary. For simplicity we assume $f(x) = x^\nu$ for some $0 < \nu < 1$ in Condition 2. Then we have the following result proved in Appendix C.

Theorem 4.6. *Suppose Condition 2 is satisfied for $\mathcal{S}_\beta(M)$ as in (39) for $f(x) = Cx^\nu$, Φ replaced by $\Phi_{n^{-k}}$ for a well-chosen k, and where C and $C_\mathcal{G}$ are independent of n. Let $\gamma_0 = \Phi(\theta_0)$ for $\theta_0 \in \mathcal{H} \cap \Theta$. Let $\Pi(\cdot|Y)$ be the corresponding sequence of posterior distributions arising for the model (1) and prior $\Pi = \Phi_{n^{-k}}\Pi_\theta$ as above. Then,*

$$\|E[\gamma|Y] - \gamma_0\|_{L^2(D)} \to 0 \quad \text{in } P_n^{\gamma_0}\text{-probability} \tag{40}$$

with rate $n^{-a\nu}$ as $n \to \infty$ for

$$a = \frac{\eta\delta}{2d\nu\eta + 2\eta\delta + d}. \tag{41}$$

Note that for weak inverse stability estimates, i.e. ν small, the obtained contraction rate approaches the usual rate (18).

5. Quantitative photoacoustic tomography problem

To test the convergence of the inclusion detection methods, we consider the following test problem in quantitative photoacoustic tomography, see [54, 27, 55]. The diffusion approximation in QPAT models light transport in a scattering medium according to an elliptic equation

$$\begin{aligned} -\nabla \cdot \mu \nabla u + \gamma u &= 0, \text{ in } D, \\ u &= g, \text{ on } \partial D, \end{aligned} \tag{42}$$

where $\mu \in L^2_{\Lambda_\mu}(D)$, $\Lambda_\mu > 0$, and $\gamma \in L^2_\Lambda(D)$ are the optical diffusion and absorption parameters, respectively. The prescribed Dirichlet boundary condition $u = g$ defines the source of incoming radiation. It is well-known that (42) has a unique solution $u \in H^1(D)$ for each $g \in H^{1/2}(\partial D)$ and for any nonzero source function $h \in H^{-1}(D)$ of (42). Furthermore, we have the estimate

$$\|u\|_{H^1(D)} \leq C(\Lambda_\mu, D)(\|g\|_{H^{1/2}(\partial D)} + \|h\|_{H^{-1}(D)}), \tag{43}$$

see for example [56, Chapter 6]. QPAT aims to reconstruct the optical parameters given the absorbed optical energy density map H, which equals the product γu up to some proportionality constant that models the photoacoustic effect. In our simplified approach, we aim to invert the forward map

$$\mathcal{G} : \gamma \mapsto H := \gamma u, \quad \mathcal{G} : L^2_\Lambda(D) \to L^2(D),$$

for a fixed $\mu \in L^2_\Lambda(D)$. For smoothness and physical accuracy we assume

$$g \in H^{3/2}(\partial\Omega) \quad \text{and} \quad 0 < g_{\min} \leq g \leq g_{\max}. \tag{44}$$

This setting allows a simple inverse stability estimate. First we have the following continuity result of $\mathcal{G}$.

Lemma 5.1. *Let $H_1 := \gamma_1 u_1$ and $H_2 := \gamma_2 u_2$ for solutions u_1 and u_2 of (42) corresponding to $\gamma = \gamma_1$, $\gamma = \gamma_2$ in $L^2_\Lambda(D)$ and g satisfying (44). Then there exists a constant C such that*

$$\|H_1 - H_2\|_{L^2(D)} \leq C\|\gamma_1 - \gamma_2\|_{L^2(D)},$$

where C depends on Λ_μ, D and $g_{\max}$.

Proof. We note that $u_1 - u_2$ solves

$$\begin{aligned} -\nabla \cdot \mu \nabla (u_1 - u_2) + \gamma_1 (u_1 - u_2) &= u_2(\gamma_2 - \gamma_1) \text{ in } D, \\ u_1 - u_2 &= 0 \text{ on } \partial D. \end{aligned}$$

Then by (43) and the maximum principle [57, Theorem 8.1]

$$\|u_1 - u_2\|_{H^1(D)} \leq \|u_2(\gamma_2 - \gamma_1)\|_{H^{-1}(D)} \leq g_{\max}\|\gamma_1 - \gamma_2\|_{L^2(D)}.$$

Since $H_1 - H_2 = \gamma_1(u_1 - u_2) + (\gamma_1 - \gamma_2)u_2$ we have

$$\begin{aligned} \|H_1 - H_2\|_{L^2(D)} &\leq \|\gamma_1(u_1 - u_2)\|_{L^2(D)} + \|(\gamma_1 - \gamma_2)u_2\|_{L^2(D)}, \\ &\leq g_{\max}(1 + M)\|\gamma_1 - \gamma_2\|_{L^2(D)}. \end{aligned}$$

□

Lemma 5.2. *Under the same assumptions of Lemma 5.1, there exists a constant $C > 0$ such that*

$$\|\gamma_1 - \gamma_2\|_{L^2(D)} \leq C\|H_1 - H_2\|_{L^2(D)}. \tag{45}$$

Proof. See also [27, Theorem 3.1] and [26, Theorem 1.2]. Note $u_1 - u_2 \in H_0^1(D)$ solves

$$\begin{aligned} -\nabla \cdot \mu \nabla (u_1 - u_2) \quad &= H_2 - H_1 \text{ in } D, \\ u_1 - u_2 &= 0 \text{ on } \partial D, \end{aligned}$$

hence by elliptic regularity

$$\|u_1 - u_2\|_{L^2(D)} \leq C(\Lambda_\mu, D) \|H_1 - H_2\|_{L^2(D)}. \tag{46}$$

Note by the trace theorem, see [58], for g as in (44) there exists $v \in H^2(\Omega)$ such that $u_2 - v \in H_0^1(\Omega)$. By a Sobolev embedding $v \in C^{0,\alpha_0}(\overline{D})$ for some $\alpha_0 > 0$ depending on $d = 2, 3$. Theorem 8.29 and the remark hereafter in [57] states that $u_2 \in C^\alpha(\overline{D})$ for some $\alpha = \alpha(d, \Lambda_\mu, \Lambda, D, \alpha_0) > 0$ and that

$$\|u_2\|_{C^\alpha(\overline{D})} \leq U_1(\sup_{x \in D} |u(x)| + U_2) =: U,$$

where $U_1 = M_1(d, \Lambda_\mu, \Lambda, D, \alpha_0) > 0$ and $U_2 = U_2(D, g)$. By the maximum principle [57, Theorem 8.1] we can collect the right-hand side to one constant $U = U(U_1, U_2, g_{\max}) > 0$. Now using the argument in [26, Lemma 12], which in return uses the Harnack inequality [57, Corollary 8.21] we conclude

$$u_2 \geq m, \tag{47}$$

where $m = m(d, \Lambda_\mu, \Lambda, D, U, \alpha, g_{\min})$ is a constant. Note

$$\begin{aligned} \gamma_1 - \gamma_2 &= \gamma_1 (1 - \frac{u_1}{u_2}) + \frac{1}{u_2}(\gamma_1 u_1 - \gamma_2 u_2), \\ &= \frac{\gamma_1}{u_2}(u_2 - u_1) + \frac{1}{u_2}(H_1 - H_2). \end{aligned}$$

Combining this with (46) and (47) we have

$$\|\gamma_1 - \gamma_2\|_{L^2(D)} \leq C(m, \Lambda, \Lambda_\mu, D) \|H_1 - H_2\|_{L^2(D)}.$$

□

We note that $\mathcal{G}$ satisfies Condition 2 for $\eta = 1$ and $f(x) = x$. We also note that $\mathcal{Y} = L^2(D)$ is a separable Hilbert space with an orthonormal basis consisting of the eigenfunctions of the Dirichlet Laplacian on D. We conclude that this problem is suitable as a test problem, and that Theorem 4.4 and 4.6 apply. In Section 7 we discuss other suitable inverse problems.

6. Numerical results

We discuss our numerical tests in detecting inclusions for the QPAT tomography problem using the pCN algorithm of Section 2.2 and the parametrizations of Section 4. For simplicity we assume $D = B(0, 1)$, the two-dimensional unit disk.

6.1. Observation model

As an approximation to the continuous observation model (1) for the numerical experiments we consider observing

$$Y_k = \langle \mathcal{G}(\gamma), e_k \rangle_{L^2(D)} + \varepsilon \xi_k, \qquad k = 1, \dots, N_d \tag{48}$$

where $\{e_k\}_{k=1}^{\infty}$ is an orthonormal basis of $L^2(D)$ consisting of the eigenfunctions of the Dirichlet Laplacian on D and $N_d \in \mathbb{N}$ is a suitable number. This observation $\mathbf{Y} = \{Y_k\}_{k=1}^{N_d}$ is the sequence of coefficients of the projection of Y from (1) to the span of $\{e_k\}_{k=1}^{N_d}$. As $N_d \to \infty$ observing $\mathbf{Y}$ is equivalent to observing Y, see for example [28, Theorem 26]. Besides being a convenient approximation, this model has numerical relevance: there exists closed-form reconstruction formulas for $\langle \mathcal{G}(\gamma), e_k \rangle_{L^2(D)}$ in the first part of the photoacoustic problem, see [59, 60]. The likelihood function then takes the form

$$p_\varepsilon^\gamma(\mathbf{Y}) := \exp\left(-\frac{1}{\varepsilon^2} \sum_{k=1}^{N_d} (Y_k - \langle \mathcal{G}(\gamma), e_k \rangle_{L^2(D)})^2 \right).$$

6.2. Approximation of the forward map

We approximate the forward map using the Galerkin finite element method (FEM) with piecewise linear basis functions $\{\psi_k\}_{k=1}^{N_m}$ over a triangular mesh of N_m vertices and N_e elements, see [54, 61]. When $\gamma \in L^2_\Lambda(D)$ is discontinuous and continuous, we approximate it by

$$\tilde{\gamma}_{N_e} = \sum_{k=1}^{N_e} \tilde{\gamma}_k \mathbb{1}_{E_k}, \quad \text{and} \quad \bar{\gamma}_{N_m} = \sum_{k=1}^{N_m} \bar{\gamma}_k \psi_k,$$

respectively. Here E_k denotes the k'th element of the triangular mesh. That gives us two approximations of the forward map:

$$\tilde{\mathcal{G}}_{N_e}(\gamma) := \tilde{\gamma}_{N_e} \tilde{u} \quad \text{and} \quad \bar{\mathcal{G}}_{N_m}(\gamma) := \bar{\gamma}_{N_m} \bar{u},$$

where $\tilde{u}$ is the FEM solution corresponding to $\tilde{\gamma}_{N_e}$ and $\bar{u}_{N_m}$ is the FEM solution corresponding to $\bar{\gamma}$. For the smooth level set parametrization we use $\bar{\mathcal{G}}_{N_m}$ with $N_m = 12708$ nodes, while for the star-shaped set parametrization we use $\tilde{\mathcal{G}}_{N_e}$ with $N_e = 25054$ elements.

We compute $\{e_k\}_{k=1}^{N_d}$ by solving the generalized eigenvalue problem arising from the FEM formulation of the Dirichlet eigenvalue problem with the MATLAB function `sptarn`. Then $\langle \mathcal{G}(\gamma), e_k \rangle_{L^2(D)}$ is approximated using the mass matrix for $k = 1, \dots, N_d$ with $N_d = N_{\text{freq}}(N_{\text{freq}} + 1)$ and $N_{\text{freq}} = 13$.

6.3. Phantom, noise and data

The phantom we seek to recover consists of two inclusions:

$$\gamma_0 = \kappa_1 + \kappa_2 \mathbb{1}_{A_1} + \kappa_3 \mathbb{1}_{A_2},$$

where $(\kappa_1, \kappa_2, \kappa_3) = (0.1, 0.4, 0.2)$ and A_1, A_2 are two star-shaped sets described by their boundaries:

$$\partial A_1 = (-0.4, 0.4) + \{0.18(\cos(\vartheta) + 0.65\cos(2\vartheta), 1.5\sin(\vartheta)), 0 \le \vartheta \le 2\pi\},$$

$$\partial A_2 = (0.4, -0.4) + \{\varphi(\vartheta)(\cos(\vartheta), \sin(\vartheta))\},$$

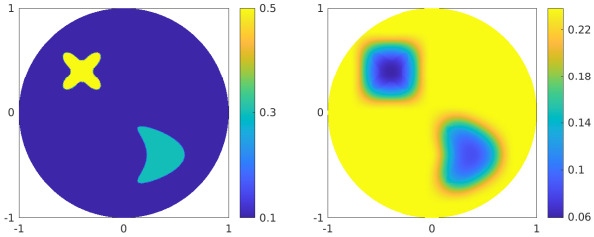

Figure 2: Simulated absorption γ_0 (left image) and diffusion μ (right image) distributions.

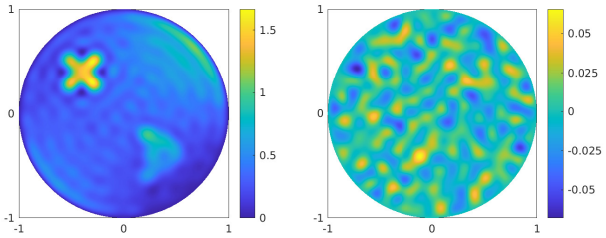

Figure 3: Projection of absorbed optical energy density H corresponding to phantom of Section 6.3 (left image) and of the white noise expansion (right image) projected onto the span of $\{e_k\}_{k=1}^{N_d}$.

where $\varphi(\vartheta) = 0.12\sqrt{0.8 + 0.8(\cos(4\vartheta) - 1)^2}$, see Figure 2. We compute and fix the optical diffusion parameter to $\mu = \frac{1}{2}\frac{1}{\gamma_0 + \mu_s(1-0.8)}$ following [61]. Here the scattering parameter μ_s equals $100\gamma_0$ smoothed with a Gaussian smoothing kernel of standard deviation 15 using the MATLAB function `imgaussfilt`. We choose an illumination g that is smooth and positive on ∂D defined by

$$g(x) = w_{m_1,s_1}(x) + w_{m_2,s_3}(x) + w_{m_2,s_3}(x),$$

where

$$w_{m,s}(x) = s \exp\left(-2\|x - m\|^2\right)$$

and $m_1 = 0.5(\sqrt{2}, \sqrt{2})$, $m_2 = 0.5(-\sqrt{2}, \sqrt{2})$, $m_3 = -m_1$, $s_1 = 10$, $s_2 = 2$ and $s_3 = 5$. This is a superposition of three Gaussians, which illuminates the target well. We simulate data $\mathbf{Y}$ as in (48) by computing $\tilde{\mathcal{G}}_{N_{e_0}}(\gamma_0)$ on a fine mesh of $N_{e_0} = 75624$ elements and $N_{m_0} = 38127$ nodes. The corresponding projection can be seen in Figure 3. We choose $\varepsilon > 0$ such that the relative error

$$\text{relative error} = \frac{\varepsilon\sqrt{\sum_{k=1}^{N_d} \xi_k^2}}{\sqrt{\sum_{k=1}^{N_d} \langle \mathcal{G}(\gamma_0), e_k\rangle_{L^2(D)}^2}}$$

is in the range $(1, 2, 4, 8, 16) \cdot 10^{-2}$. See Figure 3 for a realization of the white noise expansion (3) projected to the N_d first orthonormal vectors $\{e_k\}_{k=1}^{N_d}$ and scaled so

that it accounts for 4% relative noise.

To estimate the approximation error, we compute the vector

$$V_j = [\langle \tilde{\mathcal{G}}_{N_0}(\gamma_j), e_k\rangle_{L^2(D)} - \langle \tilde{\mathcal{G}}_{N_e}(\gamma_j), e_k\rangle_{L^2(D)}]_{k=1}^{N_d}$$

for γ_j, $j = 1, \ldots, 200$, samples of the prior for the level set parametrization introduced in Section 6.4 below. We then compute $\varepsilon_{\text{level}} = \sqrt{\frac{\text{tr}(C)}{N_d}}$, where $\text{tr}(C)$ is the trace of the sample covariance matrix C of the vectors V_j. For this choice $N(0, \varepsilon^2_{\text{level}} I)$ minimizes the Kullback-Leibler distance to $N(0, C)$, see [37]. We compute $\varepsilon_{\text{star}}$ in the same way using $\bar{\mathcal{G}}_{N_{m_0}}$, $\bar{\mathcal{G}}_{N_m}$ and samples of the prior for the star-shaped set parametrization in Section 6.4.

6.4. Choice of prior

Star-shaped sets To mirror the theoretical results of Theorem 4.4 for the phantom above, we consider a product distribution in $H^\beta(\mathbb{T}) \times H^\beta(\mathbb{T})$. To this end, consider the usual $L^2([0, 2\pi])$ real orthonormal basis of trigonometric functions $\{\phi_\ell\}_{\ell\in\mathbb{Z}}$, i.e. $\phi_1(x) = \cos(2\pi x)$ and $\phi_{-1}(x) = \sin(2\pi x)$. Consider the Karhunen-Loeve expansion

$$\theta_i = \bar{\theta} + \sum_{\ell\in\mathbb{Z}} g_{\ell,i} w_\ell \phi_\ell, \qquad g_{\ell,1}, g_{\ell,2} \overset{i.i.d.}{\sim} N(0,1), \tag{49}$$

for $i = 1, 2$ with $w_\ell = q(\tau^2 + |\ell|^2)^{-\delta/2}$ for $\delta > 1/2$, $\tau \in \mathbb{R}$, $q > 0$ and some constant $\bar{\theta} \in \mathbb{R}$. Note θ_i has a Laplace-type covariance operator, and (49) can be interpreted as the solution of a stochastic PDE [62]. Then $\theta_1, \theta_2 \in H^\beta(\mathbb{T})$ almost surely, see [8]. According to Theorem I.23 in [33] and the definition of Sobolev spaces [63, Section 4.3], $\mathcal{H} = H^\delta(\mathbb{T})$ with equivalent norms, i.e. the prior distribution of (49) satisfies Condition 3. We take as Π the distribution of

$$\gamma = \Phi(\theta_1, \theta_2) = \kappa_1 + \kappa_2 \mathbb{1}_{A(x_1,\theta_1)} + \kappa_3 \mathbb{1}_{A(x_2,\theta_2)}, \tag{50}$$

for $(\kappa_1, \kappa_2, \kappa_3) = (0.1, 0.2, 0.4)$, $x_1 = (0.37, -0.43)$ and $x_2 = (-0.44, 0.36)$. In practice, we compute (49) truncated at $|\ell| \leq N = 12$. We do not rescale as the theoretical estimates demand. Instead, we handpick a suitable q for each noise level. We use `inpoly` [64] to efficiently project γ to $\{\mathbb{1}_{E_k}\}_{k=1}^{N_e}$. We refer to Figure 4 for an example of a sample from this prior.

Level sets For the level set parametrization, we consider a prior distribution in $H^\beta(\tilde{\mathbb{T}}^2)$. Here $\tilde{\mathbb{T}}^2$ is the torus corresponding to the square $[-m, m]^2$, where we choose $m = 1.1$, since it is recommended in for example [65] to embed D in a larger domain to avoid boundary effects. Here, we consider the usual $L^2([-m, m]^2)$ real orthonormal basis of trigonometric functions $\{\phi_\ell\}_{\ell\in\mathbb{Z}^2}$. We let

$$\theta = \sum_{\ell\in\mathbb{Z}^2} g_\ell w_\ell \phi_\ell, \qquad g_\ell \overset{i.i.d.}{\sim} N(0,1), \tag{51}$$

with $w_\ell = q(\tau^2 + |\ell|^2)^{-\delta/2}$ for $\delta > 1$, $\tau \in \mathbb{R}$ and $q > 0$. Similar to above, the series exists almost surely as an element in $H^\beta(\tilde{\mathbb{T}}^2)$, see [8]. The corresponding RKHS is $\mathcal{H} = H^\delta(\tilde{\mathbb{T}}^2)$, see [33]. We choose $\mathcal{X} = D$ and consider the linear, bounded and surjective restriction $r : H^\beta(\tilde{\mathbb{T}}^2) \to H^\beta(D)$, see [63, Section 4.4]. Then $r(\theta)$ is a

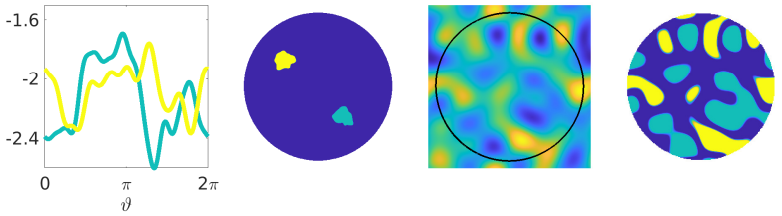

Figure 4: Samples from the star-shaped and level set priors. From left to right: Sample of θ_1 and θ_2 in (49) for $|\ell| \leq 12$, $\delta = 2.5$, $\tau = 4$, $q = 10^{3/2}/5$ and $\bar{\theta} = -2$ (first image). Sample of Π corresponding to $\Phi(\theta_1, \theta_2)$ in (50) (second image). Sample of θ in (51) for $\max(|\ell_1|, |\ell_2|) \leq 4$, $\delta = 1.2$, $\tau = 10$, $q = 5$ (third image). Sample of Π corresponding to $\Phi_\epsilon(\theta)$ in (52) for $\epsilon = 0.1$ (fourth image).

Gaussian random element in $H^\beta(D)$, and its RKHS is $r(\mathcal{H}) = H^\delta(D)$, see [32, Exercise 2.6.5]. We take as Π the distribution of

$$\gamma = \Phi_\epsilon(\theta) = \sum_{i=1}^{3} \kappa_i [H_\epsilon(\theta - c_{i-1}) - H_\epsilon(\theta - c_i)] \tag{52}$$

for $(\kappa_1, \kappa_2, \kappa_3) = (0.3, 0.1, 0.5)$ and $(c_1, c_2) = (-1, 1)$. In practice, we truncate (51) at $\max(|\ell_1|, |\ell_2|) \leq 4$. Also, we hand-pick $\epsilon > 0$ and $q > 0$ for each noise level. See Figure 4 for a sample of this prior.

6.5. Results

In this section we present the numerical results using the star-shaped and level set parametrizations in different noise regimes. We use the algorithm described in Section 2.2 with the pCN method implemented with an adaptive stepsize targeting a 30% acceptance rate. The initial stepsize is denoted by b. For an example of an implementation of this sampling method, we refer to the PYTHON package CUQIPY, see [66]. For the star-shaped set parametrization, we choose the following prior and algorithm parameters in the order $(16, 8, 4, 2, 1) \cdot 10^{-2}$ of the relative noise levels: $b = (0.1, 0.045, 0.035, 0.025, 0.015)$, $q = 10^{3/2} \cdot (7/20, 6/20, 5/20, 4/20, 3/20)$, $\delta = 2.5$, $\bar{\theta} = -2$, $\tau = 4$ and $\theta^{(0)} = (1, 1)$ corresponding to inclusions of constant radius. In the same order, we choose for the level set parametrization the following prior and sampling parameters: $b = (0.05, 0.01, 0.006, 0.003, 0.002)$, $q = 5 \cdot (5/2, 2, 3/2, 1, 3/4)$, $\delta = 1.2$, $\tau = 10$ and $\theta^{(0)} = 2\phi_{(0,-1)} \propto \sin(2\pi/2.2y)$.

For the star-shaped set parametrization, we obtain $K = 10^6$ samples after a burn-in of $5 \cdot 10^5$, whereas for the level set parametrization, we take $K = 10^6$ after $1.2 \cdot 10^6$ samples as burn-in. We find this choice suitable, since the truncation in Section 6.4 leaves us with a higher dimensional sampling problem in the level set case. We base our posterior mean approximations on Monte Carlo estimates using 10^2 equally spaced samples of the chain.

In Figure 5, we see the posterior mean of arising from the star-shaped set parametrization and observations with different noise levels. The posterior mean

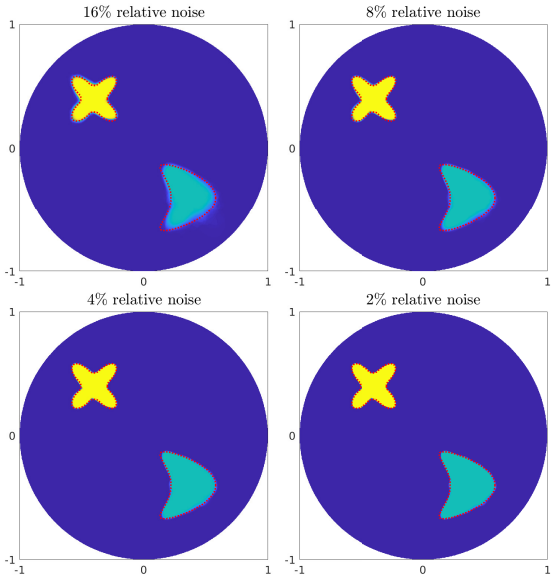

Figure 5: Posterior mean estimates of the absorption parameter using the star-shaped set parametrization in different noise regimes. The dotted red line indicates the location of γ_0.

approximates the ground truth well for all noise levels. Note that the posterior mean varies only slightly for each noise level and is approximately piecewise constant. This indicates little posterior variance. This is due to a small noise level and the fast contraction rate that this inverse problem provides by virtue of (45). The estimates are not exact, but note that the exact data is not available due to projection and discretization. Taking N_d large improves the data but also causes the likelihood function to attain larger values. This, in return, requires a smaller step size b. This means there is a computational trade-off between N_d and b. Even for 16% relative noise, the reconstruction is fairly good, and the variance of the posterior samples is visibly larger. It is a strength of this method that it is robust for large noise levels. The mixing of the sample chains in the trace plots in Figure 7 indicates that the sampling algorithm is performing well. The convergence of the posterior mean is also evident in L^2-distance as computed numerically, see Figure 8. This rate does not match the theoretical; but this is too much to expect for the observation (48), as this does not match the continuous observation (1) for which the rate is proved. Note we do not numerically scale the priors as the theoretical results require.

Figure 6 suggests that the posterior mean converges as the noise level goes to zero, as is also evident from its L^2-loss in Figure 8. Note that the reconstructions are continuous, not only because we take an average, but also because we use a continuous level set parametrization. Here, the sampling is initialized at $\theta^{(0)} = 2\phi_{(0,-1)}$, since

this guess captures some of the low frequency information of possible θ_0 that can give rise to γ_0. We report that chains with small step-size and the natural starting guess $\theta^{(0)} = 0$ often get stuck in local minima due to the number of levels in (52) and due to the fact that the pCN method does not require the gradient of either the parametrization or the forward map.

The sample diagnostics of Figure 7 indicate that sampling is harder for the level set parametrization compared to the star-shaped set parameterization. This is hard for at least two likely reasons: the first is due to the large number of coefficients θ_ℓ, $\max(|\ell_1|, |\ell_2|) \leq 4$. This was also noted in [10]. The second likely reason is that $\theta \mapsto \Phi_\epsilon(\theta)$ is not injective for any $\epsilon \geq 0$. Therefore, the prior could be multi-modal, and this can lead to correlated samples in the Markov chain. Other work suggests that the pCN method shows an underwhelming performance when applied to a correlated and multi-modal posterior, see [67] which also provides a gradient-based remedy. The level set method has found success in optimization-based approaches, in for example [68], where a descent step is taken in each iteration of an iterative algorithm. A Bayesian *maximum a posteriori* approach [21] has also been shown to find success for a smoothened level set. We expect that using gradient information in gradient-based MCMC methods would improve the performance significantly. A benefit of the level set parametrization is that we do not need to know *a priori* the number of inclusions as in the case of the star-shaped set parametrization. One could also combine the two methods as in [12]. Note in Figure 8 that, for both parametrizations, the posterior mean is stable to different noise realizations. This mirrors the convergence in probability we expect from Theorem 4.4 and 4.6.

7. Conclusions

In this paper, we provide and investigate a Bayesian approach to consistent inclusion detection in nonlinear inverse problems. The posterior consistency analysis is performed under general conditions of Hölder continuity of the parametrization and conditional well-posedness of the inverse problem. Furthermore, it gives an explicit rate. We showcase the convergence of the posterior mean in a small noise limit for a photoacoustic problem, where we note that the star-shaped set parametrization outperforms the level set parametrization. We highlight that Theorem 4.2 and 4.6 hold for any forward map satisfying Condition 2 and can be applied to other parametrizations. A different parametrization could for example arise in the related problem of crack detection. Interesting future work includes applying the inclusion detection method to other inverse problems. Similar stability estimates to that of Lemma 5.2 exist for the mathematically closely related problems of determining the absorption coefficient in acousto-optic imaging and the permittivity in microwave imaging, see [26]. This is also the case for conductivity imaging in quantitative thermoacoustic tomography, where [69] employed complex geometrical optics solutions. For the Calderón problem in two dimensions, [70] provides a stability estimate that is permitted for the star-shaped set parametrization, see also the comments after Theorem 4.2 on the regularity of γ. There is a natural Hilbert space observation setting for the Calderón problem, see [28]. Also in three dimensions and higher, conditional stability for inclusion detection in the context of the Calderón problem has been considered and shown to be logarithmic at best [71]. The generalization to three dimensions and more complex phantoms is left for future

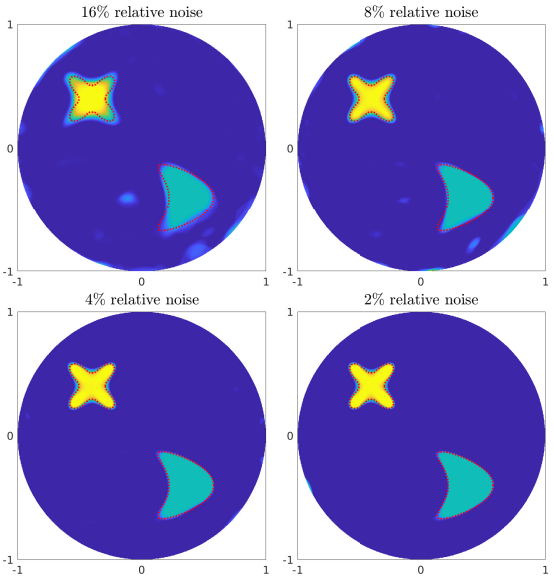

Figure 6: Posterior mean estimates of the absorption parameter using the level set parametrization in different noise regimes. The dotted red line indicates the location of γ_0.

work. An important direction in the numerical optimization of this approach is to consider gradient-based sampling methods.

Acknowledgments

The authors would like to thank Prof. Richard Nickl for many helpful discussions. The authors would also like to thank the Isaac Newton Institute for Mathematical Sciences, Cambridge, for support and hospitality during the program Rich and Nonlinear Tomography where work on this paper was undertaken, supported by EPSRC grant no EP/R014604/1. BMA, KK and AKR were supported by The Villum Foundation (grant no. 25893). TT was supported by the European Research Council (ERC) under the European Union's Horizon 2020 research and innovation programme (grant agreement no. 101001417 - QUANTOM) and the Academy of Finland (Centre of Excellence in Inverse Modelling and Imaging project 353086 and the Flagship Program Photonics Research and Innovation grant 320166).

A. Covering numbers

Consider a compact subset A of a space X endowed with a semimetric d. The covering number $N(A, d, \rho)$ denotes the minimum number of closed d-balls $\{x \in X : d(x_0, x) \leq \rho\}$ with center $x_0 \in A$ and radius $\rho > 0$ needed to cover A, see for example [33,

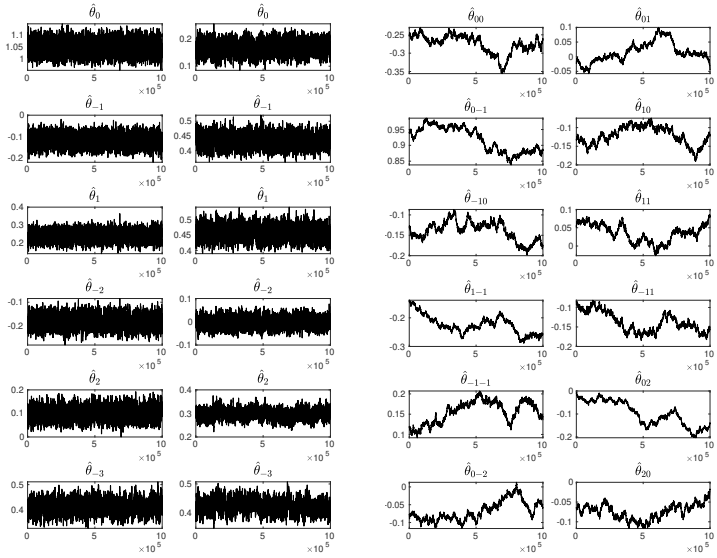

(a) (b)

Figure 7: Plot (A) shows trace plots of the first 6 Fourier coefficients of samples θ_1 (left) and θ_2 (right) from the posterior for the star-shaped set parametrization with observations subject to 4% relative noise. Plot (B) shows trace plots of the first 12 Fourier coefficients of samples θ from the posterior for the level set parametrization with observations subject to 4% relative noise.

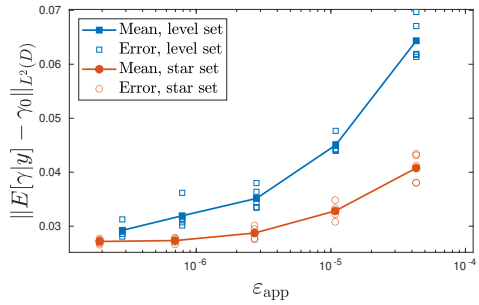

Figure 8: L^2-error of 5 realized posterior means for each noise level ε_{app} and both parametrizations. The solid markers represent the mean of the 5 error estimates.

Appendix C] or [32, Section 4.3.7]. Then the metric entropy is $\log N(A, d, \rho)$. When d is replaced by a norm, we mean the metric induced by the norm.

Lemma A.1. *Let (X, d_X) and (Y, d_Y) be two linear spaces endowed with semimetric d_X and d_Y.*

(i) If $f : X \to Y$ satisfies

$$d_Y(f(x), f(x')) \le C d_X(x, x')^\eta, \quad \forall x, x' \in A$$

for some $A \subset\subset X$ and some $\eta > 0$, then for any $\rho > 0$ we have

$$N(f(A), d_Y, C\rho^\eta) \le N(A, d_X, \rho). \tag{53}$$

(ii) For $A \subset\subset X$ and $B \subset\subset Y$,

$$N(A \times B, d_\infty, \rho) \le N(A, d_X, \rho) N(B, d_Y, \rho),$$

where $d_\infty((x, y), (x', y')) = \max(d_X(x, x'), d_Y(y, y'))$ is the product metric.

Proof. (i) We denote by $B_X(x', \rho)$ and $B_Y(y', \rho)$ the ball in X with center $x' \in X$ and radius $\rho > 0$ and the ball in Y with center $y' \in Y$ and radius $\rho > 0$, respectively. For any $\rho > 0$,

$$f(B_X(x', \rho)) \subset B_Y(f(x'), C\rho^\eta).$$

Then it follows that

$$N(f(A), d_Y, C\rho^\eta) \le N(A, d_X, \rho). \tag{54}$$

(ii) Let C_A be a finite set in A and C_B be a finite set in B such that

$$A \subset \bigcup_{x \in C_A} B_X(x, \rho) \quad \text{and} \quad B \subset \bigcup_{y \in C_B} B_Y(x, \rho).$$

Take $z = (x, y) \in A \times B$, then there exists $x_0 \in C_A$ such that $x \in B_X(x_0, \rho)$ and $y_0 \in C_B$ such that $y \in B_Y(y_0, \rho)$. Hence $z \in B_{X\times Y}((x_0, y_0), \rho) := \{z \in X \times Y : d_\infty(z, (x_0, y_0)) \le \rho\}$. It follows that

$$A \times B \subset \bigcup_{z \in C_A \times C_B} B_{X\times Y}(z, \rho),$$

and hence the wanted property follows. □

Lemma A.2. *Let $\mathcal{X}$ be a bounded Lipschitz domain in $\mathbb{R}^{d'}$ or the d'-dimensional torus and $\beta > d'/2$, then*

$$\log N(\mathcal{S}_\beta(M), \|\cdot\|_\infty, \rho) \le C\rho^{-d'/\beta},$$

where $C = C(\beta, M, d', \mathcal{X})$ and $\|f\|_\infty := \sup_{x \in \overline{\mathcal{X}}} |f(x)|$.

Proof. Corollary 4.3.38 and the remark hereafter in [32] states that the norm ball $B_\beta(M)$ of the Sobolev space $H^\beta([0, 1]^{d'})$ of radius M satisfies for $\beta > d'/2$,

$$\log N(B_\beta(M), \|\cdot\|_{L^\infty([0,1]^{d'})}, \rho) \le C(\beta, M, d')\rho^{-d'/\beta}. \tag{55}$$

If $\mathcal{X}$ is the d'-dimensional torus, we identify $H^\beta(\mathcal{X})$ with the corresponding periodic Sobolev space, which is a subset of $H^\beta([0, 1]^{d'})$, hence the wanted result follows. Now, if $\mathcal{X}$ is a bounded Lipschitz domain in $\mathbb{R}^{d'}$, we assume without loss of generality that $\mathcal{X} \subset [0, 1]^{d'}$. Indeed, if $\mathcal{X}$ is not a subset of $[0, 1]^{d'}$, we identify $f \in H^\delta(\mathcal{X})$ with

$\tilde{f} \in H^\delta(\tilde{\mathcal{X}})$ for some $\tilde{\mathcal{X}} \subset [0,1]^{d'}$ by a scaling and update M accordingly. Since $\mathcal{X}$ is Lipschitz, we let $E : H^\beta(\mathcal{X}) \to H^\beta([0,1]^{d'})$ be a continuous extension operator satisfying

$$\|Ef\|_{H^\beta([0,1]^{d'})} \leq C(d', \beta, \mathcal{X})\|f\|_{H^\beta(\mathcal{X})},$$

see for example [72]. We denote the restriction $R : H^\beta([0,1]^{d'})) \to H^\beta(\mathcal{X})$, which is a contraction in supremum norm and the left-inverse of E. Then $\mathcal{S}_\beta(M) = R(E(\mathcal{S}_\beta(M)))$ and $E(\mathcal{S}_\beta(M)) \subset B_\beta(CM)$, and hence

$$\begin{aligned} N(\mathcal{S}_\beta(M), \|\cdot\|_\infty, \rho) &= N(R(E(\mathcal{S}_\beta(M))), \|\cdot\|_\infty, \rho) \\ &\leq N(E(\mathcal{S}_\beta(M)), \|\cdot\|_{L^\infty([0,1]^{d'})}, \rho), \\ &\leq N(B_\beta(CM), \|\cdot\|_{L^\infty([0,1]^{d'})}, \rho), \\ &\leq C(\beta, M, d', \mathcal{X})\rho^{-d'/\beta}, \end{aligned} \tag{56}$$

using also Lemma A.1 (i) and (55). □

Lemma A.3. *With the notation defined in Section 3, we have for all $\rho > 0$*

$$N(B_\infty(M\rho) + \mathcal{S}_\delta(CM), \|\cdot\|_\infty, 2M\rho) \leq N(\mathcal{S}_\delta(CM), \|\cdot\|_\infty, M\rho).$$

Proof. By Lemma A.2 there exists $N > 0$ for which there is a sequence $\{\theta_i\}_{i=1}^N$ in $\mathcal{S}_\delta(CM)$ such that

$$\mathcal{S}_\delta(CM) \subset \cup_{i=1}^N B_\infty(\theta_i, M\rho).$$

By the triangle inequality,

$$B_\infty(M\rho) + \mathcal{S}_\delta(CM) \subset \cup_{i=1}^N B_\infty(\theta_i, 2M\rho), \tag{57}$$

since if $\theta = \theta^{(1)} + \theta^{(2)}$ for $\theta^{(1)} \in B_\infty(M\rho)$ and $\theta^{(2)} \in \mathcal{S}_\delta(CM)$, then there exists a θ_i such that $\|\theta^{(2)} - \theta_i\|_\infty \leq M\rho$, and hence

$$\|\theta - \theta_i\|_\infty \leq \|\theta^{(1)}\|_\infty + \|\theta^{(2)} - \theta_i\|_\infty \leq 2M\rho.$$

Then the property follows from (57). □

B. On maximum likelihood composite testing

We denote by E_n and E_n^γ the expectation with respect to P_n and P_n^γ respectively.

Lemma B.1. *Suppose for a non-increasing function $N(\rho)$, some $\rho_0 > 0$ and all $\rho > \rho_0$, we have*

$$N(\{\gamma \in A_n : \rho < d_{\mathcal{G}}(\gamma, \gamma_0) < 2\rho\}, d_{\mathcal{G}}, \rho/4) \leq N(\rho).$$

Then for every $\rho > \rho_0$, there exist measurable functions $\Psi_n : \mathcal{Y}_- \to \{0,1\}$ such that

$$E_n^{\gamma_0}(\Psi_n) \leq N(\rho)\frac{e^{-\frac{1}{8\sigma^2}n\rho^2}}{1 - e^{-\frac{1}{8\sigma^2}n\rho^2}},$$

$$\sup_{\gamma \in A_n : d_{\mathcal{G}}(\gamma,\gamma_0) > \rho} E_n^\gamma(1 - \Psi_n) \leq e^{-\frac{1}{32\sigma^2}n\rho^2}.$$

Proof. To construct the measurable functions Ψ_n we use the maximum likelihood test, see [33, Lemma D.16] and the covering argument of [23, Theorem 7.1], see also [32, Theorem 7.1.4]. Choose a finite set S_j of points in each shell

$$S_j = \{\gamma \in A_n : \rho j < d_{\mathcal{G}}(\gamma, \gamma_0) \leq \rho(1+j)\}, \quad j \in \mathbb{N},$$

so that every $\gamma \in S_j$ is within distance $\frac{j\rho}{4}$ of a point in S'_j. For $\rho > \rho_0$, there are at most $N(j\rho)$ such points. For each $\gamma_{jl} \in S'_j$, define the measurable function, $\Psi_{n,j,l} : \mathcal{Y}_- \to \{0,1\}$, known as the maximum likelihood test,

$$\Psi_{n,j,l}(y) := \mathbb{1}_{A_{n,j,l}}(y),$$

where

$$A_{n,j,l} := \{y \in \mathcal{Y}_- : \frac{p_n^{\gamma_{jl}}}{p_n^{\gamma_0}}(y) > 1\}.$$

By [33, Lemma D.16] we have

$$E_n^{\gamma_0}(\Psi_{n,j,l}) \leq e^{-\frac{1}{8\sigma^2}n(\rho j)^2}$$

and

$$\sup_{\{\gamma \in A_n : d_{\mathcal{G}}(\gamma,\gamma_{jl}) \leq \frac{\rho j}{4}\}} E_n^{\gamma}(1 - \Psi_{n,j,l}) \leq e^{-\frac{1}{32\sigma^2}n(\rho j)^2}.$$

Now, set $\Psi_n(y) := \mathbb{1}_{\cup_{j,l} A_{n,j,l}}(y)$. This is also a measurable function, since a countable union of measurable sets is measurable. Then by the union bound

$$E_n^{\gamma_0}(\Psi_n) \leq \sum_{j\in\mathbb{N}} \sum_{l=1}^{N(j\rho)} E_n^{\gamma_0}(\Psi_{n,j,l}) \leq \sum_{j\in\mathbb{N}} N(j\rho) e^{-\frac{1}{8\sigma^2}n(\rho j)^2} \leq N(\rho) \frac{e^{-\frac{1}{8\sigma^2}n\rho^2}}{1 - e^{-\frac{1}{8\sigma^2}n\rho^2}}$$

On the other hand, for any $j \geq 1$,

$$\begin{aligned}
\sup_{\gamma \in \cup_{i\geq j} S_i} E_n^{\gamma_0}(1 - \Psi_n) &= \sup_{i\geq j,l} \sup_{\gamma : d_{\mathcal{G}}(\gamma,\gamma_{i,l}) \leq \frac{\rho i}{4}} P_n^{\gamma_0}(\cap_{j',l'} A^c_{n,j',l'}), \\
&\leq \sup_{i\geq j,l} \sup_{\gamma : d_{\mathcal{G}}(\gamma,\gamma_{i,l}) \leq \frac{\rho i}{4}} E_n^{\gamma_0}(1 - \Psi_{n,i,l}), \\
&\leq \sup_{i\geq j} e^{-\frac{1}{32\sigma^2}n(\rho i)^2}.
\end{aligned}$$

For $j = 1$ we get the wanted result. □

There are other ways to prove the existence of suitable measurable functions Ψ_n used in the proof of Theorem 2.1. We mention here the approximation argument of [28, Lemma 8] that requires smoothness properties of $\mathcal{G}$.

Proof of 2.1. For the convenience of the reader, we provide what is a standard testing argument for our setting in Lemma B.1, see also [23, Theorem 7.1], implied by Condition **A.3**. Indeed, since the covering number decreases, when increasing the 'radius', we have for all $\rho > \rho_0 := 4m_0 r_n$,

$$N(A_n, d_{\mathcal{G}}, \frac{\rho}{4}) \leq N(\rho) := e^{C_3 n r_n^2}.$$

Given any $C_2 > C_1 + 4$, we set $\rho := 4mr_n$ for $m > m_0$ large enough (depending also on C_2, C_3 and σ^2 by the following) and apply Lemma B.1: there exists measurable functions $\Psi_n : \mathcal{Y}_- \to \{0,1\}$ such that

$$E_n^{\gamma_0}(\Psi_n) \leq e^{C_3 n r_n^2} \frac{e^{-2\sigma^{-2} m n r_n^2}}{1 - e^{-2\sigma^{-2} m n r_n^2}} \leq e^{-C_2 n r_n^2}.$$

In addition, choosing m such that $(4m)^2/(32\sigma^2) \geq C_2$ we note

$$\sup_{\gamma \in A_n : d_{\mathcal{G}}(\gamma, \gamma_0) > 4mr_n^2} E_n^{\gamma}(1 - \Psi_n) \leq e^{-C_2 n r_n^2}.$$

Then Theorem 28 in [31] and modifications as in the proof of Theorem 1.3.2 in [24] give the claim. □

C. Proofs of section 4

Proof of Theorem 4.4. The proof relies on satisfying Condition **A.1**, **A.2** and **A.3** for the choice $A_n = \Phi(\Theta_n)$ for

$$\Theta_n := \{\theta = \phi_1 + \phi_2 : \|\phi_1\|_\infty \leq M\bar{r}_n, \|\phi_2\|_{\mathcal{H}} \leq M\}^{\mathcal{N}} \cap \mathcal{S}_\beta(M), \quad (58)$$

where $\mathcal{S}_\beta(M)$ is defined in (30). To satisfy Condition **A.1** we follow Lemma 3.4 and note for $\theta = (\theta_1, \ldots, \theta_{\mathcal{N}})$ and $\theta_0 = (\theta_{0,1}, \ldots, \theta_{0,\mathcal{N}})$ that

$$\begin{aligned}
&\{\theta \in \Theta : d_{\mathcal{G}}(\Phi(\theta), \Phi(\theta_0)) \leq r_n\} \\
&\quad \supset \{\theta \in \Theta : \|\theta - \theta_0\|_{\mathcal{N}} \leq C\bar{r}_n, \|\theta_i - \theta_{0,i}\|_{H^\beta(\mathbb{T})} \leq \tilde{R}, i = 1, \ldots, \mathcal{N}\}, \\
&\quad \supset \{\theta \in \Theta : \|\theta_i - \theta_{0,i}\|_{\mathcal{N}} \leq C\bar{r}_n, \|\theta_i - \theta_{0,i}\|_{H^\beta(\mathbb{T})} \leq \tilde{R}, i = 1, \ldots, \mathcal{N}\}, \\
&\quad \supset \otimes_{i=1}^{\mathcal{N}} \left(\{\theta_i : \|\theta_i - \theta_{0,i}\|_{L^\infty(\mathbb{T})}\} \cap \{\theta_i : \|\theta_i - \theta_{0,i}\|_{H^\beta(\mathbb{T})} \leq \tilde{R}\} \right),
\end{aligned}$$

for some $\tilde{R} > 0$ chosen sufficiently large. Then (31) together with the argument in Lemma 3.4 implies that Condition **A.1** is satisfied. Note Θ_n in (58) is the $\mathcal{N}$-product set of (20). Then repeated use of the standard set relation $A^2 \setminus B^2 = [A \times (A \setminus B)] \cup [(A \setminus B) \times A]$ and the argument of Lemma 3.2 implies there exists $M > C(C_2, \Pi'_\theta, \delta, \mathcal{N})$ such that

$$\Pi_\theta(\Theta \setminus \Theta_n) \leq e^{-C_2 n r_n^2},$$

for any given $C_2 > 0$, hence Condition **A.2** is satisfied. Condition **A.3** is satisfied as in Lemma 3.3 using Lemma A.1 (*ii*). Then the result follows as in the proof of Theorem 3.1 and Corollary 1. □

Lemma C.1. *Let V_ϵ be defined as in (38) for $\theta_0 \in H^\beta_\diamond(\mathcal{X})$, $\beta > 1 + d'/2$ and some $c = c_{i-1} \in \overline{\mathbb{R}}$. Then for $\epsilon > 0$ sufficiently small*

$$|V_\epsilon| \leq C(\theta_0, c, \mathcal{X})\epsilon.$$

Proof. Note for $c = c_0 = -\infty$ and $c = c_{\mathcal{N}} = \infty$ this is trivially satisfied. Next, the inverse function theorem implies that any point $x_0 \in \theta^{-1}(c)$ has a neighborhood N_{x_0} that is a diffeomorphic image $\varphi_{x_0}(Q_{\epsilon_{x_0}})$ of a box

$$Q_{\epsilon_{x_0}} := \{(s,t) : |s| \leq \epsilon_{x_0}, |t| \leq \epsilon_{x_0}\}, \quad 0 < \epsilon_{x_0} < 1,$$

such that

$$\theta_0(\varphi_{x_0}(s,t)) = s|(\nabla\theta_0)(x_0)| + c,$$

(one should find the inverse of $g(x_1,x_2) = (\frac{\theta_0(x_1,x_2)-c}{|\nabla\theta_0(x_0)|}, x_2)$ in a neighborhood of x_0). Note we have a C^1 parametrization of an intersection of V_ϵ with a small neighborhood of x_0,

$$V_\epsilon \cap N_{x_0} = \{\varphi_{x_0}(s,t) : |s| \le \frac{\epsilon}{|\nabla\theta_0(x_0)|}, |t| \le \epsilon_{x_0}\},$$

for all $\epsilon \le |\nabla\theta_0(x_0)|\epsilon_{x_0}$. By the classical area formula, we have

$$|V_\epsilon \cap N_{x_0}| = \int_{|s|\le C(x_0,\theta_0)\epsilon} \int_{|t|\le\epsilon_{x_0}} |J\varphi_{x_0}(s,t)|\, ds\, dt \le C(x_0,\theta_0)\epsilon,$$

since the continuous function $J\varphi_{x_0}$ (it is a polynomial of zero'th and first order derivatives of φ_{x_0}), is integrated on a compact domain. Note $\cup_{x_0\in\mathcal{I}} N_{x_0}$ is an open cover of $\theta_0^{-1}(c)$ for some finite set $\mathcal{I} \subset \theta_0^{-1}(c)$ depending on $\mathcal{X}$ and θ_0. Take ϵ such that $V_\epsilon \subset \cup_{x_0\in\mathcal{I}} N_{x_0}$. This ϵ exists since θ_0 as defined on $\overline{\mathcal{X}}$ is a closed function, and hence there exists in $\mathbb{R}$ a neighborhood U of c such that $\theta_0^{-1}(U) \subset \cup_{x_0\in\mathcal{I}} N_{x_0}$, see [73, Theorem 1.4.13]. Then,

$$|V_\epsilon| \le \sum_{x_0\in\mathcal{I}} |V_\epsilon \cap N_{x_0}| \le C(\theta_0, c, \mathcal{X})\epsilon.$$

This is true for any $i = 1, \dots, \mathcal{N}-1$ for which the estimate is only updated by a new constant. □

Proof of Theorem 4.6. Let $\gamma_0^n = \Phi_{n^{-k}}(\theta_0)$ and $\gamma^n = \Phi_{n^{-k}}(\theta)$ for some $0 < k < 1$, which we will choose later. For any $\hat{r}_n > 0$, the triangle inequality gives

$$\begin{aligned}\{\gamma : \|\gamma-\gamma_0\|_{L^2(D)} \le C_0\hat{r}_n\} \\ \supset \left\{\gamma : \|\gamma-\gamma_0^n\|_{L^2(D)} \le \frac{1}{2}C_0\hat{r}_n, \|\gamma_0^n-\gamma_0\|_{L^2(D)} \le \frac{1}{2}C_0\hat{r}_n\right\},\end{aligned}$$

hence

$$\begin{aligned}\Pi(\gamma : \|\gamma-\gamma_0\|_{L^2(D)} \le C_0\hat{r}_n|Y) \ge \Pi(\gamma : \|\gamma-\gamma_0^n\|_{L^2(D)} \le \frac{1}{2}C_0\hat{r}_n|Y) \\ \times \mathbb{1}_{\|\gamma_0^n-\gamma_0\|_{L^2(D)}\le\frac{1}{2}C_0\hat{r}_n}. \qquad (59)\end{aligned}$$

We shall consider the two factors of the right-hand side in separate parts below:
1) We check that Condition **A.2**, **A.3**, and **A.1** are satisfied for the choice $A_n = \Phi(\Theta_n)$ with

$$\Theta_n := \{\theta = \theta_1 + \theta_2 : \|\theta_1\|_\infty \le M r_n^{\frac{1}{\eta}} n^{-k}, \|\theta_2\|_{\mathcal{H}} \le M\} \cap \mathcal{S}_\beta(M), \quad (60)$$

and k to be chosen below. For **A.2** it is clear from (37) that for each n,

$$\Pi_\theta(\Theta) = 1.$$

As in the proof of Lemma 3.2 there exists $M > C(C_2, \Pi'_\theta, \delta)$ such that Condition **A.2** is satisfied, if $a = a(k)$ is such that

$$(r_n^{\frac{1}{\eta}} n^{-k} n^{1/2-a})^{-b} = n r_n^2, \qquad (61)$$

for $b = \frac{2d}{2\delta - d}$. This is satisfied when

$$a = a(k) = \frac{\eta(\delta - dk)}{2\delta\eta + d}, \quad \text{and} \quad 0 < k < \frac{\delta}{d}, \tag{62}$$

so that $0 < a < 1/2$. Condition **A.3** follows as in the proof of Lemma A.1 with $\bar{r}_n$ replaced with $r_n^{\frac{1}{\eta}} n^{-k}$. Again it reduces to the covering number of the norm-ball in $H^\delta(\mathcal{X})$ for which we need a such that

$$(r_n^{\frac{1}{\eta}} n^{-k})^{-d/\delta} = n r_n^2$$

as in (23). This is indeed satisfied by (62). For Condition **A.1** we proceed as in the proof of Lemma 3.4 and use Lemma 4.5 to obtain

$$\{\theta \in \Theta : d_{\mathcal{G}}(\gamma^n, \gamma_0^n) \le r_n\} \supset \{\theta \in \Theta : \|\theta - \theta_0\|_\infty \le C n^{-k} r_n^{\frac{1}{\eta}}\} \cap \mathcal{S}_\beta(R),$$

where $C = C(\eta, C_{\mathcal{G}}, C_\Phi, R)$. Continuing the argument and using (37), Condition **A.1** is satisfied for some $C_1 > 0$ if again a satisfies (61). By Theorem 2.1

$$\Pi(B_{\mathcal{G}}(\gamma_0^n, C r_n) \cap A_n | Y) \to 1 \quad \text{in } P_n^{\gamma_0}\text{-probability},$$

as $n \to \infty$ for some constant $C > 0$. It follows that

$$\Pi(\gamma : \|\gamma - \gamma_0^n\|_{L^2(D)} \le C r_n^\nu | Y) \to 1 \quad \text{in } P_n^{\gamma_0}\text{-probability},$$

with rate $e^{-bnr_n^2}$, $0 < b < C_2 - C_1 - 4$ as $n \to \infty$ as in Theorem 3.1.
2) For the second factor, note that $\theta_0 \in H_\diamond^\beta(\mathcal{X})$ and Lemma 4.5 (i) implies

$$\|\gamma_0^n - \gamma_0\|_{L^2(D)} \le C'(\theta_0, \mathcal{X}, D, \mathbf{c}) n^{-k/2}.$$

Since $r_n^\nu = n^{-a(k)\nu}$ is a strictly increasing function of k (the rate becomes worse for larger k) and $n^{-k/2}$ is strictly decreasing in k, the optimal choice of k satisfies $r_n^\nu = n^{-k/2}$, which is solved by

$$k = \frac{2\delta\eta\nu}{2d\eta\nu + 2\delta\eta + d}, \tag{63}$$

which also satisfies the condition on k in (62), since $\delta > d$. Inserting this back into (62) yields (41). Finally, take $C_0 = 2\max(C, C')$ and $\hat{r}_n = r_n^\nu$ and note by (59) that

$$\Pi(\gamma : \|\gamma - \gamma_0\|_{L^2(D)} \le C_0 r_n^\nu | Y) \ge \Pi(\gamma : \|\gamma - \gamma_0^n\|_{L^2(D)} \le \frac{1}{2} C_0 r_n^\nu | Y) \to 1,$$

in $P_n^{\gamma_0}$-probability as $n \to \infty$. Then the wanted result follows as in Corollary 1. □

[1] Jari Kaipio and Erkki Somersalo. *Statistical and computational inverse problems*, volume 160 of *Applied Mathematical Sciences*. Springer-Verlag, New York, 2005.

[2] A. M. Stuart. Inverse problems: a Bayesian perspective. *Acta Numer.*, 19:451–559, 2010.

[3] V Cherepenin, A Karpov, A Korjenevsky, V Kornienko, A Mazaletskaya, D Mazourov, and D Meister. A 3d electrical impedance tomography (EIT) system for breast cancer detection. *Physiological Measurement*, 22(1):9–18, feb 2001.

[4] Minghua Xu and Lihong V. Wang. Photoacoustic imaging in biomedicine. *Review of Scientific Instruments*, 77(4):041101, 04 2006.

[5] Milad Hallaji, Aku Seppänen, and Mohammad Pour-Ghaz. Electrical impedance tomography-based sensing skin for quantitative imaging of damage in concrete. *Smart Materials and Structures*, 23(8):085001, jun 2014.

[6] Patrick Fuchs, Thorben Kröger, and Christoph S. Garbe. Defect detection in ct scans of cast aluminum parts: A machine vision perspective. *Neurocomputing*, 453:85–96, 2021.

[7] Ashish Bora, Ajil Jalal, Eric Price, and Alexandros G. Dimakis. Compressed sensing using generative models. In *Proceedings of the 34th International Conference on Machine Learning - Volume 70*, ICML'17, page 537–546. JMLR.org, 2017.

[8] Masoumeh Dashti and Andrew M. Stuart. The Bayesian approach to inverse problems. In *Handbook of uncertainty quantification. Vol. 1, 2, 3*, pages 311–428. Springer, Cham, 2017.

[9] Tan Bui-Thanh and Omar Ghattas. An analysis of infinite dimensional bayesian inverse shape acoustic scattering and its numerical approximation. *SIAM/ASA Journal on Uncertainty Quantification*, 2(1):203–222, 2014.

[10] Matthew M. Dunlop and Andrew M. Stuart. The Bayesian formulation of EIT: analysis and algorithms. *Inverse Probl. Imaging*, 10(4):1007–1036, 2016.

[11] Marco A. Iglesias, Yulong Lu, and Andrew Stuart. A Bayesian level set method for geometric inverse problems. *Interfaces Free Bound.*, 18(2):181–217, 2016.

[12] Babak Maboudi Afkham, Yiqiu Dong, and Per Christian Hansen. Uncertainty quantification of inclusion boundaries in the context of X-ray tomography. *SIAM/ASA J. Uncertain. Quantif.*, 11(1):31–61, 2023.

[13] Ana Carpio, Sergei Iakunin, and Georg Stadler. Bayesian approach to inverse scattering with topological priors. *Inverse Problems*, 36(10):105001, 29, 2020.

[14] Jeff Borggaard, Nathan E Glatt-Holtz, and Justin Krometis. A statistical framework for domain shape estimation in stokes flows. *Inverse Problems*, 39(8):085009, jun 2023.

[15] Yunwen Yin, Weishi Yin, Pinchao Meng, and Hongyu Liu. The interior inverse scattering problem for a two-layered cavity using the Bayesian method. *Inverse Probl. Imaging*, 16(4):673–690, 2022.

[16] Zhipeng Yang, Xinping Gui, Ju Ming, and Guanghui Hu. Bayesian approach to inverse time-harmonic acoustic scattering with phaseless far-field data. *Inverse Problems*, 36(6):065012, 30, 2020.

[17] Matthew M. Dunlop, Marco A. Iglesias, and Andrew M. Stuart. Hierarchical Bayesian level set inversion. *Stat. Comput.*, 27(6):1555–1584, 2017.

[18] Neil K. Chada, Marco A. Iglesias, Lassi Roininen, and Andrew M. Stuart. Parameterizations for ensemble Kalman inversion. *Inverse Problems*, 34(5):055009, 31, 2018.

[19] Jiangfeng Huang, Zhaoxing Li, and Bo Wang. A Bayesian level set method for the shape reconstruction of inverse scattering problems in elasticity. *Comput. Math. Appl.*, 97:18–27, 2021.

[20] Jiangfeng Huang, Zhiliang Deng, and Liwei Xu. A Bayesian level set method for an inverse medium scattering problem in acoustics. *Inverse Probl. Imaging*, 15(5):1077–1097, 2021.

[21] William Reese, Arvind K Saibaba, and Jonghyun Lee. Bayesian level set approach for inverse problems with piecewise constant reconstructions. *arXiv preprint arXiv:2111.15620*, 2021.

[22] François Monard, Richard Nickl, and Gabriel P. Paternain. Consistent inversion of noisy non-Abelian X-ray transforms. *Comm. Pure Appl. Math.*, 74(5):1045–1099, 2021.

[23] Subhashis Ghosal, Jayanta K. Ghosh, and Aad W. van der Vaart. Convergence rates of posterior distributions. *The Annals of Statistics*, 28(2):500 – 531, 2000.

[24] Richard Nickl. *Bayesian non-linear statistical inverse problems*. Zurich Lectures in Advanced Mathematics. EMS Press, Berlin, 2023.

[25] Sergios Agapiou, Stig Larsson, and Andrew M. Stuart. Posterior contraction rates for the Bayesian approach to linear ill-posed inverse problems. *Stochastic Process. Appl.*, 123(10):3828–3860, 2013.

[26] Mourad Choulli. Some stability inequalities for hybrid inverse problems. *C. R. Math. Acad. Sci. Paris*, 359:1251–1265, 2021.

[27] Guillaume Bal, Kui Ren, Gunther Uhlmann, and Ting Zhou. Quantitative thermo-acoustics and related problems. *Inverse Problems*, 27(5):055007, 15, 2011.

[28] Kweku Abraham and Richard Nickl. On statistical Calderón problems. *Math. Stat. Learn.*, 2(2):165–216, 2019.

[29] Matteo Giordano and Richard Nickl. Consistency of Bayesian inference with Gaussian process priors in an elliptic inverse problem. *Inverse Problems*, 36(8):085001, 35, 2020.

[30] Richard Nickl, Sara van de Geer, and Sven Wang. Convergence rates for penalized least squares estimators in PDE constrained regression problems. *SIAM/ASA J. Uncertain. Quantif.*, 8(1):374–413, 2020.

[31] Richard Nickl. Bernstein–von Mises theorems for statistical inverse problems I: Schrödinger equation. *J. Eur. Math. Soc. (JEMS)*, 22(8):2697–2750, 2020.

[32] Evarist Giné and Richard Nickl. *Mathematical foundations of infinite-dimensional statistical models*. Cambridge Series in Statistical and Probabilistic Mathematics, [40]. Cambridge University Press, New York, 2016.

[33] Subhashis Ghosal and Aad van der Vaart. *Fundamentals of nonparametric Bayesian inference*, volume 44 of *Cambridge Series in Statistical and Probabilistic Mathematics*. Cambridge University Press, Cambridge, 2017.

[34] J. Diestel and J. J. Uhl, Jr. *Vector measures*. Mathematical Surveys, No. 15. American Mathematical Society, Providence, R.I., 1977. With a foreword by B. J. Pettis.

[35] Richard M. Dudley. *Real analysis and probability*. The Wadsworth & Brooks/Cole Mathematics Series. Wadsworth & Brooks/Cole Advanced Books & Software, Pacific Grove, CA, 1989.

[36] Sebastian J. Vollmer. Posterior consistency for Bayesian inverse problems through stability and regression results. *Inverse Problems*, 29(12):125011, 32, 2013.

[37] S. L. Cotter, G. O. Roberts, A. M. Stuart, and D. White. MCMC methods for functions: modifying old algorithms to make them faster. *Statist. Sci.*, 28(3):424–446, 2013.

[38] Martin Hairer, Andrew M. Stuart, and Sebastian J. Vollmer. Spectral gaps for a Metropolis-Hastings algorithm in infinite dimensions. *Ann. Appl. Probab.*, 24(6):2455–2490, 2014.

[39] Matthew M. Dunlop, Tapio Helin, and Andrew M. Stuart. Hyperparameter estimation in Bayesian MAP estimation: parameterizations and consistency. *SMAI J. Comput. Math.*, 6:69–100, 2020.

[40] Lassi Roininen, Janne M. J. Huttunen, and Sari Lasanen. Whittle-Matérn priors for Bayesian statistical inversion with applications in electrical impedance tomography. *Inverse Probl. Imaging*, 8(2):561–586, 2014.

[41] Heinz W. Engl, Martin Hanke, and Andreas Neubauer. *Regularization of inverse problems*, volume 375 of *Mathematics and its Applications*. Kluwer Academic Publishers Group, Dordrecht, 1996.

[42] Martin Hairer. An introduction to stochastic pdes. *arXiv preprint arXiv:0907.4178*, 2009.

[43] A. W. van der Vaart and J. H. van Zanten. Adaptive Bayesian estimation using a Gaussian random field with inverse gamma bandwidth. *Ann. Statist.*, 37(5B):2655–2675, 2009.

[44] Wenbo V. Li and Werner Linde. Approximation, metric entropy and small ball estimates for Gaussian measures. *Ann. Probab.*, 27(3):1556–1578, 1999.

[45] Daria Schymura. An upper bound on the volume of the symmetric difference of a body and a congruent copy. *Adv. Geom.*, 14(2):287–298, 2014.

[46] Winfried Sickel. Pointwise multipliers of Lizorkin-Triebel spaces. In *The Maz'ya anniversary collection, Vol. 2 (Rostock, 1998)*, volume 110 of *Oper. Theory Adv. Appl.*, pages 295–321. Birkhäuser, Basel, 1999.

[47] Daniel Faraco and Keith M. Rogers. The Sobolev norm of characteristic functions with applications to the Calderón inverse problem. *Q. J. Math.*, 64(1):133–147, 2013.

[48] E Makai. Steiner type inequalities in plane geometry. *Periodica Polytechnica Electrical Engineering (Archives)*, 3(4):345–355, 1959.

[49] Alfred Gray. *Tubes*, volume 221 of *Progress in Mathematics*. Birkhäuser Verlag, Basel, second edition, 2004. With a preface by Vicente Miquel.

[50] Olav Kallenberg. *Foundations of modern probability*, volume 99 of *Probability Theory and Stochastic Modelling*. Springer, Cham, [2021] ©2021. Third edition [of 1464694].

[51] Guenther Walther. Granulometric smoothing. *Ann. Statist.*, 25(6):2273–2299, 1997.

[52] Jean-Marc Azaïs and Mario Wschebor. *Level sets and extrema of random processes and fields*. John Wiley & Sons, Inc., Hoboken, NJ, 2009.

[53] Carl Edward Rasmussen and Christopher K. I. Williams. *Gaussian processes for machine learning*. Adaptive Computation and Machine Learning. MIT Press, Cambridge, MA, 2006.

[54] T. Tarvainen, B. T. Cox, J. P. Kaipio, and S. R. Arridge. Reconstructing absorption and scattering distributions in quantitative photoacoustic tomography. *Inverse Problems*, 28(8):084009, 17, 2012.

[55] Peter Kuchment. Mathematics of hybrid imaging: A brief review. In Irene Sabadini and Daniele C Struppa, editors, *The Mathematical Legacy of Leon Ehrenpreis*, pages 183–208, Milano, 2012. Springer Milan.

[56] Lawrence C. Evans. *Partial differential equations*, volume 19 of *Graduate Studies in Mathematics*. American Mathematical Society, Providence, RI, 1998.

[57] David Gilbarg and Neil S. Trudinger. *Elliptic partial differential equations of second order*, volume 224 of *Grundlehren der mathematischen Wissenschaften [Fundamental Principles of Mathematical Sciences]*. Springer-Verlag, Berlin, second edition, 1983.

[58] J.-L. Lions and E. Magenes. *Non-homogeneous boundary value problems and applications. Vol. I*. Die Grundlehren der mathematischen Wissenschaften, Band 181. Springer-Verlag, New York-Heidelberg, 1972. Translated from the French by P. Kenneth.

[59] Leonid A. Kunyansky. A series solution and a fast algorithm for the inversion of the spherical mean Radon transform. *Inverse Problems*, 23(6):S11–S20, 2007.

[60] Mark Agranovsky and Peter Kuchment. Uniqueness of reconstruction and an inversion procedure for thermoacoustic and photoacoustic tomography with variable sound speed. *Inverse Problems*, 23(5):2089–2102, 2007.

[61] Niko Hänninen, Aki Pulkkinen, and Tanja Tarvainen. Image reconstruction with reliability assessment in quantitative photoacoustic tomography. *Journal of Imaging*, 4(12), 2018.

[62] Finn Lindgren, Hå vard Rue, and Johan Lindström. An explicit link between Gaussian fields and Gaussian Markov random fields: the stochastic partial differential equation approach. *J. R. Stat. Soc. Ser. B Stat. Methodol.*, 73(4):423–498, 2011. With discussion and a reply by the authors.

[63] Michael E. Taylor. *Partial differential equations I. Basic theory*, volume 115 of *Applied Mathematical Sciences*. Springer, New York, second edition, 2011.

[64] Jeremy Kepner, Andreas Kipf, Darren Engwirda, Navin Vembar, Michael Jones, Lauren Milechin, Vijay Gadepally, Chris Hill, Tim Kraska, William Arcand, David Bestor, William Bergeron, Chansup Byun, Matthew Hubbell, Michael Houle, Andrew Kirby, Anna Klein, Julie Mullen, Andrew Prout, and Peter Michaleas. Fast mapping onto census blocks. In *2020 IEEE High Performance Extreme Computing Conference (HPEC)*, pages 1–8. IEEE, 2020.

[65] U. Khristenko, L. Scarabosio, P. Swierczynski, E. Ullmann, and B. Wohlmuth. Analysis of boundary effects on PDE-based sampling of Whittle-Matérn random fields. *SIAM/ASA J. Uncertain. Quantif.*, 7(3):948–974, 2019.

[66] Nicolai Riis, Amal Alghamdi, Felipe Uribe, Silja Christensen, Babak Afkham, Per Christian Hansen, and Jakob Jorgensen. Cuqipy – part i: computational uncertainty quantification for inverse problems in python. *arXiv preprint arXiv:2305.16949*, 05 2023.

[67] Tiangang Cui, Kody J. H. Law, and Youssef M. Marzouk. Dimension-independent likelihood-informed MCMC. *J. Comput. Phys.*, 304:109–137, 2016.

[68] Fadil Santosa. A level-set approach for inverse problems involving obstacles. *ESAIM Contrôle Optim. Calc. Var.*, 1:17–33, 1995/96.

[69] Ilker Kocyigit, Ru-Yu Lai, Lingyun Qiu, Yang Yang, and Ting Zhou. Applications of CGO solutions to coupled-physics inverse problems. *Inverse Probl. Imaging*, 11(2):277–304, 2017.

[70] Albert Clop, Daniel Faraco, and Alberto Ruiz. Stability of Calderón's inverse conductivity problem in the plane for discontinuous conductivities. *Inverse Probl. Imaging*, 4(1):49–91, 2010.

[71] G. Alessandrini and M. Di Cristo. Stable determination of an inclusion by boundary measurements. *SIAM J. Math. Anal.*, 37(1):200–217, 2005.

[72] Ronald A. DeVore and Robert C. Sharpley. Besov spaces on domains in $\mathbf{R}^d$. *Trans. Amer. Math. Soc.*, 335(2):843–864, 1993.

[73] Ryszard Engelking. *General topology*, volume 6 of *Sigma Series in Pure Mathematics*. Heldermann Verlag, Berlin, second edition, 1989. Translated from the Polish by the author.

Appendix C

Paper C

The following appendix is the paper titled *The Bayesian approach to inverse Robin problems* authored by Ieva Kazlauskaite, Aksel Kaastrup Rasmussen, and Fanny Seizilles. It is in preparation.

THE BAYESIAN APPROACH TO INVERSE ROBIN PROBLEMS

Ieva Kazlauskaite

Department of Engineering
University of Cambridge
Cambridge, CB3 0FA, United Kingdom

Aksel Kaastrup Rasmussen
Department of Applied Mathematics and Computer Science
Technical University of Denmark
DK-2800 Kgs. Lyngby, Denmark

Fanny Seizilles
Centre for Mathematical Sciences
University of Cambridge
Cambridge, CB3 0WA, United Kingdom

Abstract. In this paper, we investigate the Bayesian approach to inverse Robin problems. These are problems for certain elliptic boundary value problems of determining a Robin coefficient on a hidden part of the boundary from Cauchy data on the observable part. Such a nonlinear inverse problem arises naturally in the initialisation of large-scale ice sheet models that are crucial in climate and sea-level predictions. We motivate the Bayesian approach for a prototypical Robin inverse problem by showing that the posterior mean converges in probability to the data-generating ground truth as the number of observations increase. Related to the stability theory for inverse Robin problems, we establish a logarithmic convergence rate for Sobolev-regular Robin coefficients, whereas for analytic coefficients we can attain an algebraic rate. The use of rescaled analytic Gaussian priors in posterior consistency for nonlinear inverse problems is new and may be of separate interest in other inverse problems.

1. Introduction

The Bayesian approach has in recent years gained traction as a powerful and flexible framework for solving inverse problems by allowing the user to model prior knowledge, regularize reconstructions and quantify uncertainty, see [48]. In this paper, we investigate the Bayesian approach to an emerging class of nonlinear inverse problems known as inverse Robin problems.

Inverse Robin problems appear in boundary value problems for partial differential equations (PDEs), where the boundary is partitioned into at least two parts: a hidden and an observable part. The hidden part carries information of a boundary effect modelled by a Robin boundary condition. Then the Robin inverse problem is the inverse problem of recovering the Robin coefficient from Dirichlet and Neumann data on the observable part of the boundary. Our focus will be on the inverse Robin

2020 *Mathematics Subject Classification.* 35R30, 62G20, 62F15.

Key words and phrases. nonlinear inverse problems, Bayesian inference, Gaussian processes, posterior consistency.

problem for a scalar Laplace equation and a Stokes' system of equations. The former is an inverse problem also known as corrosion detection and was considered in the early contribution [29]. The latter appears when initialising ice sheet models for climate and sea-level predictions. This inverse problem asks for the unknown basal drag coefficient of the ice sediment from observations of ice velocity at the surface, see [5]. Addressing this inverse problem in a statistical framework is a crucial step in improving the robustness and accuracy of ice sheet models for future sea-level projections.

Reconstruction for the inverse Robin problem for the Laplace equation has been studied using classical regularization methods based on penalized least squares, see [14, 37, 30] and the references therein. In [29, 21] accurate direct methods are provided given that the domain is sufficiently thin. The problem has been posed in a Bayesian framework in [39], which determines the Robin coefficient and the hidden boundary simultaneously. The related inverse Robin problem for the Stokes PDE has been considered in the Bayesian framework in [4, 40, 6], whereas in the two latter works the framework is similar to the general approach in [48].

Despite the success of the Bayesian approach to inverse problems, different paths of theoretical guarantees have been explored only recently. Statistical convergence analysis for the posterior distribution in nonlinear inverse problems has seen a recent interest with the framework devised in [38] based on the work in [22], see also [41]. In this approach, the main conditions of the forward map are that of forward regularity: the data should be uniformly bounded and depend continuously on the parameter given that it is sufficiently smooth, and conditional (inverse) stability: the inverse of the forward map is continuous when restricted to a sufficiently small subset of the range. For forward regularity, we require a certain smoothness of solutions of the governing equation near the observable part of the boundary. This can be achieved by classical techniques in PDEs. Inverse stability results, however, rarely come cheap and require in-depth knowledge of the inverse problem at hand. For the Stokes model we consider, some conditional stability results have been developed, see Theorem 1.5 and Remark 3.7 in [10], which quantifies the unique continuation result of [20]. Common for the inverse Robin problems is the fact that the spatially varying Robin coefficient β enters in a Robin condition of the form $\partial_\nu u + \beta u = 0$ at the hidden boundary, where ν is the outgoing unit normal and u is the solution of the governing equation. So if u is known and nonzero here, the reconstruction is a matter of algebra: $\beta = -u^{-1}\partial_\nu u$. However, determining conditions for which u in a Stokes' model is nonzero on the hidden boundary remains a largely unsolved problem, see [10]. For this reason we motivate our approach for general Robin-type inverse problems by the prototypical model for the scalar Laplace equation, see [14]. It is not uncommon that methods used in solving the Robin inverse problem for the Laplace equation have stimulated the development of approaches for solving the corresponding problem for the Stokes model, see [5] which makes use of the Kohn-Vogelius functional [31].

Inverse Robin problems are related to the Cauchy problem of determining a solution to a Laplace equation in a domain from Cauchy data on parts or the whole of the boundary. This is because the 'known' in our inverse Robin problems consists of Cauchy data on a part of the boundary. The global Cauchy problem of determining

the solution in the entire domain is known to be severely ill-posed since [26]. Conditional stability estimates of logarithmic kind exist for this global problem [2, 13, Theorem 1.9], while for stability in the interior, Hölder estimates can be obtained, see Theorem 1.7 and Remark 1.8 of [2]. Combining the latter with analytic continuation for 'uniformly' analytic (in the sense of $\mathcal{R}_2(M)$ defined below) solutions near the hidden boundary, one obtains conditional Hölder stability for the inverse Robin problem. This is essentially the content of [28], which we modify to our setting below in Lemma 2.4. We note that in [47] a Hölder stability estimate is obtained for the scalar Laplace equation, when the Robin coefficient is piecewise constant on *a priori* known sets. Using properties of the derivative of the forward map, a Lipschitz stability for the inverse problem in Stokes' model has been established in [18] given that the Robin coefficient belongs to compact and convex subset of a finite dimensional vector space. Unlike [10] it provides an estimate independent of observations of the pressure.

For inverse problems with regular forward maps and conditional stability estimates, guaranteeing the statistical convergence of the posterior distribution reduce to the choice of prior [38]. In this paper, we consider two classes of numerically tractable and popular choices of Gaussian process priors that fit the stability regimes of the inverse problem. Our theoretical results are two-fold: For a Matérn type Gaussian prior we show that as the number of observations increases, the posterior mean converges in probability to the true Robin coefficient given this has some Sobolev smoothness. Not surprisingly the convergence rate is logarithmic. On the other hand, if the Robin coefficient is analytic, the squared exponential Gaussian prior provides an algebraic rate of convergence. This is the content of Theorem 3.1 below. Our approach for the set of analytic parameters follows the approach in [38, 22, 41] using results in [50]. Unlike [50], which considers analytic Gaussian processes with a change at time scale, we consider 'rescaled' (in the sense of (9)) Gaussian processes. In Lemma C.4 we show that such priors satisfy the usual conditions for posterior consistency. This result is new and may be of independent interest in other inverse problems when modelling analytic functions. This seems to be a useful *a priori* class of functions to consider for some stability estimates, see for example [33].

In Section 2 we give the setting of two inverse Robin problems in the context of a Stokes system of PDEs and a Laplace equation in two dimensions. We state results on the regularity properties of the forward maps as well as conditional stability estimates. When not relying on existing results, these are proved in Appendix A and B. In Section 3 we recap the Bayesian approach to inverse problems, describe the observation model, and present the Matérn-type and squared exponential Gaussian priors. Here we also give the main result, Theorem 3.1, which is proved in Appendix C.

In the following, we let random variables be defined on a probability space $(\Omega, \mathcal{F}, \Pr)$. For a metric space $\mathcal{X}$ the Borel σ-algebra is denoted by $\mathcal{B}(\mathcal{X})$. Given a random element $X : \Omega \to \mathcal{X}$, i.e. $\mathcal{F} - \mathcal{B}(\mathcal{X})$ measurable, we denote its *law* or *distribution* by the probability measure $\mathcal{L}(X)$ defined by $\mathcal{L}(X)(B) = \Pr(X^{-1}(B))$ for all $B \in \mathcal{B}(\mathcal{X})$.

2. Inverse Robin problems

2.1. **Stokes' model.** We consider the constant viscosity Stokes ice sheet model for a velocity field $u : \mathcal{O} \to \mathbb{R}^d$ and pressure $p : \mathcal{O} \to \mathbb{R}$ in a bounded and smooth domain $\mathcal{O} \subset \mathbb{R}^d$, $d = 2, 3$,

$$
\begin{aligned}
-\Delta u + \nabla p &= \rho g && \text{in } \mathcal{O},\\
\nabla \cdot u &= 0 && \text{in } \mathcal{O},\\
\partial_\nu u - p\nu &= h && \text{on } \Gamma_s,\\
\partial_\nu u - p\nu + \beta u &= 0 && \text{on } \Gamma_\beta,
\end{aligned}
\tag{1}
$$

where ν is the outward unit normal, ρ is a constant density of the ice, g is the gravitational field and h is the prescribed boundary stress. Here Γ_s and Γ_β are disjoint and connected open subsets of the boundary such that $\partial\mathcal{O} = \overline{\Gamma}_s \cup \overline{\Gamma}_\beta$. We denote by Γ an open subset of Γ_s, where we make our measurements. The Robin inverse problem is then to recover β given $u|_\Gamma$, that is, to invert the nonlinear forward map

$$G : \beta \mapsto u|_\Gamma.$$

For physical accuracy, we assume β is a positive function, $\beta \geq m_\beta > 0$. We reparametrize the forward map to

$$\mathcal{G}(\theta) := G(m_\beta + e^\theta) = u|_\Gamma$$

defined on our parameter space

$$\Theta := H^1(\Gamma_\beta).$$

The choice of the parameter space Θ makes $\theta \mapsto \mathcal{G}(\theta)$ continuous into $(C(\overline{\Gamma}))^2$, which, as we shall see in Section 3, leaves us with a well-defined posterior distribution. It follows from Lax-Milgram theory in the Hilbert space of divergence-free $(H^1(\mathcal{O}))^d$-functions that there exists a unique solution $u \in (H^1(\mathcal{O}))^d$ to (1) for any positive and bounded β, hence the forward map is well-defined. Further, when β is continuous, unique continuation results [10, Corollary 1.2] imply injectivity of G, see for example [9, Proposition 3.3]. These facts are proven in the following lemma for the case $d = 2$. For $d = 3$ this follows in the same way, but for example for the choice $\Theta = H^2(\Gamma_\beta)$.

Lemma 2.1. *Let $h \in (L^2(\Gamma_s))^2$, $\rho g \in (L^2(\mathcal{O}))^2$ and $\theta, \theta_1, \theta_2 \in L^\infty(\Gamma_\beta)$. We have the following:*

(i) Set $\beta = \beta(\theta) := m_\beta + e^\theta$. Then there is a unique solution $u \in H^1(\mathcal{O})^2$ to (1).

(ii) If $\|\theta_1\|_{H^1(\Gamma_\beta)}, \|\theta_2\|_{H^1(\Gamma_\beta)} \leq M$ and $\Gamma \subset\subset \Gamma_s$, then there exists $\tilde{\alpha} > 0$ such that

$$\|\mathcal{G}(\theta_1) - \mathcal{G}(\theta_2)\|_{(C(\overline{\Gamma}))^2} \leq C(\mathcal{O}, m_\beta, h, \rho, g)\|\theta_1 - \theta_2\|^{\tilde{\alpha}}_{H^1(\Gamma_\beta)}.$$

(iii) $\Theta \ni \theta \mapsto \mathcal{G}(\theta) \in (C(\overline{\Gamma}))^2$ is injective.

2.2. **Scalar Laplace equation.** Consider the following Laplace equation for a potential $u : \mathcal{O} \to \mathbb{R}$, surface normal current $h \in H^{-1/2}(\Gamma)$ and Robin coefficient

$\beta \in L^\infty(\Gamma_\beta)$,

$$\begin{aligned} \Delta u &= 0 && \text{in } \mathcal{O}, \\ \partial_\nu u &= h && \text{on } \Gamma, \\ u &= 0 && \text{on } \Gamma_0, \\ \partial_\nu u + \beta u &= 0 && \text{on } \Gamma_\beta, \end{aligned} \tag{2}$$

where $\partial\mathcal{O} = \overline{\Gamma} \cup \overline{\Gamma}_0 \cup \overline{\Gamma}_\beta$. Here a homogeneous Dirichlet condition is introduced for the stability estimate in [1], which we use in Lemma 2.4 below. As before our goal is to invert the reparametrized forward map

$$\mathcal{G}(\theta) := G(m_\beta + e^\theta) = u|_\Gamma, \tag{3}$$

where we with a slight misuse of notation keep the notation G and $\mathcal{G}$ for this model.

Assumption 1 (Domain)**.** *We assume $\Gamma_\beta = (0,1) \times \{0\}$ and define $\Gamma_{\beta,\epsilon} := (\epsilon, 1-\epsilon) \times \{0\}$ for some $0 < \epsilon < 1$. Furthermore, we assume $\partial\mathcal{O}$ is a simple closed curve decomposed into four subarcs oriented as Γ_β, Γ_0^1, Γ, Γ_0^2, and where $\Gamma_0 = \Gamma_0^1 \cup \Gamma_0^2$.*

We assume $\Gamma_\beta = (0,1) \times \{0\}$ since we want to avoid defining Gaussian processes on manifolds. We will often tacitly identify Γ_β with $(0,1) \subset \mathbb{R}$. For the two stability estimates in Lemma 2.4 we could generalize the setting to a C^2 or analytic Γ_β, respectively. To analyze the stability of the forward map we find it useful to restrict it to two well-chosen bounded and closed subsets of Θ.

Assumption 2. *Assume first $\beta = \beta(\theta) := m_\beta + e^\theta$ for $\theta \in \Theta$ with*

$$\Theta := H^1(\Gamma_\beta).$$

Depending on the setting we accept either of the two following assumptions for some $M > 0$:

(i) Assume $\theta \in \mathcal{R}_1(M)$ with

$$\mathcal{R}_1(M) := \{\theta \in H^1(\Gamma_\beta) : \|\theta\|_{H^1(\Gamma_\beta)} \leq M\}$$

(ii) Assume $\theta \in \mathcal{R}_2(M)$ with

$$\mathcal{R}_2(M) := \{\theta \in C^\infty(\overline{\Gamma}_\beta) : \|\theta\|_{C(\overline{\Gamma}_\beta)} \leq M, \sup_{x \in \overline{\Gamma}_\beta} |(\partial^k \beta)(x)| \leq M(k!)M^k\}$$

It is well-known that β is analytic on $\overline{\Gamma}_\beta$ if and only if $\beta \in C^\infty(\overline{\Gamma}_\beta)$ with

$$\sup_{x \in \overline{\Gamma}_\beta} |(\partial^k \beta)(x)| \leq M_\beta (k!) M_\beta^k$$

for some $M_\beta > 0$, see [32, Chapter 1]. We can think of $\mathcal{R}_2(M)$ as functions that are 'uniformly' analytic with the added condition $\|\theta\|_{C(\overline{\Gamma}_\beta)} \leq M$ to ensure $\theta \mapsto \beta$ is (locally) Lipschitz continuous in both directions. The sets $\mathcal{R}_1(M)$ and $\mathcal{R}_2(M)$ are exactly the 'regularization sets' for which stability results for the inverse problem are available, see Lemma 2.4. To this end, we make the following assumption.

Assumption 3. *We assume that h is not identical to a constant and that $h \in H_1 := \{h \in H^{1/2}(\Gamma) : h \geq 0, \|h\|_{H^{1/2}(\Gamma)} \leq M_h\}$ for some $M_h > 0$.*

The positivity assumption is only needed for the stability estimate stated in Lemma 2.4 (ii), and it might be avoided as in [1]. In the following we prove a number of auxiliary results, where we specify sufficient conditions on θ and β. First, we note that the forward map is well-defined.

Lemma 2.2. *For $\beta = \beta(\theta)$ with $\theta \in L^\infty(\Gamma_\beta)$ and $h \in H^{-1/2}(\Gamma)$, there exists a unique solution $u \in H^1(\mathcal{O})$ of (2) with*

$$\|u\|_{H^1(\mathcal{O})} \leq C\|h\|_{H^{-1/2}(\Gamma)}, \tag{4}$$

for some constant $C = C(\mathcal{O}, m_\beta) > 0$.

Secondly, the forward map is Lipschitz continuous on certain bounded sets of Θ and the observations are uniformly bounded.

Lemma 2.3. *Let $h \in H_1$ and $\theta_1, \theta_2 \in L^\infty(\Gamma_\beta)$. Then,*

(i) if $\beta = \beta(\theta_1)$ and $\|\beta(\theta_1)\|_{H^1(\Gamma_\beta)} \leq M$ we have

$$\|\mathcal{G}(\theta_1)\|_{C(\overline{\Gamma})} \leq U(\mathcal{O}, m_\beta, M, M_h),$$

(ii) if $\beta_i = \beta(\theta_i)$ for $i = 1, 2$ with $\|\theta_1\|_{L^\infty(\Gamma_\beta)}, \|\theta_2\|_{L^\infty(\Gamma_\beta)} \leq M$ then

$$\|\mathcal{G}(\theta_1) - \mathcal{G}(\theta_2)\|_{L^2(\Gamma)} \leq K(\mathcal{O}, m_\beta, M)\|\theta_1 - \theta_2\|_{L^\infty(\Gamma_\beta)}.$$

(iii) if $\theta_1, \theta_2 \in \mathcal{R}_1(M)$ then there exists $\tilde{\alpha} > 0$ such that

$$\|\mathcal{G}(\theta_1) - \mathcal{G}(\theta_2)\|_{C(\overline{\Gamma})} \leq C(\mathcal{O}, m_\beta, M)\|\theta_1 - \theta_2\|^{\tilde{\alpha}}_{L^\infty(\Gamma_\beta)}.$$

The following result is that of conditional (inverse) stability, where the condition is either $\theta \in \mathcal{R}_1(M)$ or $\theta \in \mathcal{R}_2(M)$.

Lemma 2.4 (Conditional stability)**.** *Let $\mathcal{O}$ satisfy Assumption 1 and h satisfy Assumption 3.*

(i) If $\theta_i \in \mathcal{R}_1(M)$, $i = 1, 2$, then there exists constants $K_1 > 0$ and $0 < \sigma_1 < 1$ such that

$$\|\theta_1 - \theta_2\|_{L^\infty(\Gamma_{\beta,\epsilon})} \leq K_1 |\log(\|\mathcal{G}(\theta_1) - \mathcal{G}(\theta_2)\|_{L^2(\Gamma)})|^{-\sigma_1},$$

where K_1 and σ_1 depend only on $\mathcal{O}$, h, m_β, M and ϵ.

(ii) If $\theta_i \in \mathcal{R}_2(M)$, $i = 1, 2$, then there exists constants $K_2 > 0$ and $0 < \sigma_2 < 1$ such that

$$\|\theta_1 - \theta_2\|_{L^2(\Gamma_{\beta,\epsilon})} \leq K_2 \|\mathcal{G}(\theta_1) - \mathcal{G}(\theta_2)\|^{\sigma_2}_{L^2(\Gamma)},$$

where K_2 and σ_2 depend only on $\mathcal{O}$, M_h, M and ϵ.

The stability result *(ii)* generalizes to three dimensions. In this case, one technical obstacle is to analyze the smoothness of the solutions near the corner singularities.

3. The Bayesian approach

Central in the Bayesian framework is the posterior distribution, which is the normalized product of the prior distribution and the likelihood-function modelling the measurement process. In this paper we take the natural viewpoint of [41] that the measurements are discrete, taken at uniformly random locations on the observable part of the boundary, and are contaminated with Gaussian noise. In the context of Stokes' model, we let $V = \mathbb{R}^2$ and $d = 2$, whereas for the Laplace equation we set $V = \mathbb{R}$ and $d = 1$. In both cases we let $|\cdot|_V$ denote the Euclidean norm. Our observations arise as the sequence of random vectors $D_N := (Y_i, X_i)_{i=1}^N$ in $(V \times \Gamma)^N$ of the form

$$Y_i = \mathcal{G}(\theta)(X_i) + \varepsilon_i, \quad \varepsilon_i \overset{\text{i.i.d.}}{\sim} N(0,1), \quad i = 1, \ldots, N, \tag{5}$$

where $X_i \overset{\text{i.i.d.}}{\sim} \lambda$, the uniform distribution on Γ independent of the noise ε_i. More precisely, we endow Γ with a Borel σ-algebra $\mathcal{B}(\Gamma)$ generated by the open sets in Γ

with respect to arc length metric. We have $\mu(B) = |\Gamma|^{-1} \int_B dS$, where dS is the usual length measure and $|\Gamma| = \int_\Gamma dS$.

The random vectors (Y_i, X_i) are i.i.d., and we denote their law P_θ with corresponding probability density (Radon-Nikodym derivative)

$$p_\theta(y,x) \equiv \frac{dP_\theta}{d\mu}(y,x) = \frac{1}{(2\pi)^d} \exp\left(-\frac{1}{2}|y - \mathcal{G}(\theta)(x)|_V^2\right), \quad y \in V, x \in \Gamma,$$

with respect to $d\mu = dy \times d\lambda$, where dy is the Lebesgue measure on V, see [41]. We call $\theta \mapsto p_\theta(y,x)$ the likelihood function, and denote by P_θ^N the joint law of the random variables $(Y_i, X_i)_{i=1}^N$. The likelihood function is suitable to enter in the Bayesian approach: Lemma 2.1 and 2.3 imply that $x \mapsto \mathcal{G}(\theta)(x)$ is continuous and that $\Theta \ni \theta \mapsto \mathcal{G}(\theta) \in C(\overline{\Gamma})^d$, where $d = 2$ for Stokes' model and $d = 1$ for the Laplace equation. This implies $(\theta, x) \mapsto \mathcal{G}(\theta)(x)$ is jointly $\mathcal{B}(\Theta) \otimes \mathcal{B}(\Gamma) - \mathcal{B}(V)$ measurable by Lemma 4.5.1 in [3], which is enough for a well-defined posterior distribution, see [41].

Given a prior distribution Π supported in Θ, Bayes' formula, see [23, p. 7] or [41], updates Π by the likelihood function to obtain the posterior distribution $\Pi(\cdot|D_N)$ of θ given D_N,

$$\Pi(B|D_N) = \frac{\int_B e^{\ell_N(\theta)}\, \Pi(d\theta)}{\int_\Theta e^{\ell_N(\theta)}\, \Pi(d\theta)}, \quad B \in \mathcal{B}(\Theta), \tag{6}$$

where

$$\ell_N(\theta) := -\frac{1}{2} \sum_{i=1}^N |Y_i - \mathcal{G}(\theta)(X_i)|_V^2.$$

Note that $0 \leq |y - \mathcal{G}(\theta)(x)|^2 < \infty$ for all $(y,x) \in V \times \Gamma$ and $\theta \in \Theta$, and hence the normalization constant satisfies

$$0 < \int_\Theta e^{-\frac{1}{2}\sum_{i=1}^N |y_i - \mathcal{G}(\theta)(x_i)|_V^2}\, \Pi(d\theta) \leq 1$$

for all $(y_i, x_i)_{i=1}^N \in (V \times \Gamma)^N$. It follows that $B \mapsto \Pi(B|D_N)$ is a measure for each $D_N \in (V \times \Gamma)^N$ and that $\omega \mapsto \Pi(B|D_N(\omega))$ is measurable for every $B \in \mathcal{B}(\Theta)$. In particular, $\omega \mapsto \Pi(B|Y(\omega))$ is a $[0,1]$-valued random variable. Before we state our main theorem on the convergence features of the posterior distribution, we specify our choice of prior distributions.

3.1. **Choice of prior.** In this section we recall well-known prior distributions that are supported in $\mathcal{R}_j(M)$, $j = 1, 2$, allowing us to make use of the stability estimates in Lemma 2.4. Our focus will be on the Matérn-type and squared exponential Gaussian priors. For simplicity we define the Gaussian priors on the $[-\pi, \pi)$-torus $\mathbb{T}$ and restrict to Γ_β when necessary. Note any torus in which Γ_β is embedded is relevant and can be used. In the case of the Matérn priors, as we shall see, this allows us to recover any sufficiently regular Sobolev function defined on Γ_β. On the other hand, the squared exponential Gaussian processes allows us to recover analytic functions defined on Γ_β whose extension is 2π-periodic. This setting benefits from the fact that properties of Sobolev regularity and analyticity of periodic functions are straightforwardly characterized by a decay of the Fourier coefficients. We can think of this setting as an implicit choice of approximation of the ground truth by the periodic trigonometric functions. One could instead define a prior distribution on $\mathbb{R}$ with exponentially decaying spectral measure, and show that it is supported

in $\mathcal{R}_2(M)$, see [50]. This can be more technical due to the non-compactness of $\mathbb{R}$ and is unnecessary for our case.

Consider the $L^2(\mathbb{T})$ real orthonormal basis of the usual trigonometric functions $\{\phi_k\}_{k\in\mathbb{Z}}$ and for $j = 1, 2$ the random series

$$\tilde{\theta}_j = \sum_{k\in\mathbb{Z}} g_k w_{k,j}\phi_k, \qquad g_k \overset{i.i.d.}{\sim} N(0,1) \tag{7}$$

with

$$w_{k,1} = (1+k^2)^{-\alpha/2}, \quad \alpha > 1/2,$$
$$w_{k,2} = e^{-\frac{r}{2}k^2}, \quad r > 0,$$

where $\alpha > 0$ and $r > 0$ are parameters to be chosen. We consider for example $\phi_k(x) = 1/\sqrt{\pi}\cos(kx)$ for $k > 0$, $\phi_k(x) = 1/\sqrt{\pi}\sin(kx)$ for $k < 0$ and $\phi_0 = 1/\sqrt{2\pi}$. Since $w_{k,j} \in \ell^2(\mathbb{Z})$ for $j = 1, 2$, the series (7) converges for each $x \in \mathbb{T}$ in the mean-square sense. In fact it is a Gaussian random variable, see [23, p. 13], and the limit $u_j(x)$ exists almost surely. The choice of $w_{k,j}$ is here motivated by the span of $\{w_{k,j}\phi_k\}_{k\in\mathbb{Z}}$. Indeed, $\{w_{k,1}\phi_k\}_{k\in\mathbb{Z}}$ is an orthonormal basis of

$$H^\alpha(\mathbb{T}) := \{f \in L^2(\mathbb{T}) : \|f\|^2_{H^\alpha,\mathbb{T}} := \sum_{k\in\mathbb{Z}} |f_k|^2(1+k^2)^\alpha < \infty\}.$$

Here $f_k := \langle f, \phi_k\rangle_{L^2(\mathbb{T})}$ denotes the coefficients in the orthonormal basis. Note we can write $f = \sum f_k\phi_k$ in a standard complex Fourier expansion $\sum \hat{f}_k e^{ikx}$ with the usual Fourier coefficients $\hat{f}_k$ expressed in terms of f_k. Conversely, any real function in the standard complex Fourier expansion can be written as $\sum f_k\phi_k$. Then $H^\alpha(\mathbb{T})$ is the usual periodic Sobolev space of regularity α, see [49]. Similarly, $\{w_{k,2}\phi_k\}_{k\in\mathbb{Z}}$ is an orthonormal basis of

$$\mathcal{A}_r(\mathbb{T}) := \{f \in L^2(\mathbb{T}) : \|f\|^2_{r,\mathbb{T}} := \sum_{k\in\mathbb{Z}} |f_k|^2 e^{rk^2} < \infty\}.$$

A closed ball in any space of functions with exponentially decaying Fourier coefficients is in $\mathcal{R}_2(M)$ for some $M > 0$, see Lemma C.1, and so the choice of the 'square' here is only in honor of the squared exponential prior. Note both spaces are Hilbert spaces as closed subspaces of $L^2(\mathbb{T})$ with their respective obvious inner products. Note also that $\mathcal{A}_r(\mathbb{T})$ embeds continuously into $H^\alpha(\mathbb{T})$ for any $r, \alpha > 0$, which in return embeds continuously into $C(\mathbb{T})$ for $\alpha > 1/2$ by a Sobolev embedding, see [49].

3.1.1. *RKHS and support.* The random series (7) converges almost surely in $H^t(\mathbb{T})$ with $t < \alpha - \frac{1}{2}$ and $\mathcal{A}_q$ with $q < r$ for $j = 1$ and $j = 2$, respectively. Indeed, by Fubini's theorem

$$E[\|\tilde{\theta}_1\|^2_{H^t,\mathbb{T}}] = E[\sum_{k\in\mathbb{Z}} g_k^2 w_{k,1}^2(1+k^2)^t] = \sum_{k\in\mathbb{Z}}(1+k^2)^{t-\alpha} < \infty,$$

and similarly for $\tilde{\theta}_2$. Then also $\tilde{\theta}_2 \in H^t(\Gamma_\beta)$ almost surely. Likewise we define

$$\mathcal{A}_r(\Gamma_\beta) := \{f = g|_{\Gamma_\beta} : g \in \mathcal{A}_r(\mathbb{T})\},$$

endowed with the quotient norm

$$\|f\|_r = \inf_{g\in\mathcal{A}_r(\mathbb{T}):g=f \text{ in } \Gamma_\beta} \|g\|_{r,\mathbb{T}} = \|f\|_{r,\mathbb{T}}, \tag{8}$$

where the last equality holds because f has a unique analytic continuation to $\mathbb{T}$. Then $\tilde{\theta}_2 \in \mathcal{A}_q(\Gamma_\beta)$, $q < r$ almost surely.

The series (7) is the Karhunen-Loeve expansion of a Gaussian random element of $H^t(\mathbb{T})$ and $\mathcal{A}_q(\mathbb{T})$ for $j = 1$ and $j = 2$, respectively, see [15]. We set $\alpha > 3/2$ and $r > 0$ such that the laws of $\tilde{\theta}_1$ and $\tilde{\theta}_2$ define Gaussian probability measures in Θ. By a Sobolev embedding $\tilde{\theta}_1$ and $\tilde{\theta}_2$ are almost surely in $C(\overline{\Gamma}_\beta)$, the separable Banach space of continuous functions on $\overline{\Gamma}_\beta$ endowed with the usual supremum norm, which we denote by $\|\cdot\|_\infty$. Then the laws of $\tilde{\theta}_j$, $j = 1, 2$, define Gaussian probability measures on $C(\overline{\Gamma}_\beta)$, see [27, Exercise 3.39]. We denote

$$\tilde{\Pi}_j := \mathcal{L}(\tilde{\theta}_j), \quad j = 1, 2.$$

The reproducing kernel Hilbert space (RKHS) of the Gaussian random element $\tilde{\theta}_j$ is $H^\alpha(\mathbb{T})$ for $j = 1$ and $\mathcal{A}_r(\mathbb{T})$ for $j = 2$, see Theorem I.23 [23]. Since the restriction $H^\alpha(\mathbb{T}) \to H^\alpha(\Gamma_\beta)$ is onto, see [49, Section 4.4], the RKHS of the restricted Gaussian random element is $\mathcal{H}_1 := H^\alpha(\Gamma_\beta)$ in the case $j = 1$ and $\mathcal{H}_2 := \mathcal{A}_r(\Gamma_\beta)$, see [24, Exercise 2.6.5]. See also an argument in the process setting [41, Theorem 6.2.3].

3.1.2. *Covariance function.* Since $\tilde{\theta}_j(x)$ is a Gaussian random variable for each $x \in \mathbb{T}$ and $j = 1, 2$, it is in fact a Gaussian process. The covariance function $K_j : \mathbb{T} \times \mathbb{T} \to \mathbb{R}$ of the process takes the form, for $j = 1, 2$,

$$K_j(x, x') = E[\tilde{\theta}_j(x)\tilde{\theta}_j(x')] = \sum_{k\in\mathbb{Z}} w_{k,j}^2 \phi_k(x)\phi_k(x'),$$

see for example [23, p. 586]. Choosing for example $\phi_k(x) = 1/\sqrt{\pi}\cos(kx)$ for $k > 0$, $\phi_k(x) = 1/\sqrt{\pi}\sin(kx)$ for $k < 0$ and $\phi_0 = 1/\sqrt{2\pi}$, and using the identity $\cos(a)\cos(b) + \sin(a)\sin(b) = \cos(a - b)$ we find

$$\begin{aligned} K_j(x, x') &= \frac{w_{0,j}^2}{2\pi} + \frac{1}{\sqrt{\pi}} \sum_{k=1}^{\infty} w_{k,j}^2 \phi_k(x - x'), \\ &= \frac{1}{2\pi} \sum_{k\in\mathbb{Z}} w_{k,j}^2 e^{ik(x-x')}, \\ &= \sum_{k\in\mathbb{Z}} m_j(x - x' + 2\pi k), \end{aligned}$$

using the Poisson summation formula with

$$\begin{aligned} m_1(s) &= \mathcal{F}^{-1}[(1 + 4\pi^2\xi^2)^{-\alpha}](s) = Cs^{\alpha-1/2}\mathcal{K}_{\alpha-\frac{1}{2}}(s), \\ m_2(s) &= \mathcal{F}^{-1}[e^{-4\pi^2 r\xi^2}](s) = Ce^{-\frac{s^2}{4r^2}}, \end{aligned}$$

where $\mathcal{K}_\nu$, $\nu > 0$ is a modified Bessel function, see [44, Section 4.2.1]. Thus K_j is the 2π-periodization of the usual Matérn covariance function on $\mathbb{R}$ when $j = 1$ and the squared exponential covariance function on $\mathbb{R}$ when $j = 2$, which justifies our naming convention.

3.1.3. *Rescaling.* Take $\alpha > 1$ and $r > 0$ such that $\tilde{\Pi}_j(\Theta) = 1$ for $j = 1, 2$. We then let Π_j be the 'rescaled' Gaussian distribution for $j = 1, 2$,

$$\Pi_j := \mathcal{L}\left(\kappa_{N,j}\tilde{\theta}_j\right), \qquad \tilde{\theta}_j \sim \tilde{\Pi}_j, \tag{9}$$

for some decreasing sequence in N, $\kappa_{N,j}$ defined as

$$\kappa_{N,1} := N^{-1/(4\alpha+2)},$$
$$\kappa_{N,2} := \log(N)^{-1}.$$

Letting the covariance of the prior depend on the observation regime is natural: it updates the weight of the prior term in the posterior (6) formally as

$$\Pi_1(d\theta) \propto \exp\left(-\frac{N^{1/(2\alpha+1)}}{2}\|\theta\|^2_{\mathcal{H}_1}\right) d\theta$$

in the case of $j = 1$. In this way we penalize large values of $\|\theta\|_{\mathcal{H}_1}$ more. This is common in the consistency literature, see [38], and in fact sufficient for convergence of regularized least-square procedures, see [19, Section 5]. In our setting this rescaling is needed so that the prior distributions concentrate sufficiently on the totally bounded regularization sets $\mathcal{R}_1(M)$ and $\mathcal{R}_2(M)$.

3.2. **Convergence of the posterior mean.** Before we state the main result, the convergence of the posterior mean to the ground truth as $N \to \infty$, we recall some preparatory definitions. In the following we let $\Pi_j(\cdot|D_N)$ denote the posterior distribution (6) in Θ arising from the prior distribution Π_j defined in (9) for $j = 1, 2$. The posterior mean $E_j[\theta|D_N]$ is defined in the sense of a Bochner integral, see for example [16, p. 44]. Indeed, for all $D_N \in (V \times \Gamma)^N$

$$\int_\Theta \|\theta\|_\Theta \, \Pi_j(d\theta|D_N) \propto \int_\Theta \|\theta\|_\Theta e^{\ell_N(\theta)} \, \Pi_j(d\theta) \leq \int_\Theta \|\theta\|_\Theta \, \Pi_j(d\theta) < \infty,$$

by Fernique's theorem [27, Theorem 3.11], since Π_j is supported in Θ for $j = 1, 2$. Then $D_N \mapsto E_j[\theta|D_N]$ is a Θ-valued random element by the definition of the Bochner integral and since the pointwise limit of a sequence of measurable functions is measurable, see [17, Theorem 4.2.2]. Let $\epsilon_N > 0$ be some decreasing sequence in N converging to zero. We say that a sequence of real-valued random variables $\{f_N(D_N)\}_{N=1}^\infty$ converges to zero in $P^N_{\theta_0}$-probability with rate ϵ_N as $N \to \infty$ if there exists a constant $C > 0$ such that

$$\lim_{N\to\infty} P^N_{\theta_0}(D_N : |f_N(D_N)| > C\epsilon_N) = 0$$

Then we have the following convergence results for the reconstruction error of the posterior mean, where we take $f_N(D_N) = \|E_j[\theta|D_N] - \theta_0\|$ for $j = 1, 2$, and a suitable norm.

Theorem 3.1. *Consider the posterior distribution $\Pi_j(\,\cdot\,|D_N)$ arising from observations (5) in the model (3) and prior distributions Π_j, $j = 1, 2$.*

(i) If $\theta_0 \in H^\alpha(\Gamma_\beta)$, $\alpha > 3/2$, then

$$\|E_1[\theta|D_N] - \theta_0\|_{L^\infty(\Gamma_{\beta,\epsilon})} \to 0 \qquad \text{in } P^N_{\theta_0}\text{-probability}$$

with rate $|\log(C\delta_N)|^{-\sigma}$ as $N \to \infty$ for some $0 < \sigma < 1$ and constant $C > 0$ and where $\delta_N = N^{-\alpha/(2\alpha+1)}$.

(ii) If $\theta_0 \in \mathcal{A}_r(\Gamma_\beta)$, $r > 0$, then

$$\|E_2[\theta|D_N] - \theta_0\|_{L^2(\Gamma_{\beta,\epsilon})} \to 0 \qquad \text{in } P^N_{\theta_0}\text{-probability}$$

with rate δ_N^σ for some $0 < \sigma < 1$ as $N \to \infty$, and where $\delta_N = N^{-1/2}\log(N)$.

Proof. (i) This is the result of Theorem 2.3.2 [41] and [41, Exercise 2.4.4] whose conditions are satisfied by Lemma 2.3, 2.4 (i) and by the choice of prior (9) for $\alpha > 3/2$.
(ii) This fact is proven in Appendix C, since we deviate slightly from the setting of Theorem 1.3.2 in [41]. □

Remark 1. *By the local Lipschitz continuity of $z \mapsto e^z$, the case of (i) generalizes to convergence at the level of β, i.e. $\beta(E_1[\theta|D_N])$ converges to $\beta(\theta_0)$ in probability with rate $|\log(C\delta_N)|^{-\sigma}$ as $N \to \infty$. This is not as easy in the case of L^2-convergence in (ii). One straightforward remedy is to upgrade the L^2-convergence to L^∞-convergence using Sobolev interpolation. A different strategy is to replace $\theta \mapsto \beta(\theta) = m_\beta + e^\theta$ with a smoothened 'regular link function' in the sense of* [42].

This theorem justifies and quantifies the use of the Bayesian methodology for the two inverse problems. Note the theorem does not generalize immediately to the problem for Stokes' model with for example an L^2-norm on a set $K \subset\subset \Gamma_\beta$ in which $u \neq 0$ as in [10, Remark 3.7]. Indeed, the estimate includes the pressure p and its normal derivative $\partial_\nu p|_\Gamma$ at Γ. Improving this estimate to be independent of observations of the pressure remains largely open to the authors knowledge.

4. Concluding remarks

In this paper we have considered a Bayesian approach to two inverse Robin problems with theoretical convergence guarantees as the number of observations increases. We have motivated to popular and numerically tractable Gaussian priors and show under appropriate rescaling that each lead to a convergent posterior mean. If the ground true Robin coefficient is *a priori* known to be analytic, then the logarithmic convergence rate can be upgraded to a rate on the form $N^{-\tau}$ for some $\tau > 0$. Interesting future work includes generalizing Theorem 3.1 to the inverse problem for Stokes' model. In its current form, Theorem 3.1 allows recovering analytic functions in the space $\mathcal{A}_r(\Gamma_\beta)$. Another interesting future direction is to generalize this to a larger class of analytic functions on Γ_β using Gaussian processes and a continuous version of Lemma C.1. For ideas in this direction we refer to [50].

A. Forward regularity

Proof of Lemma 2.1. (i) Consider the general Stokes' equation for $f \in (L^2(\mathcal{O}))^2$, $h \in (H^{-1/2}(\Gamma))^2$ and $\tilde{h} \in (H^{-1/2}(\Gamma_\beta))^2$,

$$\begin{aligned} -\Delta u + \nabla p &= f && \text{in } \mathcal{O}, \\ \nabla \cdot u &= 0 && \text{in } \mathcal{O}, \\ \partial_\nu u - p\nu &= h && \text{on } \Gamma_s, \\ \partial_\nu u - p\nu + \beta u &= \tilde{h} && \text{on } \Gamma_\beta. \end{aligned} \tag{10}$$

The corresponding variational form is

$$\int_{\mathcal{O}} \nabla u : \nabla v + \int_{\Gamma_\beta} \beta u \cdot v = \int_{\mathcal{O}} f \cdot v + \langle h, v \rangle_{-\frac{1}{2},\frac{1}{2},\Gamma_s} + \langle \tilde{h}, v \rangle_{-\frac{1}{2},\frac{1}{2},\Gamma_\beta}, \tag{11}$$

where $\nabla u : \nabla v$ denotes the double dot product of the two matrices, $\langle \cdot, \cdot \rangle_{-\frac{1}{2},\frac{1}{2},\Gamma_s}$ denotes the $(H^{-1/2}(\Gamma_s))^2, (H^{-1/2}(\Gamma_s))^2$ dual pairing, and where $v \in V_s := \{v \in$

$(H^1(\mathcal{O}))^2 : \nabla \cdot v = 0\}$. By the generalized Poincaré inequality, see for example [12, Proposition 5.3.4],

$$\int_{\mathcal{O}} |\nabla u_i|^2 + \int_{\Gamma_\beta} u_i^2 \geq C(\mathcal{O})\|u_i\|^2_{L^2(\mathcal{O})},$$

for each $i = 1, 2$, where u_i is the $i'th$ component of the vector field u. It follows that

$$\int_{\mathcal{O}} \nabla u : \nabla u + \int_{\Gamma_\beta} \beta u \cdot u \geq C(m_\beta, \mathcal{O}) \sum_{k=1}^{2} \|u_i\|^2_{H^1(\mathcal{O})},$$

and hence the bilinear form is coercive. It is straightforward to check that it is also bounded, and likewise that the right-hand side is a bounded linear functional on V_s. By standard Lax-Milgram theory, there is a unique weak solution $u \in V_s$ to (10) satisfying

$$\|u\|_{(H^1(\mathcal{O}))^2} \leq C(\mathcal{O}, m_\beta)(\|f\|_{(L^2(\mathcal{O}))^2} + \|h\|_{(H^{-1/2}(\Gamma_s))^2} + \|\tilde{h}\|_{(H^{-1/2}(\Gamma_\beta))^2}). \tag{12}$$

Note (10) is in the form that Theorem IV.7.1 in [11] considers with the compatibility condition being satisfied by (11) for $v = 1$. The theorem then states that there is also a unique solution $p \in L^2(\mathcal{O})$ to (10). In the following we take some care in bounding this function. Initially de Rhams' theorem [11, Theorem IV2.4] gives a pressure term $\tilde{p} \in L^2_0(\mathcal{O}) = L^2(\mathcal{O})/\mathbb{R}$ unique up to a constant and satisfying $-\Delta u + \nabla \tilde{p} = f$. Take then the mean-zero solution satisfying

$$\begin{aligned} \|\tilde{p}\|_{L^2(\mathcal{O})} &\leq C(\mathcal{O})\|\nabla \tilde{p}\|_{H^{-1}(\mathcal{O})}, \\ &= C(\mathcal{O})\|\Delta u\|_{H^{-1}(\mathcal{O})} + \|f\|_{H^{-1}(\mathcal{O})}, \\ &\leq C(\mathcal{O}, m_\beta)(\|f\|_{(L^2(\mathcal{O}))^2} + \|h\|_{(H^{-1/2}(\Gamma_s))^2} + \|\tilde{h}\|_{(H^{-1/2}(\Gamma_\beta))^2}) \end{aligned} \tag{13}$$

using [11, Lemma IV.1.9] and (12). The proof of Theorem IV.7.1 in [11] shows that $p = \tilde{p} + C_0$ is the unique solution to (10) matching the boundary conditions. If $h \in (L^2(\Gamma_s))^2$ and $\tilde{h} \in (L^2(\Gamma_\beta))^2$, this constant can be bounded as

$$\begin{aligned} |C_0| \leq C(\mathcal{O})(&\|h\|_{(L^2(\Gamma_s))^2} + \|\tilde{h}\|_{(L^2(\Gamma_\beta))^2} + \|\beta\|_{L^\infty(\Gamma_\beta)}\|u\|_{L^2(\mathcal{O})} \\ &+ \|\partial_\nu u\|_{H^{-1/2}(\partial\mathcal{O})} + \|\tilde{p}\|_{L^2(\mathcal{O})}), \end{aligned}$$

hence if $\|\beta\|_{L^\infty(\Gamma_\beta)} \leq M$, then

$$\|p\|_{L^2(\mathcal{O})} \leq C(\mathcal{O}, m_\beta, M)(\|f\|_{(L^2(\mathcal{O}))^2} + \|h\|_{(L^2(\Gamma_s))^2} + \|\tilde{h}\|_{(L^2(\Gamma_\beta))^2}) \tag{14}$$

using both (12) and (13).

(ii) The difference (v, q) for $v = u_1 - u_2$ and $q = p_1 - p_2$ of solutions $(u_1, p_1), (u_2, p_2)$ of (1) corresponding to $\beta_1 = \beta(\theta_1), \beta_2 = \beta(\theta_2)$ is the unique solution of

$$\begin{aligned} -\Delta v + \nabla q &= 0 && \text{in } \mathcal{O}, \\ \nabla \cdot v &= 0 && \text{in } \mathcal{O}, \\ \partial_\nu v - q\nu &= 0 && \text{on } \Gamma_s, \\ \partial_\nu v - q\nu + \beta_1 v &= u_2(\beta_2 - \beta_1) && \text{on } \Gamma_\beta. \end{aligned}$$

Note that [9, Lemma 2.3] implies

$$\|u_2(\beta_2 - \beta_1)\|_{(L^2(\Gamma_\beta))^2} \leq \|u_2\|_{(L^2(\Gamma_\beta))^2}\|\beta_2 - \beta_1\|_{H^1(\Gamma_\beta)},$$

and hence by (i) above,

$$\begin{aligned}\|v\|_{(H^1(\mathcal{O}))^2} &\leq C(\mathcal{O}, m_\beta)\|u_2(\beta_2-\beta_1)\|_{(H^{-1/2}(\Gamma_\beta))^2},\\ &\leq C(\mathcal{O}, m_\beta, h, \rho, g)\|\beta_1-\beta_2\|_{H^1(\Gamma_\beta)}. \end{aligned} \tag{15}$$

To upgrade this we prove additional smoothness of v near Γ as follows. Define an open set $V \subset \mathcal{O}$ that meets Γ, i.e. $\Gamma \subset \overline{V}$. Define then the larger set $U \subset \mathcal{O}$ with $V \subset U$ and $\overline{U} \cap \partial\mathcal{O} \subset \Gamma_s$. We then define the smooth cutoff function $\eta \in C^\infty(U)$ with $\eta \equiv 1$ in V and $\operatorname{supp}\eta \subset \overline{U}$ (hence η is zero near Γ_β). Then $(\eta v, \eta q)$ solves the system

$$\begin{aligned} -\Delta(\eta v) + \nabla(\eta q) &= \tilde{f} && \text{in } U,\\ \nabla\cdot(\eta v) &= \nabla\eta\cdot v && \text{in } U,\\ \partial_\nu(\eta v) - (\eta q)\nu &= \eta(\partial_\nu v - q\nu) + v\partial_\nu\eta && \text{on } \partial U, \end{aligned}$$

for $\tilde{f} = v\Delta\eta + 2\nabla v\cdot\nabla\eta + q\nabla\eta \in L^2(\mathcal{O})$. Note $\eta(\partial_\nu v - q\nu) + v\partial_\nu\eta = v\partial_\nu\eta \in (H^{1/2}(\partial U))^2$. Then Theorem IV.7.1 of [11] states that

$$\|\eta v\|_{(H^2(U))^2} \leq C(U)(\|\tilde{f}\|_{(L^2(U))^2} + \|\nabla\eta\cdot v\|_{H^1(U)} + \|v\partial_\nu\eta\|_{(H^{1/2}(\partial U))^2}).$$

Since $\eta \equiv 1$ in V, using (15) and (14) gives us

$$\|v\|_{(H^2(V))^2} \leq C(\mathcal{O}, m_\beta, M, h, \rho, g)$$

By Sobolev interpolation, there exists $\bar{\alpha}, \tilde{\alpha} > 0$ such that (denoting v_i the $i'th$ component of v)

$$\begin{aligned}\sum_{i=1}^2 \|v_i\|_{(H^{7/4}(V))^2} &\leq \sum_{i=1}^2 \|v_i\|^{\bar{\alpha}}_{(H^1(V))^2}\|v_i\|^{\tilde{\alpha}}_{(H^2(V))^2},\\ &\leq C(\mathcal{O}, m_\beta, M, h, \rho, g)\sum_{i=1}^2 \|v_i\|^{\tilde{\alpha}}_{(H^1(V))^2},\\ &\leq C(\mathcal{O}, m_\beta, M, h, \rho, g)\|\beta_1-\beta_2\|^{\tilde{\alpha}}_{H^1(\Gamma_\beta)}. \end{aligned} \tag{16}$$

Now we argue that $\theta \mapsto e^\theta$ is locally Lipschitz continuous in $H^1(\Gamma_\beta)$, i.e.

$$\|\beta_1-\beta_2\|_{H^1(\Gamma_\beta)} \leq C(\Gamma_\beta, M)\|\theta_1-\theta_2\|_{H^1(\Gamma_\beta)}. \tag{17}$$

Note first by the mean value theorem that

$$\|e^{\theta_1}-e^{\theta_2}\|_{L^\infty(\Gamma_\beta)} \leq e^M\|\theta_1-\theta_2\|_{L^\infty(\Gamma_\beta)}.$$

If $\Gamma_\beta \subset \mathbb{R}$ it is clear that

$$\begin{aligned}\|\beta_1-\beta_2\|_{H^1(\Gamma_\beta)} &\lesssim \|e^{\theta_1}-e^{\theta_2}\|_{L^2(\Gamma_\beta)} + \|\nabla(e^{\theta_1})-\nabla(e^{\theta_2})\|_{L^2(\Gamma_\beta)},\\ &\leq \|e^{\theta_1}-e^{\theta_2}\|_{L^2(\Gamma_\beta)} + \|e^{\theta_1}\nabla\theta_1 - e^{\theta_2}\nabla\theta_2\|_{L^2(\Gamma_\beta)},\\ &\leq \|e^{\theta_1}-e^{\theta_2}\|_{L^2(\Gamma_\beta)} + \|\nabla\theta_1\|_{L^2(\Gamma_\beta)}\|e^{\theta_1}-e^{\theta_2}\|_{L^\infty(\Gamma_\beta)}\\ &\quad + \|e^{\theta_2}\|_{L^\infty(\Gamma_\beta)}\|\nabla\theta_1-\nabla\theta_2\|_{L^2(\Gamma_\beta)},\\ &\leq C(M)\|\theta_1-\theta_2\|_{H^1(\Gamma_\beta)}, \end{aligned}$$

using also the continuous Sobolev embedding $H^1(\Gamma_\beta) \subset C(\overline{\Gamma}_\beta)$. By the definition of Sobolev spaces on boundaries, see [25, (1,3,3,2)], the case where Γ_β is a smooth curve follows in the same way. Indeed, this amounts to showing

$$\|\beta_1\circ\phi - \beta_2\circ\phi\|_{H^1(I)} \leq C\|\theta_1\circ\phi - \theta_2\circ\phi\|_{H^1(I)}$$

for any smooth parametrization $\phi : I \to \mathbb{R}^2$ of a section of Γ_β with I an open subset of $\mathbb{R}$. In this case we just repeat the argument above. Finally, combining (16) with (17) and a Sobolev embedding it follows that

$$\|u_1 - u_2\|_{(C(\overline{\Gamma}))^2} \lesssim \sum_{i=1}^{2} \|v_i\|_{C(\overline{\Gamma})} \leq C(\mathcal{O}, m_\beta, h, \rho, g, M)\|\theta_1 - \theta_2\|_{H^1(\Gamma_\beta)}^{\tilde{\alpha}}.$$

(*iii*) This is proved in Proposition 3.3 of [9] for a stationary Neumann condition $g(x,t) = h(x)$ in $(H^{1/2}(\Gamma_s))^2$.

□

Proof of Lemma 2.2. Consider more generally the equation (2) for an inhomogeneous Robin condition $\partial_\nu u + \beta u = \tilde{h} \in H^{1/2}(\Gamma_\beta)$. The corresponding variational form is

$$\int_{\mathcal{O}} \nabla u \cdot \nabla v + \int_{\Gamma_\beta} \beta uv = \int_{\Gamma} hv + \int_{\Gamma_\beta} \tilde{h}v, \tag{18}$$

for $v \in V := \{u \in H^1(\mathcal{O}) : u|_{\Gamma_0} = 0\}$. By the generalized Poincaré inequality, see for example [12, Proposition 5.3.4],

$$\int_{\mathcal{O}} |\nabla u|^2 + \int_{\Gamma_\beta} u^2 \geq C(\mathcal{O})\|u\|_{L^2(\mathcal{O})}^2,$$

hence the left-hand side of (18) is a coercive bilinear form on V. Since h and $\tilde{h}$ are $H^{1/2}$-functions, the right-hand side is a bounded linear functional on V. By standard Lax-Milgram theory, there is a unique weak solution $u \in V$ to (18) satisfying

$$\|u\|_{H^1(\mathcal{O})} \leq C(\mathcal{O}, m_\beta)(\|h\|_{H^{-1/2}(\Gamma)} + \|\tilde{h}\|_{H^{-1/2}(\Gamma_\beta)}). \tag{19}$$

In particular, (4) is satisfied. □

Lemma A.1. *For $\beta \in H^1(\Gamma_\beta)$ with $\|\beta\|_{H^1(\Gamma_\beta)} \leq M$, h as in Assumption 3, and any $0 < s < \frac{1}{2}$ there exists a constant $C = C(\mathcal{O}, m_\beta, M, M_h, s)$ such that*

$$\|u\|_{H^{1+s}(\mathcal{O})} \leq C,$$

where u solves (2).

Proof. Far away from the 'corners' (where different boundary conditions meet) the estimate is straightforward using standard techniques. Near the corners the estimate is essentially due to [25], although we are aided by [7] in particular. Since $\beta u \in H^{1/2}(\Gamma_\beta)$ by Lemma 2.3 in [9] ($u \in H^{1/2}(\Gamma_\beta)$ by Lemma 2.2 and $\beta \in H^1(\Gamma_\beta)$ by assumption), the trace theorem in [7, Theorem 2.1] provides a function $v \in H^2(\mathcal{O})$ such that $\partial_\nu v = h$ on Γ, $v = 0$ on Γ_0 and $\partial_\nu v = -\beta u$ on Γ_β, i.e. $w = u - v$ solves

$$\begin{aligned} \Delta w &= -\Delta v && \text{in } \mathcal{O}, \\ \partial_\nu w &= 0 && \text{on } \Gamma, \\ w &= 0 && \text{on } \Gamma_0, \\ \partial_\nu w &= 0 && \text{on } \Gamma_\beta. \end{aligned} \tag{20}$$

Indeed this trace operator $T : H^2(\mathcal{O}) \to H^{1/2}(\Gamma) \times H^{3/2}(\Gamma_0) \times H^{1/2}(\Gamma_\beta)$, defined by $u \mapsto (\partial_\nu u|_\Gamma, u|_{\Gamma_0}, \partial_\nu u|_{\Gamma_\beta})$, is bounded [35] and surjective [7, Theorem 2.1], so

there exists a continuous right-inverse, see the general remark after Theorem 8.3 in [35]. Then by [9, Lemma 2.3]

$$\begin{aligned}\|v\|_{H^2(\mathcal{O})} &\leq C(\|h\|_{H^{1/2}(\Gamma)} + \|\beta u\|_{H^{1/2}(\Gamma_\beta)}),\\ &\leq C(\|h\|_{H^{1/2}(\Gamma)} + \|\beta\|_{H^1(\Gamma_\beta)}\|u\|_{H^{1/2}(\Gamma_\beta)}),\end{aligned} \tag{21}$$

The regularity decomposition of [7, Theorem 3.1.1] decomposes the unique solution $w \in H^1(\mathcal{O})$ for some $J \in \mathbb{N}$ as

$$w = w_r + \sum_{j=1}^{J} c_j S_j,$$

where $w_r \in D^2 := \{w \in H^2(\mathcal{O}) : \partial_\nu w = 0 \text{ on } \Gamma \cup \Gamma_\beta, w = 0 \text{ on } \Gamma_0\}$, $c_j = c_j(f)$ are functionals of $f = -\Delta v$ in $L^2(\mathcal{O})$, see [7, Remark 3.1.2] and S_j are certain 'singular' functions supported near the corners. They depend only on the geometry of $\mathcal{O}$, see (3.2.26) and Proposition 3.2.3 in [7], and satisfy $\Delta S_j \in L^2(\mathcal{O})$ and $S_j \in H^{1+s}(\mathcal{O})$ if and only if $s < 1/2$. Since $\Delta : D^2 \to L^2(\mathcal{O})$ is injective by uniqueness of solutions to (20), it is bijective onto its image. The open mapping theorem then states that there exists a constant $C > 0$ such that $\|w_r\|_{H^2(\mathcal{O})} \leq C\|\Delta w_r\|_{L^2(\mathcal{O})}$, and hence

$$\begin{aligned}\|w_r\|_{H^2(\mathcal{O})} &\leq C\|\Delta w_r\|_{L^2(\mathcal{O})},\\ &\leq C(\|\Delta v\|_{L^2(\mathcal{O})} + \sum_{j=1}^{J} |c_j|\|\Delta S_j\|_{L^2(\mathcal{O})}),\\ &\leq C(\mathcal{O})\|v\|_{H^2(\mathcal{O})}.\end{aligned} \tag{22}$$

Combining (22) with (21) and using the standard estimate of $\|u\|_{H^1(\mathcal{O})}$ we have

$$\begin{aligned}\|u\|_{H^{1+s}(\mathcal{O})} &\leq C(\mathcal{O})\|v\|_{H^2(\mathcal{O})} + \|\sum_{j=1}^{J} c_j S_j\|_{H^{1+s}(\mathcal{O})},\\ &\leq C(\mathcal{O}, s)\|v\|_{H^2(\mathcal{O})} \leq C.\end{aligned}$$

with $C = C(\mathcal{O}, M_h, M, m_\beta)$. □

Proof of Lemma 2.3. (i) is an immediate consequence of a Sobolev embedding and Lemma A.1.
(ii) The difference $v = u_1 - u_2$ of solutions u_1, u_2 corresponding to $\beta_1 = \beta(\theta_1), \beta_2 = \beta(\theta_2)$ is the unique solution to the equation

$$\begin{aligned}\Delta v &= 0 && \text{in } \mathcal{O},\\ \partial_\nu v &= 0 && \text{on } \Gamma,\\ v &= 0 && \text{on } \Gamma_0,\\ \partial_\nu v + \beta_1 v &= u_2(\beta_2 - \beta_1) && \text{on } \Gamma_\beta.\end{aligned}$$

Since $u_2(\beta_2 - \beta_1) \in H^{-1/2}(\Gamma_\beta)$, we use the estimate (19) with $h = 0$ and $\tilde{h} = u_2(\beta_2 - \beta_1)$ to the effect that

$$\begin{aligned}\|v\|_{H^1(\mathcal{O})} &\leq C(\mathcal{O}, m_\beta)\|u_2(\beta_2 - \beta_1)\|_{H^{-1/2}(\Gamma_\beta)},\\ &\leq C(\mathcal{O}, m_\beta)\|\beta_1 - \beta_2\|_{L^\infty(\Gamma_\beta)},\\ &\leq C(\mathcal{O}, m_\beta, M)\|\theta_1 - \theta_2\|_{L^\infty(\Gamma_\beta)},\end{aligned} \tag{23}$$

using a simple mean value theorem argument. Boundedness of the trace operator implies (ii).
(iii) By Sobolev interpolation, there exists $\bar{\alpha}, \tilde{\alpha} > 0$ such that

$$\begin{aligned}\|v\|_{H^{1+1/8}(\mathcal{O})} &\leq \|u_1 - u_2\|^{\tilde{\alpha}}_{H^1(\mathcal{O})}\|u_1 - u_2\|^{\bar{\alpha}}_{H^{1+1/4}(\mathcal{O})},\\ &\leq C(\mathcal{O}, m_\beta, M, M_h)\|\theta_1 - \theta_2\|^{\tilde{\alpha}}_{L^\infty(\Gamma_\beta)},\end{aligned}$$

where we used (23) and Lemma A.1. Then boundedness of the trace operator and a Sobolev embedding give the wanted result. □

B. Conditional stability estimates

Proof of Lemma 2.4. Notice first that the mean value theorem for a function $\tilde{\theta}(x) \in [\theta_1(x), \theta_2(x)]$ implies

$$\beta_1 - \beta_2 = e^{\theta_1} - e^{\theta_2} = e^{\tilde{\theta}}(\theta_1 - \theta_2),$$

and hence

$$\|\theta_1 - \theta_2\|_{L^q(\Gamma_\beta)} \leq C(M)\|\beta_1 - \beta_2\|_{L^q(\Gamma_\beta)},$$

for any $1 \leq q \leq \infty$, since $\|\tilde{\theta}\|_{L^\infty(\Gamma_\beta)} \leq M$ in either case of our assumptions. It is then sufficient to consider stability estimate on the level of β.
(i) Theorem 2.2 of [1] states that

$$\|\beta_1 - \beta_2\|_{L^\infty(\Gamma_{\beta,\epsilon})} \leq \tilde{K}|\log(\|\mathcal{G}(\theta_1) - \mathcal{G}(\theta_2)\|_{L^\infty(\Gamma)})|^{-\sigma} \tag{24}$$

for some $\tilde{K} > 0$ and $0 < \sigma < 1$ dependent on $\mathcal{O}$, h, M_1 and ϵ. Sobolev embedding and interpolation results gives for some $0 < \delta < \frac{1}{4}$

$$\begin{aligned}\|\mathcal{G}(\theta_1) - \mathcal{G}(\theta_2)\|_{L^\infty(\Gamma)} &\leq \|\mathcal{G}(\theta_1) - \mathcal{G}(\theta_2)\|_{H^{\frac{1}{2}+\delta}(\Gamma)},\\ &\leq \|\mathcal{G}(\theta_1) - \mathcal{G}(\theta_2)\|^p_{L^2(\Gamma)}\|\mathcal{G}(\theta_1) - \mathcal{G}(\theta_2)\|^{1-p}_{H^{\frac{1}{2}+2\delta}(\Gamma)},\\ &\leq M(\mathcal{O}, m_\beta, M_\beta, M_h, \delta)\|\mathcal{G}(\theta_1) - \mathcal{G}(\theta_2)\|^p_{L^2(\Gamma)},\end{aligned}$$

where $p = \frac{2\delta}{1+4\delta}$, and where we used Lemma A.1. Inserting this into (24) for some fixed δ gives (i) for $K = K(\tilde{K}, M)$.
(ii) We follow the argument of [28, Section 3], which relies on two auxiliary results:

(1) $\min_{x\in\overline{\Gamma}_{\beta,\epsilon}} u(x) \geq \eta$, where $\eta > 0$ is a constant dependent on ϵ, but independent of the imposed boundary condition on Γ.
(2) the solution u to (2) can be analytically extended in a fixed neighborhood U of Γ_β with $\|u\|_{H^2(U)} \leq C(M)$, where it is also harmonic.

In the presence of these two results, the estimate follows exactly as in [28, Theorem 3.1] with $K > 0$ and $0 < \sigma < 1$ depending only on M, ϵ, $\mathcal{O}$, M_h, M, and we will not repeat it here.

(1) Note first that $u(x) \geq \eta$ for any $x \in \overline{\Gamma}_{\beta,\epsilon}$, where $\eta > 0$ is some constant depending on ϵ, but independent of h. This follows from continuity of u on $\overline{\mathcal{O}}$ and maximum principles for harmonic functions as in [28, Lemma 3.2]. Indeed, one can conclude that $u \geq 0$ everywhere on $\overline{\mathcal{O}}$ by a standard contradiction argument as in [43, Theorem 9, Chap. 2]. Then [14, Lemma 2] concludes positivity on Γ_β using Hopf's lemma. The compactness argument of [28, Lemma 3.2] is then adapted to our case to show $u(x) \geq \eta$ for any $x \in \overline{\Gamma}_{\beta,\epsilon}$.

(2) Corollary 1.1 in [36, Chapter 8] shows that the solution u to (2) is analytic near and up to Γ_β. For δ small and $\tilde{U} := \overline{\mathcal{O}} \cap ((0,1) \times (-\delta, \delta))$ it further states that for $k = (k_1, k_2) \in \mathbb{N}_0^2$

$$\sup_{z \in \tilde{U}} |\partial^k u(z)| \leq C(M)(k!)C(M)^{|k|},$$

for $|k| = k_1 + k_2 \in \mathbb{N}_0$ and where $k! = k_1!k_2!$. Then the Taylor series of u in $(\alpha, 0)$ for any $\alpha \in (0,1)$ has a convergence radius of at least $r = C(M)^{-1}$. Indeed, for any (x, y) with distance at most r to $(\alpha, 0)$ we have

$$\begin{aligned} u(z) = u(x,y) &= \sum_{n_1=0}^{\infty} \sum_{n_2=0}^{\infty} \frac{\partial^n u(\alpha, 0)}{n!} (x-\alpha)^{n_1} y^{n_2}, \\ &\leq C(M) \sum_{n_1=0}^{\infty} \sum_{n_2=0}^{\infty} C(M)^{|n|} (x-\alpha)^{n_1} y^{n_2}, \\ &\leq \sum_{n_1=0}^{\infty} \sum_{n_2=0}^{\infty} (C(M)r)^{|n|} \end{aligned} \tag{25}$$

where we denoted $n = (n_1, n_2)$. Since a power series is analytic in the interior of its region of convergence, u is analytic in sufficiently small balls centered in $(\alpha, 0)$. A covering argument then gives a unique analytic extension in for example $(0,1) \times (-\tilde{\delta}, \tilde{\delta}))$ with $\tilde{\delta} = \min(\delta, (2C(M))^{-1})$. Repeating (25) for $\partial^k u(z)$ for $k = 1, 2$, we note that

$$\|u\|_{C^2((0,1)\times(-\tilde{\delta},\tilde{\delta}))} \leq C(M).$$

We also conclude $\Delta u = 0$ in $\mathcal{O} \cup ((0,1) \times (-\tilde{\delta}, \tilde{\delta}))$. Indeed, Δu is analytic in $\mathcal{O} \cup ((0,1) \times (-\tilde{\delta}, \tilde{\delta}))$ and coincides with 0 on $\mathcal{O}$ and hence is zero in $\mathcal{O} \cup ((0,1) \times (-\delta, \delta))$ by uniqueness of analytic functions. □

Using the general property of uniform analyticity up to the boundary we avoid the argument in [28, Theorem 3.1], which uses a reflection formula provided by [8]. Inspection of this reflection formula reveals that we do need a condition like $\theta_i \in \mathcal{R}_2(M)$, $i = 1, 2$, to reflect the solution to a possible small but fixed neighborhood. We can generalize our proof to stability estimates for any analytic Γ_β for $d = 2$ and $d = 3$.

C. Consistency for analytic functions

The result of Theorem 3.1 is derived from the property of posterior consistency, see [23, Chapter 8] for a general treatment. In the following we address posterior consistency for analytic functions. We start by establishing a relationship between the space $\mathcal{A}_r(\Gamma_\beta)$ and the set of functions $\mathcal{R}_2(M)$. We prove a result, which is well-known and particularly simple in the setting of the m-dimensional $[-\pi, \pi)$-torus $\mathbb{T}^m$. Analogously, it generalizes to function spaces defined by the decay of the Fourier transform by the Paley-Wiener theorem, see [45, Theorem IX.13]. We consider $m \geq 1$, since it follows in much the same way as $m = 1$. To this end, let Γ_β be an open compactly embedded subset of $[-\pi, \pi)^m$ for $m \in \mathbb{N}$. Let $\{\phi_k\}_{k \in \mathbb{Z}^m}$ be a real orthonormal Fourier basis and define for $f_k = \langle f, \phi_k \rangle_{L^2(\mathbb{T}^m)}$ the more general space

$$\mathcal{A}_{r,m}(\Gamma_\beta) := \{f = g|_{\Gamma_\beta} : g \in \mathcal{A}_r(\mathbb{T}^m)\}$$

with

$$\mathcal{A}_r(\mathbb{T}^m) = \{f \in L^2(\mathbb{T}^m) : \|f\|^2_{r,\mathbb{T}^m} := \sum_{k\in\mathbb{Z}^m} |f_k|^2 e^{r|k|} < \infty\}$$

and the corresponding quotient norm of (8), denoted $\|\cdot\|_{r,m}$. Note we write $|k| := |k_1| + \ldots + |k_m|$ and not for example $\|k\|^2$ to make a sharper result. We keep the definition of $\mathcal{R}_2(M)$ as in Assumption 2, and note that the condition

$$\sup_{x\in\overline{\Gamma}_\beta} |(\partial^k \beta)(x)| \leq M(k!)M^{|k|}$$

should be understood in multi-index notation (i.e. $\partial^k = \partial^{k_1}_{x_1} \ldots \partial^{k_m}_{x_m}$ and $k! = k_1! \ldots k_m!$) for each $k \in \mathbb{N}_0^2$. Again this is closely related to the usual characterization of analytic functions on Γ_β, see [32, Proposition 2.2.10]. We also denote $d_\infty(x, S) := \inf_{y\in S} \|x - y\|_\infty$, the sup-norm distance of the point x to the set S.

Lemma C.1. *Suppose $f \in \mathcal{A}_{r,m}(\Gamma_\beta)$, $r > 0$ with $\|f\|_r \leq M_0$. Then,*

(i) there exists an analytic extension of f to $G_r := \{z \in \mathbb{C} : d_\infty(z, \overline{\Gamma}_\beta) \leq \frac{r}{4}\}$ with

$$\sup_{z\in G_r} |f(z)| \leq M_1$$

for some $M_1 = M_1(r, M_0, m)$.

(ii) $\sup_{x\in\overline{\Gamma}_\beta} \left|(\partial^k f)(x)\right| \leq M_2(k!)M_2^{|k|}$ for some $M_2 = M_2(M_1, r)$ and $k \in \mathbb{N}_0^m$.

(iii) $f \in \mathcal{R}_2(M)$ for some $M = M(M_1)$.

Proof. We complete the proof for $m = 2$ and note that the case for other $m \in \mathbb{N}$ follows in the same way.

(i) By assumption f is the restriction of a function in $\mathcal{A}_r(\mathbb{T}^2)$ with $\|f\|_{r,\mathbb{T}^2} \leq M_0$, which implies for the usual Fourier coefficients $\hat{f}_k := \frac{1}{2\pi}\langle f, e^{ik\cdot x}\rangle_{L^2(\mathbb{T}^2)}$

$$|\hat{f}_k| \leq M_0 e^{-\frac{r}{2}|k|}.$$

Define the 'polycylinder'

$$P_\rho = \{w \in \mathbb{C}^2 : |w_1| < e^{\rho/2}, |w_2| < e^{\rho/2}\}.$$

Take a compact set $K \subset P_r$, then for any $w \in K$, the family of functions $\{\hat{f}_k w^k\}_{k\in\mathbb{N}_0^2}$ (where $w^k = w_1^{k_1} w_2^{k_2}$) is bounded. Then by the argument of [46, Corollary 1.5.9.2], the function $w \mapsto \sum_{k\in\mathbb{N}_0^2} \hat{f}_k w^k$ is complex analytic in P_r. In fact, by the same argument the four power series

$$w \mapsto \sum_{k\in\mathbb{N}_0^2} \hat{f}_{\pm k_1, \pm k_2} w^k \tag{26}$$

are complex analytic in P_r. Further, for all $w \in \overline{P}_{r/2}$

$$\left|\sum_{k\in\mathbb{N}_0^2} \hat{f}_{\pm k_1,\pm k_2} w^k\right| \leq \sum_{k\in\mathbb{N}_0^2} |\hat{f}_{\pm k_1,\pm k_2}||w|^k \leq C(M_0, r) \tag{27}$$

Now decompose the following Laurent series into four similar power series as

$$\begin{aligned}\sum_{k\in\mathbb{Z}^2}\hat{f}_k w^k &= \sum_{k_1=1}^{\infty}\sum_{k_2=0}^{\infty}\hat{f}_{-k_1,k_2}w_1^{-k_1}w_2^{k_2},\\ &+\sum_{k_1=1}^{\infty}\sum_{k_2=1}^{\infty}\hat{f}_{-k_1,-k_2}w_1^{-k_1}w_2^{-k_2},\\ &+\sum_{k_1=0}^{\infty}\sum_{k_2=0}^{\infty}\hat{f}_{k_1,k_2}w_1^{k_1}w_2^{k_2},\\ &+\sum_{k_1=0}^{\infty}\sum_{k_2=1}^{\infty}\hat{f}_{k_1,-k_2}w_1^{k_1}w_2^{-k_2}.\end{aligned}$$

Consider first the first term. This has the form $w\mapsto g(w_1^{-1},w_2)$ for a function g_1 on the form (26) complex analytic in P_ρ. The function $w\mapsto(w_1^{-1},w_2)$ is complex analytic in for example $\{w\in\mathbb{C}^2 : w_1 > e^{-r/2}, w_2 < e^{r/2}\}$, since $w\mapsto w_i$ is complex analytic everywhere and $w\mapsto w_i^{-1}$ is complex analytic for w_i away from zero, $i=1,2$, see [46, Proposition 1.2.2]. Then also $w\mapsto g_1(w_1^{-1},w_2)$ is complex analytic in $\{w\in\mathbb{C}^2 : w_1 > e^{-r/2}, w_2 < e^{r/2}\}$, since compositions of analytic functions are analytic, see again [46, Proposition 1.2.2]. Continuing this argument for each term above, we find that

$$g(w) := \sum_{k\in\mathbb{Z}^2}\hat{f}_k w^k$$

is complex analytic in the 'polyannulus' $\{w\in\mathbb{C}^2 : e^{-r/2} < w_i < e^{r/2}, i=1,2\}$. Using that $z\mapsto e^z$ is entire on $\mathbb{C}$ and again the composition rule, we find that

$$z\mapsto g(e^{iz_1},e^{iz_2}) = \sum_{k\in\mathbb{Z}^2}\hat{f}_k e^{ik\cdot z}$$

is complex analytic in $\{z\in\mathbb{C}^2 : |\mathrm{Im}(z_i)| < r/2, i=1,2\}$. Moreover, since (27) is a bound for each of the four power series which make up f and G_r is a subset of the strip of where it is defined, we conclude

$$\sup_{z\in G_r}|f(z)| \le M_1(r,M_0). \tag{28}$$

(ii) The Cauchy integral inequality in [46, Theorem 1.3.3] gives the estimate

$$\sup_{|z_i|<r/4,i=1,2}|(\partial^k f)(z)| \le (k!)(r/4)^{|k|}\sup_{|z_i|=r/4,i=1,2}|f(z)|.$$

Since $\overline{\Gamma}_\beta$ is compact, we can cover it by real translations of $\{z\in\mathbb{C}^2 : |z_i| < r/4, i=1,2\}$ and conclude by (28) that there exists a constant $M_2 = M_2(M_1,r)$ such that

$$\sup_{x\in\overline{\Gamma}_\beta}|(\partial^k f)(x)| \le M_2(k!)M_2^{|k|}.$$

(iii) Since $z\mapsto e^z$ is entire, also $z\mapsto e^{f(z)}$ is complex analytic in G_r with a bound $\sup_{z\in G_r}|e^{f(z)}| \le e^{M_1}$. Repeating the same arguments as of (ii) we conclude that $f\in\mathcal{R}_2(M)$ for some $M = M(M_1)$. □

We now return to the question of consistency, which involves precise statements on the prior we use. Since $\tilde{\Pi}_2$ is a Gaussian measure in $C(\overline{\Gamma}_\beta)$, a covering number bound of the unit norm-ball in the RKHS $\mathcal{H}_2 = \mathcal{A}_r(\Gamma_\beta)$, yields a bound on the measure of small norm balls, see [34]. To make use of this, we define the notion

of covering numbers as follows. Let the covering number $N(A, d, \rho)$ for $A \subset X$ of some space X endowed with a semimetric d, denote the minimum number of closed d-balls $\{x \in X : d(x_0, x) \leq \rho\}$ with center $x_0 \in A$ and radius $\rho > 0$ needed to cover A, see for example [23, Appendix C] or [24, Section 4.3.7]. When d is replaced by a norm, we mean the metric induced by the norm. The following consequence of [23, Proposition C.9] allows us to bound the unit norm ball of $\mathcal{A}_r(\Gamma_\beta)$.

Lemma C.2. *The class $A(M_1)$ of all functions $f : [0,1]^m \to \mathbb{R}$ that can be extended to a complex analytic function on G_r with $\sup_{z \in G_r} |f(z)| \leq M_1$ for some $M_1 > 0$ and $r > 0$, satisfies for all $\rho > 0$ sufficiently small*

$$\log N(A(M_1), \|\cdot\|_\infty, \rho) \leq C(r, m, M_1) \log(\rho^{-1})^{1+m}. \tag{29}$$

Proof. Proposition C.9 in [23] states that

$$\log N(A(1), \|\cdot\|_\infty, \rho) \leq C(m) r^{-m} \log(\rho^{-1})^{1+m}$$

for all $0 < \rho < 1/2$. Since $\|\cdot\|_\infty \leq \|\cdot\|_{C([0,1]^m)}$, [24, eq. (4.172)] gives

$$\log N(A(1), \|\cdot\|_\infty, \rho) \leq \log N(A(1), \|\cdot\|_{C([0,1]^m)}, \rho).$$

Then, combining the two last displays with [24, eq. (4.171)] we have

$$\begin{aligned} \log N(A(M_1), \|\cdot\|_\infty, \rho) &= \log N(A(1), \|\cdot\|_\infty, \rho M_1^{-1}), \\ &\leq \log N(A(1), \|\cdot\|_{C([0,1]^m)}, \rho M_1^{-1}), \\ &\leq C(r, m) \log(M_1 \rho^{-1})^{1+m}. \end{aligned}$$

By the convexity of $x \mapsto x^{1+m}$, $m \geq 1$, we have the inequality $(x+y)^{m+1} \leq 2^m(x^{m+1} + y^{m+1})$ for $x, y \in \mathbb{R}$. Then for ρ small enough,

$$\log(M_1 \rho^{-1})^{1+m} \leq C(M_1, m) \log(\rho)^{1+m},$$

and hence (29) is satisfied. □

Since we constructed Π_2 for $m = 1$, we consider from now only this case, although everything generalizes to higher dimensions. See also Remark 2 below. To this end, denote the unit norm ball of $\mathcal{H}_2 = \mathcal{A}_r(\Gamma_\beta)$ by

$$B_{\mathcal{H}_2} := \{f \in \mathcal{H}_2 : \|f\|_{\mathcal{H}_2} \leq 1\}.$$

Note that $B_{\mathcal{H}_2} \subset A(M_1)$ for some $M_1 = M_1(r)$ by Lemma C.1 (i).

Lemma C.3. *Let $\phi(\rho) := -\log \tilde{\Pi}_2(\theta \in C(\overline{\Gamma}_\beta) : \|\theta\|_\infty \leq \rho)$ where $\tilde{\Pi}_2$ is dependent on $r > 0$. For all $\rho > 0$ sufficiently small,*

$$\phi(\rho) \leq C(r) \log(\rho^{-1})^2. \tag{30}$$

Proof. We follow [50, Lemma 4.6]. Theorem 1.2 of [34] initially gives the rough estimate

$$\phi(\rho) \leq C(r, M_1) \rho^{-2}, \tag{31}$$

for all $\rho > 0$ sufficiently small, since

$$\log N(B_{\mathcal{H}_2}, \|\cdot\|_\infty, \rho) \leq C(r) \rho^{-1},$$

for all $\rho > 0$ sufficiently small by Lemma C.2 for $m = 1$. The first display of the proof of Lemma 4.6 in [50] provides the inequality

$$\phi(2\rho) \leq \log N(B_{\mathcal{H}_2}, \|\cdot\|_\infty, 2\rho[2\phi(\rho)]^{-1/2}).$$

Inserting (31) into this and using Lemma C.2 again, then gives (30). □

The following result corresponds to Theorem 2.2.2 of [41] for rescaled Gaussian priors for analytic functions. We define $d_{\mathcal{G}}(\theta_1,\theta_2) := \|\mathcal{G}(\theta_1)-\mathcal{G}(\theta_2)\|_{L^2(\Gamma)}$ for all $\theta_1,\theta_2\in\Theta$.

Lemma C.4. *Let $\theta_0\in\mathcal{H}_2=\mathcal{A}_r(\Gamma_\beta)$, $r>0$, and Π_2 be as defined in (9). Set,*

$$\delta_N = N^{-1/2}\log(N). \tag{32}$$

Let $U>0$ be large enough depending on $\tilde{\Pi}_2$, r and such that $\|\mathcal{G}(\theta_0)\|_{C(\overline{\Gamma})}\le U$. Then, there exists Borel measurable sets Θ_N such that

(i) $\Pi(\theta : d_{\mathcal{G}}(\theta,\theta_0)\le\delta_N, \|\mathcal{G}(\theta)\|_{C(\overline{\Gamma})}\le U) \ge e^{-C_1N\delta_N^2}$ *for some $C_1>0$,*

(ii) $\Pi_2(\Theta_N^c)\le e^{-C_2N\delta_N^2}$ *for $C_2>C_1+2$.*

(iii) $\log N(\Theta_N, d_{\mathcal{G}}, m_0\delta_N)\le C(C_2,r)N\delta_N^2$ *for $m_0>0$ large enough*

for all N sufficiently large.

Proof. First we give the form of Θ_N. Define $B_{\mathcal{H}_2}(\delta)$ and $B_\infty(\delta)$ to be the closed norm balls of radius $\delta>0$ in $\mathcal{H}_2$ and $C(\overline{\Gamma}_\beta)$, respectively. That is,

$$B_{\mathcal{H}_2}(\delta) := \{f\in\mathcal{H}_2 : \|f\|_{\mathcal{H}_2}\le\delta\},$$
$$B_\infty(\delta) := \{f\in C(\overline{\Gamma}_\beta) : \|f\|_\infty\le\delta\},$$

Recall, also that $B_{\mathcal{H}_2}(M_0)\subset A(M_1)$ for some $M_1=M_1(r,M_0)$ by Lemma C.1 (i). Then we take

$$\Theta_N := (B_{\mathcal{H}_2}(M)+B_\infty(M\delta_N))\cap\mathcal{R}_2(M). \tag{33}$$

for $M>0$ sufficiently large determined by (ii) below.

We also recall the following triangle inequality fact needed for (ii) below: a $C\delta_N$-covering of $B_{\mathcal{H}_2}(M)$ is a $(M+C)\delta_N$-covering of $B_{\mathcal{H}_2}(M)+B_\infty(M\delta_N)$ so that

$$N(B_{\mathcal{H}_2}(M)+B_\infty(M\delta_N),\|\cdot\|_\infty,(M+C)\delta_N)\le N(B_{\mathcal{H}_2}(M),\|\cdot\|_\infty,C\delta_N).$$

This implies for $\tilde{C}$ large enough that

$$N(\Theta_N,\|\cdot\|_\infty,\tilde{C}\delta_N)\le N(B_{\mathcal{H}_2}(M),\|\cdot\|_\infty,(\tilde{C}-M)\delta_N). \tag{34}$$

In addition, we will use repeatedly below that

$$\kappa_{N,2}=\frac{1}{\sqrt{N}\delta_N}.$$

Finally, we need the scaled RKHS $\mathcal{H}_{2,N}:=\kappa_{N,2}\mathcal{H}_2=\{\kappa_{N,2}h : h\in\mathcal{H}_2\}$ with norm $\|h\|_{\mathcal{H}_{2,N}}=\kappa_{N,2}^{-1}\|h\|_{\mathcal{H}_2}$. This is the RKHS associated with Π_2, see [27] or [24, Exercise 2.6.5].

(i) We proceed as in [41, Theorem 2.2.2]. Recall that $\tilde{\Pi}_2(\mathcal{A}_q(\Gamma_\beta))=1$ for any $0<q<r$. Hence also $\Pi_2(\mathcal{A}_q(\Gamma_\beta))=1$. Fernique's theorem [24, Theorem 2.1.20] initially gives that $E[\|\tilde{\theta}_2\|_q]\le D$ for some constant D depending only on the prior $\tilde{\Pi}_2$, and next

$$\begin{aligned}\Pi_2(\theta:\|\theta\|_q>M_0) &= \tilde{\Pi}_2(\tilde{\theta}:\|\tilde{\theta}\|_q>M_0\sqrt{N}\delta_N),\\ &\le \tilde{\Pi}_2(\tilde{\theta}:\|\tilde{\theta}\|_q-E[\|\tilde{\theta}\|_q]>\frac{1}{2}M_0\sqrt{N}\delta_N),\\ &\le e^{-CM_0^2N\delta_N^2},\end{aligned} \tag{35}$$

for some sufficiently large constant $M_0 = M_0(D)$ and some constant $C = C(\tilde{\Pi}_2)$. By Lemma C.1, this implies

$$\Pi_2(\theta : \|\theta\|_{H^1(\Gamma_\beta)} > M_1) \leq e^{-CM_0^2 N\delta_N^2} \leq \frac{1}{2}, \tag{36}$$

for M_0 large enough depending on C and $M_1 = M_1(M_0, r)$. Note we have

$$\|\theta - \theta_0\|_{H^1(\Gamma_\beta)} \leq M_1 \quad \Rightarrow \quad \|\theta\|_{H^1(\Gamma_\beta)} \leq M_1 + \|\theta_0\|_{H^1(\Gamma_\beta)} \equiv \bar{M},$$

which by Lemma 2.3 implies $\|\mathcal{G}(\theta)\|_{C(\overline{\Gamma})} \leq U = U(\bar{M})$, since

$$\|e^\theta\|_{H^1(\Gamma_\beta)} \lesssim \|e^\theta\|_\infty (1 + \|\theta\|_{H^1(\Gamma_\beta)}).$$

Using again Lemma 2.3 and Corollary 2.6.18 [24] permitted since $\theta_0 \in \mathcal{H}_2$ and $\Pi_2(\Theta) = 1$, we get

$$\begin{aligned}
\Pi_2(d_{\mathcal{G}}(\theta, \theta_0) \leq \delta_N, \|\mathcal{G}(\theta)\|_{C(\overline{\Gamma})} \leq U) \\
&\geq \Pi_2(d_{\mathcal{G}}(\theta, \theta_0) \leq \delta_N, \|\theta - \theta_0\|_{H^1(\Gamma_\beta)} \leq M_1), \\
&\geq \Pi_2(\|\theta - \theta_0\|_\infty \leq K^{-1}\delta_N, \|\theta - \theta_0\|_{H^1(\Gamma_\beta)} \leq M_1), \\
&\geq e^{-\frac{1}{2}\|\theta_0\|^2_{\mathcal{H}_{2,N}}} \Pi_2(\|\theta\|_\infty \leq K^{-1}\delta_N, \|\theta\|_{H^1(\Gamma_\beta)} \leq M_1), \\
&\geq e^{-C(\theta_0)\kappa_{N,2}^{-2}} \Pi_2(\|\theta\|_\infty \leq K^{-1}\delta_N) \Pi_2(\|\theta\|_{H^1(\Gamma_\beta)} \leq M_1),
\end{aligned}$$

where we used the Gaussian correlation inequality, see [41, Theorem 6.2.2], and the relation $\|\theta_0\|_{\mathcal{H}_{2,N}} = \kappa_{N,2}^{-1}\|\theta_0\|_{\mathcal{H}_2}$ for the last line. We also note that K depends on M_1. Lemma C.3 implies

$$\begin{aligned}
-\log \Pi_2(\theta : \|\theta\|_\infty \leq K^{-1}\delta_N) &= -\log \tilde{\Pi}_2(\tilde{\theta} : \|\tilde{\theta}\|_\infty \leq \kappa_{N,2}^{-1} K^{-1}\delta_N) \\
&\leq C(r) \log\left(\frac{K\kappa_{N,2}}{\delta_N}\right)^2, \\
&= C(r) \log\left(K\sqrt{N}\log(N)^{-2}\right)^2, \\
&\leq C(r)\left[\log(K) + \frac{1}{2}\log(N) - 2\log(\log(N))\right]^2, \\
&\leq C(K, r)\log(N)^2, \\
&\leq C(K, r) N\delta_N^2, \qquad (37)
\end{aligned}$$

for a sufficiently large constant $C = C(K, r)$. Equation (36) shows

$$\Pi_2(\theta : \|\theta\|_{H^1(\Gamma_\beta)} \leq M_1) \geq 1 - \frac{1}{2} = \frac{1}{2}.$$

The three last displays shows (i) for (32) and a constant $C_1 = C_1(\theta_0, K, M_1, r)$. (ii) Lemma C.1 implies there exists $M = M(q, M_0)$ such that

$$\{f \in \mathcal{A}_q(\Gamma_\beta) : \|f\|_q \leq M_0\} \subset \mathcal{R}_2(M),$$

and hence by (35) we can pick M_0 large enough dependent on C_2 such that

$$\Pi_2(\mathcal{R}_2(M)^c) \leq \frac{1}{2} e^{-C_2 N\delta_N^2}.$$

We simply pick $q = r/2$ to fix constants. Then it suffices to prove

$$\Pi_2(B_{\mathcal{H}_2}(M) + B_\infty(M\delta_N)) \geq 1 - \frac{1}{2} e^{-C_2 N\delta_N^2}.$$

We prove the stronger bound

$$\Pi_2(B_{\mathcal{H}_2}(M) + B_\infty(M\delta_N)) \geq 1 - e^{-2C_2N\delta_N^2}.$$

By similar computations as with (37) for $M \geq 1$, we find

$$\begin{aligned} -\log \Pi_2(\theta : \|\theta\|_\infty \leq M\delta_N) &\leq C(r)\log(\delta_N^{-1}), \\ &\leq C(r)(1/2\log(N) - \log\log(N)), \\ &\leq 2C_2\log(N)^2, \\ &\leq 2C_2N\delta_N^2, \end{aligned}$$

for any given $C_2 > 0$ and N sufficiently large. As in [41, Theorem 2.2.2] we denote

$$B_N = -2\Phi^{-1}(e^{-2C_2N\delta_N^2}),$$

where Φ is the standard normal cumulative distribution function. Then by [23, Lemma K.6] we have

$$B_N \leq 2\sqrt{2\log(e^{2C_2N\delta_N^2})} \leq 4\sqrt{C_2}\sqrt{N}\delta_N.$$

Then for $M > 4\sqrt{C_2}$ such that $B_N \leq M\sqrt{N}\delta_N$ we use the isoperimetric inequality [24, Theorem 2.6.12] to conclude that

$$\begin{aligned} \Pi_2(B_{\mathcal{H}_2}(M) + B_\infty(M\delta_N)) &= \tilde{\Pi}_2(B_{\mathcal{H}_2}(M\sqrt{N}\delta_N) + B_\infty(M\sqrt{N}\delta_N^2)), \\ &\geq \tilde{\Pi}_2(B_{\mathcal{H}_2}(B_N) + B_\infty(M\sqrt{N}\delta_N^2)), \\ &\geq \Phi(\Phi^{-1}[\tilde{\Pi}_2(B_\infty(M\sqrt{N}\delta_N^2))] + B_N), \\ &\geq \Phi(\Phi^{-1}[e^{-2C_2N\delta_N^2}] + B_N), \\ &= \Phi(-\Phi^{-1}[e^{-2C_2N\delta_N^2}]), \\ &= 1 - \Phi(\Phi^{-1}[e^{-2C_2N\delta_N^2}]), \\ &= 1 - e^{-2C_2N\delta_N^2}, \end{aligned}$$

using also $\Phi(-x) = 1 - \Phi(x)$.
(iii) We recall that $B_{\mathcal{H}_2}(M) \subset A(M_1)$ for some $M_1 = M_1(M, r)$ by Lemma C.1 so that Lemma C.2 gives

$$\begin{aligned} \log N(B_{\mathcal{H}_2}(M), \|\cdot\|_\infty, \delta_N) &\leq C(r, M)\log(\delta_N^{-1})^2, \\ &\leq C(r, M)\left(1/2\log(N) - \log\log(N)\right)^2, \\ &\leq C(r, M)N\delta_N^2, \end{aligned}$$

for N large enough. Then using Lemma 2.3 with $m_0 = m_0(K, M)$ sufficiently large and (34) we get

$$\begin{aligned} \log N(\Theta_N, d_{\mathcal{G}}, m_0\delta_N) &\leq \log N(\Theta_N, \|\cdot\|_\infty, K^{-1}m_0\delta_N), \\ &\leq \log N(B_{\mathcal{H}_2}(M), \|\cdot\|_\infty, (K^{-1}m_0 - M)\delta_N), \\ &\leq C(r, M)N\delta_N^2, \end{aligned}$$

Note M depends only on r and C_2 through M_0. □

Remark 2. *Extending Lemma C.3 and C.4 to $m > 1$ and other exponential decay is straightforward. Indeed, define a Gaussian prior by the restriction to $\Gamma_\beta \subset [-\pi, \pi)^m$ of the random series*

$$\tilde{\theta}_2 = \sum_{k \in \mathbb{Z}^m} g_k e^{-\frac{r}{2}|k|} \phi_k, \qquad g_k \overset{i.i.d.}{\sim} N(0,1).$$

This is an element of $\mathcal{A}_{q,m}(\Gamma_\beta)$ a.s for $q < r$ and its RKHS is $\mathcal{H}_2 = \mathcal{A}_{r,m}(\Gamma_\beta)$. Then Lemma C.3 follows in the same way by noting $B_{\mathcal{H}_2} \subset A(M_1)$ for some $M_1 = M_1(r)$ by Lemma C.1 (i). Given a Lipschitz continuous forward map $\mathcal{G}$, Lemma C.4 follows for $\delta_N = N^{-1/2} \log(N)^\zeta$ for some exponent ζ dependent on m.

Proof of 3.1 (ii). By Lemma C.4, conditions (1.32) and (1.33) of Theorem 1.3.2 [41] are satisfied for the choice (33) of Θ_N. Lemma C.4 (*ii*) and the bound on the Hellinger distance $h(p_\theta, p_\vartheta) \leq \frac{1}{2} d_{\mathcal{G}}(\theta, \vartheta)$, see [41, Proposition 1.3.1], implies

$$N(\tilde{\Theta}_N, h, \frac{1}{2} m_0 \delta_N) \leq N(\Theta_N, d_{\mathcal{G}}, m_0 \delta_N) \leq e^{C(C_2, r) N \delta_N^2} \tag{38}$$

hence for all $\varepsilon > 2 m_0 \delta_N$

$$N(\tilde{\Theta}_N, h, \frac{\varepsilon}{4}) \leq e^{C(C_2, r) N \delta_N^2},$$

with

$$\tilde{\Theta}_N := \{p_\theta : \theta \in \Theta_N\}.$$

Note the right-hand side of (38) is independent of such ε. Setting $\varepsilon = m \delta_N$ for $m > 2 m_0$, Theorem 7.1.4 of [24] gives the existence of statistical tests $\Psi_N : (\mathbb{R} \times \Gamma)^N \to \{0, 1\}$ satisfying

$$P_{\theta_0}^N (\Psi_N = 1) \to 0,$$

as $N \to \infty$, and for the expectation E_θ^N with respect to P_θ^N

$$\sup_{\theta \in \Theta_N : h(p_\theta, p_{\theta_0}) > m \delta_N} E_\theta^N (1 - \Psi_N) \leq e^{-\kappa N \delta_N^2}$$

for m large enough also depending on $C(C_2, r)$ and κ. Then the proof of Theorem 1.3.2 [41] implies that for all $0 < b < C_2 - C_1 - 2$ we can choose $C_0 = C_0(C_1, C_2, r, m_0, b, U)$ large enough such that

$$P_{\theta_0}^N \left(\Pi_N (\theta \in \Theta_N : d_{\mathcal{G}}(\theta, \theta_0) \leq C_0 \delta_N | D_N) \leq 1 - e^{-b N \delta_N^2} \right) \to 0.$$

Lemma 2.4 (ii) implies

$$\{\theta \in \Theta_N : d_{\mathcal{G}}(\theta, \theta_0) \leq C_0 \delta_N\} \subset \{\theta \in \Theta_N : \|\theta - \theta_0\|_{L^2(\Gamma_{\beta, \epsilon})} \leq K C_0^\sigma \delta_N^\sigma\}$$

so that we also have

$$P_{\theta_0}^N \left(\Pi_N (\theta \in \Theta_N : \|\theta - \theta_0\|_{L^2(\Gamma_{\beta, \epsilon})} \leq K C_0^\sigma \delta_N^\sigma | D_N) \leq 1 - e^{-b N \delta_N^2} \right) \to 0.$$

Then the argument of Theorem 2.3.2 [41] applies in the same way here to the effect that

$$\|E_2[\theta | D_N] - \theta_0\|_{L^2(\Gamma_{\beta, \epsilon})} \to 0 \qquad \text{in } P_{\theta_0}^N\text{-probability}$$

with rate δ_N^σ as $N \to \infty$. □

Acknowledgements

The authors would like to thank Prof. Richard Nickl for helpful discussions on Bayesian nonparametrics. The authors would also like to thank Prof. Kim Knudsen for helpful discussions on mixed boundary value problems. IK was funded by a Biometrika Fellowship awarded by the Biometrika Trust. AKR was supported by The Villum Foundation (grant no. 25893). FS was supported by Cantab Capital Institute for Mathematics of Information.

References

[1] G. Alessandrini, L. Del Piero, and L. Rondi. Stable determination of corrosion by a single electrostatic boundary measurement. *Inverse Problems*, 19(4):973–984, 2003.

[2] Giovanni Alessandrini, Luca Rondi, Edi Rosset, and Sergio Vessella. The stability for the Cauchy problem for elliptic equations. *Inverse Problems*, 25(12):123004, 47, 2009.

[3] Charalambos D. Aliprantis and Kim C. Border. *Infinite dimensional analysis*. Springer, Berlin, third edition, 2006. A hitchhiker's guide.

[4] Robert J. Arthern. Exploring the use of transformation group priors and the method of maximum relative entropy for bayesian glaciological inversions. *Journal of Glaciology*, 61(229):947–962, 2015.

[5] Robert J. Arthern and G. Hilmar Gudmundsson. Initialization of ice-sheet forecasts viewed as an inverse Robin problem. *Journal of Glaciology*, 56(197):527–533, 8 2010.

[6] O. Babaniyi, R. Nicholson, U. Villa, and N. Petra. Inferring the basal sliding coefficient field for the stokes ice sheet model under rheological uncertainty. *The Cryosphere*, 15(4):1731–1750, 2021.

[7] J. Banasiak and G. F. Roach. On mixed boundary value problems of Dirichlet oblique-derivative type in plane domains with piecewise differentiable boundary. *J. Differential Equations*, 79(1):111–131, 1989.

[8] Boris P. Belinskiy and Tatiana V. Savina. The Schwarz reflection principle for harmonic functions in $\mathbb{R}^2$ subject to the Robin condition. *J. Math. Anal. Appl.*, 348(2):685–691, 2008.

[9] Muriel Boulakia, Anne-Claire Egloffe, and Céline Grandmont. Stability estimates for a Robin coefficient in the two-dimensional Stokes system. *Math. Control Relat. Fields*, 3(1):21–49, 2013.

[10] Muriel Boulakia, Anne Claire Egloffe, and Céline Grandmont. Stability estimates for the unique continuation property of the Stokes system and for an inverse boundary coefficient problem. *Inverse Problems*, 29(11), 11 2013.

[11] Franck Boyer and Pierre Fabrie. *Mathematical tools for the study of the incompressible Navier-Stokes equations and related models*, volume 183 of *Applied Mathematical Sciences*. Springer, New York, 2013.

[12] Susanne C. Brenner and L. Ridgway Scott. *The mathematical theory of finite element methods*, volume 15 of *Texts in Applied Mathematics*. Springer, New York, third edition, 2008.

[13] S. Chaabane, I. Fellah, M. Jaoua, and J. Leblond. Logarithmic stability estimates for a Robin coefficient in two-dimensional Laplace inverse problems. *Inverse Problems*, 20(1):47–59, 2004.

[14] Slim Chaabane and Mohamed Jaoua. Identification of Robin coefficients by the means of boundary measurements. *Inverse Problems*, 15(6):1425–1438, 1999.

[15] Masoumeh Dashti and Andrew M. Stuart. The Bayesian approach to inverse problems. In *Handbook of uncertainty quantification. Vol. 1, 2, 3*, pages 311–428. Springer, Cham, 2017.

[16] J. Diestel and J. J. Uhl, Jr. *Vector measures*. Mathematical Surveys, No. 15. American Mathematical Society, Providence, R.I., 1977. With a foreword by B. J. Pettis.

[17] Richard M. Dudley. *Real analysis and probability*. The Wadsworth & Brooks/Cole Mathematics Series. Wadsworth & Brooks/Cole Advanced Books & Software, Pacific Grove, CA, 1989.

[18] Anne-Claire Egloffe. Lipschitz stability estimate in the inverse Robin problem for the Stokes system. *C. R. Math. Acad. Sci. Paris*, 351(13-14):527–531, 2013.

[19] Heinz W. Engl, Martin Hanke, and Andreas Neubauer. *Regularization of inverse problems*, volume 375 of *Mathematics and its Applications*. Kluwer Academic Publishers Group, Dordrecht, 1996.

[20] Caroline Fabre and Gilles Lebeau. Prolongement unique des solutions de l'equation de Stokes. *Comm. Partial Differential Equations*, 21(3-4):573–596, 1996.
[21] Dario Fasino and Gabriele Inglese. An inverse Robin problem for Laplace's equation: theoretical results and numerical methods. *Inverse Problems*, 15(1):41–48, 1999. Conference on Inverse Problems, Control and Shape Optimization (Carthage, 1998).
[22] Subhashis Ghosal, Jayanta K. Ghosh, and Aad W. van der Vaart. Convergence rates of posterior distributions. *The Annals of Statistics*, 28(2):500 – 531, 2000.
[23] Subhashis Ghosal and Aad van der Vaart. *Fundamentals of nonparametric Bayesian inference*, volume 44 of *Cambridge Series in Statistical and Probabilistic Mathematics*. Cambridge University Press, Cambridge, 2017.
[24] Evarist Giné and Richard Nickl. *Mathematical foundations of infinite-dimensional statistical models*. Cambridge Series in Statistical and Probabilistic Mathematics, [40]. Cambridge University Press, New York, 2016.
[25] P. Grisvard. *Elliptic problems in nonsmooth domains*, volume 24 of *Monographs and Studies in Mathematics*. Pitman (Advanced Publishing Program), Boston, MA, 1985.
[26] Jacques Hadamard. *Lectures on Cauchy's problem in linear partial differential equations*. Dover Publications, New York, 1953.
[27] Martin Hairer. An introduction to stochastic pdes. *arXiv preprint arXiv:0907.4178*, 2009.
[28] Guanghui Hu and Masahiro Yamamoto. Hölder stability estimate of Robin coefficient in corrosion detection with a single boundary measurement. *Inverse Problems*, 31(11):115009, 20, 2015.
[29] Gabriele Inglese. An inverse problem in corrosion detection. *Inverse Problems*, 13(4):977–994, 1997.
[30] Bangti Jin. Conjugate gradient method for the Robin inverse problem associated with the Laplace equation. *Internat. J. Numer. Methods Engrg.*, 71(4):433–453, 2007.
[31] Robert V. Kohn and Michael Vogelius. Relaxation of a variational method for impedance computed tomography. *Comm. Pure Appl. Math.*, 40(6):745–777, 1987.
[32] Steven G. Krantz and Harold R. Parks. *A primer of real analytic functions*. Birkhäuser Advanced Texts: Basler Lehrbücher. [Birkhäuser Advanced Texts: Basel Textbooks]. Birkhäuser Boston, Inc., Boston, MA, second edition, 2002.
[33] Christophe Labreuche. Stability of the recovery of surface impedances in inverse scattering. *J. Math. Anal. Appl.*, 231(1):161–176, 1999.
[34] Wenbo V. Li and Werner Linde. Approximation, metric entropy and small ball estimates for Gaussian measures. *Ann. Probab.*, 27(3):1556–1578, 1999.
[35] J.-L. Lions and E. Magenes. *Non-homogeneous boundary value problems and applications. Vol. I*, volume Band 181 of *Die Grundlehren der mathematischen Wissenschaften*. Springer-Verlag, New York-Heidelberg, 1972. Translated from the French by P. Kenneth.
[36] J.-L. Lions and E. Magenes. *Non-homogeneous boundary value problems and applications. Vol. III*, volume Band 183. Springer-Verlag, New York-Heidelberg, 1973. Translated from the French by P. Kenneth.
[37] Jijun Liu and Gen Nakamura. Recovering the boundary corrosion from electrical potential distribution using partial boundary data. *Inverse Probl. Imaging*, 11(3):521–538, 2017.
[38] François Monard, Richard Nickl, and Gabriel P. Paternain. Consistent inversion of noisy non-Abelian X-ray transforms. *Comm. Pure Appl. Math.*, 74(5):1045–1099, 2021.
[39] Ruanui Nicholson and Matti Niskanen. Joint estimation of Robin coefficient and domain boundary for the Poisson problem. *Inverse Problems*, 38(1):Paper No. 015008, 23, 2022.
[40] Ruanui Nicholson, Noémi Petra, and Jari P. Kaipio. Estimation of the Robin coefficient field in a Poisson problem with uncertain conductivity field. *Inverse Problems*, 34(11):115005, 26, 2018.
[41] Richard Nickl. *Bayesian non-linear statistical inverse problems*. Zurich Lectures in Advanced Mathematics. EMS Press, Berlin, 2023.
[42] Richard Nickl, Sara van de Geer, and Sven Wang. Convergence rates for penalized least squares estimators in PDE constrained regression problems. *SIAM/ASA J. Uncertain. Quantif.*, 8(1):374–413, 2020.
[43] Murray H. Protter and Hans F. Weinberger. *Maximum principles in differential equations*. Springer-Verlag, New York, 1984. Corrected reprint of the 1967 original.
[44] Carl Edward Rasmussen and Christopher K. I. Williams. *Gaussian processes for machine learning*. Adaptive Computation and Machine Learning. MIT Press, Cambridge, MA, 2006.

[45] Michael Reed and Barry Simon. *Methods of modern mathematical physics. II. Fourier analysis, self-adjointness*. Academic Press [Harcourt Brace Jovanovich, Publishers], New York-London, 1975.
[46] Volker Scheidemann. *Introduction to complex analysis in several variables*. Birkhäuser Verlag, Basel, 2005.
[47] E. Sincich. Lipschitz stability for the inverse Robin problem. *Inverse Problems*, 23(3):1311–1326, 2007.
[48] A. M. Stuart. Inverse problems: a Bayesian perspective. *Acta Numer.*, 19:451–559, 2010.
[49] Michael E. Taylor. *Partial differential equations I. Basic theory*, volume 115 of *Applied Mathematical Sciences*. Springer, New York, second edition, 2011.
[50] A. W. van der Vaart and J. H. van Zanten. Adaptive Bayesian estimation using a Gaussian random field with inverse gamma bandwidth. *Ann. Statist.*, 37(5B):2655–2675, 2009.

Appendix D

Technical report

The following appendix is the technical report titled *Direct method for stroke detection with electrical impedance tomography in three dimensions* authored by Kim Knudsen and Aksel Kaastrup Rasmussen in 2023.

DIRECT METHOD FOR STROKE DETECTION WITH ELECTRICAL IMPEDANCE TOMOGRAPHY IN THREE DIMENSIONS

Kim Knudsen and Aksel Kaastrup Rasmussen*

Technical University of Denmark
Department of Applied Mathematics and Computer Science
DK-2800 Kgs. Lyngby, Denmark

Abstract. In this paper we revisit the regularized, direct reconstruction method for three dimensional Electrical Impedance Tomography (EIT) based on complex geometrical optics solutions and a non-physical scattering transform. The method solves the full non-linear problem directly without relying on iterations or linearization. We demonstrate via computational experiments that the method applies to the challenging situation of stroke detection, where the weakly conducting skull is a barrier. Our results suggest that detecting a hemorrhagic stroke is possible and robust to noise perturbations, while detecting an ischemic stroke is highly challenging. Further, our results suggest that the direct method is a promising candidate for a portable and nearly real-time stroke-EIT system.

1. Introduction

Electrical Impedance Tomography (EIT) is a non-invasive medical imaging modality that aims to recover a body's electrical conductivity based on surface measurements of currents and voltages through electrodes attached to the skin. Applications are diverse: lung EIT has shown great promise (see [1] and references therein), but also for the monitoring of fast electrical brain activity [2] and stroke detection, EIT seems feasible [3, 4]. A great challenge in brain EIT is the weakly conducting skull: It is difficult to get the electric energy to pass beyond the skull and propagate information about the brain's inner structures to the surface measurements.

The mathematical problem behind EIT was formulated by Calderón in 1980 [5] as follows: consider a bounded and smooth domain $\Omega \subset \mathbb{R}^3$ representing the electrically conducting body. We assume the conductivity distribution is isotropic and hence described by a bounded and strictly positive function γ. The experiment consists of applying an electrical potential to the boundary of Ω and measuring the corresponding current flux through

Key words and phrases. electrical impedance tomography, stroke detection, ill-posed problem, regularization, direct method.

* Corresponding author.

the boundary. Indeed, under conservation of charge, the boundary potential, as modelled by a continuous function f on the boundary $\partial\Omega$, induces an electrical potential u inside Ω that solves uniquely the conductivity equation

$$\begin{aligned} \nabla \cdot (\gamma \nabla u) &= 0 \quad \text{in } \Omega, \\ u &= f \quad \text{on } \partial\Omega. \end{aligned} \tag{1}$$

The corresponding current field is $\gamma\nabla u$, and on the boundary the normal component $g = \nu \cdot (\gamma \nabla u)|_{\partial\Omega}$ can be measured. Here ν denotes the outward unit normal to $\partial\Omega$. The Dirichlet-to-Neumann map (Voltage-to-Current map) Λ_γ takes any voltage f to the corresponding current $g = \Lambda_\gamma f$; it models and encodes all possible boundary experiments.

The inverse problem in EIT is two-fold: it asks whether the boundary measurements represented by Λ_γ determines uniquely the conductivity distribution γ, and assuming this is the case, it asks for a stable reconstruction of the conductivity γ given the boundary measurements Λ_γ. This is the so-called Calderón problem.

The Calderón problem is non-linear and known to be severely ill-posed. The uniqueness question for the full 3D problem was answered in the affirmative in [6] using complex geometrical optics (CGO) solutions, and a theoretical reconstruction method was developed by Nachman [7] and Novikov [8] using a non-physical scattering transform. The method was implemented as a computational algorithm in [9, 10, 11], and finally stabilized via rigorous regularization analysis in [12]. See also [13] for a closely related study using a simplified CGO-based method with the complete electrode model.

The aim of this paper is to investigate computationally whether the algorithm applies to the situation of stroke-EIT. Theoretically this is already guaranteed with mild smoothness assumptions on γ, but since the inverse problem is severely ill-posed and stroke-EIT needs to deal with the weakly conducting skull, difficulties are expected to occur. To this end we develop two numerical phantoms modelling a hemorrhagic and an ischemic stroke. We simulate the electrode measurements by numerically solving (1), and use this data for solving the inverse problem in different noise regimes.

The outline of the paper is as follows: In section 2 we outline the theoretical method and a regularized adaptation for the case of noisy data. In section 3 we detail the numerical scheme for the reconstruction method. Then in section 4 we describe the method for solving the forward problem, and finally in section 5 we give the numerical results.

2. Full nonlinear reconstruction

The full nonlinear reconstruction of γ is a method of three steps. It builds on a certain family of functions ψ_ζ (CGO) for which $\gamma^{-1/2}\psi_\zeta$ solves (1) with $\gamma = 1$ near $\partial\Omega$ [6]. These solutions are indexed by a complex frequency $\zeta \in \mathbb{C}^3$ which satisfy $\zeta \cdot \zeta = 0$. Construction of such solutions involves the

Fadeev Green's function

$$G_\zeta(x) := e^{i\zeta\cdot x} g_\zeta(x) \qquad g_\zeta(x) := \frac{1}{(2\pi)^3}\int_{\mathbb{R}^3} \frac{e^{ix\cdot\xi}}{|\xi|^2 + 2\zeta\cdot\xi} d\xi,$$

which share the same singularity as the usual Green's function G_0 for the negative Laplacian. That is, $H_\zeta := G_\zeta - G_0$ is a harmonic function.

The first step involves recovering the trace of CGO solutions ψ_ζ for a sequence of large frequencies ζ. This is possible by solving the boundary integral equations

$$\psi_\zeta|_{\partial\Omega} + \mathcal{S}_\zeta(\Lambda_\gamma - \Lambda_1)(\psi_\zeta|_{\partial\Omega}) = e^{i\zeta\cdot x}|_{\partial\Omega}, \tag{2}$$

where $\mathcal{S}_\zeta : H^{-1/2}(\partial\Omega) \to H^{1/2}(\partial\Omega)$ is the boundary single-layer operator corresponding to the kernel G_ζ. That is,

$$(\mathcal{S}_\zeta\varphi)(x) := \int_{\partial\Omega} G_\zeta(x-y)\varphi(y)\, d\sigma(y), \quad x \in \partial\Omega.$$

There is a unique solution to (2) if the complex frequency is of large magnitude, namely

$$|\zeta| > C_0\|\gamma\|_{C^2(\Omega)}, \tag{3}$$

for some positive constant C_0 depending on a lower bound on $\gamma \in C^2(\Omega)$, see for example [7]. Intuitively, one can think of this step as identifying the surface potentials that extract the right current information from the relative measurements $\Lambda_\gamma - \Lambda_1$.

The second step involves a non-physical scattering transform, which we can compute if we restrict ζ to the subset $\mathcal{V}_\xi$ of $\mathbb{C}^3$ on the form

$$\mathcal{V}_\xi = \{\zeta \in \mathbb{C}^3 \mid \zeta\cdot\zeta = (\zeta+\xi)\cdot(\zeta+\xi) = 0\}.$$

Then the scattering transform takes the form

$$\mathbf{t}(\xi, \zeta(\xi)) = \int_{\partial\Omega} e^{ix\cdot(\xi+\zeta(\xi))}(\Lambda_\gamma - \Lambda_1)\psi_\zeta(x)\, d\sigma(x). \tag{4}$$

Integration by parts in (4) reveals a relationship with $q := \gamma^{-1/2}\Delta(\gamma^{1/2})$ under the assumption that $\gamma \in C^2(\Omega)$. In fact, the scattering transform resembles the Fourier transform of q in the sense that

$$\lim_{|\zeta(\xi)|\to\infty} \mathbf{t}(\xi, \zeta(\xi)) = \hat{q}(\xi)$$

for all ξ in $\mathbb{R}^3$. We note $\mathcal{V}_\xi$ is sufficiently large to contain a sequence tending to infinity [14]. We can then recover q from the inverse Fourier transform and in the last step γ by solving a boundary value problem.

The method is summarized as follows:

$$\Lambda_\gamma \xrightarrow{(1)} \mathbf{t} \xrightarrow{(2)} q \xrightarrow{(3)} \gamma$$

Step 1: For each fixed ξ in $\mathbb{R}^3$, solve the boundary integral equation (2) for all $\zeta(\xi) \in \mathcal{V}_\xi$. Compute $\mathbf{t}(\xi, \zeta(\xi))$ by (4).
Step 2: Compute $\hat{q}(\xi)$ and then $q(x)$ by the inverse Fourier transform.

Step 3: Solve the boundary value problem

$$\begin{aligned}(-\Delta+q)\gamma^{1/2}&=0 \quad \text{in } \Omega,\\ \gamma^{1/2}&=1 \quad \text{on } \partial\Omega.\end{aligned}$$

and extract γ.

We consider now the case of inexact data. Say we measure a perturbed Dirichlet-to-Neumann map

$$\Lambda_\gamma^\varepsilon = \Lambda_\gamma + \mathcal{E},$$

where $\mathcal{E}$ is a bounded linear operator from $H^{1/2}(\partial\Omega)$ to $H^{-1/2}(\partial\Omega)$ with some operator norm bounded by $\varepsilon>0$ of small size. In this case, [11, 12] proposes an adaptation of the direct method as follows.

Step 1$^\varepsilon$: Let $M=M(\varepsilon)>0$ be determined by a sufficiently small ε. For each fixed ξ with $|\xi|<M$, take $\zeta(\xi)\in\mathcal{V}_\xi$ and recover $\psi_\zeta^\varepsilon|_{\partial\Omega}$ from

$$\psi_\zeta^\varepsilon|_{\partial\Omega} + \mathcal{S}_\zeta(\Lambda_\gamma^\varepsilon-\Lambda_1)(\psi_\zeta^\varepsilon|_{\partial\Omega}) = e^{i\zeta\cdot x}|_{\partial\Omega}.$$

Compute the truncated scattering transform by

$$\mathbf{t}_M^\varepsilon(\xi) = \begin{cases}\int_{\partial\Omega} e^{-ix\cdot(\xi+\zeta)}(\Lambda_\gamma^\varepsilon-\Lambda_1)\psi_\zeta^\varepsilon(x)d\sigma(x) & |\xi|<M,\\ 0 & |\xi|\geq M,\end{cases}$$

Step 2$^\varepsilon$: Set $\widehat{q^\varepsilon}(\xi):=\mathbf{t}_M^\varepsilon(\xi)$ and compute the inverse Fourier transform to obtain q^ε.

Step 3$^\varepsilon$: Solve the boundary value problem

$$\begin{aligned}(-\Delta+q^\varepsilon)(\gamma^\varepsilon)^{1/2}&=0 \qquad \text{in } \Omega,\\ (\gamma^\varepsilon)^{1/2}&=1 \qquad \text{on } \partial\Omega.\end{aligned}$$

and extract γ^ε.

We shall refer to this as the regularized method.

Remark 1. There are several several strategies for picking $\zeta(\xi)$. One suggestion is to pick $\zeta(\xi)$ such that $|\zeta(\xi)|=M^p$ for $p>3/2$. This is a sufficient condition to show that the method is a convergent regularization scheme given M is sufficiently slowly growing in ε [12]. In practice, one may choose ζ in a pragmatic fashion and take for example $|\zeta(\xi)|=M$ or $\zeta(\xi)=\frac{\xi}{\sqrt{2}}$ such that $|\zeta|$ is minimal in the admissible set.

3. Implementation of the method

For simplicity we let $\Omega=B(0,1)$. The unit ball setting allows a simple orthonormal basis of $L^2(\partial\Omega)$ consisting of spherical harmonics

$$Y_n^m(\theta,\phi)=P_n(\cos(\theta))e^{im\phi}, \quad n\in\mathbb{N}_0, |m|\leq n,$$

where P_n is the associated Legendre polynomial of degree n. This particular basis is useful for a Nyström type discretization of the boundary integral equation [10, 11].

We aim to recover γ^ε everywhere in Ω from frequency information in a ball of radius M. By Shannon sampling it is sufficient to sample $\widehat{q^\varepsilon}$ in an equidistant grid Ξ sufficiently dense in $[-M, M]^3$. Each $\xi \in \Xi$ defines together with a strategy for picking $|\zeta(\xi)|$ an admissible $\zeta(\xi) \in \mathcal{V}_\xi$ on the form

$$\zeta(\xi) = \zeta_1 + i\zeta_2,$$

where $\zeta_1 = -\frac{\xi}{2} + \xi^\perp$, $|\zeta_1| = |\zeta_2| = \kappa$ for some $\kappa \geq \frac{|\xi|}{2}$, and $\{\xi, \xi^\perp, \zeta_2\}$ is an orthogonal set.

For each $\zeta(\xi)$, $\xi \in \Xi$ we solve a discretized boundary integral equation following [11] for which we briefly recall the setup. We let L_N denote an approximated projection onto the space $\mathbb{H}_N$ spanned by the spherical harmonics of degree less than or equal to N. Indeed, for any $f \in C^0(\partial\Omega)$

$$L_N f = \sum_{n=0}^{N} \sum_{m=-n}^{n} c_{n,m}(\mathbf{f}) Y_n^m,$$

for a suitable quadrature rule on $\partial\Omega$ approximating the inner products as

$$c_{n,m}(\mathbf{f}) = \sum_{k=0}^{K} \alpha_k f(x_k) Y_n^{-m}(x_k),$$

for weights α_k and quadrature points x_k on $\partial\Omega$. A natural choice is a combination of a Gauss-Legendre quadrature rule of order $N+1$ and a trapez rule of order $2N+2$ resulting in $K = 2(N+1)^2$, see for example [11]. Here, we denote $\mathbf{f}$ the vector of elements $\mathbf{f}_k = f(x_k)$.

We can then approximate the action of $\Lambda_\gamma - \Lambda_1$ on any continuous function f by $(\Lambda_\gamma - \Lambda_1) L_N f$ and evaluate as

$$(\Lambda_\gamma - \Lambda_1) f(x_k) \simeq [\mathbf{Q}_\gamma \mathbf{f}]_k := \sum_{n=0}^{N} \sum_{m=-n}^{n} c_{n,m}(\mathbf{f}) (\Lambda_\gamma - \Lambda_1) Y_n^m(x_k).$$

Based on L_N and a matching quadrature approximation of the boundary integral operator corresponding to the regular kernel H_ζ, [11] proposes the discretization

$$(\mathbf{I} + \mathbf{S}_\zeta \mathbf{Q}_\gamma) \boldsymbol{\psi}_\zeta = \mathbf{e}_\zeta,$$

where the k'th element of the right-hand side is $e^{i\zeta \cdot x_k}$ and

$$[\mathbf{S}_\zeta]_{kk'} = \alpha_{k'} H_\zeta(x_k - x_{k'}) + \frac{\alpha_{k'}}{4\pi} \sum_{n=0}^{N} P_n(x_k \cdot x_{k'}).$$

We use a one-dimensional integral formula for the Fadeev Green's function based on [15, Chapter 6] to compute $H_\zeta(x) = G_\zeta(x) - G_0(x)$ as

$$H_\zeta(x) = \frac{e^{-\kappa|x|}}{4\pi|x|} - \frac{\kappa}{4\pi} \int_{\frac{\zeta_2}{\kappa} \cdot \frac{x}{|x|}}^{1} e^{-\kappa|x|u} \frac{J_1(\kappa|x|\sqrt{1-u^2})}{\sqrt{1-u^2}}\, du - \frac{1}{4\pi|x|},$$

where J_1 is the first order Bessel function of the first kind.

From $\boldsymbol{\psi}_\zeta$ we compute $\mathbf{t}_M^\varepsilon(\xi)$ using the quadrature rule on $\partial\Omega$ and compute the inverse FFT to obtain q^ε sampled in an equidistant grid. In the final step we solve the boundary value problem using the finite element method. See [11] for more details and [16] for an implementation.

4. Data simulation

To simulate data we compute $(\Lambda_\gamma - \Lambda_1)Y_n^m(x_k)$ using the finite element method [17] in a unit ball mesh. We rewrite the conductivity equation (1) with Dirichlet condition $f = Y_n^m$ to

$$\begin{aligned} \nabla\cdot(\gamma\nabla w) &= -\nabla\cdot(\gamma\nabla v_n^m) && \text{in } \Omega,\\ w &= 0 && \text{on } \partial\Omega, \end{aligned}$$

where $u = w + v_n^m$ with

$$v_n^m(r,\theta,\phi) = r^n Y_n^m(\theta,\phi).$$

A stable way of recovering the $\mathbb{H}_N$ basis coefficients of $(\Lambda_\gamma - \Lambda_1)Y_n^m$ is to consider the weak formulation

$$\langle(\Lambda_\gamma - \Lambda_1)Y_n^m, Y_{n'}^{m'}\rangle_{L^2(\partial\Omega)} = \int_\Omega (\gamma - 1)\nabla(w + v_n^m)\cdot\nabla v_{n'}^{m'}\,dx.$$

We approximate this integral using a Gauss-Legendre-Jacobi quadrature rule on Ω, see [10]. Note it is possible to compute the gradients ∇v_n^m accurately by computing the derivatives of the associated Legendre polynomials [18]. Then

$$(\Lambda_\gamma - \Lambda_1)Y_n^m(x_k) \simeq \sum_{n'=0}^{N}\sum_{m'=-n'}^{n'} \langle(\Lambda_\gamma - \Lambda_1)Y_n^m, Y_{n'}^{m'}\rangle_{L^2(\partial\Omega)} Y_{n'}^{m'}(x_k),$$

which gives the matrix representation $\mathbf{Q}_\gamma$. We simulate noisy measurements by adding to each element in the matrix representation $\mathbf{Q}_\gamma$ a Gaussian random variable. This means we simulate

$$\mathbf{Q}_\gamma^\varepsilon = \mathbf{Q}_\gamma + \delta\mathbf{E},$$

where $[\mathbf{E}]_{\ell,\ell'}$ are independent Gaussian random variables of zero mean and unit variance, and $\delta > 0$ is chosen such that $\frac{\delta\|\mathbf{E}\|}{\|\mathbf{Q}_\gamma\|}$ is the specified relative noise level for a suitable matrix norm $\|\cdot\|$. See [12] for the choice of norm and a small discussion on noise models.

5. Numerical experiments

We model a simple head phantom in $B(0,1)$ by considering a weakly conducting ellipsoidal shell representing the skull. In the interior we place a either a highly or a weakly conductive ball inclusion representing the stroke. We let a constant background $\gamma = 1$ represent the scalp and the interior of the brain. Our experiments consists of two specific phantoms summarized in table 1 and visualized in figure 1. The parameters are chosen in agreement with existing stroke-EIT simulations [3]. We simulate $\mathbf{Q}_\gamma$ for each phantom

setting $N = 25$ and test further the regularized method on the hemorrhagic stroke phantom in the presence of noise.

	Width	Outer radius	Center	γ
Skull	0.04	$(0.9, 0.95, 0.95)$	$(0, 0, 0)$	0.2
Hemorrhagic stroke		0.15	$(0.3, 0.3, 0)$	3
Ischemic stroke		0.15	$(0.3, 0.3, 0)$	0.7

TABLE 1. Summary of piecewise constant stroke phantoms

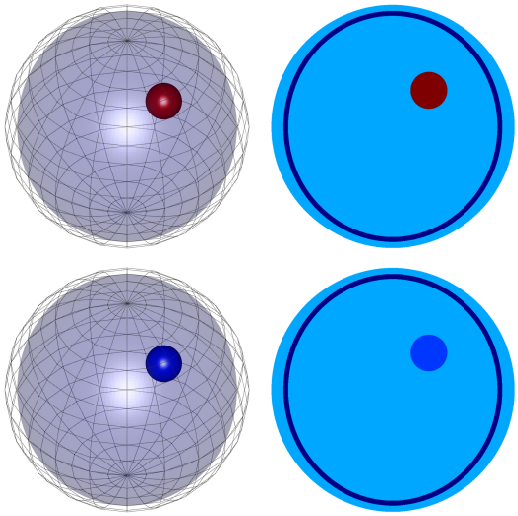

FIGURE 1. Piecewise constant stroke phantoms in a 3D view and the planar cross section $x_3 = 0$.

Figure 2 and 3 show reconstructed conductivities from $\mathbf{Q}_\gamma$ for the hemorrhagic and ischemic stroke phantoms. For both phantoms, the truncation radius M and complex frequency magnitude $|\zeta(\xi)|$ was chosen optimally in terms of visual similarity with the true conductivity distribution. The hemorrhagic stroke is accurately recovered. Here, $M = 13.8$ is chosen with $\zeta(\xi)$ minimal in the admissible set to increase stability of the reconstruction as indicated in [11]. In contrast, a more conservative $M = 10$ and fixed $|\zeta| = 1.2\frac{M}{\sqrt{2}}$ is chosen for the ischemic stroke phantom to promote the ischemic stroke inclusion. Looking hard at figure 3 there is some indication of

a weaker conductivity signal at the location of the ischemic stroke, but it is insignificant in the presence of the weakly conductive skull for this method. Note also, there are some visible 'donut'-type artefacts in the interior of the ellipsoidal shell in both cases. We believe this is a Gibbs-type behavior from the truncation of the high frequency signal.

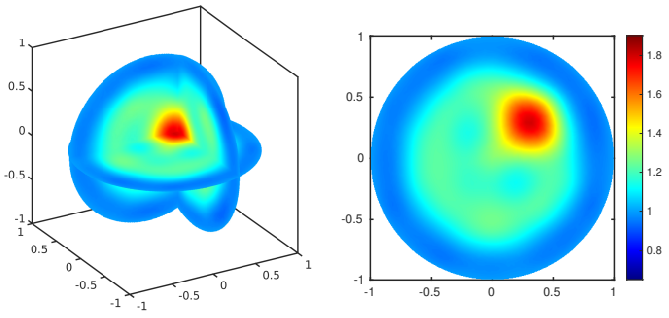

(A) (B)

FIGURE 2. Reconstruction of the hemorrhagic stroke from the simulated Λ_γ without added noise using the regularized method. (A) shows the cross sections $x_3 = 0$, $x_2 = 0.35$ and $x_2 = 0.35$, whereas (B) shows the plane corresponding to $x_3 = 0$. The parameters used are $M = 13.8$, $L = 11$ and $\zeta(\xi) = \frac{\xi}{\sqrt{2}}$ as was determined by visual inspection.

Recovering a high-frequency signal demands the choice of a large $|\zeta(\xi)|$ by (3), which in return amplifies the noise, see [12]. In figure 4 we see cross-sectional plots of reconstructed conductivities from $\mathbf{Q}_\gamma^\varepsilon$ corresponding to 0.1% and 0.5% relative noise. For both data sets we choose $\zeta(\xi) = \frac{\xi}{\sqrt{2}}$ and M small. In the 0.1% case a truncation radius of 8.2 allowed a reasonable reconstruction, where a hemorrhagic stroke is recovered. For the 0.5% case, a smaller truncation radius is chosen for a stable reconstruction. In both cases this yields low resolution and a low frequency reconstruction, but allows an identification of the stroke and its location.

Computationally, the steps 2^ε and 3^ε of the regularized method consisting of an inverse FFT and solving a linear system are almost negligible. This makes approximations to this method fast and popular alternatives [13]. See also [11] for a comparison of different approximations suggesting the full reconstruction method is the most accurate. In its current implementation, which is not optimized, the main computational challenge is assembling and solving the boundary integral equations. As an example, the reconstruction in figure 4 (left) was completed on an Intel Xeon Processor 2660v3 (2.60GHz) in 3915 seconds CPU time. Parallelization on 20 cores gave a speed-up to

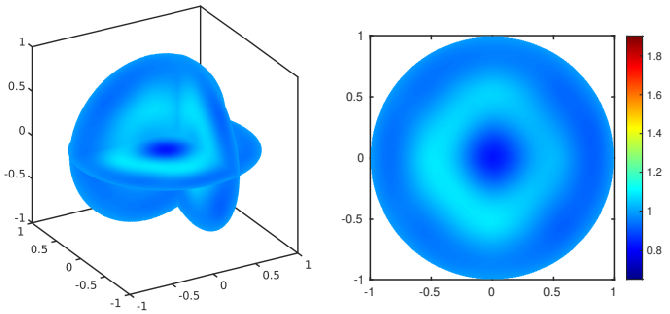

(A) (B)

FIGURE 3. Reconstruction of the ischemic stroke from the simulated Λ_γ without added noise using the regularized method. (A) shows the cross sections $x_3 = 0$, $x_2 = 0.35$ and $x_2 = 0.35$, whereas (B) shows the plane corresponding to $x_3 = 0$. The parameters used are $M = 10$, $L = 9$ and $|\zeta(\xi)| = 1.2\frac{M}{\sqrt{2}}$.

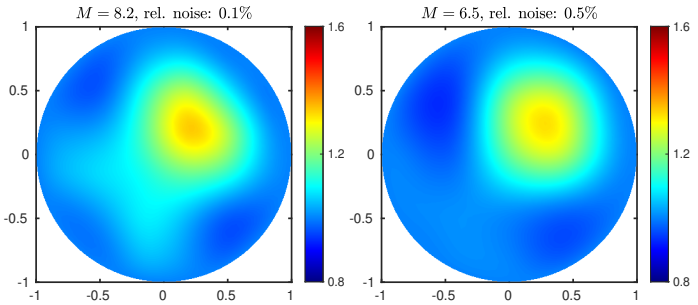

FIGURE 4. Cross sections ($x_3 = 0$) of reconstructions of the hemorrhagic stroke using the regularized method on noisy Dirichlet-to-Neumann maps. The relative noise levels are 0.1% (left) and 0.5% (right) for which $M = 8.2$ and $M = 6.5$ (resp.) was chosen. To increase stability $\zeta(\xi)$ was chosen minimally as $\frac{\xi}{\sqrt{2}}$.

583 seconds in wall time. We believe this can be optimized considerably giving near real-time reconstructions.

6. Conclusions

In this paper we have investigated a direct regularized EIT reconstruction method for the challenging problem of stroke detection. Our computational experiments suggest that detecting a hemorrhagic stroke is possible and robust to noise. Separating an ischemic stroke from the background in the presence of a weakly conductive skull remains a challenge for future work. The method serves as a promising candidate for a near real-time hemorrhagic stroke detection.

Acknowledgments

AKR and KK were supported by The Villum Foundation (grant no. 25893).

References

[1] Martins T d C, Sato A K, de Moura F S, de Camargo E D L B, Silva O L, Santos T B R, Zhao Z, Möeller K, Amato M B P, Mueller J L, Lima R G and Tsuzuki M d S G 2019 *Annual Reviews in Control* **48** 442–471 ISSN 18729088, 13675788

[2] Aristovich K Y, Packham B C, Koo H, Santos G S d, McEvoy A and Holder D S 2016 *Neuroimage* **124** 204–213 ISSN 10959572, 10538119

[3] Agnelli J P, Cöl A, Lassas M, Murthy R, Santacesaria M and Siltanen S 2020 *Inverse Problems* **36** 115008 ISSN 13616420, 02665611

[4] Candiani V and Santacesaria M 2022 *Math. eng.* **4** 1–22 ISSN 26403501

[5] Calderón A P 1980 On an inverse boundary value problem *Seminar on Numerical Analysis and its Applications to Continuum Physics (Rio de Janeiro, 1980)* (Soc. Brasil. Mat., Rio de Janeiro) pp 65–73

[6] Sylvester J and Uhlmann G 1987 *Ann. of Math. (2)* **125** 153–169 ISSN 0003-486X

[7] Nachman A I 1988 *Ann. of Math. (2)* **128** 531–576 ISSN 0003-486X

[8] Novikov R G 1988 *Funktsional. Anal. i Prilozhen.* **22** 11–22, 96 ISSN 0374-1990

[9] Delbary F, Hansen P C and Knudsen K 2011 *Journal of Physics: Conference Series (print)* **290** 012003 ISSN 17426596, 17426588

[10] Delbary F, Hansen P C and Knudsen K 2012 *Applicable Analysis* **91** 737–755 ISSN 1563504x, 10267360, 00036811

[11] Delbary F and Knudsen K 2014 *Inverse Probl. Imaging* **8** 991–1012 ISSN 19308345, 19308337

[12] Knudsen K and Rasmussen A K 2022 *Inverse Probl. Imaging* **16** 871–894 ISSN 1930-8337,1930-8345 URL https://doi.org/10.3934/ipi.2022002

[13] Hamilton S J, Isaacson D, Kolehmainen V, Muller P A, Toivainen J and Bray P F 2021 *Inverse Probl. Imaging* **15** 1135–1169 ISSN 1930-8337

[14] Cornean H, Knudsen K and Siltanen S 2006 *J. Inverse Ill-Posed Probl.* **14** 111–134 ISSN 0928-0219

[15] Newton R G 1989 *Inverse Schrödinger scattering in three dimensions* Texts and Monographs in Physics (Springer-Verlag, Berlin) ISBN 3-540-50563-6

[16] Delbary F, Knudsen K, Rasmussen A K and Hansen P C 2022 crEITive https://github.com/akselkaastras/crEITive

[17] Logg A, Mardal K A, Wells G N *et al.* 2012 *Automated Solution of Differential Equations by the Finite Element Method* (Springer) ISBN 978-3-642-23098-1

[18] Zhang S and Jin J 1996 *Computation of special functions* (New York: Wiley) ISBN 0471119636

Email address: kiknu@dtu.dk
Email address: akara@dtu.dk

Appendix E

Notation and notes

E.1 Notation

In this section, we comment on the notation used in this thesis. The notation is standard and consistent with [GN16, GvdV17], but included here for reference.

For definitions related to Sobolev spaces, we refer to [Gri85] and [Tay11]. For basic notation and definitions related to probability theory, some of which we repeat below, we refer to [Kah85, Chapter 1] or [Dud02].

For a metric space $(\mathcal{Z}_1, d)$ the Borel σ-algebra is denoted by $\mathcal{B}(\mathcal{Z}_1)$. If $f : \mathcal{Z}_1 \to \mathcal{Z}_2$ is a measurable map between the measure space $(\mathcal{Z}_1, \mathcal{B}(\mathcal{Z}_1), m)$ and the measurable space $(\mathcal{Z}_2, \mathcal{B}(\mathcal{Z}_2))$, then fm denotes the push-forward measure defined by $fm(B) = m(f^{-1}(B))$ for all $B \in \mathcal{B}(\mathcal{Z}_1)$. This is slightly unusual notation, but for example found in [Pol02].

Unless stated otherwise, we let random variables and elements be defined on a probability space $(\Omega, \mathcal{F}, \Pr)$. A random element $\mathcal{Z}_1$ is a Borel measurable function $Z : \Omega \to \mathcal{Z}_1$. In the special case where $\mathcal{Z}_1 = \mathbb{R}$, we call Z a random variable. We call $Z\Pr$ the *law* or *distribution* of Z. Writing $\Pr(Z \in B)$ for some $B \in \mathcal{B}(\mathcal{Z}_1)$, we simply mean

$$\Pr(Z \in B) = \Pr(\omega \in \Omega : Z(\omega) \in B) = (Z\Pr)(B).$$

When $Z \in B$ is defined by a relation $R(Z)$, we write $\Pr(R(Z))$ instead of $\Pr(Z \in B)$. We sometimes call probability measures defined on $\mathcal{B}(\mathcal{Z}_1)$ Borel distributions.

For a Borel measurable function $f : \mathcal{Z}_1 \to \mathbb{R}$, we denote by $E[f(Z)]$ the expectation of the random variable $f(Z) : \omega \to \mathbb{R}$ defined by

$$E[f(Z)] = \int_\Omega f(Z(\omega)) \Pr(d\omega) = \int_{\mathcal{Z}_1} f(z) \, (Z\Pr)(dz).$$

For remarks on the expectation of more general random elements, we refer to Appendix E.2.2. For two measurable spaces $(\mathcal{Z}_1, \Sigma_1)$ and $(\mathcal{Z}_2, \Sigma_2)$, the σ-algebra for the product space $\mathcal{Z}_1 \times \mathcal{Z}_2$ is called the *product σ-algebra* and defined by

$$\Sigma_1 \otimes \Sigma_2 = \sigma(\{B_1 \times B_2 : B_1 \in \Sigma_1, B_2 \in \Sigma_2\}),$$

i.e. the intersection of all σ-algebras containing $\{B_1 \times B_2 : B_1 \in \Sigma_1, B_2 \in \Sigma_2\}$. The *support* of the measure m on $(\mathcal{Z}_1, \mathcal{B}(\mathcal{Z}_1))$ we define as the set of all points in $z \in \mathcal{Z}_1$ for which every open neighborhood of z has positive measure under m. Given two σ-finite measures m_1, m_2 on $(\mathcal{Z}_1, \mathcal{B}(\mathcal{Z}_1))$, if there is a Borel measurable function $f : \mathcal{Z}_1 \to [0, \infty)$ such that for any $B \in \mathcal{B}(\mathcal{Z}_1)$

$$m_2(B) = \int_B f(z) \, m_1(dz),$$

then we write $f = \frac{dm_2}{dm_1}$ and call f the Radon-Nikodym derivative. We will often, somewhat loosely, say that m_2 has a density f with respect to m_1.

Consider a compact subset A of a space $\mathcal{Z}_1$ endowed with a semimetric $\tilde{d}$. The covering number $N(A, \tilde{d}, \rho)$ denotes the minimum number of closed $\tilde{d}$-balls $\{z \in \mathcal{Z}_1 : \tilde{d}(z_0, z) \leq \rho\}$ with center $z_0 \in A$ and radius $\rho > 0$ needed to cover A, see for example [GvdV17, Appendix C] or [GN16, Section 4.3.7]. We call $\log N(A, \tilde{d}, \rho)$ the metric entropy of A. When $\tilde{d}$ is replaced by a norm, we mean the metric induced by the norm.

Generic constants are denoted C. We denote dependence of a constant on certain parameters $a, b, c, \ldots$ by $C = C(a, b, c, \ldots)$.

E.2 Notes

E.2.1 Measurability of posterior ratios

Note first the following general property. If $f : (\Omega, \mathcal{F}) \to (\mathbb{R}, \mathcal{B}(\mathbb{R}))$ is a measurable function, then

$$g(\omega) := \begin{cases} \frac{1}{f(\omega)} & \text{if } f(\omega) \neq 0, \\ 0 & \text{if } f(\omega) = 0, \end{cases}$$

is also a measurable function. Indeed, take $A \in \mathcal{B}(\mathbb{R})$ and consider the following cases. If $\{0\} \notin A$, then

$$g^{-1}(A) = \{\omega : 1/f(\omega) \in A\} = f^{-1}(h^{-1}(A)),$$

where $h(z) = 1/z$. Note h is continuous on the open set $\{z : z \neq 0\}$, and hence $h^{-1}(A)$ is measurable. Then $f^{-1}(h^{-1}(A)) \in \mathcal{F}$ by measurability of f. If $\{0\} \in A$, then $g^{-1}(A) = g^{-1}(\{0\}) \cup g^{-1}(A \setminus \{0\})$, where $g^{-1}(\{0\}) = \{\omega : f(\omega) = 0\}$. Then $g^{-1}(A) \in \mathcal{F}$ by repetition of the previous argument and since countable unions and intersections of measurable sets are measurable. This concludes that $g : \Omega \to \mathbb{R}$ is measurable.

In the setting of Section 3.1, this property implies that $g : (\mathcal{Y}, \mathcal{B}(\mathcal{Y})) \to (\mathbb{R}, \mathcal{B}(\mathbb{R}))$ defined by

$$g(y) := \begin{cases} \frac{1}{p_n(y)} & \text{if } p_n(y) \neq 0, \\ 0 & \text{if } p_n(y) = 0, \end{cases}$$

is Borel measurable. In fact, $(\gamma, y) \mapsto 1/p_n(y)$ jointly $\mathcal{B}(\Gamma) \otimes \mathcal{B}(\mathcal{Y}) - \mathcal{B}(\mathbb{R})$ measurable. Since products of measurable functions are measurable, also

$$\pi_y(\gamma) := \begin{cases} \frac{p_n^\gamma(y)\pi(\gamma)}{p_n(y)} & \text{if } p_n(y) \neq 0, \\ 0 & \text{if } p_n(y) = 0, \end{cases}$$

is jointly Borel measurable. Then also $y \mapsto \Pi(B|y)$ is measurable for all $B \in \mathcal{B}(\Gamma)$, see [Pol02, Theorem 20, Chapter 4]. This also holds for $(\mathcal{Y}, \mathcal{B}(\mathcal{Y}))$ replaced with $(\Omega, \mathcal{F})$ and $y \mapsto \Pi(B|y)$ replaced with $\omega \mapsto \Pi(B|Y(\omega))$ in the white noise setting of Section 4.1.

E.2.2 Measurability of posterior means

We initially consider a Borel subset Γ of $\mathcal{X} = \mathbb{R}^k$. For any non-negative measurable function $f : \Gamma \to \mathbb{R}$, there exists an increasing sequence of simple functions

such that $s_n \to f$ pointwise [RF10]. Simple means that each s_n has the form $s_n = \sum_{k=1}^{K_n} \alpha_{k,n} \mathbb{1}_{A_{k,n}}$ for measurable sets $A_{k,n} \in \mathcal{B}(\Gamma)$ that are disjoint for each fixed n and constants $\alpha_{k,n}$. By definition of the Lebesgue integral,

$$\int_\Gamma f(\gamma)\,\Pi(d\gamma|y) = \lim_{n\to\infty} \int_\Gamma s_n(\gamma)\,\Pi(d\gamma|y) = \lim_{n\to\infty} \sum_{k=1}^{K_n} \alpha_{k,n} \Pi(A_{k,n}|y),$$

and hence the integral is measurable in y, since $y \mapsto \Pi(A_{k,n}|y)$ is measurable and pointwise limits of measurable functions are measurable. Then each component of the vector $E[\gamma|y] \in \mathbb{R}^k$ is Borel measurable in y by decomposing each function $\gamma \mapsto \gamma_i$ into a positive and negative part. Then also $E[\gamma|y]$ is Borel measurable. We can also see this fact directly from Theorem 20 [Pol02, Chapter 4].

When Γ is as general as a Borel subset of a Banach space $\mathcal{X}$ endowed with a σ-algebra $\mathcal{B}(\Gamma)$, we define the posterior mean as a Bochner integral, the notion of which we obtain from [DU77, p. 44]. A Borel measurable function $f : \Gamma \to \mathcal{X}$ is called Bochner integrable (with respect to $\Pi(\cdot|Z(\omega))$) if there exists a sequence of simple functions $s_n : \Gamma \to \mathcal{X}$ such that

$$\lim_{n\to\infty} \int_\Gamma \|s_n(\gamma) - f(\gamma)\|_{\mathcal{X}}\,\Pi(d\gamma|Z(\omega)) = 0.$$

Here, we mean simple by functions on the form $s_n(\gamma) = \sum_{k=1}^{K_n} \gamma_{k,n} \mathbb{1}_{A_{k,n}}$ for measurable sets $A_{k,n} \in \mathcal{B}(\Gamma)$ that are disjoint for each fixed n and elements $\gamma_{k,n} \in \mathcal{X}$. For Bochner integrable functions f, the Bochner integral is defined as

$$\begin{aligned}\int_\Gamma f(\gamma)\,\Pi(d\gamma|Z(\omega)) &= \lim_{n\to\infty} \int_\Gamma s_n(\gamma)\,\Pi(d\gamma|Z(\omega)),\\ &= \lim_{n\to\infty} \sum_{k=1}^{K_n} \gamma_{k,n} \Pi(A_{k,n}|Z(\omega)),\end{aligned}$$

where the limit is in $\mathcal{X}$. Note that $\omega \mapsto \Pi(A_{k,n}|Z(\omega))$ is measurable and that pointwise limits of measurable functions are measurable, even when they take values in Banach spaces, see [Dud02, Theorem 4.2.2]. Then also $\omega \mapsto E[\gamma|Z(\omega)]$ is measurable.

E.2.3 Lower bound of the posterior denominator

Proposition E.1 *Let $y \in B^m(r) := \{y \in \mathbb{R}^m, \|y\| \le r\}$, and $\pi(B) > 0$ for some bounded set $B \subset \Gamma$. Then*

$$C(r, B, \mathcal{G}, \varepsilon_n) \le p_n(y) \le C(\varepsilon_n).$$

PROOF. Note

$$p_n(y) = \int_{\mathbb{R}^m} p_n^\gamma(y)\pi(\gamma)\,d\gamma \le C(\varepsilon_n)\int_{\mathbb{R}^m}\pi(\gamma)\,d\gamma = C(\varepsilon_n).$$

On the other hand,

$$\begin{aligned}\inf_{(\gamma,y)\in B\times B^m(r)} p_n^\gamma(y) &= C(\varepsilon_n)\inf_{(\gamma,y)\in B\times B^m(r)}\exp\left(-\frac{1}{2\varepsilon_n^2}\|\mathcal{G}(\gamma)-y\|^2\right),\\ &\ge C(\varepsilon_n)\inf_{(\gamma,y)\in B\times B^m(r)}\exp\left(-\frac{1}{\varepsilon_n^2}\|\mathcal{G}(\gamma)\|^2-\frac{1}{\varepsilon_n^2}\|y\|^2\right),\\ &\ge C(r,B,\mathcal{G},\varepsilon_n),\end{aligned}$$

by continuity of $\mathcal{G}$ on $\overline{B}$. This implies

$$p_n(y) \ge C(\varepsilon_n,r,B,\mathcal{G})\int_B \pi(\gamma)\,d\gamma \ge C(\varepsilon_n,r,B,\mathcal{G}).$$

□